

UNCLASSIFIED

AD NUMBER

ADB013275

LIMITATION CHANGES

TO:

Approved for public release; distribution is unlimited.

FROM:

Distribution authorized to U.S. Gov't. agencies only; Test and Evaluation; MAR 1976. Other requests shall be referred to Air Force Avionics Laboratory, Wright-Patterson AFB, OH 45433.

AUTHORITY

afal ltr, 23 mar 1979

THIS PAGE IS UNCLASSIFIED

THIS REPORT HAS BEEN DELIMITED  
AND CLEARED FOR PUBLIC RELEASE  
UNDER DOD DIRECTIVE 5200.20 AND  
NO RESTRICTIONS ARE IMPOSED UPON  
ITS USE AND DISCLOSURE.

DISTRIBUTION STATEMENT A

APPROVED FOR PUBLIC RELEASE;  
DISTRIBUTION UNLIMITED,

AFAL-TR-76-33

62

## INTERFEROMETRIC LENS TESTING

National Bureau of Standards  
Washington, D.C.

*September 1976*

Technical Report AFAL-TR-76-33  
Final Report for Period March 1971 - February 1973

ADB013275

Distribution limited to U.S. Government agencies only, test and evaluation, March 1976. Other requests for this document must be referred to AFAL/RWI.

AIR FORCE AVIONICS LABORATORY  
AIR FORCE WRIGHT AERONAUTICAL LABORATORIES  
AIR FORCE SYSTEMS COMMAND  
WRIGHT-PATTERSON AIR FORCE BASE, OHIO 45433

AD No.  
DDC FILE COPY

B013275

Replacement for cataloging



NOTICE

When Government drawings, specifications, or other data are used for any purpose other than in connection with a definitely related Government procurement operation, the United States Government thereby incurs no responsibility nor any obligation whatsoever; and the fact that the government may have formulated, furnished, or in any way supplied the said drawings, specifications, or other data, is not to be regarded by implication or otherwise as in any manner licensing the holder or any other person or corporation, or conveying any rights or permission to manufacture, use, or sell any patented invention that may in any way be related thereto.

This report was prepared by National Bureau of Standards, Washington, D.C. The work was performed under Air Force Contract F33615-71-M-5007, Project 76460412. The program was under the technical direction of William C. Martin, AFAL/RWI, Air Force Avionics Laboratory, Wright-Patterson AFB, Ohio.

This report has been reviewed and is approved for publication.

*William C. Martin*  
WILLIAM C. MARTIN  
Physicist  
AFAL/RWI

*Ronald N. Hubbard*  
RONALD N. HUBBARD  
E-O Sensors Group  
E-O & Reconnaissance Branch

*Robert E. Deal*  
ROBERT E. DEAL, Chief  
Electro-Optics & Reconnaissance Br.  
Reconnaissance & Weapon Delivery Div.  
Air Force Avionics Laboratory

Copies of this report should not be returned unless return is required by security considerations, contractual obligations, or notice on a specific document.

**UNCLASSIFIED**

SECURITY CLASSIFICATION OF THIS PAGE (When Data Entered)

REPORT DOCUMENTATION PAGE		READ INSTRUCTIONS BEFORE COMPLETING FORM
1. REPORT NUMBER <i>(18) AFAL-TR-76-33</i>	2. GOVT ACCESSION NO.	3. RECIPIENT'S CATALOG NUMBER
4. TITLE (and Subtitle) <i>(6) INTERFEROMETRIC LENS TESTING.</i>	5. TYPE OF REPORT & PERIOD COVERED <i>(9) Final Report. Mar 1971 - Feb 1973,</i>	
7. AUTHOR(s) <i>(10) John M. Jerke D. Nyysonen</i>	8. CONTRACT OR GRANT NUMBER(s) <i>(15) F33615-71-M-5007 new</i>	
9. PERFORMING ORGANIZATION NAME AND ADDRESS <i>National Bureau of Standards Washington, D. C. 20234</i>	10. PROGRAM ELEMENT, PROJECT, TASK AREA & WORK UNIT NUMBERS <i>(16) AF-7646 04 12 (17) 764604</i>	
11. CONTROLLING OFFICE NAME AND ADDRESS <i>Air Force Avionics Laboratory Wright-Patterson Air Force Base, Ohio 45433</i>	12. REPORT DATE <i>(11) Sep 1976</i>	
14. MONITORING AGENCY NAME & ADDRESS (if different from Controlling Office)	13. NUMBER OF PAGES <i>(12) 35 p.</i>	
	15. SECURITY CLASSIFICATION (of this report) <b>UNCLASSIFIED</b>	
	15a. DECLASSIFICATION/DOWNGRADING SCHEDULE	
16. DISTRIBUTION STATEMENT (of this Report) <b>Distribution limited to U. S. Government agencies only, test and evaluation, March 1976. Other requests for this document must be referred to AFAL/RWI.</b>		
17. DISTRIBUTION STATEMENT (of the abstract entered in Block 20, if different from Report)		
18. SUPPLEMENTARY NOTES		
19. KEY WORDS (Continue on reverse side if necessary and identify by block number) <b>Interferogram scanning, lens aberrations, lens testing, optical transfer function, wavefront shearing interferometer.</b>		
20. ABSTRACT (Continue on reverse side if necessary and identify by block number)		
<b>ABSTRACT</b>		
<p>Interferometric testing of optical systems measures the pupil function, or wavefront deviations from a reference sphere, of the lenses and mirrors. From this pupil function, the optical transfer function (OTF), spread function, and aberration coefficients may be computed.</p>		

**UNCLASSIFIED**

SECURITY CLASSIFICATION OF THIS PAGE(When Data Entered)

20.

In the present study, a wavefront shearing interferometer (WSI) is developed and applied to the on-axis testing of lenses. The simple cube interferometer has all the interferometric adjustments built in during assembly. In contrast to most interferometric test systems, the WSI is inexpensive, portable, relatively insensitive to vibration, does not need laser illumination, and requires only a minimum of experimental time and operational expertise.

Scanning the interferograms and subsequent data reduction are the major effort in testing with the WSI. A computer program for reducing input fringe data to the pupil function, OTF, and aberration coefficients is described; a program to plot the pupil function and OTF is included. Also, a computer program for deriving fringe locations from density data obtained with automatic scanning of the interferograms is described. Sample outputs of the computer programs are given.

Aberrations introduced by the cube interferometer, which is equivalent to a glass plate, are determined. Corrections are automatically made in the computer program for spherical aberration. Defocus can be compensated during testing. Asymmetrical aberrations for test systems greater than  $f/5$  are less than 0.05 wavelength if the cube face is aligned normal to the test-system optical axis within  $1/2^\circ$ .

Results of testing two  $f/8.7$  collimators and an  $f/8$  OTF Standard Test Lens on the WSI are presented. These test results show that one collimator is highly aberrated and the other collimator is nearly diffraction limited. For the OTF Standard Test Lens, the WSI test results are compared with other published test results.

All of the present tests are on axis. Alignment of the lens is a critical factor in determining the on-axis performance and repeating test measurements. Present testing techniques have resulted in root-mean-square differences of less than 0.04 wavelength.

ACCESSION NO.	
NTIS	White Section <input type="checkbox"/>
BCC	Black Section <input checked="" type="checkbox"/>
UNMARKED/UNCLASSED	
JUSTIFICATION	
BY	
DISTRIBUTION/AVAILABILITY CODES	
Dist.	AVAIL. AND/OR SPECIAL
B	

**UNCLASSIFIED**

SECURITY CLASSIFICATION OF THIS PAGE(When Data Entered)

## PREFACE

This report describes a wavefront shearing interferometer system for testing lenses. In addition to the test system and representative data, a complete data-reduction procedure for the resulting interferograms is described. This system can be used to evaluate the in-situ performance of large diameter collimators located at Air Force facilities.

This effort was administered under direction of the Air Force Avionics Laboratory, Dayton, Ohio. The program monitor was Mr. William C. Martin.

Special acknowledgement is made to Richard E. Swing for technical consultation and to Geraldine Hailes for computer programming. The theoretical analysis and the development of algorithms used in computer programming were done by Diana Nyssonen. The experimental portion of the program, the major part of the written draft, and program management were the responsibility of John M. Jerke.

TABLE OF CONTENTS

	PAGE
I. INTRODUCTION	1
II. DESCRIPTION OF WSI	3
III. ANALYSIS OF OPERATION	7
IV. DATA REDUCTION	11
V. OPTICAL TRANSFER FUNCTION	19
V.1. Computation	19
V.2. Variation with Focus Position	22
VI. CUBE INTERFEROMETER	25
VI.1. Parameters	25
VI.2. Aberrations	28
VII. AUXILIARY LENS	37
VIII. ERROR ANALYSIS	41
VIII.1. Cube Quality and Alignment	41
VIII.2. Experimental	42
VIII.3. Interferogram Quality, Scanning, and Registration	45
IX. AUTOMATIC SCANNER	57
IX.1. Description	57
IX.2. Calibration	59
IX.3. Data Reduction	61
X. WSI FRINGE PATTERNS	65
X.1. Analytic Form	65
X.2. Test Cases	67
XI. TEST SYSTEM AND PROCEDURES	79
XI.1. Testing Mode	79
XI.2. Components	79

TABLE OF CONTENTS (CONTINUED)

	PAGE
XI.3. Alignment	82
XI.4. Interferogram Photography	85
XII. TEST RESULTS	87
XII.1. Collimator A	87
XII.2. Collimator B	95
XII.3. OTF Standard Test Lens	106
XIII. COMPUTER PROGRAMS	113
XIV. CONCLUSIONS	117
XV. RECOMMENDATIONS	119
Appendix A. Computer Program to Reduce WSI Fringe Data	121
Appendix B. Computer Program to Plot WSI Test Data	255
Appendix C. Computer Program to Obtain WSI Fringe Data from Automatic-Scanner Density Data	283
Appendix D. Registration of Interferograms	343
Appendix E. Assembly and Adjustment of WSI Cubes	349
REFERENCES	355

## LIST OF ILLUSTRATIONS

<u>FIGURE NO.</u>	<u>TITLE</u>	<u>PAGE</u>
1	WSI cube	4
2	WSI system for finite-conjugate lens testing	5
3	WSI system for infinite-conjugate lens testing	6
4	WSI system parameters	8
5	Typical WSI interferogram	8
6	Grid for interpolated fringe-order array	13
7	Schematic of light path in WSI cube of thickness $t$ and in equivalent glass plate of thickness $2t$	26
8	Minimum WSI cube dimension as a function of f-number for given shear angles $\phi$	27
9	Schematic of convergent light beam passing through glass plate of thickness $2t$	30
10	Maximum values of defocus and third-order spherical aberration introduced by 13-mm-thick WSI cube; $\lambda = 546.1 \text{ nm}$	33
11	Maximum values of third-order coma introduced by 13-mm-thick WSI cube for given angles of incidence $\theta + \phi$ ; $\lambda = 546.1 \text{ nm}$	34
12	Maximum values of third-order $0^\circ$ astigmatism introduced by 13-mm-thick WSI cube for given angles of incidence $\theta + \phi$ ; $\lambda = 546.1 \text{ nm}$	35
13	Parameters and coordinates for computation of effects of auxiliary lens on WSI fringe pattern	38
14	Photograph of fixture for rotating WSI cube, relay lens, and film plane	43
15	Comparison of test results for fringe data obtained from automatic and manual scanning of same pair of WSI interferograms; $f/8.7$ collimator and $\lambda = 546.1 \text{ nm}$	49
16	Photograph of automatic-scanning microdensitometer with magnetic-tape transport unit	58

LIST OF ILLUSTRATIONS (CONTINUED)

<u>FIGURE NO.</u>	<u>TITLE</u>	<u>PAGE</u>
17	Photograph of 1951 USAF tri-bar target	60
18	Comparison of WSI interferogram with fringe-peak locations obtained from automatic scanning	62
19	Schematic of WSI interferograms for $2\lambda$ of third-order x coma	66
20	Schematic of WSI interferograms for $2\lambda$ of third-order $0^\circ$ astigmatism	68
21	Schematic of WSI interferograms for $2\lambda$ of third-order $45^\circ$ astigmatism	69
22	Schematic of WSI interferogram for $2\lambda$ of third-order spherical aberration	71
23	Isocontours of pupil-function phase for test cases of WSI fringe patterns with $1\lambda$ and $2\lambda$ of third-order spherical aberration	73
24	Isocontours of MTF for test cases of WSI fringe patterns with $1\lambda$ and $2\lambda$ of third-order spherical aberration	74
25	MTF for test cases of WSI fringe patterns with $1\lambda$ and $2\lambda$ of third-order spherical aberration	75
26	Isocontours of PTF for test cases of WSI fringe patterns with $1\lambda$ and $2\lambda$ of third-order spherical aberration	76
27	PTF for test cases of WSI fringe patterns with $1\lambda$ and $2\lambda$ of third-order spherical aberration	77
28	Photograph of single-pass WSI test system for infinite-conjugate testing	80
29	Schematic of Boys-point method to align test lens in WSI system	84
30	On-axis WSI test results in plane of best focus for f/8.7 collimating doublet (collimator A); $\lambda = 546.1$ nm	89

LIST OF ILLUSTRATIONS (CONTINUED)

<u>FIGURE NO.</u>	<u>TITLE</u>	<u>PAGE</u>
31	On-axis WSI test results in plane of best focus for f/8.7 collimating doublet (collimator B); $\lambda = 632.8 \text{ nm}$	96
32	On-axis WSI test results in plane of best focus for f/8.7 collimating doublet (collimator B) stopped down to f/10; $\lambda = 632.8 \text{ nm}$	102
33	On-axis WSI test results in plane of best focus for f/8 OTF Standard Test Lens; $\lambda = 546.1 \text{ nm}$	108
34	Flow diagram of complete data-reduction procedures for WSI interferogram	114
35	Schematic of x and y-sheared WSI interferograms showing measured parameters for input to data-reduction computer program	133
36	Coordinate system for WSI interferograms	343
37	Schematic of test lens with cross hairs, fiducial marks, and identification patterns as viewed from cube interferometer	344
38	Schematic of WSI fringe pattern with cross hairs and identification patterns	345
39	Schematic of WSI interferograms marked with coordinate axes to preserve relative orientation	346
40	Schematic of superimposed WSI interferograms with punched holes for manual-scanning alignment	347
41	Schematic of placement of WSI interferograms for scanning	347
42	Schematic of pair of 45°-90°-45° prisms for WSI cube	349
43	Photograph of device for assembling WSI cube	351
44	Schematic of cylindrical holder for WSI cube	354

LIST OF TABLES

<u>TABLE NO.</u>	<u>TITLE</u>	<u>PAGE</u>
1	Aberration terms for WSI data reduction and comparison with terms in USAF lens design program FROLIC	16
2	WSI cube parameters	29
3	Comparison of maximum aberrations resulting from scanning same pair of WSI interferograms with manual and automatic scanners	52
4	Comparison of maximum aberrations, RMS values, and residual symmetric aberrations resulting from three scans of same pair of WSI interferograms	54
5	Pattern spatial frequencies for 1951 USAF tri-bar target	60
6	Maximum aberrations for test cases of $1\lambda$ and $2\lambda$ of third-order spherical aberration	72
7	Maximum aberrations for f/8.7 collimating doublet (collimator A)	94
8	Maximum aberrations for f/8.7 collimating doublet (collimator B)	101
9	Maximum aberrations for f/8.7 collimating doublet (collimator B) stopped down to f/10	105
10	Maximum aberrations for f/8 OTF Standard Test Lens	111
11	Execution time and storage requirement for WSI computer programs	115

## I. INTRODUCTION

Optical testing is a necessary step in the design, evaluation and acceptance of optical systems. As a major procurer of lenses, it is important that the sponsor have a viable technique for accurate testing. A standard approach to optical-systems evaluation is the measurement of the optical transfer function (OTF). Methods of measuring the OTF generally fall into one of the following categories [1,2,3]: (1) spatial-frequency analysis of the image of a target of known content; and (2) interferometric determination of the pupil function from which the OTF and spread function may be calculated.

Although most commercially available OTF equipment is based on the first method, the use of targets for frequency analysis is subject to numerous errors. These systems use edges, sine waves, square waves, or slits as either object or scanning aperture. The system is assumed to be incoherent and, therefore, the ratio of the frequency content of the image to that of the object for each frequency yields the modulation transfer function (MTF) of the system without ambiguity. The phase portion of the OTF, or phase transfer function (PTF), is generally determined by measurement of the shift of the image with respect to the object. The accuracy of this method depends on exact knowledge of the transmittance functions of the object and of the scanning aperture. The accuracy also depends on the relative incoherence of the system and, for determining the PTF, depends on the ability to accurately detect small image shifts. For frequencies under 100 cycles/mm, it is not difficult to meet these requirements; however, as the frequency increases, it becomes more difficult to meet them. As the targets of scanning apertures become smaller, analysis of their frequency content depends on microdensitometry. This is presently a very inexact method for determination of the transmittance function of small objects, due mainly to the nonlinear effects of the instrument [4]. With increased frequency, the relative incoherence (and linearity) of the system becomes more difficult to assure. Also, detection of small image shifts becomes more difficult when measuring the PTF. For these reasons, high-frequency system analysis favors the improved accuracy of interferometric measurement.

Interferometric testing basically measures the pupil function of the system. From the pupil function, a wealth of other information such as the aberration coefficients, the OTF and the spread function may be obtained to satisfy the particular interests of the systems user [4,5,6]. The pupil function, which cannot be extracted from frequency analysis of an object, is the fundamental quantity of interest when dealing with cascaded optical systems [7] as well as systems employing partially or fully coherent illumination [8]. Measurement of the pupil function is, therefore, necessary to properly evaluate systems of these types and to make accurate predictions of performance.

Most interferometric testing systems are expensive, time consuming and require operational expertise. The wavefront shearing interferometer (WSI) which was chosen for development under the present study eliminates some of the undesirable features of most interferometric testing systems. Since most of the interferometric adjustments are built in at manufacture, the WSI is easy to use with a comparatively short time required for experimental measurements. The WSI is also portable and may be set up quickly on most optical benches. It does not require laser illumination and is relatively insensitive to vibration. In addition, the WSI is inexpensive to manufacture and install.

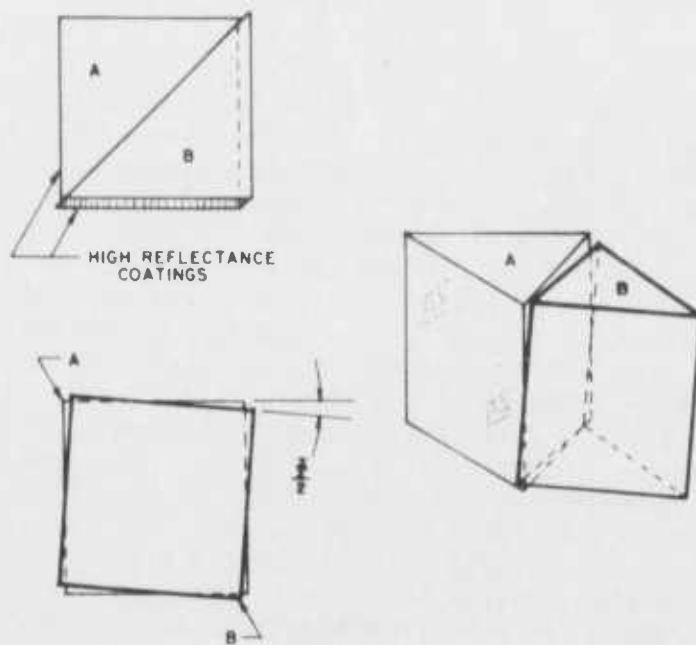
The WSI interferograms cannot be directly interpreted upon simple inspection, in terms of wavefront aberrations [9]. Hence, the major portion of time and cost in routine operation of this system involves data reduction and analysis. However, with the availability of high-speed computers and fast methods of data accumulation and reduction, the WSI system becomes an inexpensive and reasonable choice for lens testing.

## II. DESCRIPTION OF WSI

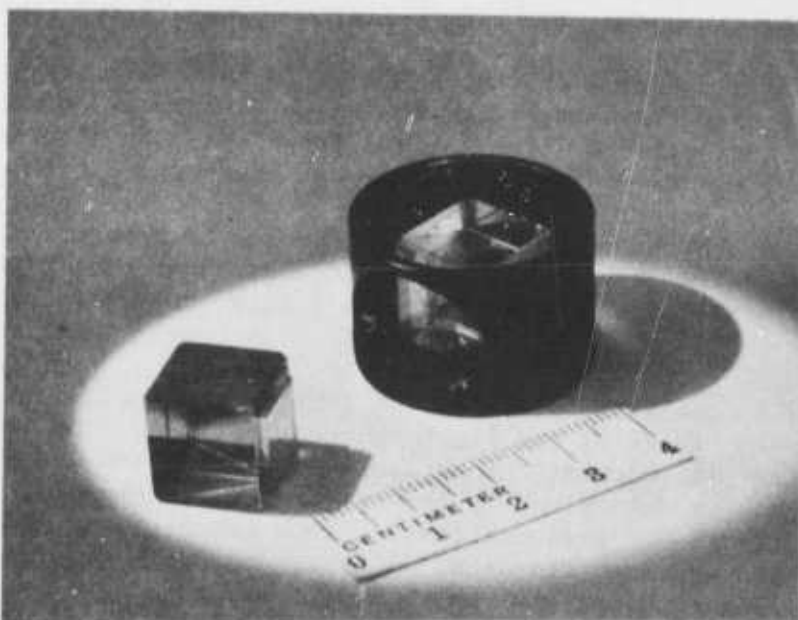
The major component of the wavefront shearing interferometer system described in this report is the cube interferometer of Saunders [10]. As shown in figure 1, this cube represents a compact form of a Michelson interferometer. Figure 1(a) and figure 1(b) show a schematic and photograph of an assembled WSI cube. The cube consists of two identical  $45^{\circ}$ - $90^{\circ}$ - $45^{\circ}$  prisms cemented along their hypotenuse faces, one of which is coated to transmit and reflect partially. A beam entering the cube is amplitude-divided, and the angle between the axes of the two emerging beams is adjusted to a fixed value  $\Phi$  by rotating one prism relative to the other about an axis normal to the beam-dividing face. This rotational adjustment is made when the prisms are cemented together. In addition, the zero-order fringe position is permanently adjusted to lie in the center of the cube, thereby assuring equal optical paths for the two beams in the interferometer. Equal light paths allow the use of relatively broadband spectral sources, rather than restricting the use of the WSI to lasers. A discussion of cube parameters is given in section VI.1, and the assembly and adjustment of the WSI cube are discussed in appendix E.

The WSI cube may be used for testing lenses at either finite or infinite conjugates as shown in figures 2 and 3, respectively. The test system shown in figure 2 is a single-pass system. For infinite-conjugate testing, the test system may be used in a single or double-pass mode as shown in figures 3(a) and 3(b), respectively. In the arrangements shown in figure 3, a high-quality collimator or mirror is used. If a nearly diffraction-limited collimator or mirror is not available, then the aberrations in the collimator or mirror must be measured and removed from the WSI test data. An alternative, which requires no additional optics, can be used for infinite-conjugate testing of lenses with relatively short focal lengths. In this alternate approach, the pinhole light source is located at a distance from the test lens greater than the lens hyperfocal distance (about twenty or more times the focal length); this test system is single pass.

In all the test systems, the WSI cube is placed in the beam near the image of the light source. Hence, the cube may be treated as an element of an image-forming system. The size of the point source is determined by the degree of coherence required to produce fringes of good contrast. Since coherence is also a function of the propagation distance, shorter-conjugate testing requires smaller light sources and vice versa. For recording the interferogram, an auxiliary lens relays the interference pattern onto the film plane. A stable optical bench forms the basis of the test system; one right-angle arm is required for a single-pass system, two are required for a double-pass system. All elements of the test



(a) Schematic of cube; A and B are  $45^\circ - 90^\circ - 45^\circ$  prisms and  $\Phi$  is shear angle.



(b) Photograph of assembled cube and cube in holder.

Figure 1.- WSI cube.

system are standard optical equipment with the exception of the cube interferometer and the test-lens nodal slide that has a 90° rotation adjustment about the test-lens optical axis. An alternate procedure to rotating the test lens is to rotate the cube, auxiliary lens, and film plane as a unit about the test-system optical axis. This alternative requires a suitable rotating fixture.

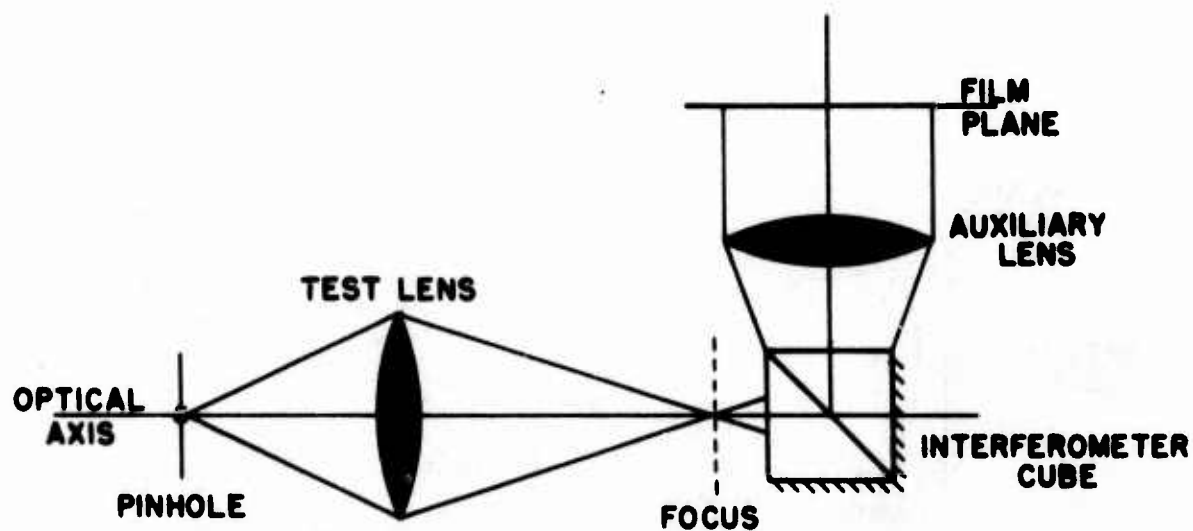
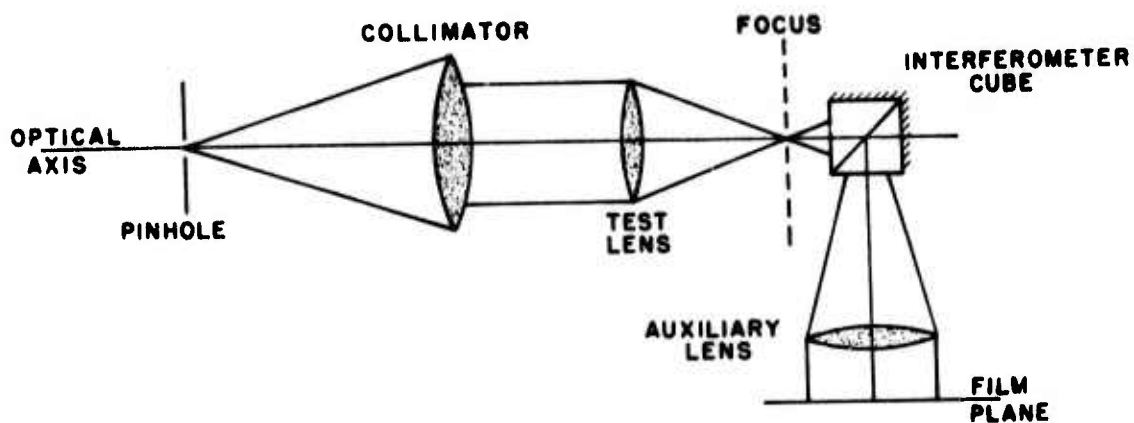
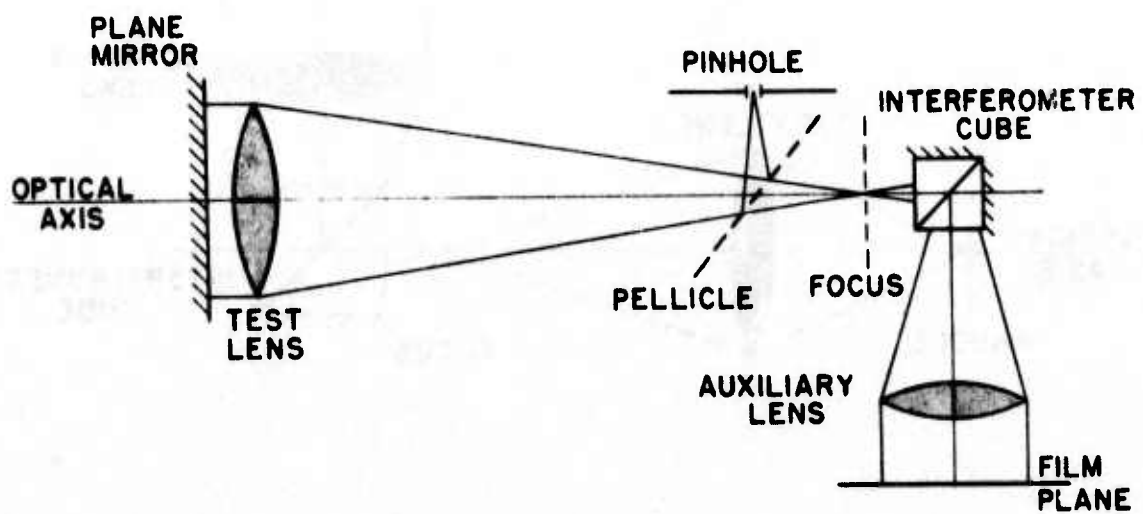


Figure 2.- WSI system for finite-conjugate lens testing.



(a) Single-pass mode.



(b) Double-pass mode.

Figure 3.- WSI system for infinite-conjugate lens testing.

### III. ANALYSIS OF OPERATION

As noted earlier, the cube interferometer operates by amplitude dividing the incoming wavefront into two equal parts and introducing a small angular shear  $\phi$  (approximately 4 to 40 mrad) into one of the beams. For a cube consisting of  $45^\circ$ - $90^\circ$ - $45^\circ$  prisms, the pivot points of the rotation lies in the plane of the back face of the cube as shown in figure 4. With the cube placed near the focus of a converging beam, a small amount of lateral shear  $\ell\phi$  is also introduced. Only for short focal length lenses, however, does the lateral shear become a significant portion of the total shear  $\ell\phi + z_2\phi$ .

Let the wavefront at the exit pupil of the test lens be given by

$$F(x,y) \exp \left\{ -ik \left[ \left( \frac{x^2+y^2}{2x_2} \right) + \varphi(x,y) \right] \right\} \quad (1)$$

where  $x$  and  $y$  are Cartesian coordinates in the exit pupil,  $x_2$  is the radius of the reference sphere [11],  $F(x,y)$  is the amplitude transmittance of the exit pupil,  $\varphi(x,y)$  is the aberration function or deviations of the wavefront from the reference sphere, and  $k = 2\pi/\lambda$ . The pupil function is defined as the complex quantity obtained by removing the reference sphere from equation (1), viz

$$F(x,y) \exp \left[ -ik \varphi(x,y) \right]. \quad (2)$$

In the present investigation, the amplitude transmittance is considered to have a constant value of unity over the exit pupil. Pupil functions with nonuniform amplitude can also be treated using the methods of the present investigation; only minor changes in the computation scheme for the pupil function and OTF would be necessary. However, in most cases of practical interest, the variation of the amplitude is very small and can be considered constant.

The WSI interference pattern, as seen in the exit pupil of the test lens, has the form

$$\begin{aligned} L(x,y) = & |F(x,y)|^2 + |F(x-\ell\phi-z_2\phi, y)|^2 + 2|F(x,y)F(x-\ell\phi-z_2\phi, y)| \\ & \times \gamma_{12}(\tau) \cos \left[ \frac{k\ell\phi x}{x_2} - \frac{k(\ell\phi)^2}{2x_2} + k\varphi(x,y) - k\varphi(x-\ell\phi-z_2\phi, y) \right] \end{aligned} \quad (3)$$

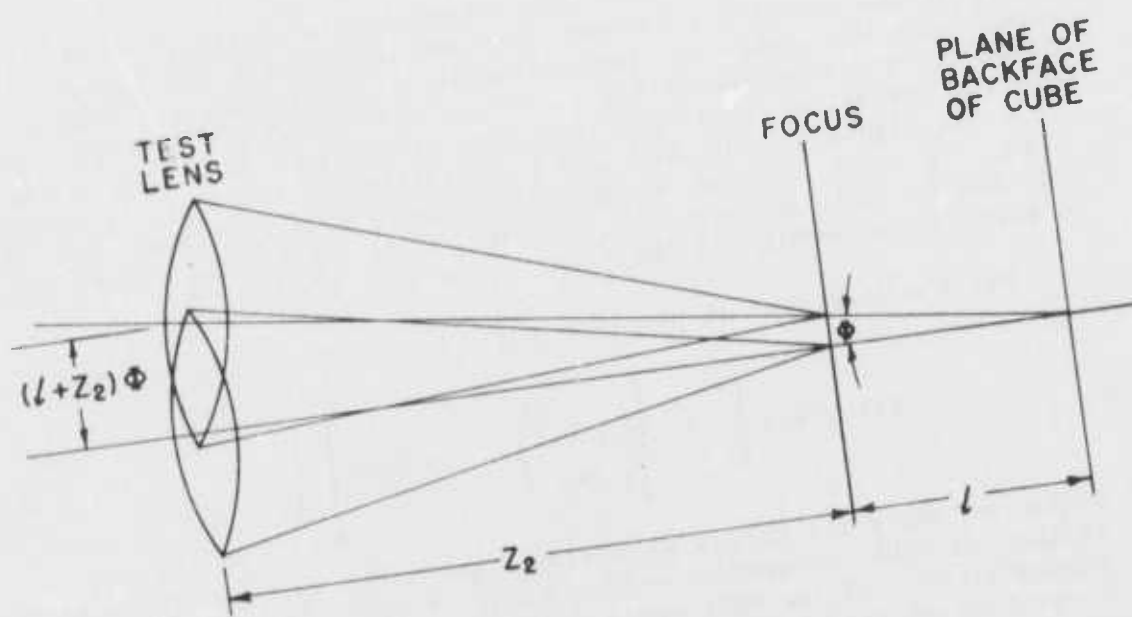


Figure 4.- WSI system parameters.



Figure 5.- Typical WSI interferogram.

where  $\gamma_{12}(\tau)$  is the degree of coherence [12] between points on the overlapping wavefronts, and  $l$ ,  $\phi$ , and  $z_2$  are parameters of the system as shown in figure 4. This form of the interference pattern was derived in previous reports [13,14] and is given here in the more general form to account for variations in the amplitude of the pupil function. The interference pattern consists of straight-line reference fringes of frequency  $k\phi/z_2$  with local displacements of  $\varphi(x,y) - \varphi(x-l\phi - z_2\phi, y)$  where the shear has been taken in the positive  $x$ -direction and the displacement of one wavefront with respect to the other is  $l\phi + x_2\phi$  (shear distance). A photograph of a typical WSI interferogram is shown in figure 5. Since a single interferogram yields information only in the direction of shear, two interferograms are required with shear in orthogonal directions in order to determine the phase of the pupil function  $\varphi(x,y)$ .

#### IV. DATA REDUCTION

The basic data from the WSI system are contained in the two film transparencies of the interference patterns which result from shearing the test-lens wavefront in each of two mutually perpendicular directions. In the present study, these interferograms are enlargements of the fringe patterns photographed with a 35-mm camera in the test set-up. In processing and exposing the enlargements, an effort is made to preserve the maximum detail in the film-density variation at the fringe peaks to permit a more accurate determination of their position. A detailed discussion of interferogram quality is given in section VIII.3.

The interferograms were scanned to locate the fringe peaks either manually using a Grant Comparator or automatically with an Optronics Photoscan P-1000 microdensitometer [15]; one of these automatic digital microdensitometers has also been installed at the sponsor's facilities. When scanned automatically, additional data reduction is required as described in section IX.3 and appendix C. The fringes are, therefore, described by an array of numbers ( $p_{ij}$ ,  $x_{ij}$ ,  $y_{ij}$ ) where  $p_{ij}$  is the integer order of interference associated with the fringe peak located at  $(x_{ij}, y_{ij})$  in the scanning-device coordinate system.

The two interferograms, or frames, representing the wavefront sheared in orthogonal directions must be oriented in the scanner so that the resulting fringe-peak data can eventually be registered in a common coordinate system. The direction of scanning is generally along the shear direction, and, therefore, the fringe-peak coordinates in one frame must undergo a coordinate transformation to account for a  $90^\circ$  lens rotation or a  $90^\circ$  cube rotation. Fiducial marks must be used to either align the interferograms for scanning or to correct the resulting scan data, thereby reducing registration errors. A discussion of registration errors is presented in section VIII.3, and a technique for registration is given in appendix D.

Given the fringe-peak location array ( $p_{ij}$ ,  $x_{ij}$ ,  $y_{ij}$ ), computation of the pupil function is based on equation (2). If we set the argument of the cosine equal to the order of interference  $p(x)$  for any point in the aperture, we get

$$\frac{k\ell\phi x}{z_2} - \frac{k(\ell\phi)^2}{2z_z} + k(x, y) - k(x-\ell\phi-z_2\phi, y) = 2\pi p(x) \quad (4)$$

with a similar equation for the y-sheared interferogram. In order to solve for  $\phi(x, y)$ , a set of such equations must be generated for a

regular array of points  $(X_m, Y_n)$  as shown in figure 6. Since only fringe peaks can be located accurately, this requirement necessitates fringe-order values  $p(x)$  to be interpolated at the selected coordinates  $(X_m, Y_n)$ . Using the available data for fringe peaks corresponding to integral order numbers, an interpolation scheme based on a spline fit [16], which fits a changing third-degree polynomial to adjacent data points, was chosen. This interpolation method is analogous to reading points from a smoothed curve drawn with a draftman's spline passing through adjacent data points. Because a spline fit makes the first and second derivatives continuous as well as the function, this interpolation is more satisfactory than a linear or second-order interpolation technique whenever the pupil-function variations are large compared to the data-sampling interval. When the variations are small, these methods produce equivalent results. Since fringes do not occur in the lune area of the interferogram, interpolated fringe orders are not available for grid points common to the lens aperture and the lune area; rather than extrapolating fringe orders into the lune area, the calculated pupil function is eventually extrapolated into a small portion of this area where values are not available from solution of the following equations.

If we let the spacing of the grid points be equal to the shear distance  $\ell\phi + z_2\phi$  and

$$\left. \begin{aligned} X_m &= x/(\ell\phi + z_2\phi) = m + \text{constant} \\ Y_n &= y/(\ell\phi + z_2\phi) = n + \text{constant} \end{aligned} \right\} \quad (5)$$

and

where  $m$  and  $n$  are integers, then equation (4) reduces to

$$\left( \frac{\ell\phi}{\lambda z_2} \right) m(\ell\phi + z_2\phi) + \text{constant} + \varphi(X_m, Y_n)/\lambda - \varphi(X_{m-1}, Y_n)/\lambda = p(X_m). \quad (6)$$

If we denote the ratio of shear distance to reference fringe spacing as

$$R = \frac{(\ell\phi + z_2\phi)}{\left( \frac{\lambda z_2}{\ell\phi} \right)} \quad (7)$$

Equation (6) reduces to

$$\varphi(X_m, Y_n)/\lambda - \varphi(X_{m-1}, Y_n)/\lambda = p(X_m) - Rm + \text{constant}. \quad (8)$$

A similar equation results for the same grid points in the y-sheared interferogram. If we define  $p(X_m) - Rm$  as the interpolated fringe-

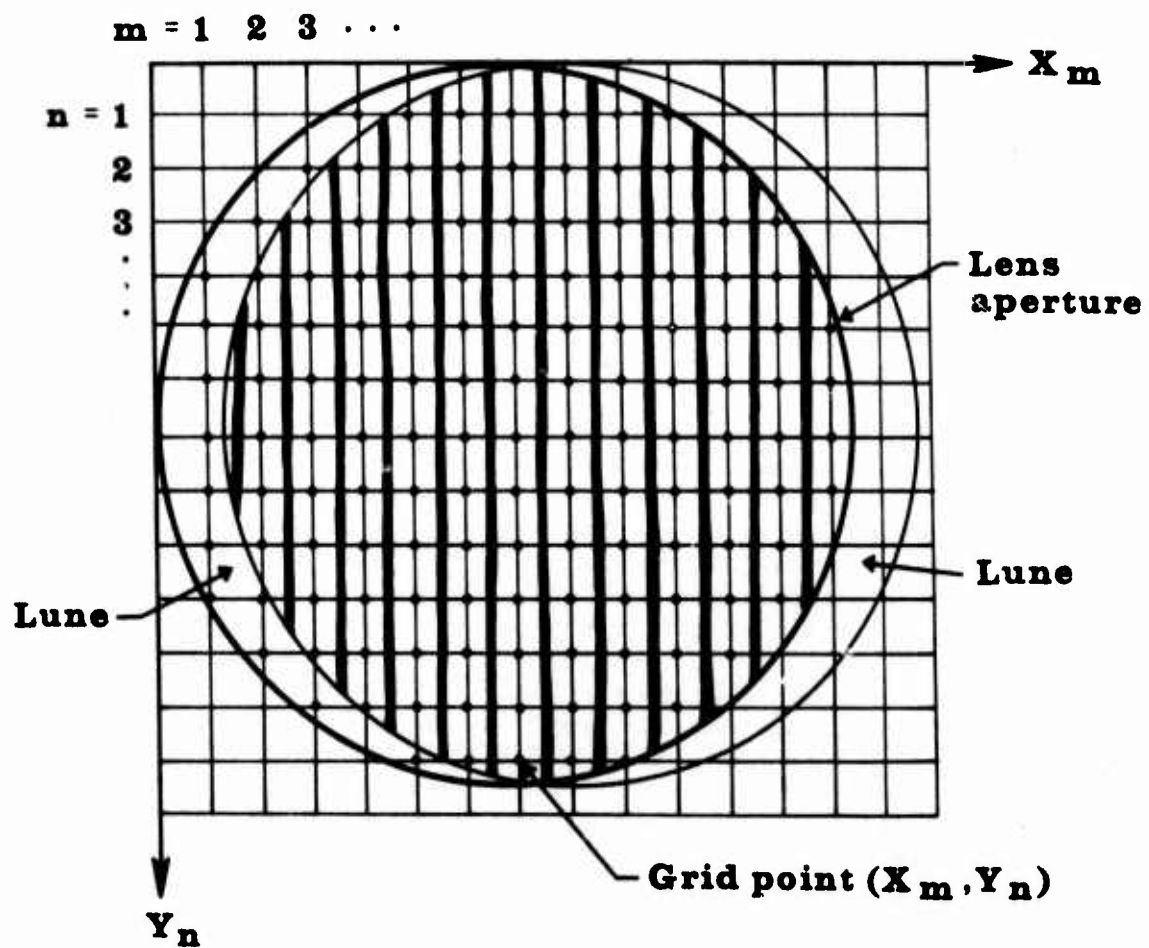


Figure 6.- Grid for interpolated fringe-order array.

order deviations  $Q_{m,n}$  for the grid points  $(X_m, Y_n)$  and similarly define  $p(Y_n) - R_n$  as  $S_{m,n}$  for the y-sheared interferogram, we have a set of equations

$$\begin{aligned}\varphi(X_m, Y_n)/\lambda - (X_{m-1}, Y_n)/\lambda &= Q_{m,n} + K_x \\ \varphi(X_m, Y_n)/\lambda - (X_n, Y_{n-1})/\lambda &= S_{m,n} + K_y\end{aligned}\quad (9)$$

for each grid point with two unknown constants  $K_x$  and  $K_y$  for the whole array. For most grid points, a pair of such difference equations exists, always resulting in more than enough equations to solve for  $\varphi(X_m, Y_n)$ ; where more than one equation applies to a grid point, the equations are summed so that all data are used.

The set of difference equations is solved by first assuming that the pupil-function phase is zero at some grid point, preferably near the center of the aperture. The equation for each grid point is then solved successively from this point outward; the unknown constants  $K_x$  and  $K_y$  will introduce a linear phase term if the solution path is outward from a point in the aperture. For computation of the OTF, a linear phase term will not affect the results [17]. However, if the function  $\varphi(X_m, Y_n)$  is expanded in a polynomial with terms corresponding to common lens aberrations, the linear phase term will automatically be isolated and may be removed from a plot of the wavefront. This method of solution was adopted after it was shown that iterative techniques such as that used by Saunders and Bruening [18] did not converge properly near the edges of the exit pupil. Combining the set of equations as in equation (9) results in far fewer equations than unknowns and, thus, requires more boundary conditions than the single, zero-value reference point used in the present investigation.

The lens aberrations are determined by least-squares fitting the polynomial containing the appropriate aberration coefficients to the computed  $\varphi(X_m, Y_n)$ . The least-squares fitting requires the minimization of the square of the difference between the input wavefront based on interferometric data and the analytic wavefront described by the twenty-three term polynomial in  $X$  and  $y$ , viz,

$$b_n \left\{ \sum_i \left[ \varphi_i(x,y) - \sum_{n=1}^{23} b_n P_n(x,y)_i \right]^2 \right\} = 0 \quad (10)$$

where  $P_n(x,y)$  is the set of polynomials describing the aberrations, and  $b_n$ 's are constant coefficients. In the present investigations, the pupil-function values that were determined by

setting  $(X_m, Y_n) = 0$  for one grid point and successively solving equation (9) were then substituted into equation (10). Various polynomials may be used, including a power series in Cartesian coordinates or polar coordinates [19]. The terms in the series are frequently grouped so that they may be identified with particular aberrations. The series used here is similar to that of reference 20 and for axial images contains the terms shown in table 1(a). An alternate polynomial of the form

$$\sum_m \sum_n c_{m,n} x^n y^m$$

may be used as in the current USAF Lens Design Program FROLIC. The equivalent relationships between these coefficients and those used on the present study are given in table 1(b). Although these twenty-three terms do not include all the terms resulting from a general eight-order power-series expansion of the wavefront, the terms corresponding to third and fifth-order aberrations such as coma, astigmatism and seventh-order spherical aberrations, which are commonly treated in lens design, have been included. After determining the  $b_n$ 's of the aberration coefficients from equation (10) by use of matrix theory, the resulting analytic wavefront or pupil function expressed in actual lens coordinates can be written as

$$\varphi(x,y) = \sum_{n=1}^{23} b_n P_n(x,y) \quad (11)$$

from which the constant term  $b_1$ , the x-tilt term  $b_2x$ , and the y-tilt term  $b_3y$  are subtracted to give the pupil function with respect to the exit-pupil plane. This data reduction is performed by the computer program described in appendix A.

TABLE 1. - ABERRATION TERMS FOR WSI DATA REDUCTION  
AND COMPARISON WITH TERMS IN USAF LENS  
DESIGN PROGRAM FROLIC

(a) ABERRATION TERMS

n	$F_n(r, \theta)$	$F_n(x, y)$	Type
1	constant	constant	constant
2	$r \cos \theta$	x	x tilt
3	$r \sin \theta$	y	y tilt
4	$r^2$	$x^2 + y^2$	focus
5	$r^2 \cos 2\theta$	$x^2 - y^2$	$0^\circ$ astigmatism (3rd)
6	$r^2 \sin 2\theta$	$2xy$	$45^\circ$ astigmatism (3rd)
7	$r^3 \cos \theta$	$x(x^2 + y^2)$	x coma (3rd)
8	$r^3 \sin \theta$	$y(x^2 + y^2)$	y coma (3rd)
9	$r^3 \cos 3\theta$	$x(x^2 - 3y^2)$	x clover (3rd)
10	$r^3 \sin 3\theta$	$y(3x^2 - y^2)$	y clover (3rd)
11	$r^4$	$(x^2 + y^2)^2$	3rd spherical
12	$r^4 \cos 2\theta$	$x^4 - y^4$	$0^\circ$ astigmatism (5th)
13	$r^4 \sin 2\theta$	$2xy(x^2 + y^2)$	$45^\circ$ astigmatism (5th)
14	$r^2 \cos 4\theta$	$x^4 - 6x^2y^2 + y^4$	
15	$r^4 \sin 4\theta$	$4xy(x^2 - y^2)$	
16	$r^5 \cos \theta$	$x(x^2 + y^2)^2$	x coma (5th)
17	$r^5 \sin \theta$	$y(x^2 + y^2)^2$	y coma (5th)
18	$r^5 \cos 3\theta$	$x^5 - 2x^3y^2 - 3xy^4$	x clover (5th)
19	$r^5 \sin 3\theta$	$3x^4y + 2x^2y^3 - y^5$	y clover (5th)
20	$r^5 \cos 5\theta$	$x^5 - 10x^3y^2 + 5xy^4$	
21	$r^5 \sin 5\theta$	$5x^4y - 10x^2y^3 + y^5$	
22	$r^6$	$(x^2 + y^2)^3$	5th spherical
23	$r^8$	$(x^2 + y^2)^4$	7th spherical

TABLE 1. - CONTINUED

## (b) COMPARISON OF COEFFICIENTS FOR FROLIC AND WSI

Polynomial term	FROLIC coefficient, $c_{m,n}$	WSI coefficient, $b_n$
1	$c_{0,0}$	$b_1$
x	$c_{1,0}$	$b_2$
$x^2$	$c_{2,0}$	$b_4 + b_5$
$x^3$	$c_{3,0}$	$b_7 + b_9$
$x^4$	$c_{4,0}$	$b_{11} + b_{12} + b_{14}$
$x^5$	$c_{5,0}$	$b_{16} + b_{18} + b_{20}$
$x^6$	$c_{6,0}$	$b_{22}$
$x^8$	$c_{8,0}$	$b_{23}$
y	$c_{0,1}$	$b_3$
xy	$c_{1,1}$	$2b_6$
$x^2y$	$c_{2,1}$	$b_8 + 3b_{10}$
$x^3y$	$c_{3,1}$	$2b_{13} + 4b_{15}$
$x^4y$	$c_{4,1}$	$b_{17} + 3b_{19} + 5b_{21}$
$y^2$	$c_{0,2}$	$b_4 - b_5$
$xy^2$	$c_{1,2}$	$b_7 - 3b_9$
$x^2y^2$	$c_{2,2}$	$2b_{11} - 6b_{14}$
$x^3y^2$	$c_{3,2}$	$2b_{16} - 2b_{18} - 10b_{20}$
$x^4y^2$	$c_{4,2}$	$3b_{22}$
$x^6y^2$	$c_{6,2}$	$4b_{23}$
$y^3$	$c_{0,3}$	$b_8 - b_{10}$
$xy^3$	$c_{1,3}$	$2b_{13} - 4b_{15}$
$x^2y^3$	$c_{2,3}$	$2b_{17} + 2b_{19} - 10b_{21}$

TABLE 1. - CONCLUDED

(b) CONCLUDED

Polynomial term	FROLIC coefficient, $c_{m,n}$	WSI coefficient, $b_n$
$y^4$	$c_{0,4}$	$b_{11} - b_{12} + b_{14}$
$xy^4$	$c_{1,4}$	$b_{16} - 3b_{18} + 5b_{20}$
$x^2y^4$	$c_{2,4}$	$3b_{22}$
$x^4y^4$	$c_{4,4}$	$6b_{23}$
$y^5$	$c_{0,5}$	$b_{17} - b_{19} + b_{21}$
$y^6$	$c_{0,6}$	$b_{22}$
$x^2y^6$	$c_{2,6}$	$4b_{23}$
$y^8$	$c_{0,8}$	$b_{23}$

## V. OPTICAL TRANSFER FUNCTION

### V.1. Computation

The two-dimensional optical transfer function (OTF) of a lens can be written as the autocorrelation of the pupil function, viz,

$$\text{OTF}(k_x, k_y) = \frac{1}{A} \iint_{\sigma} \exp \left\{ -\frac{2\pi i}{\lambda} \left[ \varphi(x + k_x, y + k_y) - \varphi(x, y) \right] \right\} dx dy \quad (12)$$

where  $k_x$  and  $k_y$  are reduced spatial frequencies,  $\sigma$  is the region of integration defined by the convolved aperture, and  $A$  is the area of the exit pupil. In the present case, the phase of the pupil function  $\varphi(x, y)$  is determined for grid points with a spacing of  $\Delta x$  and  $\Delta y$ ; therefore the reduced spatial frequency coordinates will be given by

$$\begin{aligned} k_x &= m \Delta x \\ k_y &= n \Delta y \end{aligned} \quad | \quad (13)$$

where  $\Delta x$  and  $\Delta y$  were both chosen equal to the shear distance, and  $m$  and  $n$  are integers.

The evaluation of the OTF as given by equation (12) can be rather inaccurate or time consuming if a conventional approach to integration such as Simpson's Rule is employed. The difficulty arises from the occurrence of a rapidly changing phase over a small region of integration in the presence of lens aberrations. Other methods for evaluating equation (12), such as those of Hopkins [21] and Barakat [22], represent a tradeoff between accuracy and computation time. A modification of the Hopkins method utilizing the computed aberration coefficients was chosen in the present study.

Expanding the phase part of the pupil function in a two-dimensional Taylor Series about the point  $(x, y)$ , we can write

$$\begin{aligned} \varphi(x + k_x, y + k_y) - \varphi(x, y) &= k_x \left[ \frac{\partial \varphi(x, y)}{\partial x} \right] + k_y \left[ \frac{\partial \varphi(x, y)}{\partial y} \right] \\ &+ \frac{1}{2} \left[ k_x^2 \frac{\partial^2 \varphi(x, y)}{\partial x^2} + 2k_x k_y \frac{\partial^2 \varphi(x, y)}{\partial x \partial y} + k_y^2 \frac{\partial^2 \varphi(x, y)}{\partial y^2} \right] \\ &+ \frac{1}{6} \left[ k_x^3 \frac{\partial^3 \varphi(x, y)}{\partial x^3} + 3k_x^2 k_y \frac{\partial^3 \varphi(x, y)}{\partial x^2 \partial y} + \dots \right] + \dots \quad (14) \end{aligned}$$

Substituting the polynomial representation of  $\varphi(x, y)$ , as given by equation (11), into equation (14) we get

$$V(x, y, k_x, k_y) = \frac{1}{\lambda} \sum_{n=1}^{23} b_n \left( k_x \frac{\partial}{\partial x} + k_y \frac{\partial}{\partial y} + \frac{k_x^2}{2} \frac{\partial^2}{\partial x^2} + k_x k_y \frac{\partial^2}{\partial x \partial y} + \frac{k_y^2}{2} \frac{\partial^2}{\partial y^2} + \frac{k_x^3}{3} \frac{\partial^3}{\partial x^3} + k_x k_y \frac{\partial^3}{\partial x^2 \partial y} + \dots \right) P_n(x, y) . \quad (15)$$

Therefore, equation (12) may be written as

$$OTF(k_x, k_y) = \frac{1}{A} \iint \exp \left[ -2\pi i V(x, y, k_x, k_y) \right] dx dy \quad (16)$$

which is the integral to be evaluated. The phase of the pupil function was determined earlier at grid points  $(X_m, Y_n)$  with grid spacing  $\Delta x$ . Over an elemental area defined by  $x = X_m \pm \Delta x/2$  and  $y = Y_n \pm \Delta y/2$ , a two-dimensional Taylor expansion of  $V(x, y, k_x, k_y)$  can be performed in which the first three terms determine the contribution of that region of integration to a good approximation. Writing the first three terms of the expansion about the point  $(X_m, Y_n)$ , we have

$$V_{m,n} = V(x, y, k_x, k_y) = V(X_m, Y_n, k_x, k_y) + \frac{\partial V(X_m, Y_n, k_x, k_y)}{\partial x} (x - X_m) + \frac{\partial V(X_m, Y_n, k_x, k_y)}{\partial y} (y - Y_n) . \quad (17)$$

Therefore, the integral of equation (15) becomes

$$\text{OTF}(k_x, k_y) = \frac{1}{(\Delta x)^2} \exp \left\{ -2\pi i v_{m,n} \right\} \times \int_{(X_m - \frac{\Delta x}{2})}^{(X_m + \frac{\Delta x}{2})} \int_{(Y_n - \frac{\Delta x}{2})}^{(Y_n + \frac{\Delta x}{2})} \exp \left\{ -2\pi i \left[ \frac{\partial v_{m,n}}{\partial x} \cdot (x - X_n) + \frac{\partial v_{m,n}}{\partial y} \cdot (y - Y_n) \right] \right\} dx dy. \quad (18)$$

After a change of variables and integration, we obtain

$$\text{OTF}(k_x, k_y) = \frac{1}{(\Delta k)^2} \exp \left\{ -2\pi i v_{m,n} \right\} \times \left\{ \text{sinc} \left[ 2\pi \frac{x}{2} \frac{\partial v_{m,n}}{\partial x} \right] \right. \\ \left. \times \text{sinc} \left[ 2\pi \frac{y}{2} \frac{\partial v_{m,n}}{\partial y} \right] \right\} \quad (19)$$

where

$$\text{sinc } x = (\sin x)/x.$$

Assuming that the contribution of equation (18) for each elemental area is accepted or rejected depending on whether or not it lies within the region of integration, the OTF may be written as

$$\text{OTF}(k_x, k_y) = \frac{1}{N} \sum_m \sum_n \exp \left\{ -2\pi i v_{m,n} \right\} \times \left\{ \text{sinc} \left[ 2\pi \frac{\Delta x}{2} \frac{\partial v_{m,n}}{\partial x} \right] \right. \\ \left. \times \text{sinc} \left[ 2\pi \frac{\Delta y}{2} \frac{\partial v_{m,n}}{\partial y} \right] \right\} \quad (20)$$

where  $N$  is the total number of grid points for which there are data in the lens aperture. The reduced coordinates may be converted to real spatial frequencies by the relations  $\mu_x = k_x/\lambda z_2$  and  $\mu_y = k_y/\lambda z_2$ .

This method of computation of the two-dimensional OTF was found to have superior accuracy especially for rapidly varying phase functions. For 25 fringes (approximately 400 sampling points) the two-dimensional OTF can be computed on the Univac 1108 computer [15] in less than two minutes. The present approach determines the two-dimensional OTF for all grid points ( $X_m, Y_n$ ); computation time can be reduced significantly by calculating only tangential and sagittal cross sections of the OTF. While fast Fourier transforms [23] applied to an equivalent two-dimensional array of grid points would reduce computation time, the accuracy would not be equivalent without a considerable increase in array size; optimizing the computation of the OTF for both time and accuracy is under study.

## V.2. Variation with Focus Position

As noted in equation (3), the nominal frequency  $k\ell\phi/z_2$  of the fringes seen in the interferograms is a function of the displacement  $\ell$  of the cube backface from the test-lens focal plane. For a given interferogram, the total distance  $\ell + z_2$  is fixed by the test system. This sum of  $\ell + z_2$  must be measured and used to calculate the shear distance  $\Delta X$  which, in turn, is used in the data reduction. (See equations (5)-(7).) The ratio of  $\ell$  to  $z_2$ , however, may be arbitrarily specified. The effect of changing this ratio would be to change the frequency or spacing of the reference fringes from which the local fringe deviations are measured. This change is equivalent to changing the radius of the reference sphere [11] and thereby, the focus position. The ratio of  $\ell$  to  $z_2$  corresponding to a different focus position would be substituted into equation (7); the resulting set of equations given by equation (9) would be solved, and a new OTF would be calculated.

An easier approach to calculating the OTF for a focus change is to alter the pupil function computed for the original value of  $z_2$ . To describe the pupil function for a different focus position  $z'_2$  where  $z_2 = z'_2 + \Delta$ , we can rewrite equation (1) as

$$F(x,y) \exp \left\{ -ik \left[ \left( \frac{x^2 + y^2}{2(z'_2 + \Delta)} \right) + \varphi(x,y) \right] \right\} \quad (21)$$

Since the reference sphere now becomes

$$\exp \left\{ -ik \left( \frac{x^2 + y^2}{2z'_2} \right) \right\}, \quad (22)$$

we regroup equation (21) in the form

$$F(x,y) = \exp \left\{ -ik \left[ \left( \frac{x^2 + y^2}{2z'_2} \right) + f(x,y,\Delta) + \varphi(x,y) \right] \right\} \quad (23)$$

where

$$f(x,y,\Delta) = \frac{x^2 + y^2}{2(z'_2 + \Delta)} - \frac{x^2 + y^2}{2z'_2} \quad (24)$$

or

$$f(x,y,\Delta) = - \frac{\Delta(x^2 + y^2)}{2z'_2(z'_2 + \Delta)}. \quad (25)$$

Therefore, the new pupil function is given by

$$F(x,y) = \exp \left\{ -ik \left[ \left( \frac{x^2 + y^2}{2z'_2} \right) + \varphi_{\Delta}(x,y) \right] \right\} \quad (26)$$

where

$$\varphi_{\Delta}(x,y) = \varphi(x,y) - \frac{\Delta(x^2 + y^2)}{2z'_2(z'_2 + \Delta)}. \quad (27)$$

Thus, if  $F(x,y)$  is known for any one focus position, the pupil function for any other may be determined from equations (26) and (27).

The change of focus as expressed by equation (25) corresponds to changing only the defocus term in the polynomial representation of the pupil function,

$$(\delta b_4)(x^2 + y^2) = - \frac{\Delta(x^2 + y^2)}{2z'_2(z'_2 + \Delta)} \quad (28)$$

where  $\delta b_4$  is the difference between the defocus coefficient obtained from the original pupil function and the defocus coefficient corresponding to a different focal position  $z_2$ . The choice of  $\Delta$ , which is the difference in focal positions along the optical axis, is arbitrary, but should depend on the nominal depth of focus expected from the test lens. The present version of the computer program to reduce WSI fringe data has the option of incrementing the focus position in fractional units of the Rayleigh depth-of-focus criterion [24] given by

$$\Delta = F \left[ \pm 3.2 \left( \frac{\lambda}{2\pi} \right) \left( \frac{z_2}{a} \right)^2 \right] \quad (29)$$

where  $F$  is the fractional value,  $a$  is the aperture radius of the test lens,  $z_2$  is the nominal focal length or image conjugate of the test lens, and  $\lambda$  is the radiation wavelength. Using equations (27), (28), and (29), the pupil function is computed. This procedure is repeated for different values of  $\Delta$  on both sides of the original focus position  $z_2$  until the minimum value for the root-mean-square of the wavefront is obtained. The resulting value of  $z'_2$  represents the optimum focal plane.

## VI. CUBE INTERFEROMETER

### VI.1. Parameters

Since the cube is equivalent to a glass plate of dimensions  $t \times t \times 2t$ , the relationship of the minimum cube dimension  $t_{\min}$  to f-number of the system under test is determined by the focal position as shown in figure 7. If the acceptance angle of the cube is  $\mu$ , then

$$f\# = 1/(2\tan\mu). \quad (30)$$

Using Snell's law, the acceptance angle becomes  $\mu'$  inside the cube and

$$\sin \mu = N \sin \mu' \quad (31)$$

where  $N$  is the index of refraction of the cube glass. Because the beam is focused a distance  $l$  from the backface of the cube, the relationship of maximum acceptance angle  $\mu'$  to the cube dimension is given by

$$\tan \mu' = \frac{t/2}{t + l} \quad (32)$$

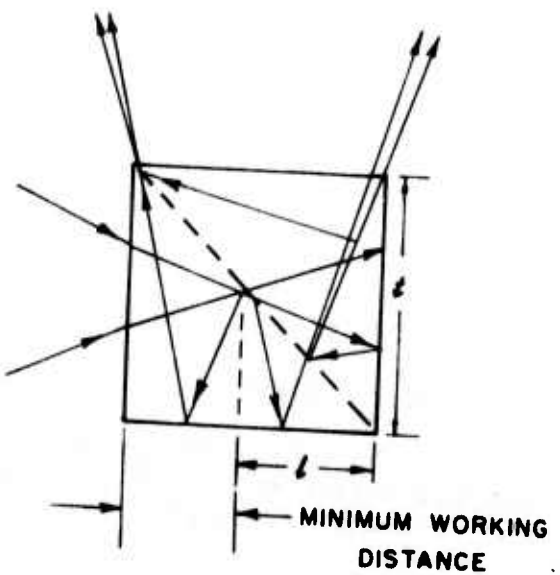
Combining equation (30), (31) and (32) and letting the fringe spacing equal the shear distance ( $l = \lambda/\phi^2$ ) yields

$$f\# = \frac{5t^2 - N^2t^2 + 8\lambda t/\phi^2 + 4\lambda^2/\phi^4}{4N^2t^2}. \quad (33)$$

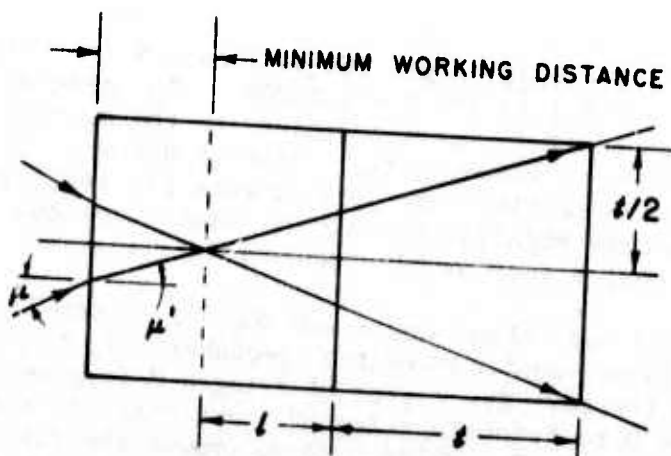
The f-number versus  $t_{\min}$  is plotted in figure 8 for several cube shear angles with  $\lambda = 546.1$  nm and  $N = 1.46008$ . In general, the minimum working distance ( $t-l$ ) corresponding to the distance from the lens surface or flange to focus, rather than f-number, is the limiting parameter in selecting the proper cube for testing; however, this limitation becomes significant only for high numerical-aperture, short focal-length optics such as microscope objectives.

The choice of shear angle for the WSI system is governed by the number of fringes required and the f-number of the optical system system being tested. The number of fringes  $M$  is given by the ratio of lens diameter  $D$  to fringe spacing  $\Delta F$  where  $D$  is related to f-number and conjugate  $z_2$  by  $D = z_2/f\#$ . If we choose the fringe spacing equal to the shear distance, then  $\Delta F \approx z_2\phi$  for  $z_2 \gg l$  and combining these expressions yields the relationship

$$\phi = 1/M f\#. \quad (34)$$



(a) WSI cube.



(b) Equivalent glass plate.

Figure 7.- Schematic of light path in WSI cube of thickness  $t$  and in equivalent glass plate of thickness  $2t$ .

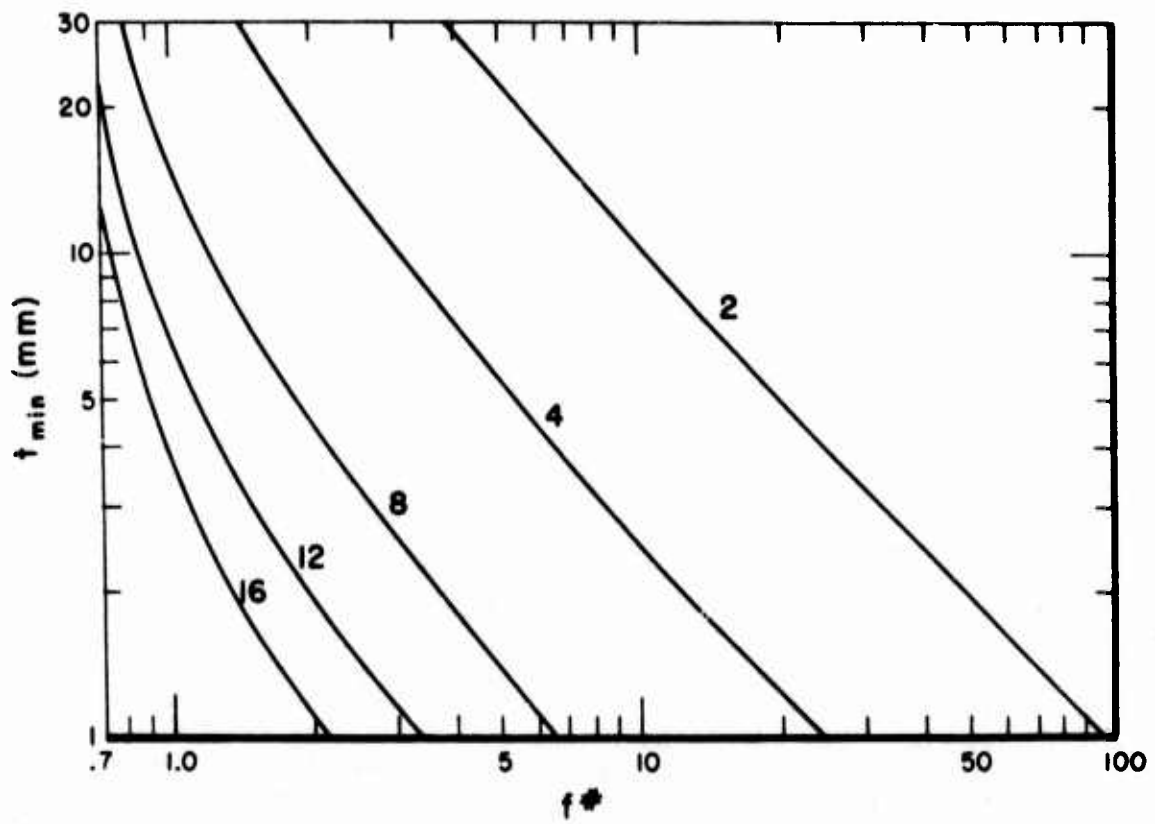


Figure 8.- Minimum WSI cube dimension as a function of f-number for given shear angles  $\Phi$ .

If we let  $M$  equal 25 in equation (34), we obtain the values shown in table 2(a) for the best choice of shear angles to be used with testing a wide range of optical systems. These values are based on straight-line, equally-spaced fringes characteristic of well-corrected optical systems, fringe spacing equal to the shear distance, and  $z_2 \gg l$ ; for highly aberrated lenses or in cases where the ratio  $l/z_2$  is greater than approximately 0.1, it may be necessary to use a different shear angle to produce 25 fringes. The choice of 13 mm for the cube dimension exceeds the minimum requirements of equation (33) and furthermore, it is not difficult to polish such cube surfaces to  $\lambda/10$  flatness. Hence, the optimum choice of cube parameters is governed by the quality of the test lens, its f-number, and focal length. For a high-quality lens, table 2(a) represents a selection of cubes which would satisfy most lens-testing requirements.

The parameters for the set of cubes delivered to the sponsor are given in table 2(b). A comparison with table 2(a) shows that the optimum values of shear angles, or values very close to the optimum, were obtained in fabricating the cubes for the sponsor. This set of cubes should be adequate for testing most of the sponsor's optical systems, such as collimators, with f-numbers down to about  $f/1$  as originally intended in this program. For these systems,  $z_2 \gg l$  and, therefore, the available working distance ( $t-l$ ) will not be the limiting factor as in the case of testing microscope objectives. However, as discussed in the next section, several hundred wavelengths of third-order spherical aberration may be introduced when testing an  $f/1$  system. The resulting fringe pattern for 25 fringes would exhibit highly curved fringes, and the error in locating the fringe peak could be significant. Even though the computer program would automatically remove this large aberration from the data, it is not likely that a measurement accuracy of even  $0.01 \lambda$  could be maintained.

#### VI.2. Aberrations

Because the WSI cube is part of the imaging system as described earlier, the effects of the cube on the test results are important. The cube is equivalent to a thick glass plate of thickness  $2t$  where  $t$  is the length of a cube side. The path traversed by a converging beam of light as it passes through a glass plate is illustrated in figure 9. If the faces of the cube are of interferometer quality and the glass homogeneous, the increase in optical path length introduced by the cube may be calculated from figure 9. Although it is known [25] that a thick glass plate introduces defect of focus and spherical aberration for the case where the optical axis is normal to the face

TABLE 2. - WSI CUBE PARAMETERS<sup>a</sup>

## (a) GENERAL LENS TESTING

f-number of test element	Shear angle, $\phi$ (milliradians)	Displacement, $\ell$ (mm)	Minimum working distance (mm)
11.0	3.6	42.1	not limited
8.0	5.0	21.8	not limited
5.6	7.1	10.8	2.2
4.0	10.0	5.46	7.54
2.8	14.2	2.71	10.29
2.0	20.0	1.36	11.64
1.4	28.6	.67	12.33
1.0	40.0	.34	12.66

## (b) ASSEMBLED FOR SPONSOR

f-number of test element	Shear angle, $\phi$ (milliradians)	Displacement, $\ell$ (mm)	Minimum working distance (mm)
11.0	3.6	42.1	not limited
8.0	5.7	16.8	not limited
5.6	7.8	9.0	4.0
4.0	10.0	5.46	7.54
2.8	13.9	2.81	10.19
2.0	20.0	1.36	11.64
1.4	28.5	.68	12.32
1.0	40.2	.34	12.66

<sup>a</sup> 13-mm-thickness; 25 fringes; and  $\lambda = 546.1$  nm.

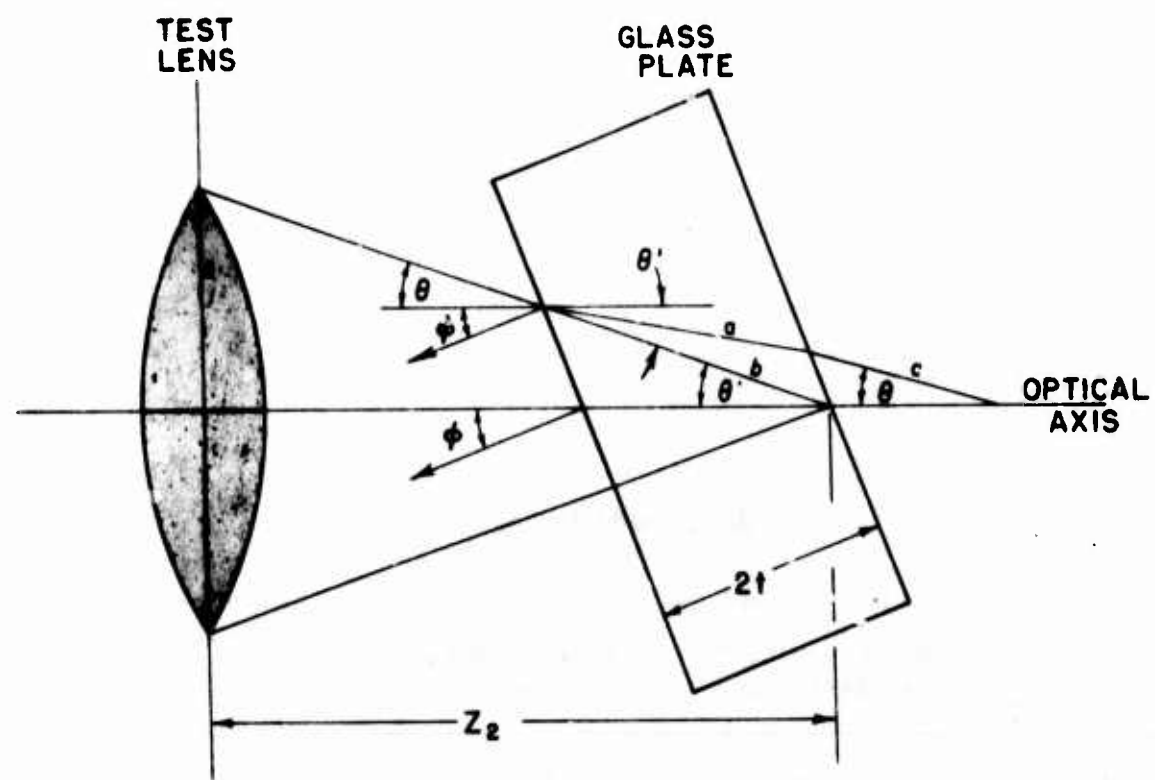


**Figure 9.- Schematic of convergent light beam passing through glass plate of thickness  $2t$ .**

of the plate and the beam is converging, the derivation was not available in the suitable form to use as a correction to the pupil-function data. Therefore, the optical-path differences were computed for the general case which allows for both symmetric and asymmetric aberrations.

From figure 9, we denote the optical path differences as

$$OPD = (Na + c - b)/\lambda \quad (35)$$

where  $N$  is the index of refraction of the cube. For a ray with angle of incidence  $\theta + \phi$ ,

$$\left. \begin{aligned} Na &= \frac{Nt}{\cos(\theta' + \phi)}, \\ b &= \frac{t}{\cos(\theta + \phi)} \\ \text{and} \quad c &= \frac{t}{\cos(\theta + \phi)} \left[ 1 - \frac{\cos(\theta + \phi)}{N \cos(\theta' + \phi)} \right] \end{aligned} \right\} \quad (36)$$

where

$$\left. \begin{aligned} \cos(\theta' + \phi) &= \sqrt{1 - \frac{\sin^2(\theta + \phi)}{N^2}}, \\ \text{and} \quad \sin^2(\theta + \phi) &= \frac{y^2 + (x \cos \phi - z_2 \sin \phi)^2}{x^2 + y^2 + z_2^2} \end{aligned} \right\} \quad (37)$$

Since we are not concerned with a constant increase or decrease in path length, we adjust the optical path differences to zero at the axis by subtracting  $(N^2 - 1)/(N^2 - \sin^2 \phi)^{1/2}$ . The resulting expression for the optical-path difference is

$$OPD = \frac{t}{\lambda} (N^2 - 1) \left\{ \left[ N^2 - \sin^2(\theta + \phi) \right]^{-1/2} - \left[ N^2 - \sin^2 \phi \right]^{-1/2} \right\}. \quad (38)$$

The above expression for OPD may be used as an exact point-by-point correction to the wavefront or may be curve-fitted to the polynomial containing the various aberration terms. Using the polynomial of table 1(a), the terms were computed for a cube with  $t = 13$  mm and  $N = 1.46008$  (fused silica at  $\lambda = 546.1$  nm). The aberrations introduced by the cube are shown in figures 10 through 12 for a range of test-lens f-numbers. These primary aberrations include defocus, spherical aberration, coma, and  $0^\circ$  astigmatism. Other aberrations, including higher orders of spherical, astigmatism, and coma, are not significant for the given f-numbers and angles. These angular values represent the angle between the test-system optical axis and the normal to the entrance face of the cube.

If the cube is normal to the optical axis, only the symmetric aberrations, defocus and third-order spherical, are significant. Third-order spherical aberration becomes significant (greater than  $0.1 \lambda$ ) when testing systems with f-numbers below f/8. However, defocus is relatively large for most optical systems of interest. The defocus introduced by the cube can be compensated during testing if the recommended test procedure discussed in section XI.3 is followed. This procedure requires that the null-fringe position be located by moving the cube until an infinitely-wide dark or light fringe covers the entire test aperture; at this position, the lateral shear  $l\phi$  is zero. The cube is then moved away from the null-fringe position to the  $l$  setting calculated to produce a desirable number of fringes. If the shear distance  $l\phi + z_2\phi$  used in scanning the interferograms is based on this  $l$  setting, then any resulting defocus in the focal plane at  $z_2$  is due entirely to the lens. If this test procedure is not used, then the data-reduction computer program may be triggered to correct for the defocus introduced by the cube. (See appendix A.) Corrections for third, fifth, and seventh order spherical aberration are automatically made in the computer program. In the present version of the program, the value for the index of refraction  $N$  of the cube is 1.46008 (fused silica at  $\lambda = 546.1$  nm). For testing lenses at a wavelength other than 546.1 nm, there will be a very slight error in the corrections for aberrations since  $N$  varies slightly with wavelength.

If the entrance face of the cube is not normal to the optical axis during the lens test, the asymmetrical aberrations of coma and  $0^\circ$  astigmatism may significantly affect the test results. Figure 11 shows that coma can be as large as  $0.1 \lambda$  for testing an f/5.6 lens whenever the angle between the normal to the cube face and the test-system optical axis is from  $1^\circ$  to  $2^\circ$ . Whereas, figure 12 shows that the  $0^\circ$

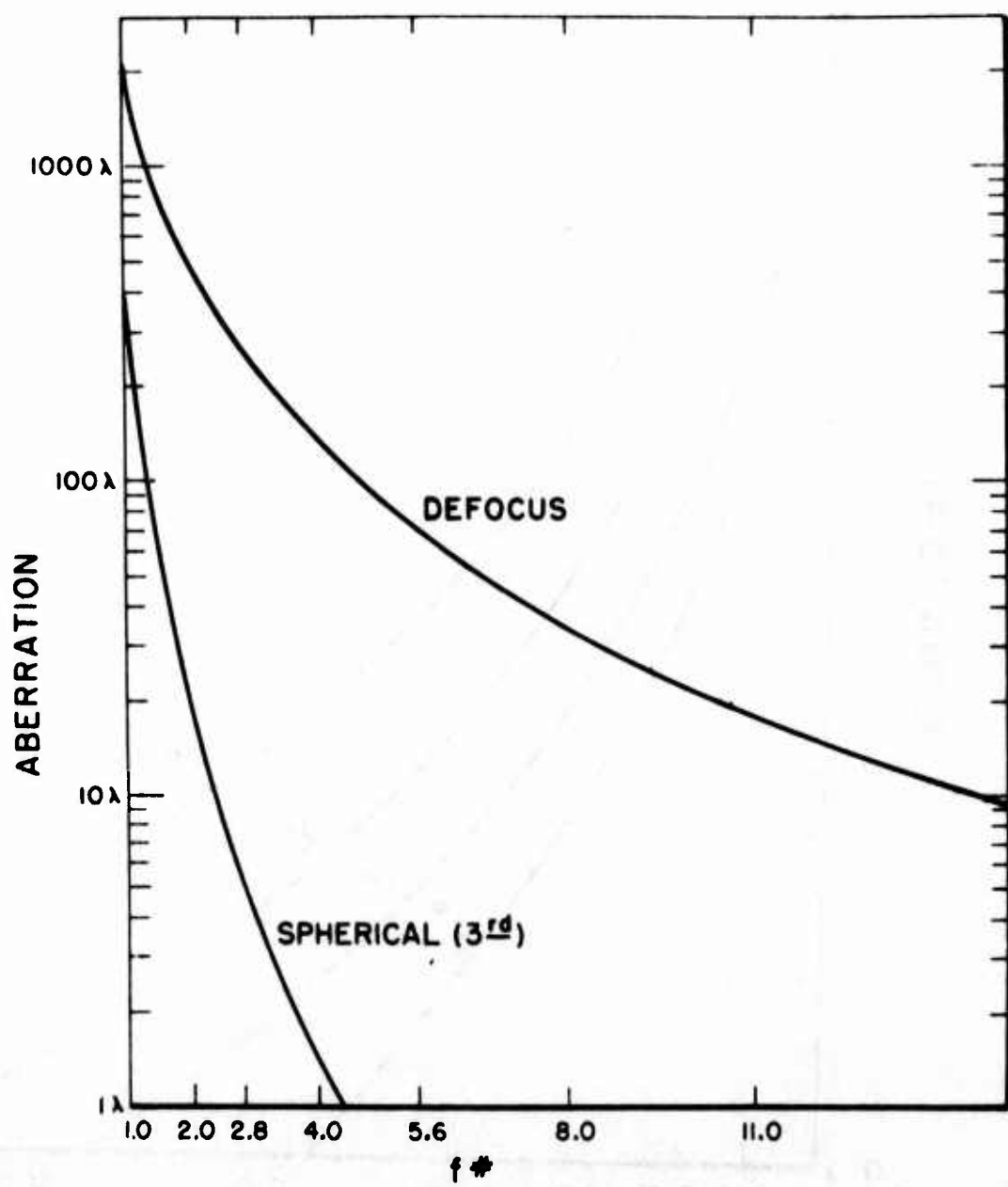


Figure 10.- Maximum values of defocus and third-order spherical aberration introduced by 13-mm-thick WSI cube;  $\lambda = 546.1$  nm.

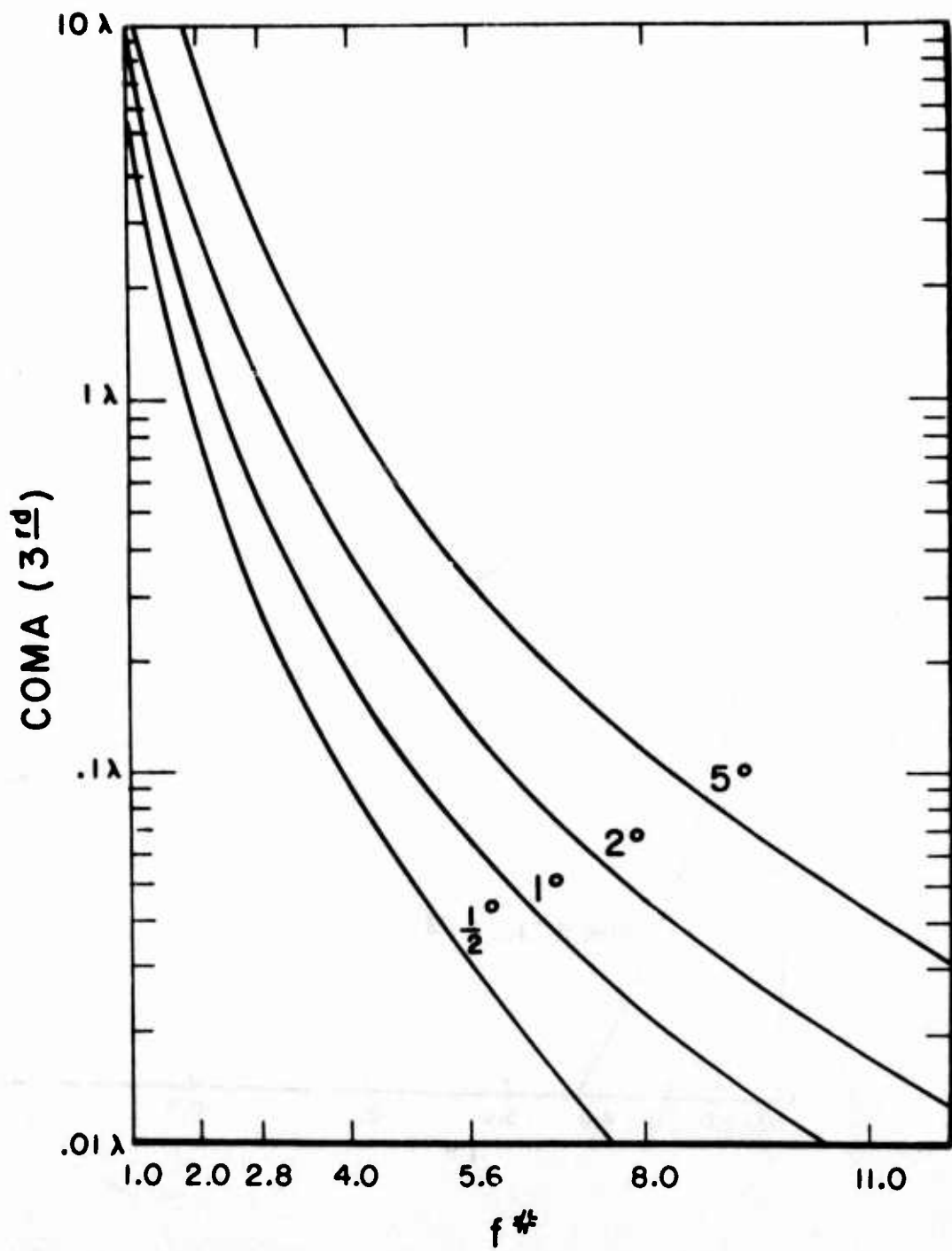


Figure 11.- Maximum values of third-order coma introduced by 13-mm-thick WSI cube for given angles of incidence  $\theta + \phi$ ;  $\lambda = 546.1$  nm.

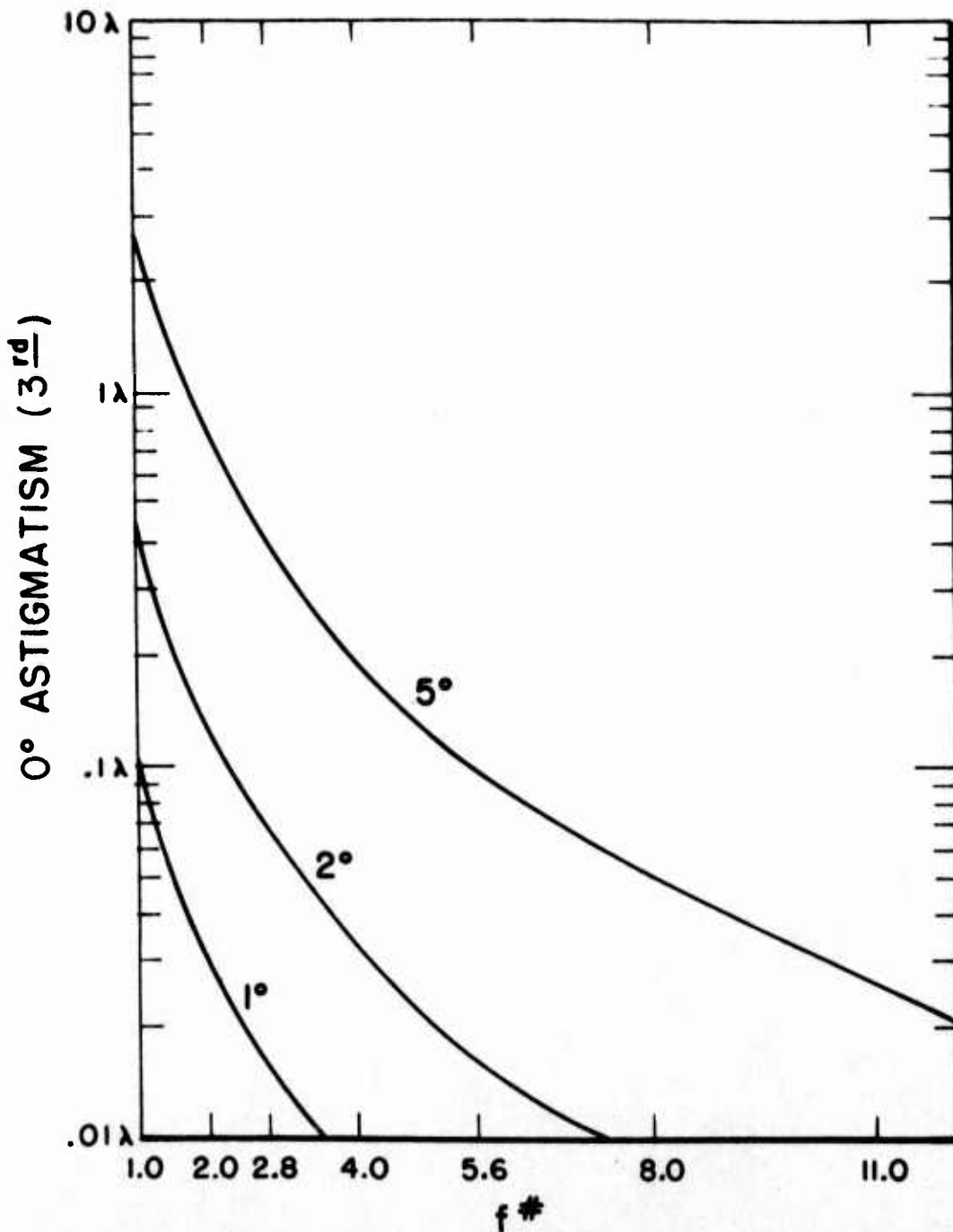


Figure 12.- Maximum values of third-order  $0^\circ$  astigmatism introduced by 13-mm-thick WSI cube for given angles of incidence  $\theta + \phi$  ;  $\lambda = 546.1$  nm.

astigmatism introduced by this cube misalignment would not be more than about  $0.015 \lambda$  for testing the f/5.6 lens. Corrections for these asymmetrical aberrations are not included in the computer program. Their magnitude would depend on a measurement of the cube misalignment, and the cube could just as well be aligned during the measurement procedure. A simple technique for aligning the cube is described in section XI.3; this approach permits cube alignment to within 30 seconds which is sufficiently small to eliminate asymmetrical aberrations greater than about  $0.01 \lambda$  for most lens systems.

Other cube properties such as glass homogeneity and surface flatness may also introduce aberrations. These possible sources of error in the test data are discussed in section VIII.1.

## VII. AUXILIARY LENS

The lens that relays the interferogram onto the film plane is operating in a coherent mode and has its own pupil function; therefore it is essential to know its effect on the measured fringe displacements. It is preferable to use this relay lens as a collimator placed a focal length away from the focus of the test lens. The interference pattern will then be a plane wavefront, and distortion will not be introduced for low f numbers.

In coherent systems, the complex amplitude distribution is propagated through the system, and the squared modulus of the result yields the intensity distribution at the film plane. In the present case, the complex amplitude distribution in one dimension (corresponding to the direction of shear) is the sum of the two sheared wavefronts at the exit pupil of the test lens and is given by

$$\exp\left(\frac{ikx^2}{2z_2}\right) \left\{ \varphi(x) + \varphi(x - l\phi - z_2\phi) \exp\left[-ik(l\phi x - l^2\phi^2/2)/z_2\right] \right\} \quad (38)$$

where the first exponential term represents the reference sphere and  $\varphi(x)$  is the pupil function of the test lens as given by equation (1). If we let the expression in braces in equation (38) be denoted by  $D(x)$ , the squared modulus of  $D(x)$  yields the interference pattern (in one dimension) of equation (3). Propagating the above distribution to the film plane yields an intensity distribution given by

$$I(w) = \left| K \int D(x) \exp\left(\frac{ikx^2}{2z_2}\right) \exp\left[-\frac{ik(u-x)^2}{2(z_2+f)}\right] G(u) \exp\left(\frac{iku^2}{2f}\right) \times \exp\left[-\frac{ik(w-u)^2}{2S}\right] dx du \right|^2 \quad (39)$$

where the coordinates and parameters are shown in figure 13, K is a constant, and  $G(u)$  is the pupil function of the auxiliary lens of focal length  $f$ . After simplifying,

$$I(w) = \left| K \int \left( \int D(x) \exp\left\{ ik \left[ \frac{x^2}{2} \left( \frac{1}{z_2} - \frac{1}{z_2+f} \right) + \frac{ux}{z_2+f} \right] \right\} dx \right) G(u) \times \exp\left\{ ik \left[ \frac{u^2}{2} \left( \frac{1}{f} - \frac{1}{z_2+f} - \frac{1}{S} \right) + \frac{uw}{S} \right] \right\} du \exp\left(-\frac{ikw^2}{2S}\right) \right|^2. \quad (40)$$

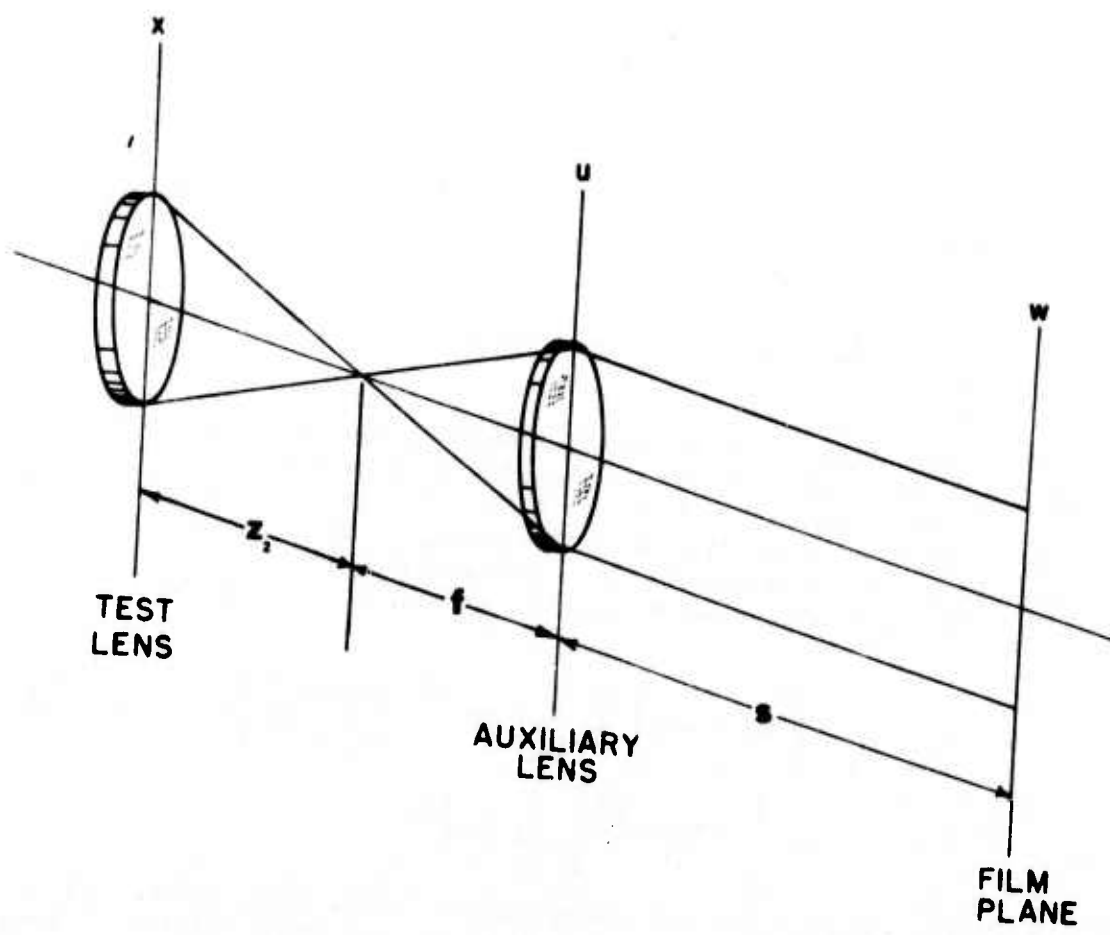


Figure 13.. Parameters and coordinates for computation of effects  
of auxiliary lens on WSI fringe pattern.

Since  $D(x)$  is slowly varying compared to the exponential in the  $x$  integral, the Fresnel Integral may be solved by the method of stationary phase [26]. After  $x$  integration by this method,

$$I(w) = \left| K' \int D\left(-\frac{uz_2}{f}\right) G(u) \exp\left[ik\left(-\frac{u^2}{2S} + \frac{uw}{S}\right)\right] du \exp\left(-\frac{ikw^2}{2S}\right) \right|^2. \quad (41)$$

The remaining  $u$  integral may be solved in the same manner yielding

$$I(w) = K'' \left| D\left(-\frac{wz_2}{f}\right) G(u) \right|^2. \quad (42)$$

For an auxiliary lens of uniform amplitude transmittance, the modulus squared of  $G(u)$  is a constant, and we are left with  $|D[-(wz_2)/f]|^2$ , which is the desired interferogram inverted and scaled by the ratio of  $z_2/f$ . Hence, the aberrations of the auxiliary lens, other than distortion, do not effect the measurement of fringe locations.

## VIII. ERROR ANALYSIS

### VIII.1. Cube Quality and Alignment

The quality of the glass prisms used in fabricating the WSI cubes should be of interferometric quality and thereby, reasonably free of bubbles, inclusions, and other scattering centers. (See appendix E.) Scattered light will reduce fringe contrast, and these scatterers can also appear on the final interferograms. Such patterns can result in fringe-location errors, particularly if coherent illumination is used for testing. In this respect, it is also important to keep the entrance and exit faces of the cube clean. Furthermore, the index of refraction should remain constant throughout the glass. Otherwise, the optical paths for the two beams traversing the WSI may differ and lead to a size difference in the two overlapping sheared images. The data interpretation requires that the two sheared images represent the identical wavefront scaled to the same size. The flatness requirements ( $\lambda/10$  or better for 546.1 nm) on all prism surfaces used to transmit or reflect light are necessary to limit wavefront errors which could not feasibly be separated from those of the test-lens. The assembled cube can be inspected for residual aberrations by techniques discussed in appendix E.

There are additional aberrations such as defocus, spherical aberration, and coma, introduced by the cube and discussed previously in section VI.2. These aberrations, in contrast to the material and surface errors in the cube, can be calculated and removed from the test data. It should be noted that for testing high-quality lenses (aberrations less than  $1\lambda$ ) with f-numbers below about f/2, the defocus and spherical aberration become relatively large (greater than  $100\lambda$ ), and the resulting test data would be highly suspect. It is, therefore, generally recommended that the WSI not be used to test optical systems with f-numbers much below about f/2.

The WSI cube should be positioned in the test system so that the cube entrance face is perpendicular to the test-system optical axis. Provided that the test lens is aligned with its optical axis along the test-system optical axis, the cube entrance face is also perpendicular to the test-lens optical axis. In this arrangement, no asymmetrical aberrations will be introduced by the cube. The effect of cube misalignment is discussed previously in section VI.2. As noted in that discussion, it should be just as easy to align the cube to within a few degrees as it is to measure the misalignment which is required if a correction is to be applied to the wavefront. The only requirement for the lateral position of the cube face in a plane perpendicular to the test-system optical axis is to avoid clipping, or vignetting, of the fringe pattern; no differences in fringe patterns should be observed for different lateral positions of the cube provided that the cube glass is homogeneous.

## VIII.2. Experimental

There are several possible sources of error in the experimental set up. Those sources found to be important as a result of testing several lenses include lens alignment, method used to obtain the second or y-sheared interferogram, experimental parameters required as input data for computer reduction of test data, and use of an auxiliary lens to photograph fringe patterns.

A test-system optical axis must first be established for testing lenses with the WSI. Alignment of the test lens along this test-system is required to a high degree of accuracy in order to obtain repeatable measurements of the OTF to within a few percent. This requirement is particularly important when testing multi-element lenses or collimators with a relatively narrow field of view. As an example, repeated tests with an f/8.7 collimator realigned in a nodal slide that could not be accurately positioned showed a variation of up to  $0.15 \lambda$  in the asymmetric aberrations, such as astigmatism. An improved nodal slide resulted in a reproducibility of less than  $0.05 \lambda$  in the wavefront. This level of precision was obtained even though the lens was realigned for the y-sheared interferogram. The method used to align the test lens is discussed in section XI.3.

The original approach to obtaining the second or y-sheared interferogram was to rotate the test lens  $90^\circ$ . The nodal slide used for mounting the test lens did not maintain the initial lens alignment as the lens was rotated  $90^\circ$ . Therefore, the lens had to be realigned after the  $90^\circ$  rotation. Successive tests in which the lens was realigned showed non-repeatable values for astigmatism. The realignment of the lens at the  $90^\circ$  setting most likely displaced the lens along the optical axis and, therefore, introduced astigmatism. As a result, a fixture which rotates the relay lens, film plane, and cube as a fixed unit about the optical axis has been built and is used for current lens testing; a photograph of this fixture is shown in figure 14. This fixture maintains the cube at a fixed location along the optical axis during rotation. Furthermore, the ball-pivot assembly for holding the cube permits the cube to be angularly realigned, with essentially no linear displacement, in order to maintain the cube entrance face normal to the optical axis for both the  $0^\circ$  and  $90^\circ$  settings. It is not required that the axis of rotation for this fixture be coincident with the test-system optical axis; as noted earlier, a lateral movement of the cube during rotation should not alter the fringe pattern if the cube material is homogeneous. The effect of an angular error in the  $90^\circ$  setting of the fixture has not been determined; however, for high-quality optics with pupil functions that change very little across the aperture, an error of a few degrees would probably have an insignificant effect on the test results. This fixture also keeps the film plane at the same distance from the test lens for the  $0^\circ$  and  $90^\circ$  settings, thereby reducing any magnification changes in the x and y-sheared interferograms.

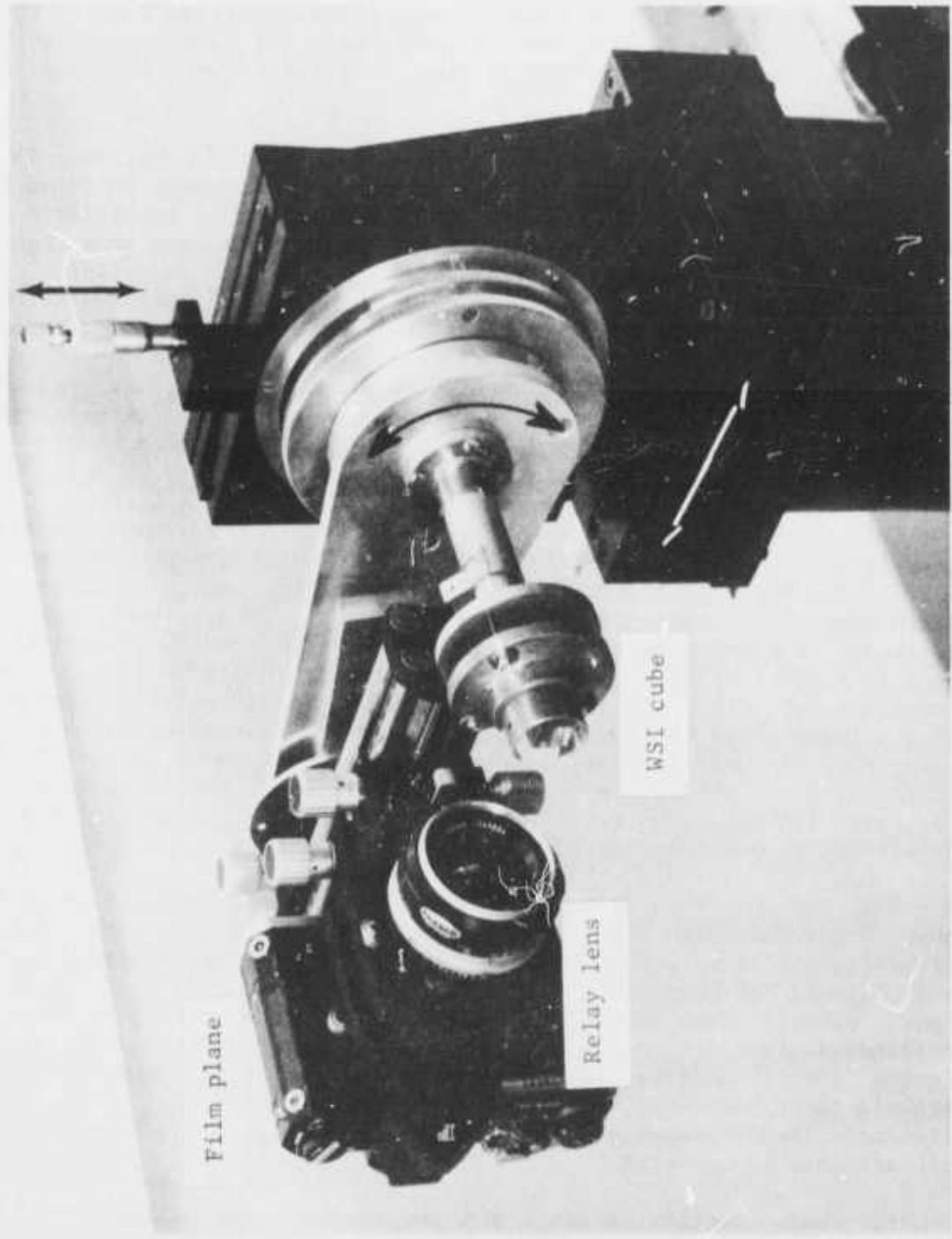


Figure 14.- Photograph of fixture for rotating WSI cube, relay lens, and film plane.

The experimental parameters that are used as input values in the reduction of the interferogram data are the cube shear angle  $\phi$ , cube thickness  $t$ , radiation wavelength  $\lambda$ , and the sum of  $l + z_2$ . The shear angle  $\phi$  must be known accurately since an error in this parameter will generate an error in the calculated shear distance  $\phi(l+z_2)$  and, subsequently, in the scanned fringe positions. The cube shear angle can be measured to within  $\pm 0.05$  mrad using the techniques described in appendix E.

The cube thickness should be known to within  $\pm 0.1$  mm. This thickness is used to calculate the symmetric aberrations introduced by the cube as discussed in section VI.2. For testing lenses with f-numbers approaching  $f/2$ , these aberrations are significant and, therefore, an error in cube thickness should be more important. For example, an error in cube thickness of 0.1 mm for a  $f/2.8$  test lens would give errors of about  $2\lambda$  of defocus and about  $0.04\lambda$  of third-order spherical aberration in the aberrations removed from the fringe pattern during data reduction. Considering that the defocus introduced by the cube can be compensated by the experimental procedure described in section VI.2, the remaining error would be about  $0.04\lambda$ .

The value of the radiation wavelength used to illuminate the test lens is used throughout the data-reduction computer program such as in solving the basic equations for the pupil function and the aberrations introduced by the cube. (See equations (9) and (37), respectively.) Although an assessment of errors in the wavelength value has not been made it appears that the result of such an error would be to alter the magnitude of the pupil-function values and the OTF values. Provided that a laser or an arc source with a filter of measured or known mean wavelength is used as a light source, the wavelength value should not be a source of error. Also, any filters used should produce a spectral transmission function which is symmetrical about the mean wavelength in order not to distort the cosine fringes.

The sum of  $l + z_2$  is measured directly from the test set up after positioning the cube at the axial position that will give the number of fringes desired for scanning. (See figure 4.) The distance  $z_2$  is the distance from the second principal plane of the test lens to the focal plane. For testing a lens at infinite conjugates with a collimated light source,  $z_2$  is equivalent to the effective focal length (EFL); however, when testing at finite conjugates with a pinhole light source situated at a distance less than the hyperfocal distance (about twenty or more times the EFL),  $z_2$  is not equal to the EFL and must be measured.

For both testing modes, the second principal plane should be physically located using a nodal slide; thus, the total distance  $l + z_2$  could be determined by measuring from this plane to the backface

of the cube. However, for infinite-conjugate testing, the EFL furnished by the lens manufacturer could be used for  $z_2$ ; if this value is incorrect, there will be an error associated with the pupil function as discussed below. In either case if the defocus introduced by the cube is to be eliminated experimentally, a separate measurement of  $l$  is required to position the cube to give the desired number of fringes.

The refractive effect of the cube will lead to a slight error in the measured value of the sum  $l + z_2$  since this value should be measured totally in air. Consequently, there will be a slight error in the calculated shear distance ( $\Delta X = \phi(l+z_2)$ ) used for sampling fringe data from the interferograms and an error in the resulting pupil function. For most lenses, the shear-distance error would be typically less than a few percent; furthermore, most pupil functions are not rapidly varying over the shear distance, so the effect on the calculated pupil function and OTF will be small.

### VIII.3. Interferogram Quality, Scanning, and Registration

The errors introduced by the quality of the interferogram are somewhat dependent on the mode of scanning and data reduction used. For any scanning method, a serious attempt should be made to produce interferograms which have density variations approaching a cosine distribution across the light or dark fringes, uniform density values along the fringe peaks, absence of spurious fringe patterns, and are relatively free of pinholes and other film defects. Some of these factors can be controlled in the experimental set up, and others during film processing.

Spurious fringe patterns can be largely avoided by not using a laser for a test light source. As discussed earlier, the WSI cubes are adjusted for chromatic compensation, and, therefore, a filtered white-light source can be used. If a laser is used, special care must be taken to clean all optical surfaces in the test system in order to eliminate diffraction patterns arising from scattering centers. The light source should also illuminate the test lens uniformly so that there will not be a significant variation in film density along a fringe peak.

It should be noted that although the WSI is relatively insensitive to mechanical vibrations and thermal drifts, these effects can still affect the interferogram quality. For a test lens with a relatively long  $z_2$  value, mechanical vibrations and thermal drifts near the test lens can result in a vibrating or changing interference pattern. If the vibration or thermal sources cannot be eliminated, then short exposure times, depending on the frequency of the disturbance, may help to reduce the problem.

If both light and dark fringes exhibit a flat density distribution across the peak and valley, the interferogram should be discarded, and the interference pattern should be rephotographed. These flat density distributions can result from the improper combination of film and exposure times or in the processing used to make the enlargements for scanning. However, for interferograms in which only the light, or the dark, fringes exhibit finesse, these fringes can be scanned.

There are two types of errors which are dependent on the number of fringes in the interferogram rather than the interferogram quality. The first of these errors may be called the reading error RE and defined as the scanner reading error  $\epsilon$  divided by the fringe spacing  $\Delta F$  in the interferogram, viz,

$$RE = \frac{\epsilon}{\Delta F} . \quad (43)$$

For a given interferogram, we can write the fringe spacing  $\Delta F$  as the test-lens aperture diameter D (on the interferogram) divided by the number of fringes M, viz,

$$WF = \frac{D}{M} . \quad (44)$$

Substituting equation (44) into equation (43), we obtain

$$RE = \frac{\epsilon M}{D} . \quad (45)$$

For the manual scanner (Grant comparator),  $\epsilon = 0.005$  mm,  $D = 50$  mm, and typically  $M = 25$ ; thus,  $RE = 0.0025$  (units of wavelength). For the automatic scanner (Photoscan P-1000),  $\epsilon = 0.050$  mm,  $D = 100$  mm, and typically  $M = 25$ ; thus,  $RE = 0.0125$  (units of wavelength).

The other error which is dependent on the number of fringes in the interferogram is the fringe interpolation error. As discussed in section 4, fringe-order values must be interpolated at coordinates on a grid in order to determine the pupil function. The interpolation approach used in the data-reduction computer program is based on a spline fit. For a lens which has a maximum wavefront error of  $2\lambda$  spherical aberration and a WSI interferogram with 22 fringes, the interpolation error is less than  $0.001\lambda$ . Although this error is much smaller than the reading error discussed previously, it should be remembered that the interpolation error for the spline fit will depend on the type and magnitude of errors in the test lens and the number of fringes in the interferogram.

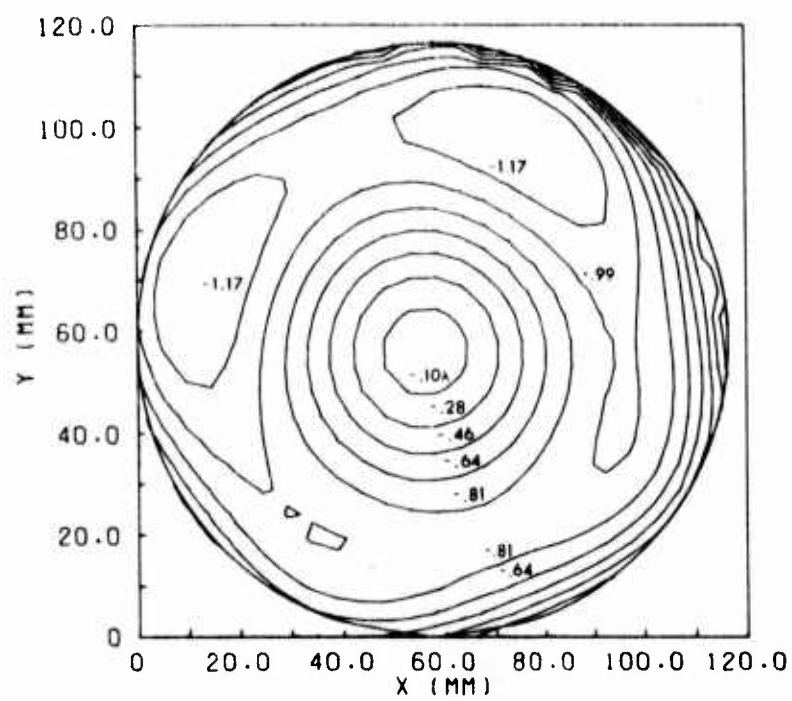
The scanning errors are, of course, directly dependent on the type of facility used for interferogram scanning. The two basic methods of scanning are manual and automatic. The manual approach usually relies on a visual judgment of fringe-peak location, whereas the automatic approach provides film-density data that can be processed to determine fringe-peak locations. The scanner properties which bear directly on the quality of the resulting data are resolution, accuracy, reproducibility, and linearity. Since these properties vary widely depending on the particular scanner and a general discussion of their effects would be lengthy, it is not appropriate to include an analysis in this report. The positional accuracy of placing the interferogram in the scanner is also important, particularly since the data from two WSI interferograms must eventually be registered. This registration is discussed in appendix D, and the possible errors from registration are discussed in the present section.

In order to determine possible differences in fringe data from the automatic scanner (Photoscan P-1000) and the manual scanner (Grant comparator) used in the present tests, interferograms of the same test lens were scanned on each instrument. Since the size of the interferograms used for the two scanning systems is different, two pairs of enlargements were prepared from the original interferogram. The resulting fringe-peak data from both scanners were scaled to the actual lens coordinate system by using the appropriate magnification. The magnification for each pair of interferograms was determined by using an optical comparator to measure a scale appearing in the interferogram; the scale was located near the test-lens exit pupil and was photographed along with fringe pattern. The scaled fringe data from the two scanners were plotted, and these plots were superimposed to provide a direct comparison. These fringe patterns showed a two percent difference in magnification. An alternate approach to determine the magnification of each interferogram pair is to use a microdensitometer to trace the scale in the interferograms; this approach showed that the magnification difference can be reduced to about 1 percent. In any event, a quantitative comparison of fringe locations is not possible without scaling both sets of fringe data to exactly the same size lens aperture. The comparison did show, however, that the measured magnification can be a source of error in the comparison of fringe data obtained on different instruments that require different size interferograms. For this reason, both sets of fringe data were reduced, and the results are shown in figure 15 and table 3.

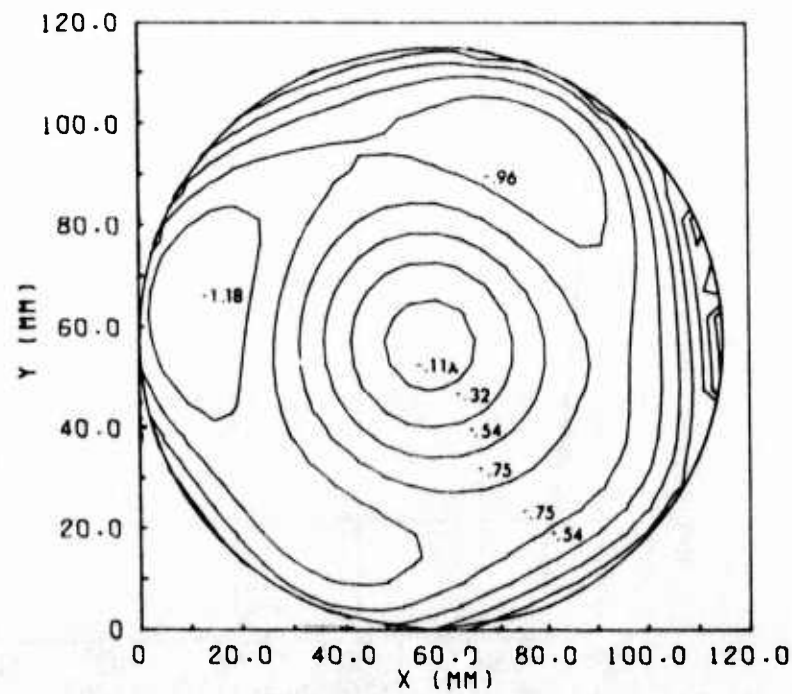
The data shown in figure 15 are for an f/8.7 collimator in the plane of best focus. Figures 15(a), 15(c), and 15(e) are data reduced from interferograms scanned on the automatic scanner, and figures 15(b), 15(d), and 15(f) are data reduced from interferograms scanned on the manual scanner. A comparison of the aperture diameters in figures 15(a) and 15(b) shows the 1-percent difference in the magnification used to scale each set of fringe data. A comparison of the isocontours for the pupil functions in these two figures shows that these distributions appear essentially the same. The root mean square (RMS) of the difference of these two wavefronts normalized to the same coordinate system was calculated to be  $0.12 \lambda$ . This difference is probably due primarily to registration errors, particularly in the data from the automatic scanner. The improved registration technique discussed in appendix D should eliminate some of these errors.

A comparison of figures 15(c) and 15(d) shows only minor differences in the MTF values resulting from the two sets of scanner data. A comparison of figures 15(e) and 15(f), however, shows large differences in the PTF values. The accuracy of these PTF values for the upper spatial frequencies is not very high. The PTF is defined as the arctangent of the ratio of the imaginary and real parts of the OTF. As discussed in section V.1, the method used to compute the OTF was found to have superior accuracy even for highly aberrated lenses, i.e., lenses with a rapidly varying pupil-function phase. However, at the higher spatial frequencies, the computational accuracy is reduced since fewer points lie within the region of integration. (See equation (20).) Moreover, for highly aberrated lenses such as the collimator discussed in figure 15, the real and imaginary parts of the OTF are very small and fluctuate in sign starting at the mid-range spatial frequencies. Therefore, the calculation of the PTF involves the ratio of very small and rapidly changing values, and the resultant PTF exhibits large and rapid changes in both magnitude and sign as shown in figures 15(e) and 15(f).

A comparison of the maximum aberration values for the manual and automatic scanning in table 3 show that differences between the same type of asymmetric aberrations are less than about  $0.05 \lambda$  for most of these terms. Only third-order y coma and third-order  $45^\circ$  astigmatism show differences much greater than  $0.1 \lambda$ . As noted earlier, part of the difference in the two wavefronts is probably due to registration errors. Such errors could result in differences in the  $45^\circ$ -astigmatism term. (See section X.1.) Although there are large differences between the same type of symmetrical aberration for the manual and automatic-scanner data, the difference in the net sums of these symmetrical aberrations is only  $0.04 \lambda$ . Therefore, the differences in the aberration terms resulting from the two sets of

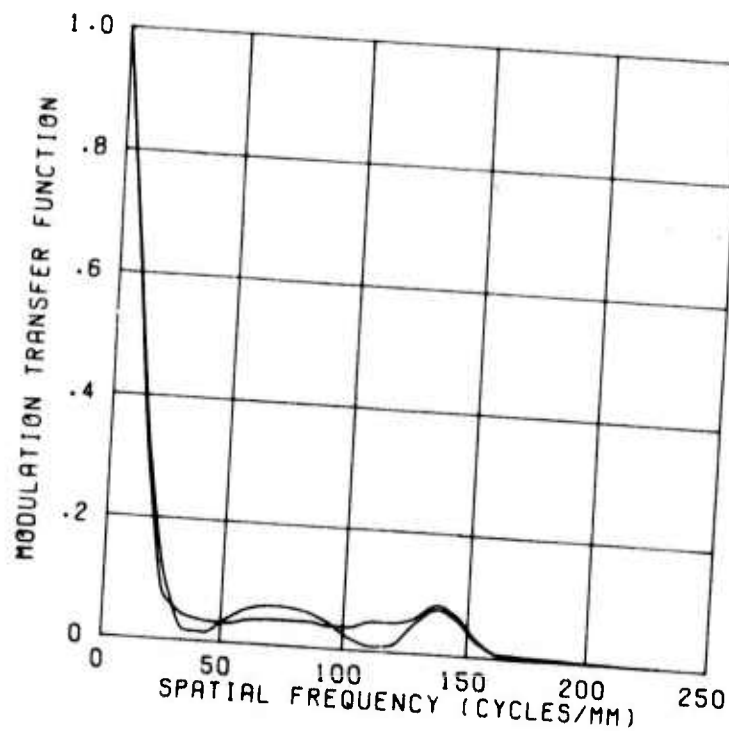


(a) Pupil-function phase; automatic scanner.

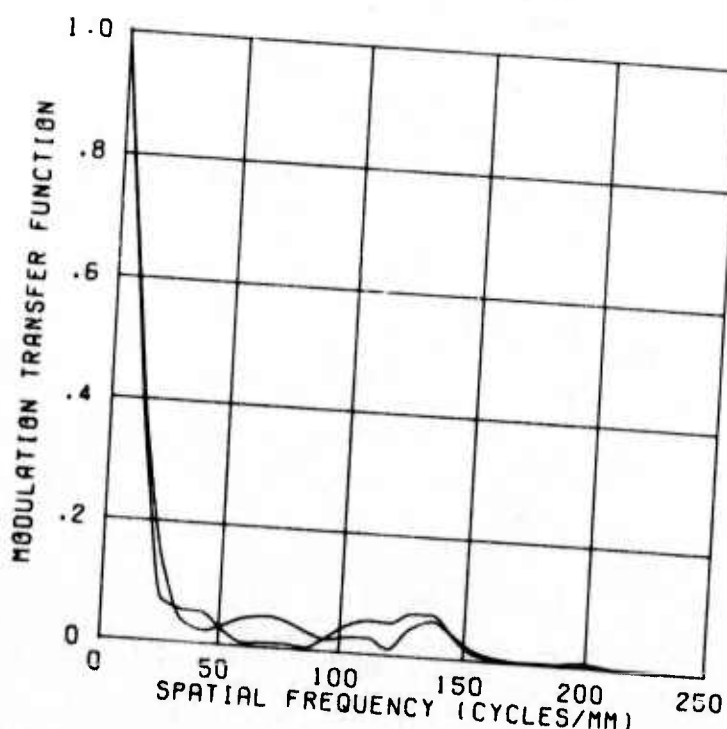


(b) Pupil-function phase; manual scanner.

**Figure 15.- Comparison of test results for fringe data obtained from automatic and manual scanning of same pair of WSI interferograms; f/8.7 collimator and  $\lambda = 546.1$  nm.**

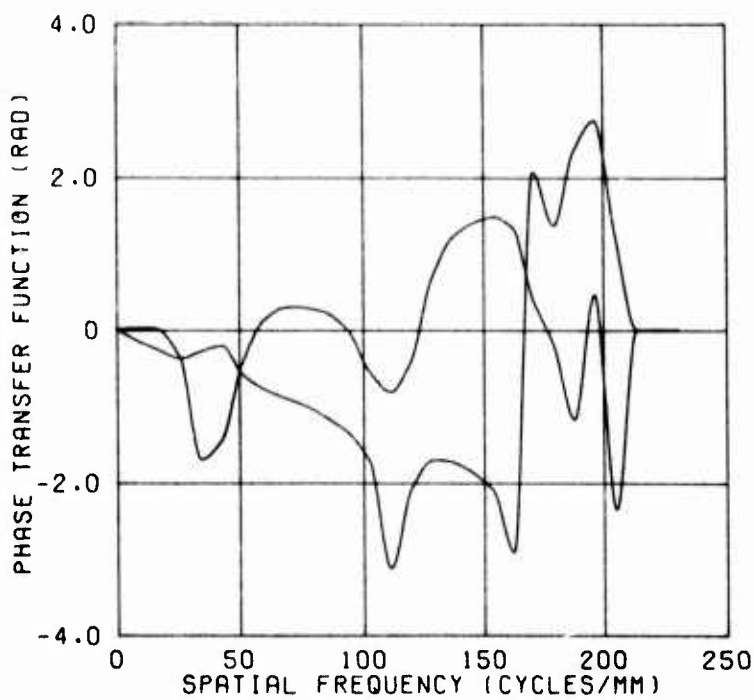


(c) MTF; automatic scanner.

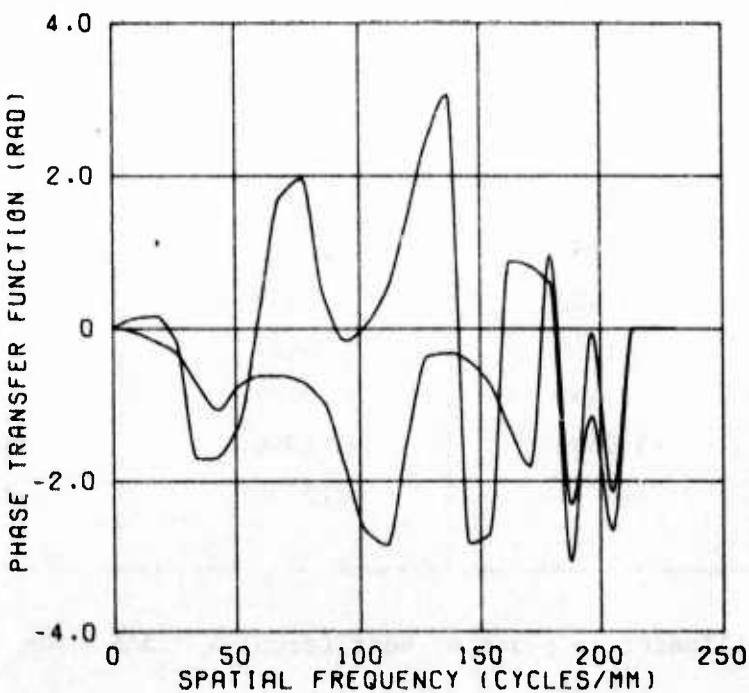


(d) MTF; manual scanner.

Figure 15.- Continued.



(e) PTF; automatic scanner.



(f) PTF; manual scanner.

Figure 15.- Concluded.

TABLE 3. - COMPARISON OF MAXIMUM ABERRATIONS RESULTING FROM  
SCANNING SAME PAIR OF WSI INTERFEROGRAMS WITH  
MANUAL AND AUTOMATIC SCANNERS<sup>a</sup>

n	Maximum aberrations, units of $\lambda$		Type
	Manual	Automatic	
4	-4.821	-5.250	focus
5	- .1062	- .1314	0° astigmatism
6	.2080	- .0461	45° astigmatism
7	.6441	.1573	x coma (3rd)
8	- .3685	- .6316	y coma (3rd)
9	.2209	.1750	x clover (3rd)
10	- .1603	- .0934	y clover (3rd)
11	7.1699	8.3341	3rd spherical
12	.1365	.1378	0° astigmatism (5th)
13	.1297	- .0020	45° astigmatism (5th)
14	.0336	.0101	
15	.2568	.2698	
16	- .1396	.0503	x coma (5th)
17	.3120	.3054	y coma (5th)
18	- .0188	- .0727	x clover (5th)
19	.1405	.1033	y clover (5th)
20	.1164	.0821	
21	.0155	.0192	
22	-3.8634	-5.5946	5th spherical
23	1.4013	2.3383	7th spherical

<sup>a</sup> f/8.7 collimator in plane of best focus;  $\lambda = 546.1$  nm.

scanning data are significant only for the asymmetric terms. It should be noted that differences in a given aberration term for two or more sets of data from different scanners or repeated scans on the same scanner should not always be considered at face value. Even for data from different lenses, the comparison of the same aberration term may be misleading. The polynomial solution for the wavefront is sensitive to random fluctuations in the fringe data, particularly for the higher order terms. Random errors in the fringe-peak positions can result from the scanner and noise in the interferogram.

Repeated scans of interferograms for an f/8.7 collimator were made on the manual scanner in order to determine an over-all RMS value for the scanning process. Resulting aberration values and RMS values for the plane of best focus are given in table 4 for each of the three repeat scannings. Except for the various orders of spherical aberration, focus defect, and y-coma (third and fifth order), the aberration values for the different scans do not differ by more than about  $0.05 \lambda$ . The least-squares fitting of the data to the 23-term polynomial is far more sensitive to the higher-order terms, such as the fifth and seventh-order spherical aberrations; thus, their greater variation for small differences in input fringe data is expected. Furthermore, it is important to look at the net result of adding the focus defect and spherical-aberration terms since this total or residual is more representative of the overall wavefront deviations. Therefore, a comparison of the residual values of these symmetric aberrations as given in table 4(b) shows that the differences between repeated scans is about  $0.01 \lambda$ ; thus, the aberrations in this test lens are primarily coma. A comparison of the RMS of the wavefront for the plane of best focus in table 4(b) shows that these values do not differ by more than  $0.01 \lambda$ . A better indication of the RMS for the scanning process than either the RMS of the wavefront or aberrations [27] is shown in table 4(c). This table gives the RMS of the difference of two wavefronts from the repeat scannings. These values indicate that the repeatability for scanning process on the manual scanner is about  $0.02 \lambda$ . A similar test is planned for the automatic scanner.

As discussed in appendix D, the proper registration of two WSI interferograms requires that each interferogram be scanned parallel to the shear axis. Provided that this axis has been located and marked accurately on each interferogram, the interferogram should be placed in the scanner so that scan axis is parallel to the shear axis. An approach for accomplishing the proper orientation of the interferogram in a scanner is described in appendix D. A modification to the computer software for reducing the data from the automatic scanner could be made to include this approach; the modification would probably be a correction to the fringe-peak data based on the angular tilt of the interferogram. The primary aberration introduced by an

TABLE 4. - COMPARISON OF MAXIMUM ABERRATIONS, RMS VALUES, AND RESIDUAL SYMMETRIC ABERRATIONS RESULTING FROM THREE SCANS OF SAME PAIR OF WSI INTERFEROGRAMS<sup>a</sup>

(a) MAXIMUM ABERRATIONS

n	Maximum aberrations, units of $\lambda$			Type
	Scan 1	Scan 2	Scan 3	
4	-.395	-.495	-.470	
5	.0391	.0357	.0426	focus
6	.0091	.0119	-.0533	0° astigmatism
7	.1796	.1796	.1479	45° astigmatism
8	.0463	.0858	.0952	x coma (3rd)
9	.0463	.0642	.0778	y coma (3rd)
10	.0111	.0241	.0316	x clover (3rd)
11	.9927	1.6469	1.4857	y clover (3rd)
12	-.0304	-.0028	-.0024	3rd spherical
13	.0328	.0373	.0387	0° astigmatism (5th)
14	-.0265	-.0202	-.0230	45° astigmatism (5th)
15	-.0526	-.0050	.0019	
16	-.1372	-.1800	-.1679	x coma (5th)
17	-.1907	-.0424	-.0474	y coma (5th)
18	-.0658	-.0590	-.0655	x clover (5th)
19	-.0877	-.0728	-.0840	y clover (5th)
20	-.0053	-.0057	-.0057	
21	-.0165	.0150	.0156	
22	-1.2698	-2.3947	-2.1077	5th spherical
23	.6658	1.2664	1.1085	7th spherical

<sup>a</sup>f/8.7 collimator in plane of best focus;  $\lambda = 632.8 \text{ nm}$ .

TABLE 4. - CONCLUDED

## (b) RMS VALUES AND RESIDUAL SYMMETRIC ABERRATIONS

	Scan 1	Scan 2	Scan 3
RMS	$\lambda/20.625$	$\lambda/25.754$	$\lambda/24.547$
Residual symmetric aberrations <sup>a</sup>	-.006 $\lambda$	-.019 $\lambda$	.017 $\lambda$

<sup>a</sup>  $b_4 F_4 + b_{11} F_{11} + b_{22} F_{22} + b_{23} F_{23}$  where  $b_n F_n$  is the nth aberration.

## (c) RMS OF DIFFERENCE OF TWO WAVEFRONTS

	Scan 1 and Scan 2	Scan 2 and Scan 3	Scan 1 and Scan 3
RMS	.017 $\lambda$	.013 $\lambda$	.023 $\lambda$

angular error in one or both of the interferograms during scanning is  $45^\circ$  astigmatism. For example, a rotational difference of about  $1^\circ$  in the scanning orientation of the two interferograms could introduce about  $0.2 \lambda$  of third-order  $45^\circ$  astigmatism.

In addition to defining the shear direction on an interferogram, a fiducial system must differentiate between the x and y-sheared interferograms and must show the positive or negative directions for a coordinate system common to both interferograms. The registration discussed in appendix D includes both these requirements. The magnitude of errors that would result from improper interferogram identification or improper scanning direction have not been determined. Their values would depend, to a large extent, on the differences in the two interferograms, i.e., whether the test lens has significant asymmetrical aberrations.

## IX. AUTOMATIC SCANNER

### IX.1 Description

A high-speed digital microdensitometer (Photoscan P-1000; Optronics International Inc. [15]) was used for automatic scanning of the WSI interferograms. This scanner incorporates an electro-optical rotating drum which converts photometric data on film transparencies to digital form for computer processing. Figure 16 is a photograph of the scanner with a magnetic-tape transport unit. The sampling interval in both the x and y directions can be set at 12.5, 25, or 50  $\mu\text{m}$ . For a film optical-density ranging from 0 to 2 or 0 to 3, a total of 256 gray levels can be resolved. The following discussion of scanner calibration and data reduction is not restricted to this particular scan system; these procedures are generally applicable to any automatic microdensitometer that can be used to scan WSI interferogram transparencies.

The interference patterns obtained from the WSI test set up were typically 1 to 2 cm in diameter on 35-mm film. In order to take advantage of the scanner resolution and to present the fringe pattern in a format suitable for scanning with the Photoscan System, it was necessary to make enlargements of the original interferograms. Thus, 12.7 cm x 12.7 cm (5 in. x 5 in.) transparencies with a nominal 9-cm-diameter fringe pattern were made for scanning. The requirements for high-quality film transparencies suitable for scanning have been discussed earlier in section VIII.3. It should be added that an effort was made to limit the optical density of the enlargements to a value of 3.0 (0.10 percent transmission) since this represents the upper detectable gray level for the scanner.

During automatic scanning, a transparency is digitized into density data over the entire selected scan window. For the typical enlargement with a 9-cm-diameter fringe pattern and a sampling interval of 50  $\mu\text{m}$  along both the x and y axes, a total of about 4 million density data are generated, and the scanning time is about 30 minutes. From these data, it is necessary to extract the following two items: (1) test-lens aperture boundary with the sense of orientation preserved; and (2) fringe-peak locations. As discussed in the following subsections, the entire 4 million density values are not required to extract this information. However, the resolution required to determine the fringe-peak locations essentially demands the smallest available sampling interval across the fringe width. It is desirable to interface a computer to the scanner to permit automatic control of the sampling interval (both raster and aperture settings) over the entire film transparency. Ideally, the WSI interferograms would have to be scanned at only about 25 equally-spaced scans across the fringes. The sponsor's Photoscan System is currently interfaced to a mini-computer which permits the raster setting (along the



Figure 16.- Photograph of automatic-scanning microdensitometer with magnetic-tape transport unit.

rotating drum axis) to be under program control; in addition, the data from a single scan can be processed prior to the successive scan, thereby dramatically reducing the total density data accumulated or stored on magnetic tape.

#### IX.2. Calibration

Calibration tests to determine the resolution, density response, and dimensional fidelity of the scanner should be made prior to scanning interferograms. These tests were conducted on the Photoscan System as installed at the sponsor's facilities. It is further suggested that these calibration tests be repeated during the future use of the scanner to maintain proper performance.

A positive transparency of a resolution test chart, such as the 1951 USAF tri-bar target [28] shown in figure 17, is recommended for checking the scanner resolution. For the 12.5- $\mu\text{m}$  raster and aperture, the test chart should have patterns with spatial frequencies higher than about 40 cycles/mm. The 1951 USAF target may include patterns up to about 230 cycles/mm as listed in table V. After scanning the resolution test target, the resultant density data are inspected to determine for which pattern groups the bars and spaces can be detected.

The density response of the scanner can be determined by scanning a calibrated photographic step tablet such as those offered by the National Bureau of Standards (NBS) [29]. These NBS tablets have about 20 density steps ranging from an optical density of 0.05 to 3.00 with an accuracy of the larger of 0.01 optical density or 1 percent. After scanning the step tablet, the resultant density data, or gray levels, are plotted against the calibrated density levels of the step tablet; this curve should be linear over the entire density range of the scanner. If the density response is not linear, the scanner should be adjusted.

The dimensional fidelity of the scanner may be determined by scanning a positive transparency of an orthogonal grid. The x and y coordinates of the intersections of the grid lines should be known by an independent approach, such as an optical comparator, to better than the expected position accuracy of the scanner. These known grid coordinates are compared to those obtained from the scanner. Usually the scanner data will have to be corrected for tilt since it is difficult to align the grid to better than the positional accuracy of the scanner.

Group No.	Element No.	Cycles/mm	Group No.	Element No.	Cycles/mm	Group No.	Element No.	Cycles/mm
2	1	.250	2	1	4.00	5	1	32.0
	2	.280		2	4.49		2	38.0
	3	.315		3	5.04		3	40.3
	4	.351		4	4.68		4	45.3
	5	.397		5	6.35		5	50.8
	6	.445		6	7.13		6	57.0
-1	1	0.500	3	1	8.00	6	1	64.0
	2	.561		2	8.98		2	71.8
	3	.630		3	10.1		3	80.6
	4	.707		4	11.3		4	90.5
	5	.793		5	12.7		5	102.
	6	.891		6	14.3		6	114.
0	1	1.000	4	1	16.0	7	1	128.
	2	1.12		2	17.95		2	144.
	3	1.28		3	20.16		3	161.
	4	1.41		4	22.63		4	181.
	5	1.59		5	25.39		5	202.
	6	1.78		6	28.51		6	224.
1	1	2.00						
	2	2.24						
	3	2.52						
	4	2.83						
	5	3.17						
	6	3.58						

Table 5.- Pattern spatial frequencies for 1951 USAF tri-bar target.

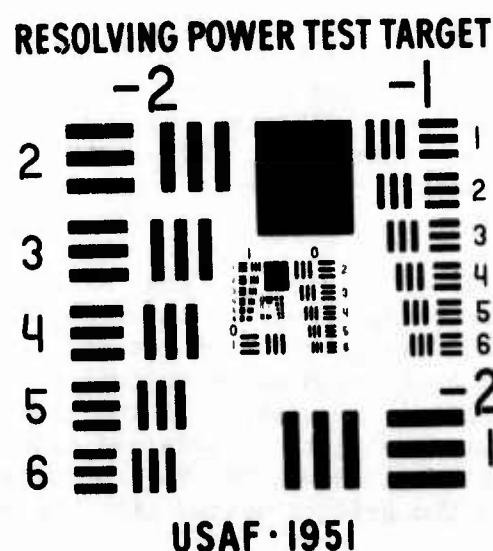


Figure 17.- Photograph of 1951 USAF tri-bar target.

### IX.3. Data Reduction

The computer program for reducing the density data obtained with the automatic scanner is outlined in appendix C. Two subroutines contained in this program locate both the test-lens aperture boundary and the fringe peaks. These two data-reduction steps produce the basic input data for the subsequent calculation of the test-lens properties, and they comprise the major portion of computer time in the reduction of automatic-scanner data; thus, both steps are discussed separately in this section.

Of the 4 million data samples recorded with the 50- $\mu\text{m}$ -sampling intervals, one quarter are used to locate the test-lens aperture boundary. Searching for specific information in a million samples is time consuming even for a high-speed computer. Methods of using the density variations in the photograph to identify the aperture boundary are even more time consuming. Most of these techniques depend on differentiation, autocorrelation, or other similar techniques. To reduce the number of required operations in the search and to reduce the possibility of errors, a method of punching small holes (about 1 mm in diameter) in the transparency at the beginning and end of every fringe was adopted. These holes not only clearly define the boundary, but also help to locate the fringe peaks and to assign fringe-order numbers. A typical interferogram with these punched holes is shown in figure 18(a).

The computer program searches for the holes by testing for density levels less than a given threshold value. If such a value is found, the scan is restricted to adjacent points, and all values below the threshold are counted. Since noise or pinholes in the transparency will sometimes result in values below the threshold, less than a given number in such a count is considered to be noise and ignored; whereas a sufficiently high count indicates that a hole has been located. The average location of the values below the threshold is noted, and the scan is continued over the entire transparency. The locations of the holes are then sorted and paired as the beginning and end of a fringe. After sorting the hole locations, they are curve-fitted to a circular lens aperture.

From the 2,000 or more recorded scans obtained with the 50- $\mu\text{m}$ -raster setting, those scans within the aperture, spaced at intervals corresponding to multiples of the shear distance, are chosen for locating the fringe peaks. Since only 20 to 30 scans are used, the computer time required to perform this search is relatively short. The fringe peaks are located in the following manner. By a process which most nearly corresponds to differentiation, the approximate location of a fringe peak is noted. Because of the noise in the photograph and lack of finesse in the fringes, this operation is not

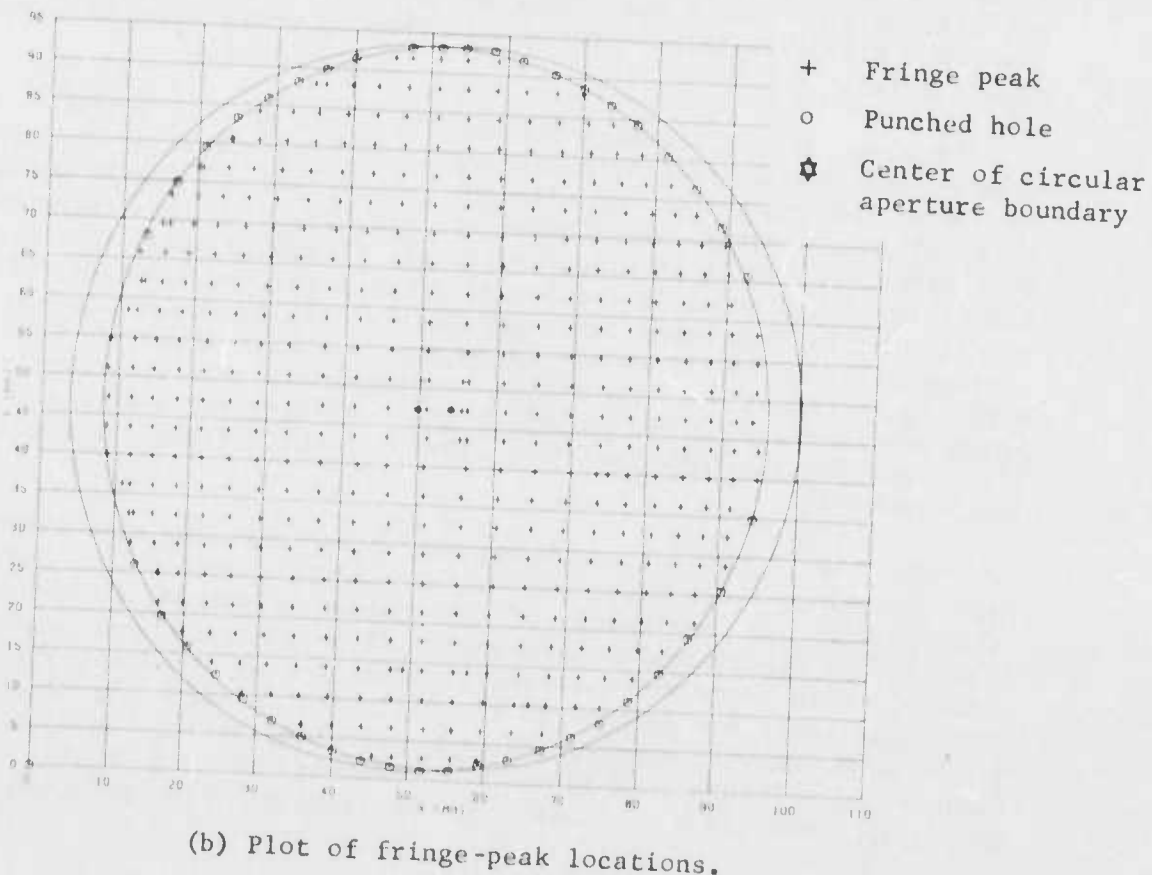
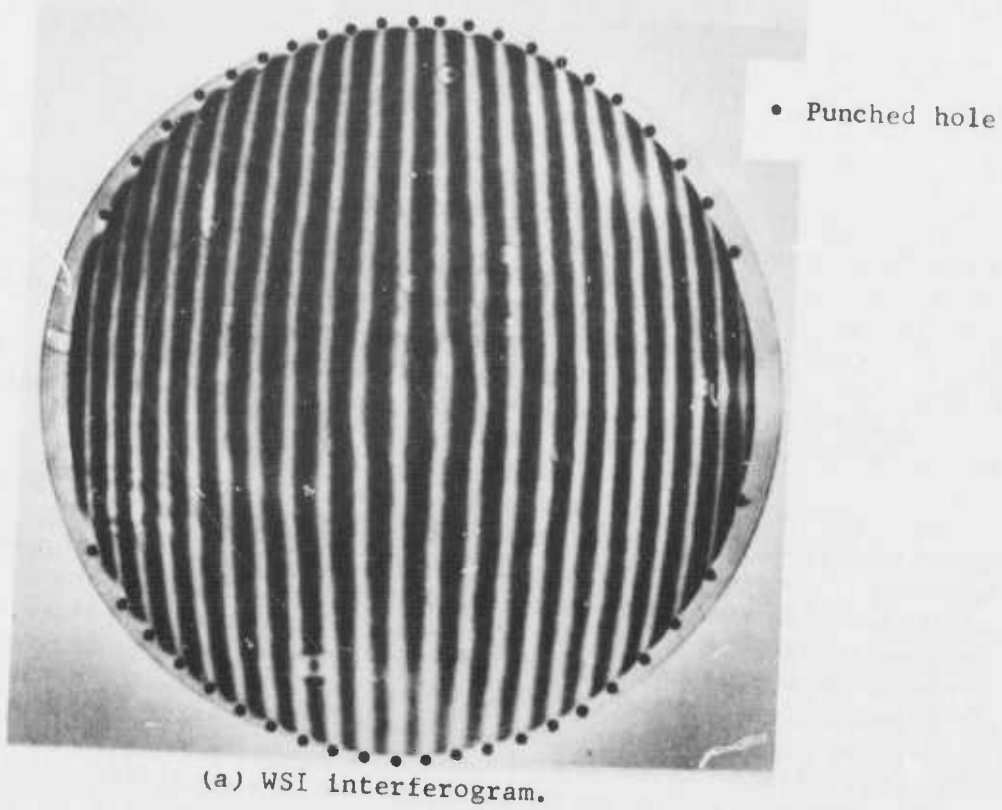


Figure 18.- Comparison of WSI interferogram with fringe-peak locations obtained from automatic scanning.

sufficiently accurate. Therefore, in the region of the peak, an interval of the scan corresponding to one cycle of the cosine is used to perform an autoconvolution. The location of the peak of the autoconvolution function corresponds to the fringe peak. The effects of photographic noise are minimized by this technique which approximates the operation performed by the operator using the Grant comparator. This procedure is performed over all cycles of the scans used.

The resulting locations of fringe peaks are then assigned order numbers in the following manner. Since the holes corresponding to the beginning and ends of fringes have already been sorted and the fringes assigned order numbers in increasing values of  $x$ , the fringe locations in the first scan are assigned the same order number as the hole to which they are closest. Subsequent scans are compared with the locations of peaks in the previous scan and assigned order values similarly. If more than one peak location appears at the same order number because of noise or other anomalies in the photograph, the one which is closest to the previous  $x$  value is assigned that fringe number and the other discarded. This technique works extremely well for current interferograms. There is minimal noise in the interferograms and seldom any real problem with incorrect choices of fringe-order numbers. The only major problem in using this program has occurred because holes were punched in the wrong place on the interferogram. If the holes do not touch the fringe terminals, or are displaced horizontally, the proper assignment of order number may not be made.

Figure 18(b) is a computer-generated plot of the fringe-peak locations from the automatic data reduction for the WSI interferogram in figure 18(a). The location of the punched holes is also shown; one of these holes is incorrectly plotted at the origin of the coordinate axes. The two circles shown correspond to the sheared and unsheared aperture boundaries of the test lens. In some areas, there are two closely spaced values for a fringe-peak location. The additional values usually result from noise in the interferogram, such as diffraction patterns from the aperture boundary or dust on the test lens. An apparent fringe for which holes are not punched is also shown; this fringe is only partially visible in figure 18(a) and was not treated as useable data.

## X. WSI FRINGE PATTERNS

### X.1. Analytic Form

Discussions of shearing interferograms resulting from various types of lens aberrations may be found throughout the literature [30, 31]. For the present cube interferometer, the general form of the interferograms for shear in the x direction may be found by setting the cosine argument of equation (3) equal to  $2\pi p$ , viz,

$$\frac{x\ell\phi}{\lambda z_2} + \frac{\varphi(x,y)}{\lambda} - \frac{\varphi(x-\ell\phi-z_2, y)}{\lambda} = p \quad (46)$$

where  $p$  is an integer corresponding to fringe peaks,  $x$  is the fringe location measured from the center of the lens aperture, and the term  $k(\ell\phi)^2/2z_2$  corresponding to a small constant displacement of the fringe pattern has been omitted. In order to simplify the solution of equation (46) for fringe locations, we may rewrite it in a normalized form, viz,

$$x + c \left[ \varphi(x,y) - \varphi(x-1, y) \right] = p \quad (47)$$

where the ideal fringes are assumed to be at unit spacing ( $\ell\phi/\lambda z_2 = 1$ ), the shear distance is assumed unity ( $\ell\phi + z_2\phi = 1$ ), and  $c$  is a constant ( $c = \frac{C_1}{\lambda}$ ;  $C_1 = \text{constant}$ ). A similar equation results for the y-sheared interferogram.

From table 1(a), we can write an analytical form of  $\varphi(x,y)$  for specific aberrations. Substituting this form of  $\varphi(x,y)$  into equation (47) and solving for  $x$  will give the fringe pattern for the x-sheared interferogram. For example, with third-order x coma, equation (47) becomes

$$x + cx(x^2 + y^2) - c_1(x-1) \left[ (x-1)^2 + y^2 \right] = p . \quad (48)$$

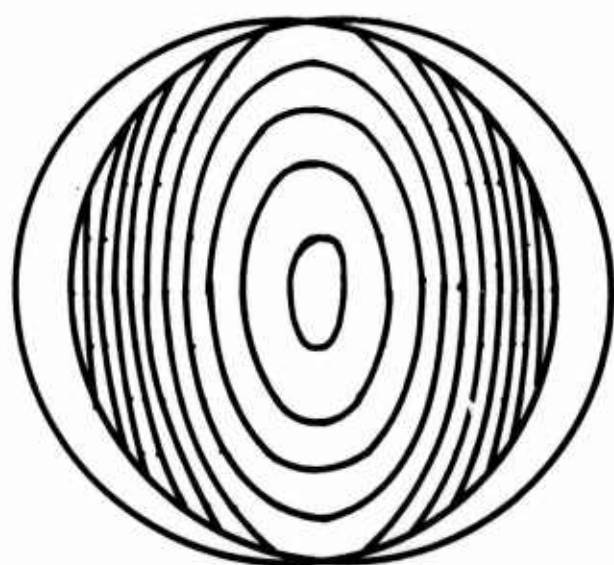
The y-sheared interferogram for this aberration is given by

$$y + cy(x^2 + y^2) - cx \left[ x^2 + (y-1)^2 \right] = p . \quad (49)$$

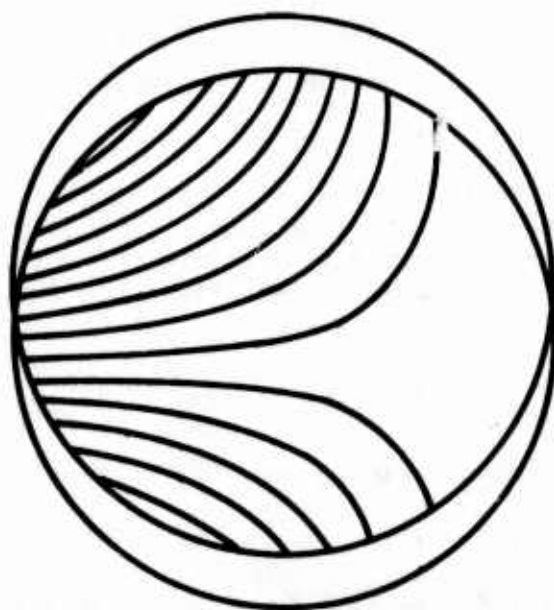
Solving equation (48) and (49) for  $2\lambda$  of third-order x coma gives the fringe patterns shown in figures 19(a) and 19(b).

As another example, consider third-order  $0^\circ$  astigmatism; for this aberration, we can write

$$x + c(x^2 - y^2) - c \left[ (x-1)^2 - y^2 \right] = p \quad (50)$$



(a) x-sheared interferogram.



(b) y-sheared interferogram.

Figure 19.- Schematic of WSI interferograms for  $2\lambda$  of third-order x coma.

for the x-sheared interferogram; and

$$y + c(x^2 - y^2) - c \left[ x^2 - (y - 1)^2 \right] = p$$

for the y-sheared interferogram. Solving these equations for  $2\lambda$  of third-order  $0^\circ$  astigmatism gives the fringe patterns shown in figures 20(a) and 20(b). The resulting fringe are straight in both interferograms, but the fringe spacing is different. The other component of astigmatism given in table 1(a), viz, third-order  $45^\circ$  astigmatism, also produces straight-line fringes, but with different slopes or orientations in the x and y-sheared interferograms. The fringe patterns for  $2\lambda$  of third-order  $45^\circ$  astigmatism are shown in figures 21(a) and 21(b).

## X.2. Test Cases

One approach to check the logic and accuracy of the computer data-reduction program outlined in appendix A is to input data representing a lens with a known aberration and compare the resulting pupil function and aberrations with the input value. Consider a lens with third-order spherical aberration; for this aberration, equation (47) becomes

$$x + c(x^2 + y^2)^2 - c \left[ (x - 1)^2 + y^2 \right]^2 = p. \quad (52)$$

Since spherical aberration is rotationally symmetric, both the x and y-sheared interferograms will be identical. Solving equation (52) for x yields a cubic equation with real solutions at  $x = A + B$  where

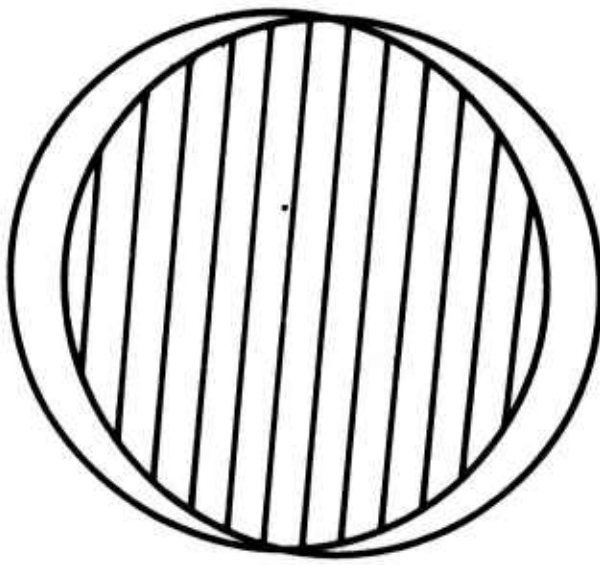
$$A = \sqrt[3]{\frac{b}{2} + \sqrt{\frac{b^2}{4} + \frac{a^3}{27}}} \quad (53)$$

$$B = \sqrt[3]{\frac{b}{2} - \sqrt{\frac{b^2}{4} + \frac{a^3}{27}}}$$

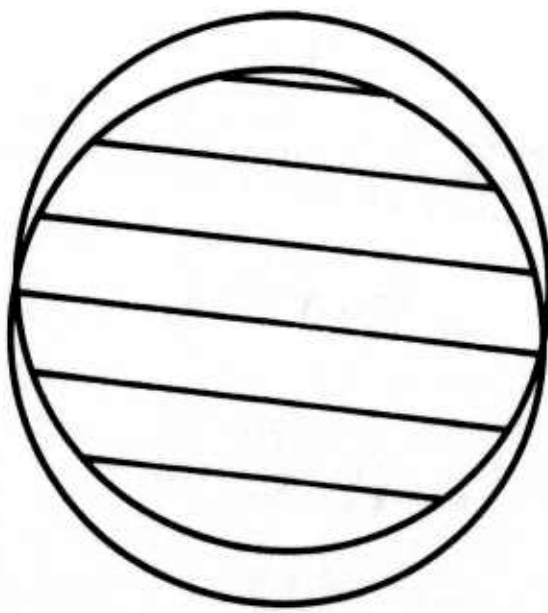
and

$$a = y^2 + \frac{1}{2}$$

$$b = \frac{3}{8} - \frac{m}{4}.$$

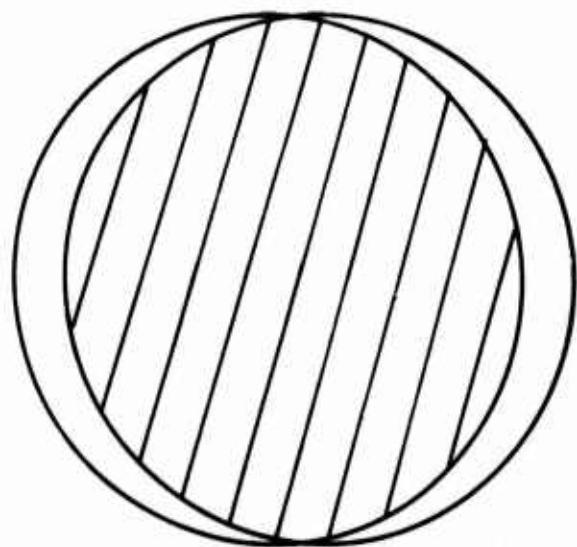


(a) x-sheared interferogram.

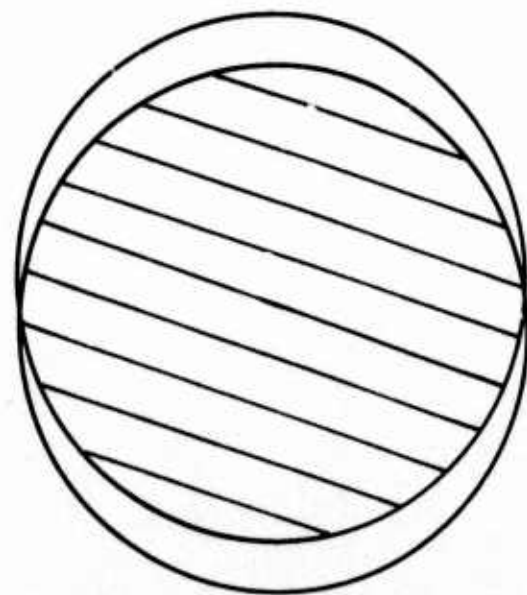


(b) y-sheared interferogram.

Figure 20.- Schematic of WSI interferograms for  $2\lambda$  of third-order  
 $0^\circ$  astigmatism.



(a) x-sheared interferogram.



(b) y-sheared interferogram.

Figure 21.- Schematic of WSI interferograms for  $2\lambda$  of third-order  
45° astigmatism.

Solving equations (52) and (53) for  $2\lambda$  of third-order spherical aberration gives the fringe pattern shown in figure 22. These fringe locations were used as input to the computer data-reduction program. The resulting maximum aberrations are given in table 6; also given in this table are the maximum aberrations for the case of  $1\lambda$  of third-order spherical aberration. The pupil-function phases for these two cases are shown in figures 23(a) and 23(b). The isocontours of the MTF's are shown in figures 24(a) and 24(b); the two-dimensional MTF's are shown in figure 25(a) and 25(b). The isocontours of the PTF's are shown in figures 26(a) and 26(b); the two-dimensional PTF's are shown in figures 27(a) and 27(b). For these plots, wavelength is unity and the radius of the lens aperture is 12 units; the spatial frequency is normalized. For both cases, the computed pupil functions are accurate to  $\lambda/10^4$ . The computed MTF's and PTF's agree with the calculations of reference 32 to within plotting accuracy. Since spherical aberration is symmetrical, as readily apparent from figure 23, there should be no differences between the sagittal and tangential MTF's. For the PTF's, there are large differences between the sagittal and tangential values above 0.6 cycles/mm. These differences are due primarily to computational inaccuracies as discussed in section 8.2 and do not signify a real difference in the sagittal and tangential PTF's.

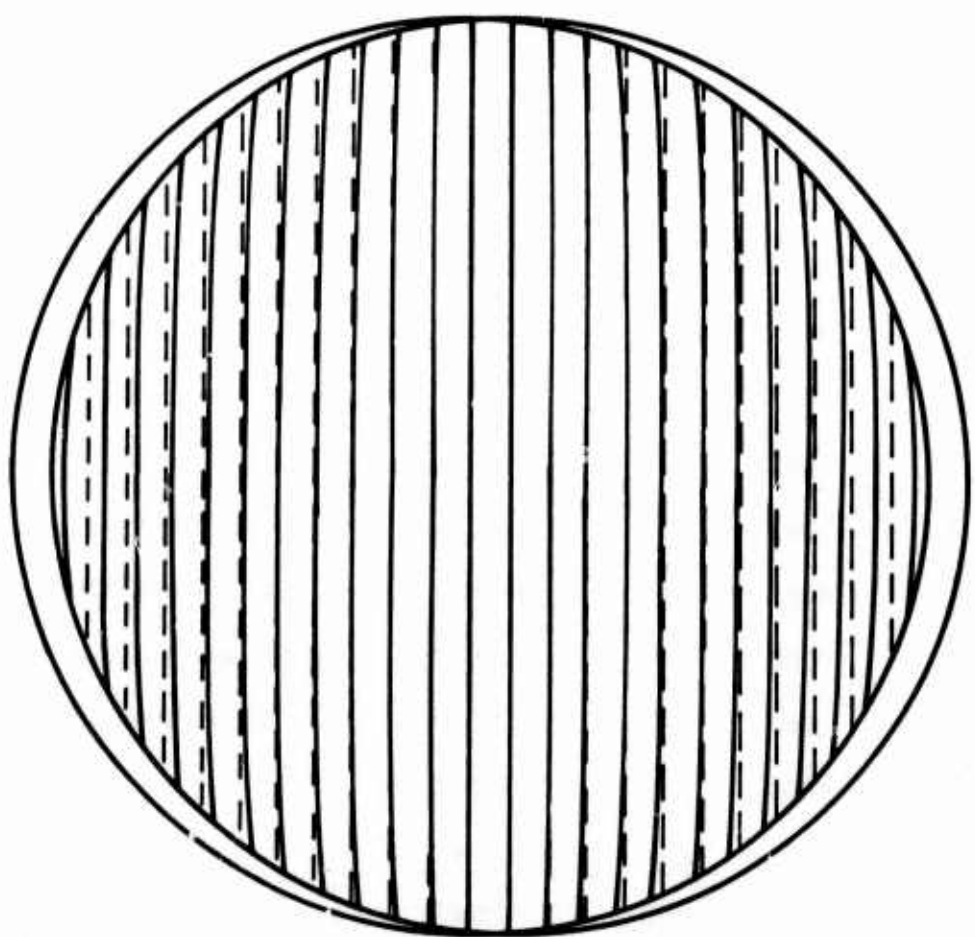
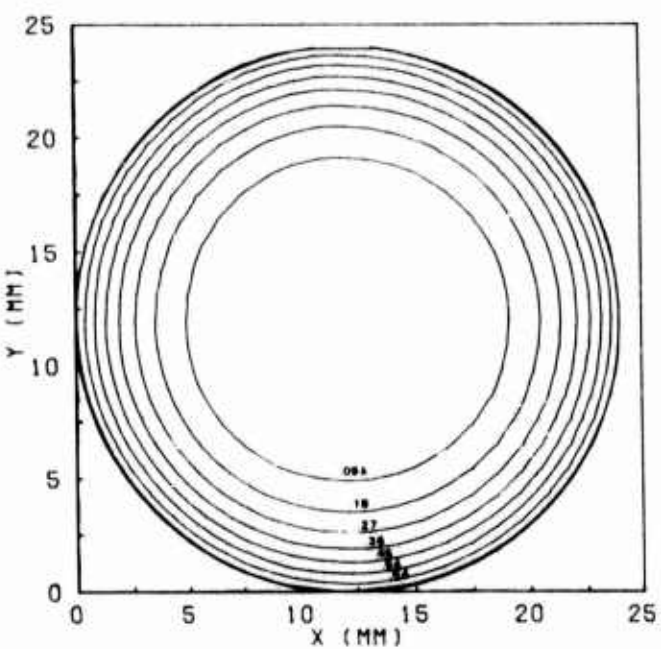


Figure 22.- Schematic of WSI interferogram for  $2\lambda$  of third-order spherical aberration. (Dashed lines represent equally spaced, straight-line reference fringes for aberration-free lens.)

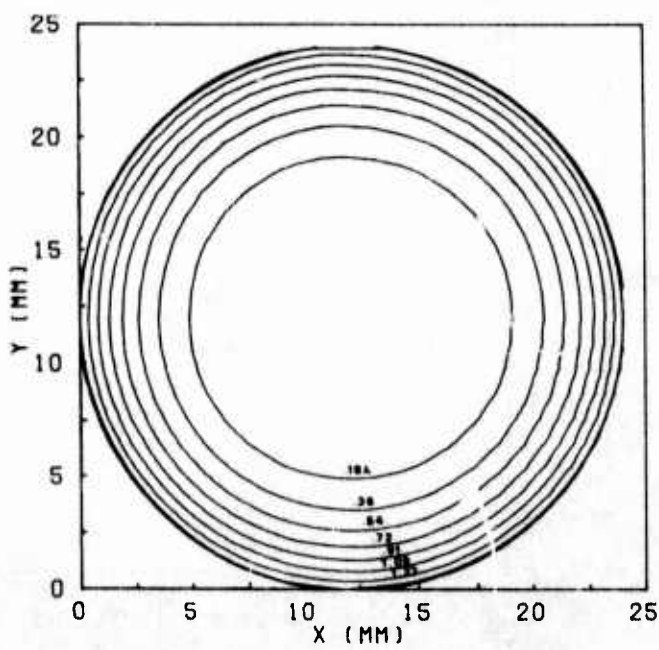
TABLE 6.- MAXIMUM ABERRATIONS FOR TEST CASES OF  $1\lambda$  AND  $2\lambda$  OF  
THIRD-ORDER SPHERICAL ABERRATIONS<sup>a</sup>

n	$1\lambda$ spherical	$2\lambda$ spherical	type
4	- .0010	.0014	focus
5	- .0000	.0002	0° astigmatism
6	.0000	- .0000	45° astigmatism
7	- .0017	- .0011	x coma (3rd)
8	- .0009	- .0010	y coma (3rd)
9	.0002	.0021	x clover (3rd)
10	.0043	.0013	y clover (3rd)
11	1.0065	1.9955	3rd spherical
12	.0000	- .0002	0° astigmatism (5th)
13	- .0000	.0000	45° astigmatism (5th)
14	.0000	.0001	
15	.0000	.0000	
16	.0016	.0009	x coma (5th)
17	.0008	.0011	y coma (5th)
18	- .0003	- .0026	x clover (5th)
19	- .0054	- .0012	y clover (5th)
20	- .0002	- .0001	
21	.0000	- .0015	
22	- .0106	.0038	5th spherical
23	.0063	- .0016	7th spherical

<sup>a</sup> $\lambda = 1.0$

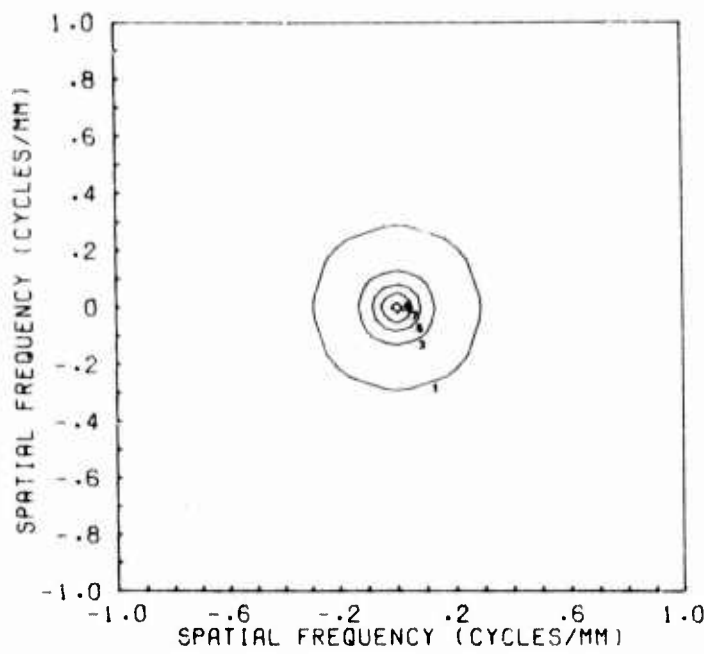


(a)  $1\lambda$  spherical aberration.

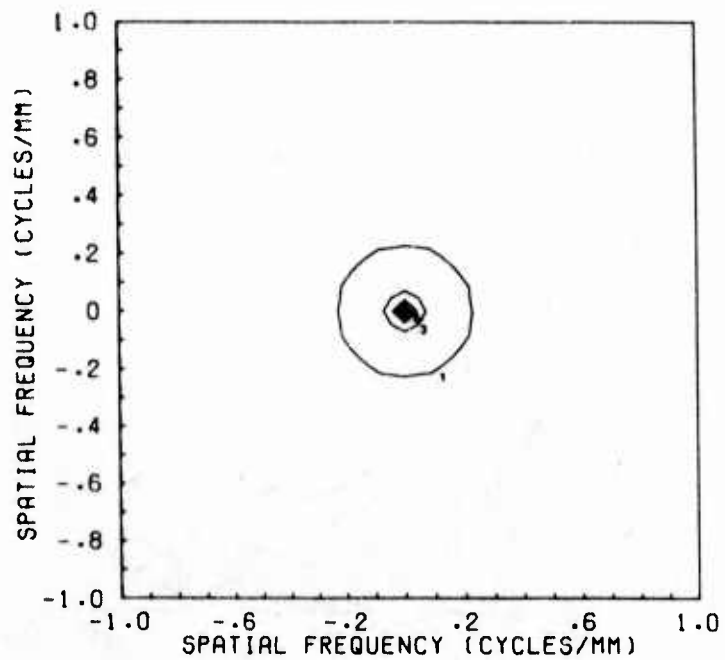


(b)  $2\lambda$  spherical aberration.

Figure 23.- Isocontours of pupil-function phase for test cases of WSI fringe patterns with  $1\lambda$  and  $2\lambda$  of third-order spherical aberration.

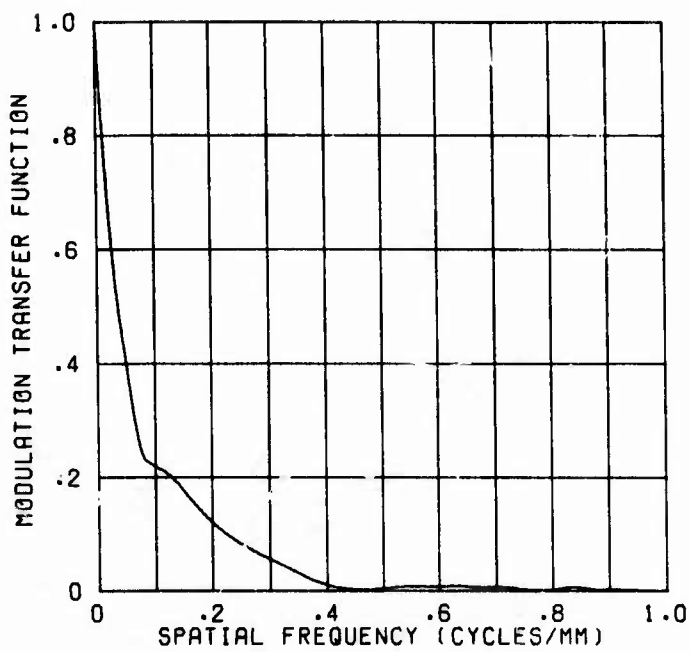


(a)  $1\lambda$  spherical aberration.

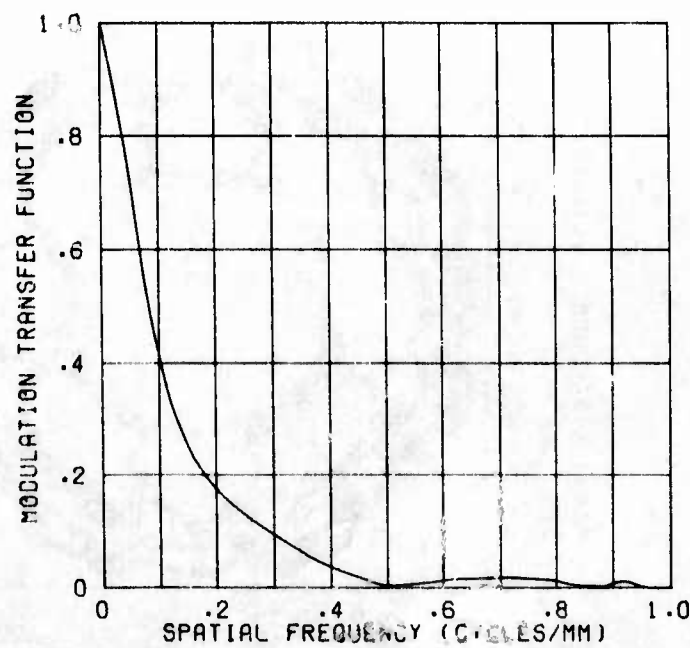


(b)  $2\lambda$  spherical aberration.

**Figure 24.- Isocontours of MTF for test cases of WSI fringe patterns with  $1\lambda$  and  $2\lambda$  of third-order spherical aberration.**

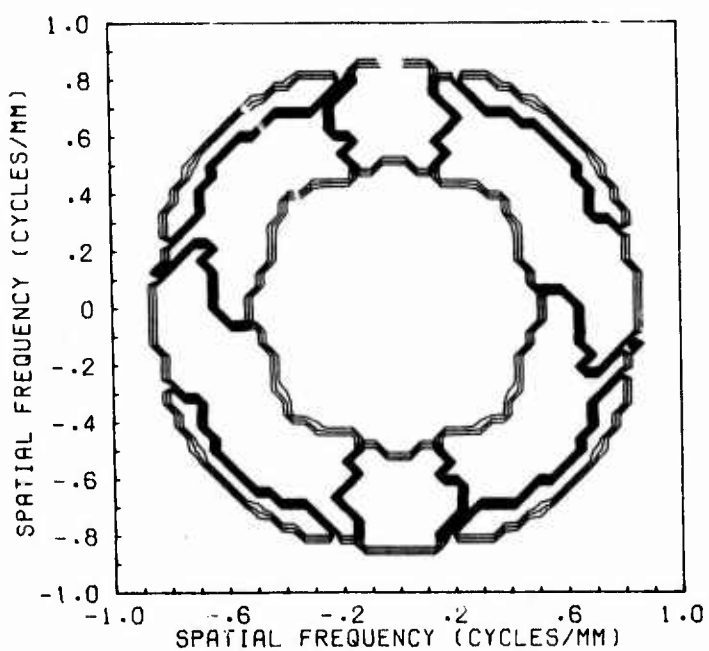


(a)  $1\lambda$  spherical aberration.

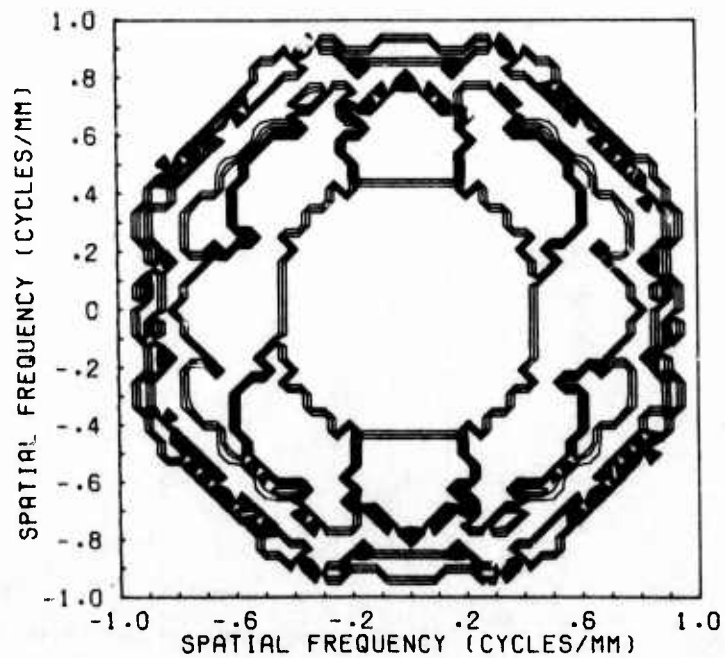


(b)  $2\lambda$  spherical aberration.

Figure 25.- MTF for test cases of WSI fringe patterns with  $1\lambda$  and  $2\lambda$  of third-order spherical aberration.

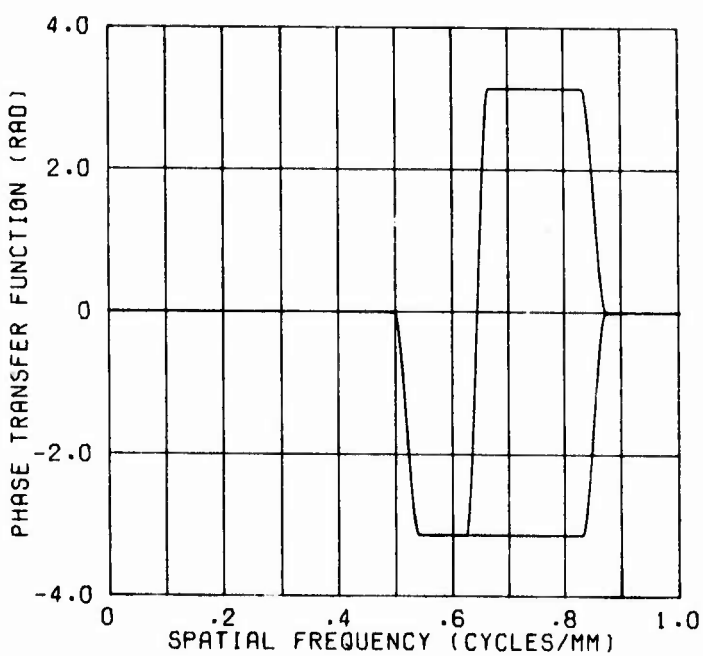


(a)  $1\lambda$  spherical aberration.

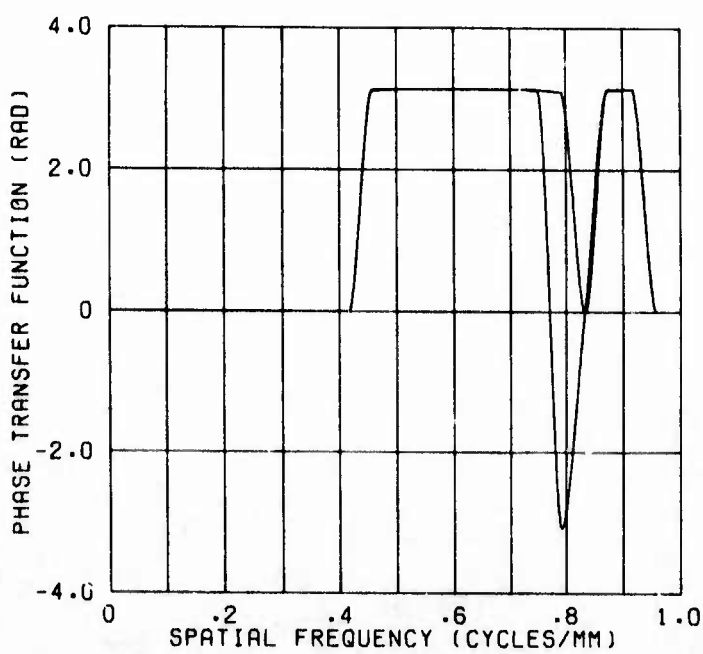


(b)  $2\lambda$  spherical aberration.

Figure 26.- Isocontours of PTF for test cases of WSI fringe patterns with  $1\lambda$  and  $2\lambda$  of third-order spherical aberration.



(a)  $1\lambda$  spherical aberration.



(b)  $2\lambda$  spherical aberration.

Figure 27.- PTF for test cases of WSI fringe patterns with  $1\lambda$  and  $2\lambda$  of third-order spherical aberration.

## XI. TEST SYSTEM AND PROCEDURES

The test system and experimental procedures used for testing lenses in the WSI system have, to a great extent, been discussed throughout previous sections. These items are collected in this section to serve as a guideline in the set up and use of a WSI test system.

### XI.1. Testing Mode

As shown previously in figures 2 and 3, the WSI system can be arranged for testing lenses at either finite or infinite conjugates. Although the double-pass mode is the usual arrangement for infinite-conjugate testing, this approach is not satisfactory for testing relatively short focal-length lenses. For such lenses in a double-pass mode, the available working distance is not long enough to allow a pellicle or beam splitter to be positioned between the pellicle and cube. An alternative for testing most lenses at infinite conjugates is to use a diffraction-limited or high quality collimator in a single-pass mode as shown in figure 28. If a aberration-free collimator is unavailable, a third approach, which is also a single-pass system, is to place the test lens at a distance from the light source beyond the hyperfocal distance.

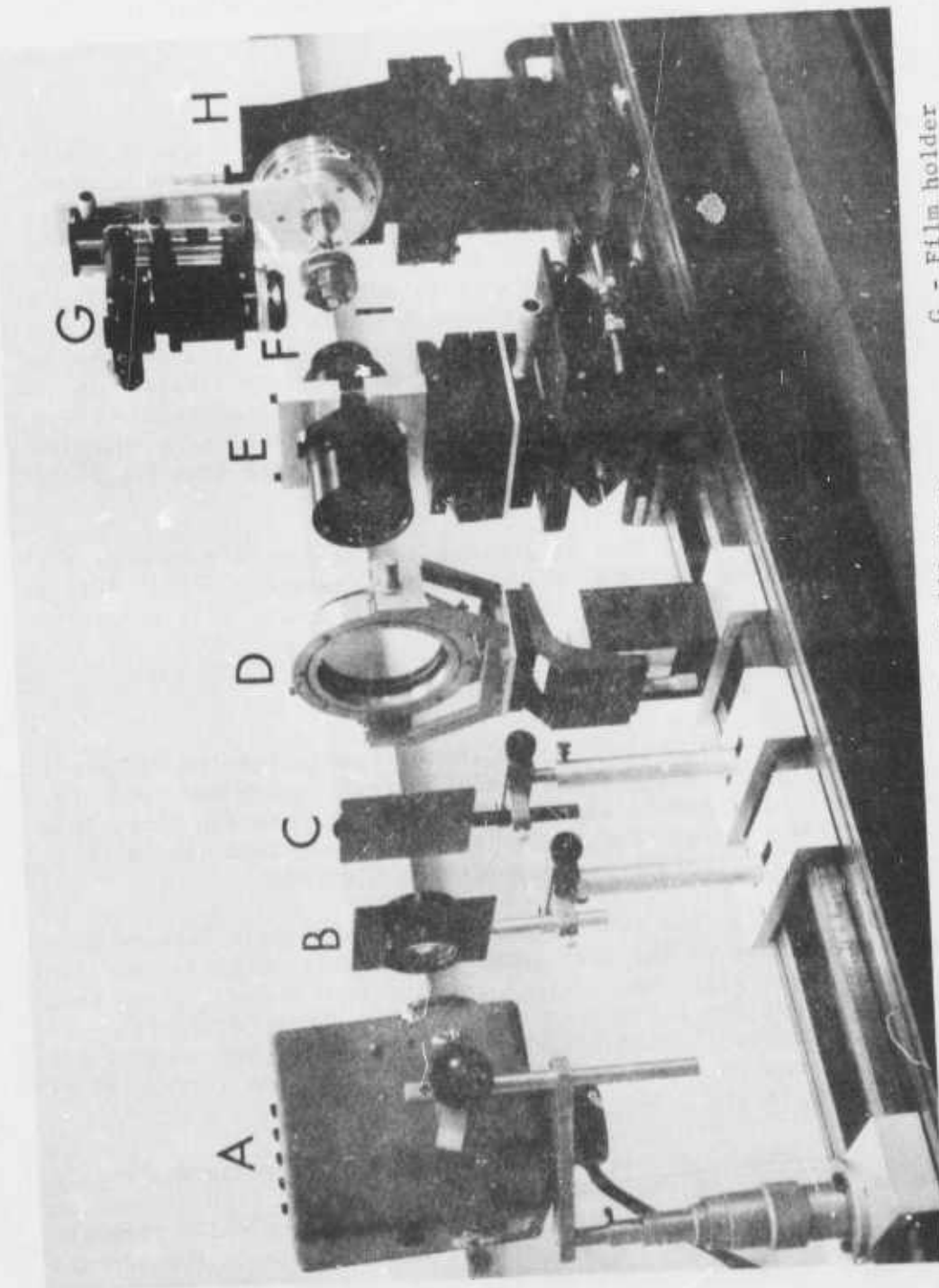
It should be noted that in testing in the double-pass mode the test-lens wavefront aberrations are doubled. Therefore, the fringe displacements are automatically halved during computer data reduction for this case.

### XI.2. Components

The basic components required for lens testing with the WSI are a set of cube interferometers, optical bench, light source and pinhole, auxiliary lens, and nodal slide or fixture for rotating cube, film plane, and auxiliary lens. For infinite-conjugate testing, a flat mirror and pellicle or collimator may also be required.

The choice of a WSI cube with a fixed shear angle depends primarily on the f-number of the test lens. (See table 2(a).) A set of eight or nine cubes with shear angles ranging from about 2 to 40 mrad should be sufficient for testing lenses with f-numbers from f/15 to f/1. However, it should be noted that testing lenses below about f/2 should generally not be undertaken since the aberrations introduced by the cube are very large. (See section VI.2.)

The optical bench should dampen external vibrations, remain straight over the span of the test system, and exhibit high dimensional stability. For the present tests, an optical bench which remained level to within 0.1 mm over 1 m was used. Vibrations of the fringe patterns were detected occasionally even though the bench was relatively heavy steel. The test-system components were mounted at



A - Light source      D - Collimator  
B - Condenser      E - Test lens  
C - Pinhole      F - Relay lens  
G - Film holder      H - Rotating fixture  
I - WSI cube

Figure 28.- Photograph of single-pass WSI test system for infinite-conjugate testing.

about 30 cm above the top surface of the bench, and, therefore, introduced a mass at the end of a relatively long lever arm; this design probably led to the observed vibrations.

The light source can be filtered polychromatic light or a laser. A 100-watt mercury-arc lamp with a monochromatic filter and a 15-mW He-Ne laser were both used in the present tests. A pinhole is used for a point source, and the size of the pinhole is determined by the degree of coherence required to produce fringes of good contrast. For the present tests, a 100- $\mu\text{m}$ -diameter pinhole was used to test a 1-m focal-length lens, and a 10- $\mu\text{m}$ -diameter pinhole was used to test a 50-mm focal length lens. In addition, condenser optics are generally necessary to produce a high-energy, focused image of the light source at the pinhole. These condenser optics should be selected and adjusted so that the cone of light diverging from the pinhole fills the test lens completely and uniformly.

The choice of an auxiliary lens to image the interference pattern on the film plane is related to both the f-number of the test system and the desired image size of the interferogram. Since the auxiliary lens should be placed a distance equal to its focal length away from the test-lens focal plane, the diameter of the resulting interferogram D will be given by  $D = f_c/f^{\#}$  where  $f_c$  is the focal length of the auxiliary lens and  $f^{\#}$  is the f-number of test lens. For the f/8 and f/8.7 lenses in the present tests, an auxiliary lens with  $f_c = 105$  mm at f/2.5 was used to give an interferogram with  $D \sim 12$  mm.

Ideally, a nodal slide that maintains test-lens alignment during rotation to the 90° or y-sheared setting should be used. If such a lens mount is not available, two alternatives are to (1) rotate the auxiliary lens, film plane, and cube as a fixed unit about the test-system axis; or (2) realign the test lens after the 90° rotation. The latter approach was used in the present tests. However, since completion of these tests, a fixture for rotating the auxiliary lens, film plane, and cube was built and is currently used for lens testing with the WSI; it is generally recommended that such a fixture be used rather than realigning the lens after rotation. (See figure 12.)

The flat mirror that may be required for infinite-conjugate testing should ideally not introduce any wavefront deviations greater than the smallest repeatable deviations detected with the WSI test system. Present testing techniques with the WSI have shown that wavefront deviations down to about  $0.04 \lambda$  can be repeated. The 14-cm-diameter mirror used as a retro-reflector in the present tests was inspected with a Twyman-Green interferometer and found to give wavefront deviations (peak to valley) no greater than about  $0.10 \lambda$ . The largest surface deviations, as with most flat mirrors, occurred near the mirror edge. For the present tests, only the central mirror area with a diameter of about 11 cm was used; thus, the wavefront deviations introduced by the mirror were probably far less than  $0.10 \lambda$ . For current testing, a 20-cm-diameter mirror with a maximum peak-to-valley deviation of only  $0.03 \lambda$  is used.

If a beam splitter is required to fold optically the WSI test system, a pellicle rather than a glass-plate should be used. A glass plate, like the cube interferometer, will introduce aberrations. Since a glass-plate beamsplitter is commonly used with light incident at 45° to the glass surface, significant asymmetrical aberrations would be added to the wavefront. A nominally 5- $\mu\text{m}$ -thick, 8-cm-diameter pellicle with an optical flatness of a few wavelengths over the diameter was used in the present tests. A pellicle area measuring from only 0.5 to 1 cm in diameter was actually used to transmit and reflect the wavefront.

If a collimator is used to provide a plane wavefront for infinite-conjugate testing, the collimator should be tested first to determine its performance. One of the f/8.7 collimators tested in the present study and discussed in the following section was found to be nearly diffraction limited; thus, this collimator is currently used to test lenses at infinite conjugates on the WSI. It should be noted that special care must be taken to align a collimator in the WSI test system since many collimators are designed with a very narrow angular field of view of 1 or 2 degrees; otherwise, off-axis aberration will be introduced even for a collimator that is diffraction-limited on axis.

### XI.3. Alignment

After mounting the test-system components on the optical bench, it is necessary to establish an optical axis and to align the components along this axis. As noted earlier, an optical axis, which did not vary in height more than 0.1 mm over a 1-m length, was defined at about 30 cm above the top surface of the bench. To establish this axis, the centers of a cross hair and an alignment target were fixed at the same height and transverse position by visual sighting through an alignment telescope (theodolite). Thus, the optical axis could be "reconstructed" at any time by simply reinstalling the cross hair and alignment target on the optical bench.

The system components, excluding the WSI cube, test lens, and auxiliary lens, were centered to within 0.5 mm of the test-system optical axis by means of the alignment telescope. For a test system using a pellicle to fold optically the light source, the pellicle must be angularly adjusted in order to center the image of the point source.

The cube interferometer is roughly centered on the optical axis by visual sighting. Other than avoiding any non-homogeneities in the cube, the cube must be located so that no vignetting of the interference pattern occurs. For systems that rotate the cube 90° to obtain the y-sheared interferogram, these requirements, of course, apply to both angular settings. A 1-mW He-Ne laser was used to align the front face of the cube normal to the optical axis. After aligning the laser beam along the optical axis, the cube was adjusted angularly until the beam reflected from the front face returned through the laser aperture. With this approach, the cube face was aligned to within 15 arc minutes, thereby eliminating asymmetric aberrations which arise from a tilted cube. The cube should be aligned to well within 15 arc minutes when testing lenses below f/4; otherwise, significant coma may be introduced. This angular alignment must also be maintained if the cube is rotated for the y-sheared interferogram.

The rotational position of the cube about the optical axis is related to interferogram registration and, therefore, is discussed in appendix D. The cube position or *l* setting along the optical axis is discussed following the test-lens alignment since this cube setting is dependent on test-lens location and alignment.

The test lenses were aligned by the Boys-point method [33] which uses subsidiary images of the light source formed by reflections from the front and back surfaces of the test-lens. A schematic of this technique is shown in figure 29. In this technique the test lens is alternately translated and tilted until a subsidiary image formed behind the lens and one formed in front of the lens are both centered on the optical axis. During alignment the subsidiary images can be seen on the cross hairs and alignment target; the centers of the cross hairs and alignment target define the optical axis as noted earlier. In the present tests, the test lenses were aligned to within two arc minutes. For infinite-conjugate testing, with a collimator, the position of the test lens along the optical axis is not important; however, for infinite-conjugate testing without a collimator, the test lens must be placed at a distance from the light source beyond the hyperfocal distance. For finite-conjugate testing, it is important to position the test lens at the required distance from the light source.

After positioning and aligning the test lens, the cube interferometer is moved along the optical axis until the null-fringe position is located. This is the cube position in which the fringe field is either all dark or all light, i.e., a dark or light fringe of infinite extent denotes the null-fringe position. At this position, the backface of the cube is located in the plane of the test-lens

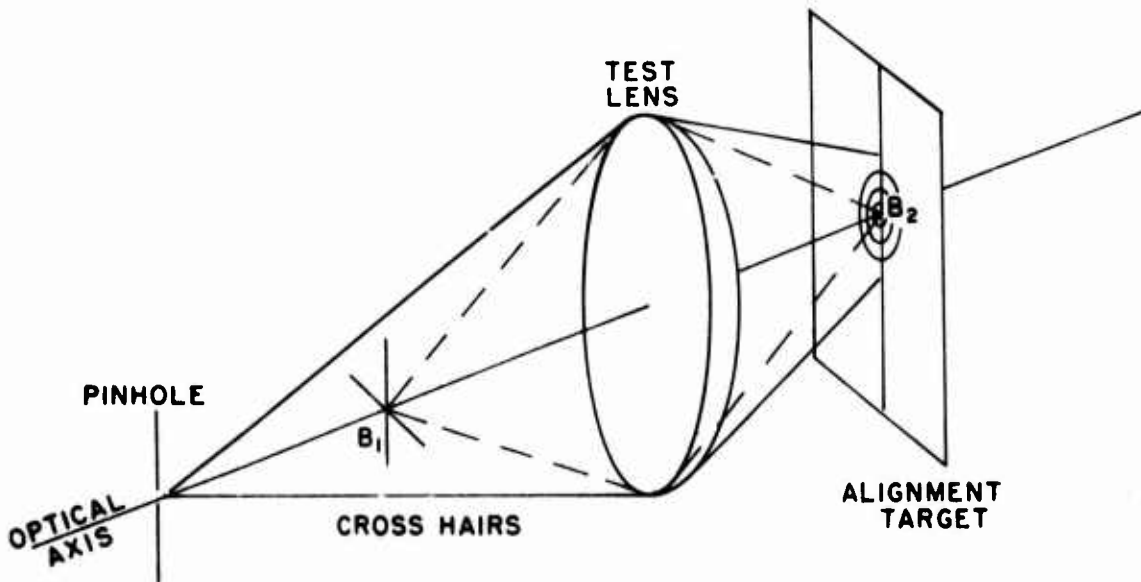


Figure 29.- Schematic of Boys-point method to align test lens in WSI system.  
( $B_1$  and  $B_2$  are subsidiary images formed by test lens.)

focus and, therefore, there is no lateral shear or  $\ell\phi = 0$ . (See figure 4.) Since the depth of focus for a lens increases with increasing f-number [24], the null-fringe position is less repeatable for lenses with higher f-numbers. For example, the null-fringe position in the present tests with the f/8.7 lens could be repeated to within 0.1 mm. This is consistent with the focal properties of the test lens since the depth of focus for an f/8.7 lens at  $\lambda = 0.50 \mu\text{m}$  is about 0.1 mm. Thus, the error in locating and repeating the null fringe position may be no larger than the depth of focus for the test lens. The cube interferometer is then moved along the optical axis a predetermined distance  $\ell$  away from the null-fringe position. Although the same fringe pattern can be obtained for the same  $\ell$  setting on either side of focus, it is recommended that the cube be moved outside of the test-lens focus. This setting is consistent with the present data-reduction technique which requires  $\ell + z_2$  as an input parameter where  $\ell > 0$ . The  $\ell$  distance is determined by first choosing the total number of fringes  $M$  to appear in the interferogram. From equation (44), the fringe spacing  $\Delta F$  is given by  $D/M$  and from equation (7), the reference fringe spacing for a given  $\ell$  is  $\lambda z_2/\ell\phi$ . Equating these two expressions for fringe spacing gives

$$\frac{D}{M} = \frac{\lambda z_2}{l\phi} . \quad (54)$$

Solving equation (54) for  $l$  yields

$$l = \frac{M\lambda z_2}{D\phi} \quad (55)$$

which is used to determine the axial position of the cube as measured from the null-fringe position.

The auxiliary lens must be positioned so that the interference pattern incident on the film plane is collimated, unobstructed, and relatively free of distortion. After fixing the axial, angular, and rotational settings of the cube interferometer, the auxiliary lens should be centered with respect to the beam exiting from the cube and opened to the lowest f-stop. Furthermore, the auxiliary lens should be roughly aligned along the exit-beam axis so that lens distortion is kept to a minimum. This alignment can be done visually by inspecting the image geometry on the film plane. Assuming that the film is normal to the exit-beam axis, the image should be round for a test lens with a circular aperture. The auxiliary lens must also be located axially so that the fringe pattern is collimated. This can be checked by comparing the image diameter at the film plane with the image diameter at some distance relatively far behind the film plane; the image diameter is constant for collimated light.

#### XI.4. Interferogram Photography

The choice of film for recording fringe patterns in the test system and making enlargements suitable for scanning depend upon many variables such as film speed, resolution, and range of contrast obtainable under various processing conditions. As discussed in section VIII.3, the requirements for a high-quality interferogram ideally include a density variation that approaches a cosine distribution across the fringe pattern and a transparency which is free of pinholes, scratches, and other similar defects. Any film and subsequent processing which can produce an interferogram that approaches these conditions will be suitable.

For the majority of the present tests, 35-mm AHU microfilm (ASA 64) at exposure times of 1/4 to 1 second was found to give satisfactory interferograms. In a few instances, 35-mm TRI-X pan film (ASA 400) at exposure times of 1/30 to 1/8 second was used and also gave satisfactory interferograms. Ortho sheet film - Type 3 (ASA 10) and Ortho Super Speed Portrait sheet film (ASA 125) were used to make enlargements for scanning. Depending on the quality of the original 35-mm interferogram, the exposure and processing for the enlargements were often varied to produce acceptable interferograms.

As discussed in appendix D, roll film is recommended over sheet film for original interferograms. With roll film, the proper orientation between x and y-sheared interferograms can be preserved more easily.

## XII. TEST RESULTS

In the present study, three lenses were tested on axis with the WSI. These lenses were: (1) f/8.7 collimating doublet (collimator A); (2) f/8.7 collimating doublet (collimator B); and (3) f/8 OTF Standard Test Lens. Although test procedures, test-system components, and data-reduction procedures were improved throughout the testing of these three lenses, the data presented are representative of WSI test data and accurately reflect the test-lens performance.

### XII.1. Collimator A

The f/8.7 collimating doublet has a clear aperture of 11.5 cm and a nominal effective focal length of 1 m. This collimator was reported by the supplier to be diffraction limited over a 1.9-cm field of view ( $1.1^\circ$ ) from 510 nm to 610 nm.

The collimator was tested at infinite conjugates since it is designed to be used under these conditions. The test system was arranged in a double-pass mode using a 14-cm-diameter plane mirror as shown in figure 3. A 100-W high-pressure mercury-arc lamp with a monochromatic interference filter ( $\lambda = 546.1$  nm), condensing optics, and a nominally 100- $\mu\text{m}$ -diameter pinhole were used for the light source. A cube interferometer with  $\Phi = 4.55$  mrad was used.

The initial fringe pattern observed for the collimator was highly curved, thereby indicating that this lens was not diffraction limited or large errors were being introduced by the test system. Possible sources of errors in the test system were, therefore, investigated. The retro-reflecting plane mirror was tested on a Twyman-Green interferometer and found to give wavefront deviations (peak to valley) no greater than about  $0.10 \lambda$  over the entire 14-cm diameter; deviations were much smaller over the 11.5-cm-diameter portion used to reflect the test wavefront. The pellicle, which was used to fold optically the light source, was repositioned several times, but no change in the fringe pattern was observed; furthermore, the substitution of two other pellicles did not change the fringe pattern. The cube interferometer was also replaced by several other cubes with different shear angles, and after adjustments to obtain the same number of fringes in all cases, the resulting fringe pattern was the same. The collimator was also reversed front to back in the nodal slide since many achromats, like the collimator, are designed to be used only with the point source on the back side of the lens; however, no change in fringe pattern was observed. Finally, the collimator was very carefully realigned to well within the  $1.1^\circ$  angular field of view. The resulting fringe pattern was essentially identical to the

initial pattern, thereby demonstrating that the fringes accurately reflected the lens performance. Thus, interferograms were scanned, and the resulting pupil function, MTF, and PTF for the plane or best focus are shown in figures 30(a), 30(b), 30(c), 30(d), and 30(e). The resulting maximum aberrations are given in table 7.

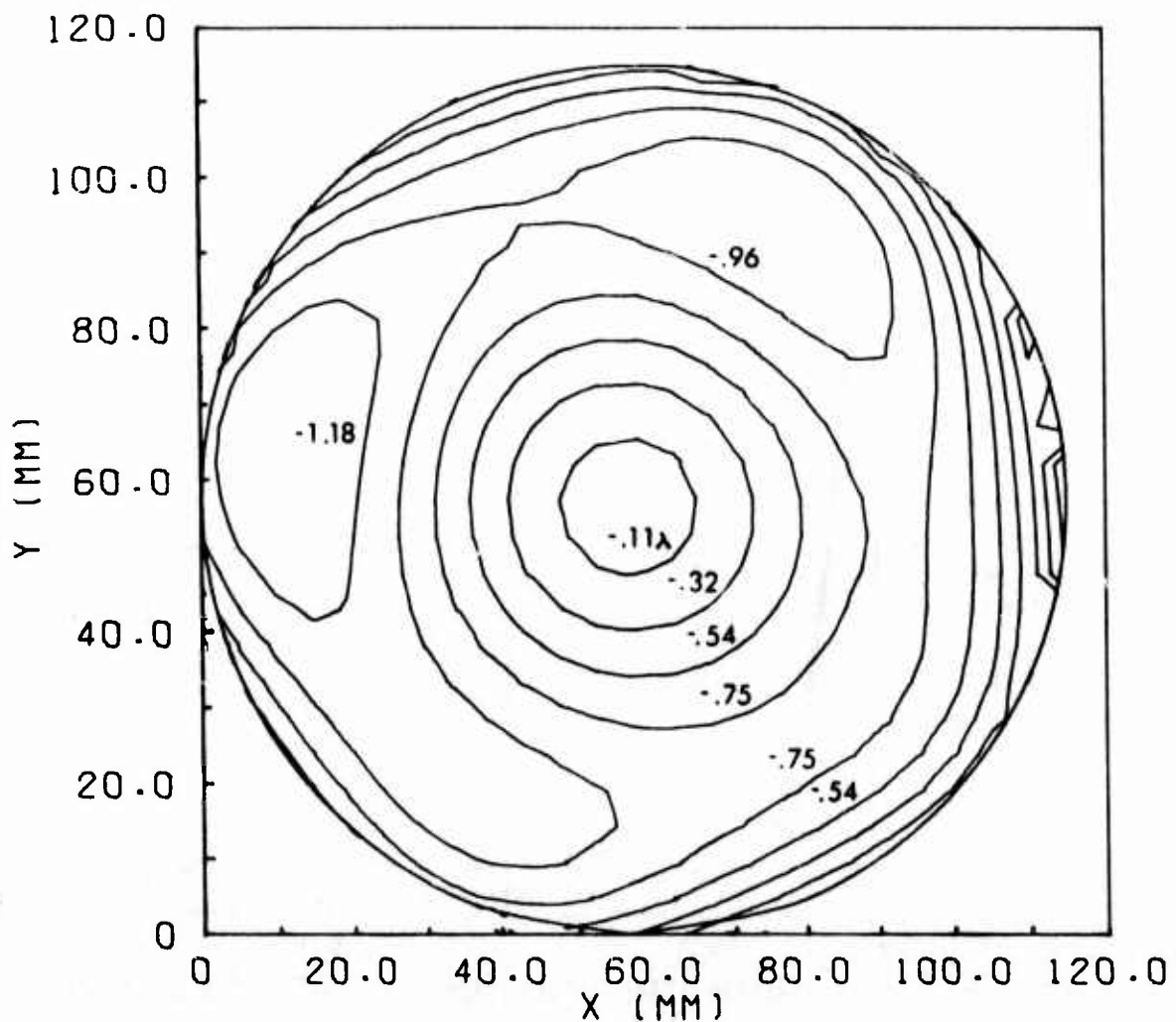
The pupil-function plot in figure 30(a) shows that there are both symmetrical and asymmetrical aberrations in the collimator. The maximum deviation of the wavefront is about  $2.1 \lambda$ , and the RMS of the wavefront is about  $\lambda/3$ . Inspection of table 7 shows that the net symmetrical aberration, which results from combining defect of focus and spherical aberration, is about  $-0.1 \lambda$ . The significant asymmetrical aberrations are third-order x coma ( $-0.6 \lambda$ ), third-order y coma ( $-0.4 \lambda$ ), and fifth-order y coma ( $0.3 \lambda$ ). The coma may arise from a decentration error [34] since the collimator was tested on axis, or at the center of the field, and coma arising from improper shape of the lens surface does not occur on axis. On the other hand, the astigmatism at the center of field does not result from decentration of the lens elements; this error results from imperfect lens surfaces.

The MTF for the diffraction-limited lens ( $\lambda = 546.1$  nm) with the same f-number as the collimator is also shown in figure 30(b). The large differences between the collimator and a diffraction-limited lens are readily apparent.

Isocontours of the MTF for the collimator are shown in figure 30(c). The zero value of spatial frequency occurs at the center of the lens aperture; the spatial-frequency values given along the coordinate axes apply to values along lens diameters drawn parallel to these axes.

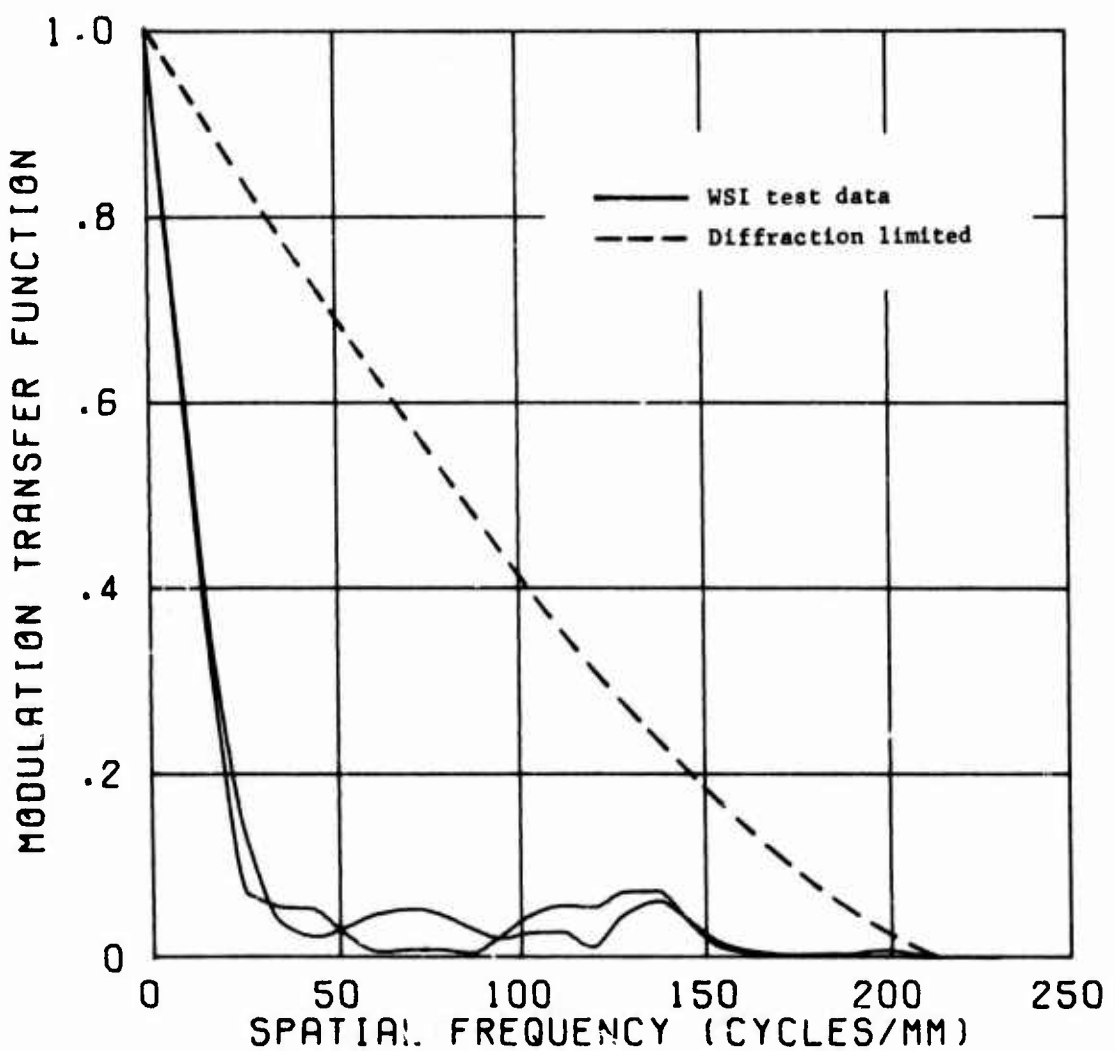
The PTF for the collimator is given in figure 30(d). However, as noted earlier in section VIII.3, the accuracy of these phase values is probably not very high since their calculation involved very small and rapidly changing values of the OTF. The isocontours of the PTF are shown in figure 30(e). The intricate pattern of this plot results, to some degree, from the same computational inaccuracies indicated above. However, this plot does illustrate the ability of the test system and data-reduction program to handle a lens with a rapidly varying OTF.

Since the collimator performance was found to be considerably less than diffraction limited, it was returned to the supplier. Follow-up testing by the supplier confirmed the test results obtained with the WSI test system.



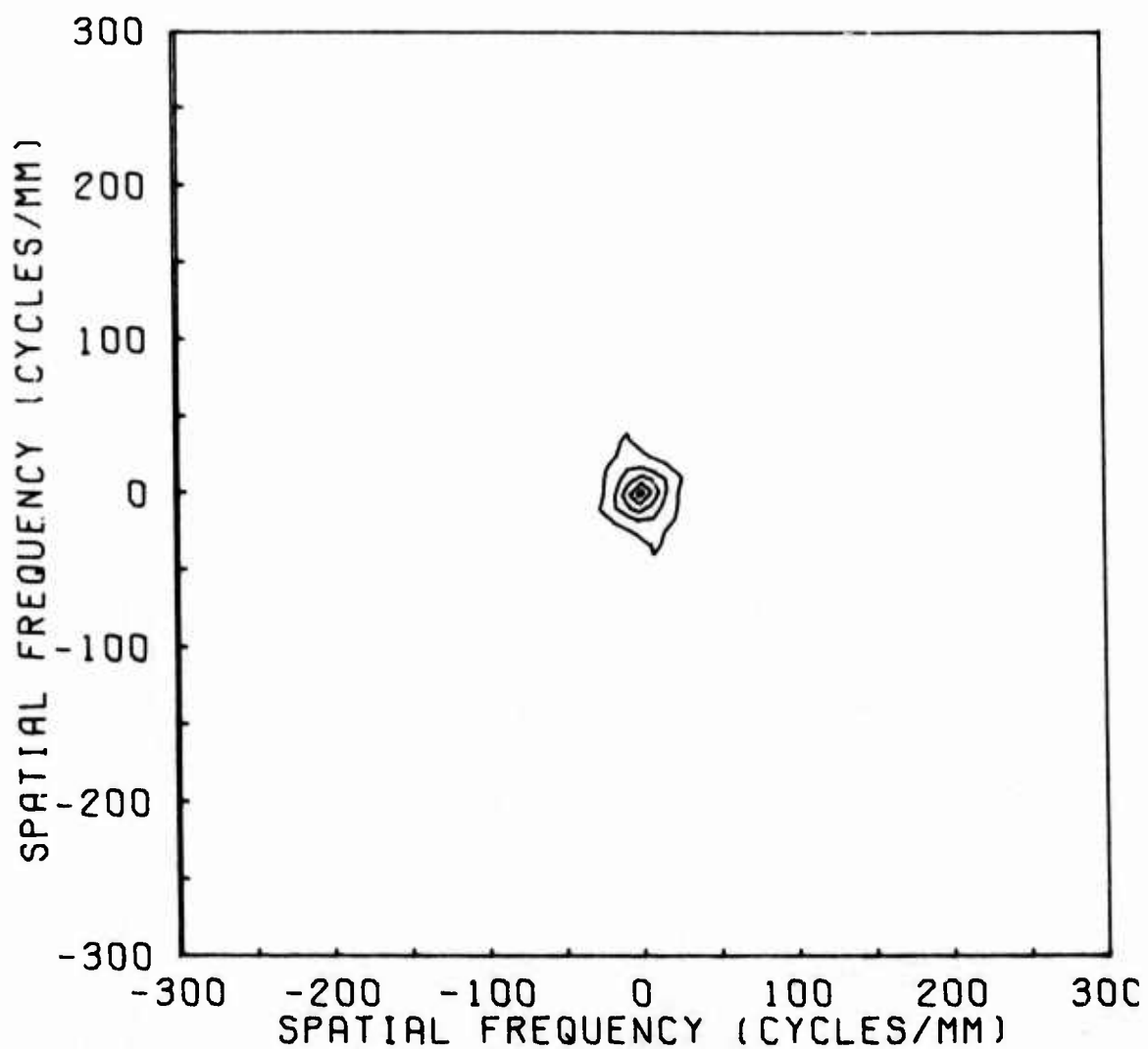
(a) Isocontours of pupil-function phase.

Figure 30.- On-axis WSI test results in plane of best focus for f/8.7 collimating doublet (collimator A);  $\lambda = 546.1$  nm.



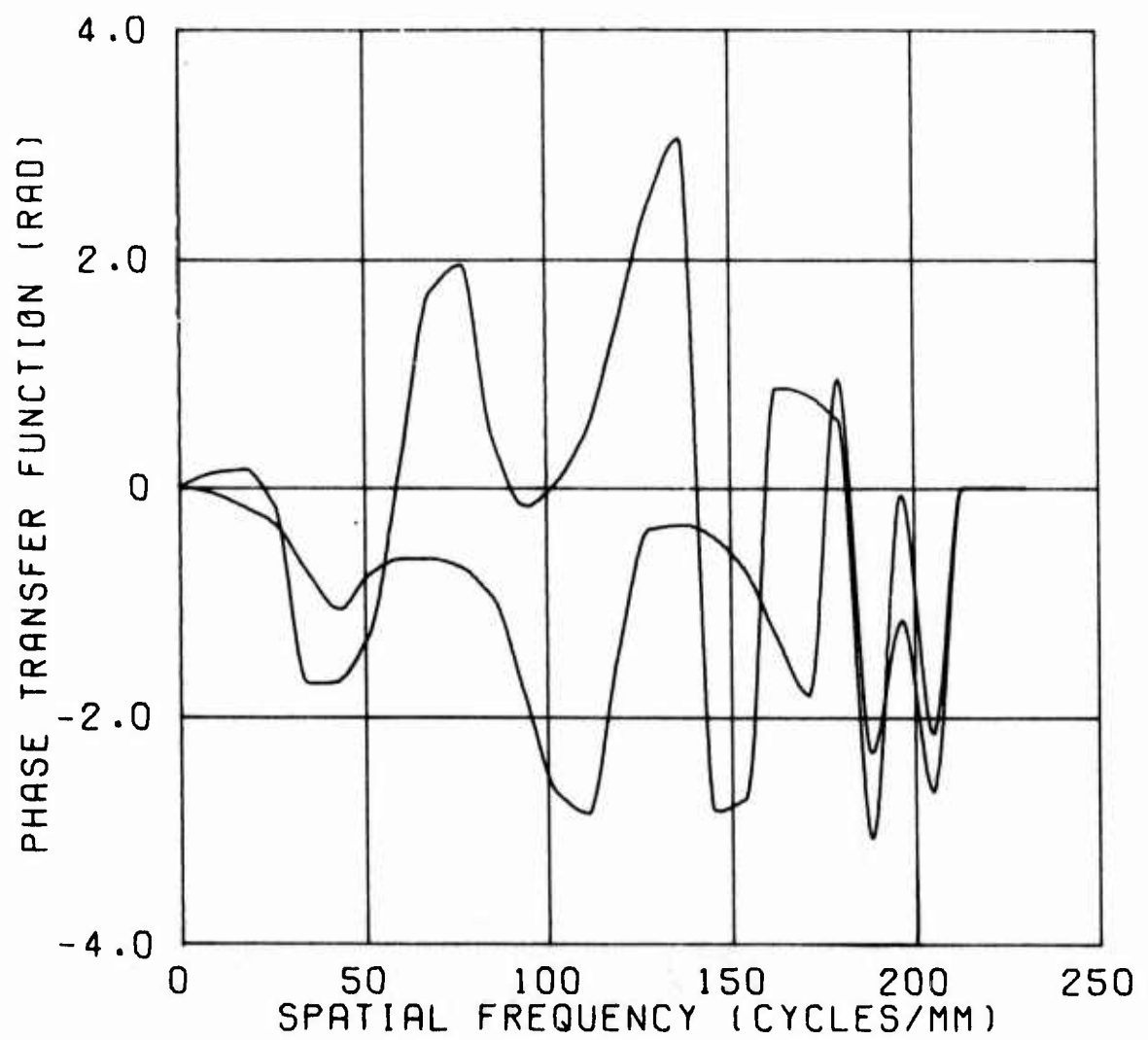
(b) Tangential and sagittal MTF.

Figure 30.- Continued.



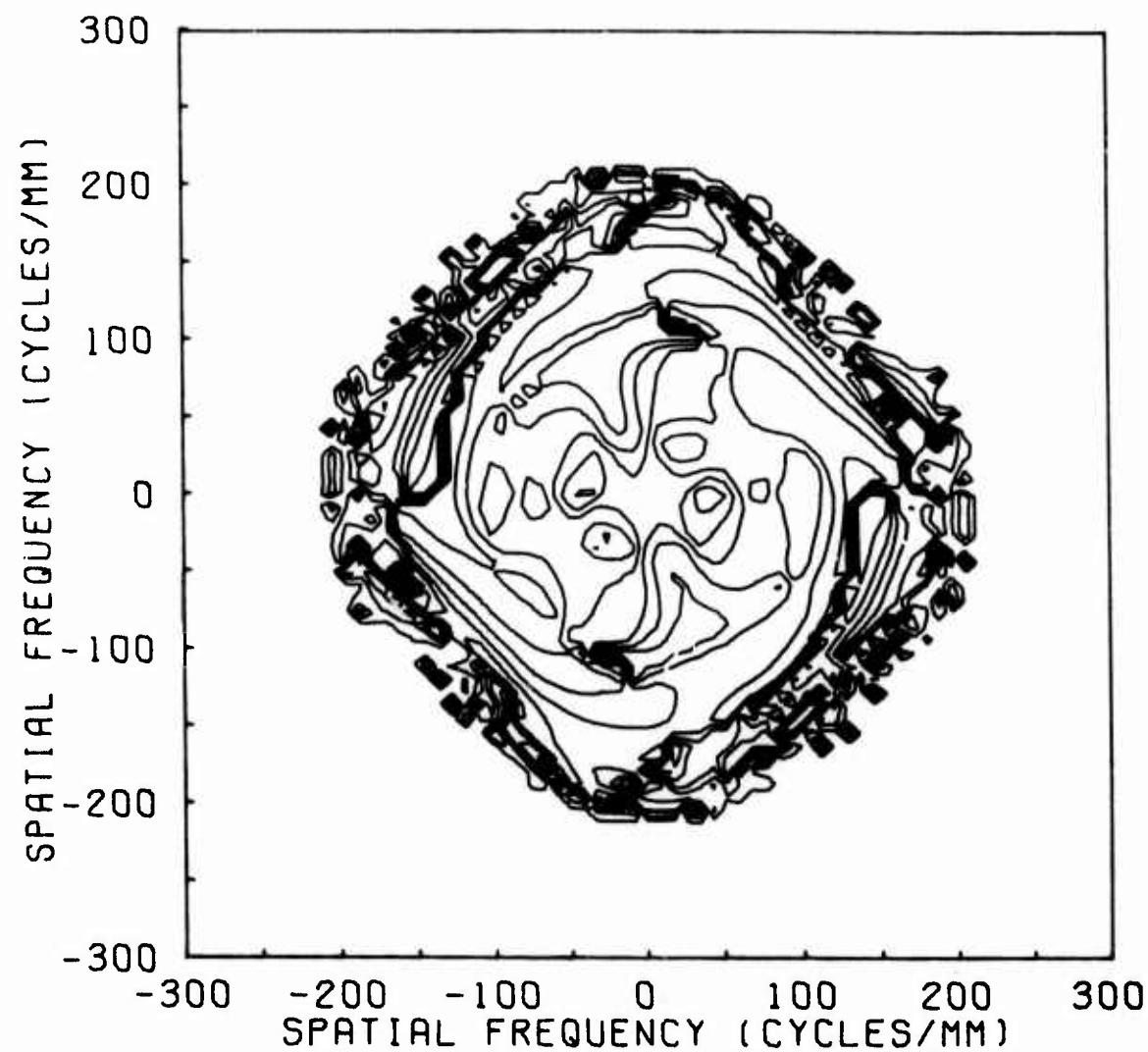
(c) Isocontours of MTF.

Figure 30.- Continued.



(d) Tangential and sagittal PTF.

Figure 30.- Continued.



(e) Isocontours of PTF.

Figure 30.- Concluded.

TABLE 7. - MAXIMUM ABERRATIONS FOR f/8.7 COLLIMATING  
DOUBLET (COLLIMATOR A)<sup>a</sup>

n	Maximum aberrations, units of $\lambda$	Type
4	-4.821	focus
5	-.1062	0° astigmatism
6	.2080	45° astigmatism
7	.6441	x coma (3rd)
8	-.3685	y coma (3rd)
9	.2209	x clover (3rd)
10	-.1603	y clover (3rd)
11	7.1699	3rd spherical
12	.1365	0° astigmatism (5th)
13	.1297	45° astigmatism (5th)
14	.0336	
15	.2568	
16	.1390	x coma (5th)
17	.3120	y coma (5th)
18	-.0188	x clover (5th)
19	-.1405	y clover (5th)
20	.1164	
21	.0155	
22	-3.8634	5th spherical
23	1.4013	7th spherical

<sup>a</sup>In plane of best focus;  $\lambda = 546.1$  nm.

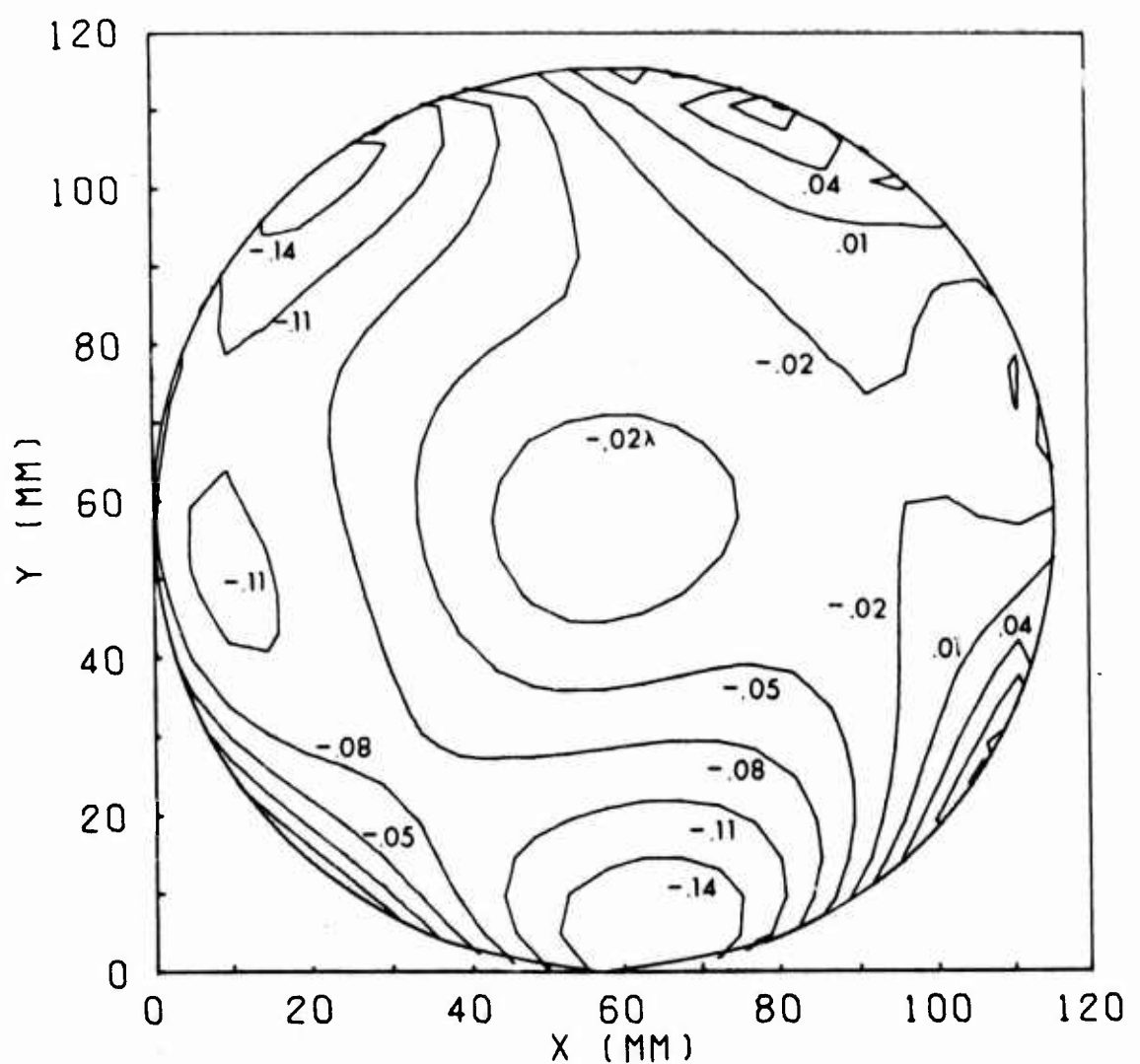
## XII.2. Collimator B

This collimator has the same nominal f-number of f/8.7 and effective focal length of 1 m as the previous collimator. The supplier of collimator B also reported this collimator to be diffraction limited over a 1.9-cm (0.75 in.) field of view ( $1.1^\circ$ ) from 510 nm to 610 nm.

Collimator B was also tested at infinite conjugates as shown in figure 3. However, for this collimator, a 15-mW He-Ne laser ( $\lambda = 632.8$  nm) with a beam expander and 16- $\mu\text{m}$ -diameter pinhole was used. An initial attempt to use the filtered mercury-arc lamp with a 10- $\mu\text{m}$ -diameter pinhole, rather than the 100- $\mu\text{m}$ -diameter pinhole used earlier, was made. The diameter of the Airy disc [35] for a diffraction-limited f/8.7 lens is about 12  $\mu\text{m}$ ; therefore, a 100- $\mu\text{m}$ -diameter pinhole may lead to off-axis illumination. In any case, sufficient energy for reasonably short photographic exposures was not available with the mercury-arc lamp and the 10- $\mu\text{m}$ -diameter pinhole. A special effort was made to keep the collimator and test-system components free of dust which might cause spurious fringe patterns in laser illumination. An improved nodal slide, which offered finer controls for lens alignment, was used. The same cube interferometer with  $\phi = 4.55$  mrad was used. The resulting pupil function, MTF's, and PTF's for the plane of best focus are shown in figure 31. Table VIII lists the resulting maximum aberrations.

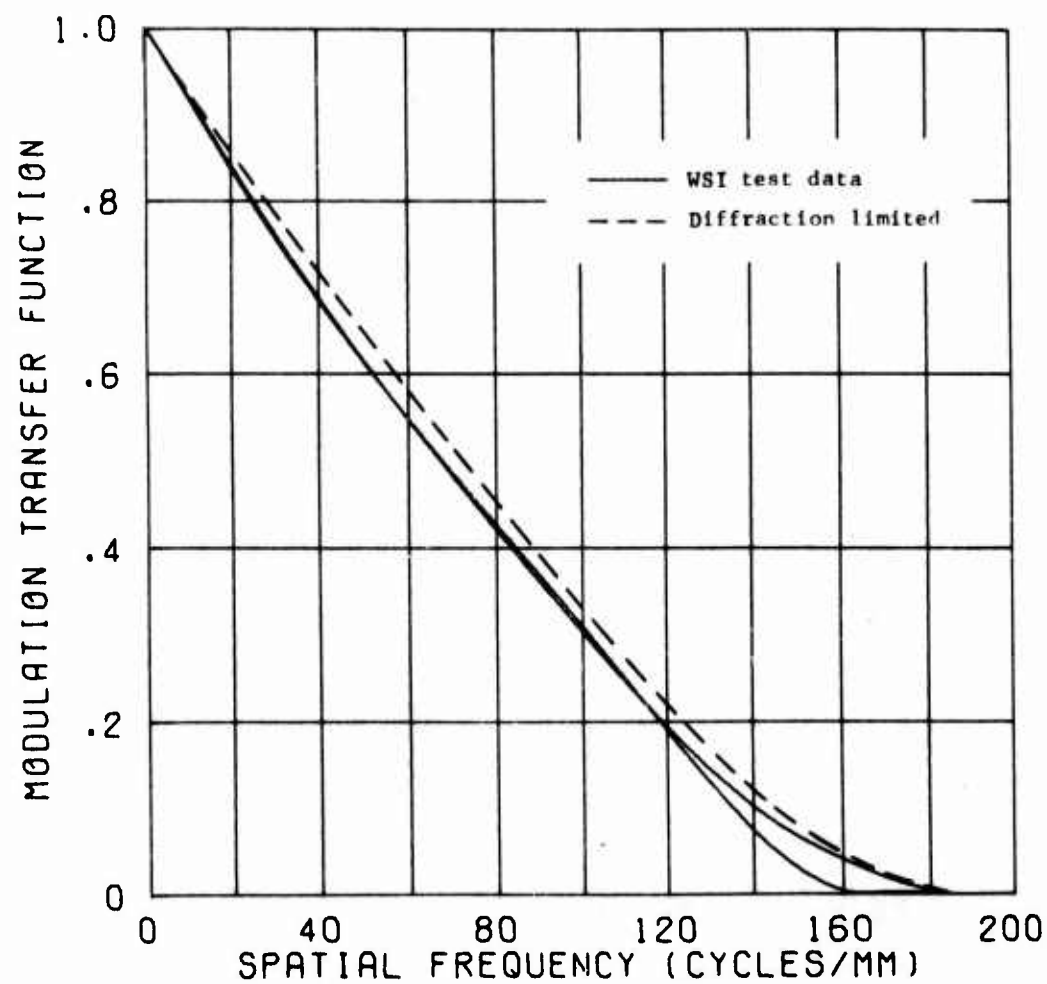
Figure 31(a) shows that the pupil function exhibits primarily asymmetrical aberrations. The net result of the symmetrical aberrations listed in table 8 is about  $-0.01\lambda$ . The primary asymmetrical aberrations appear to be x and y coma (third and fifth-order). The maximum value for each of these aberrations is about  $\pm 0.2\lambda$ ; this value is also the maximum deviation of the wavefront which has an RMS of  $\lambda/21$ . As noted in the previous section, this coma, which occurs on axis, may be due to a decentration error, i.e., one or both lens elements in the collimator doublet may not be centered exactly. The effective focal length for the plane of best focus was determined to be 999.566 mm.

The MTF for diffraction-limited performance of an f/8.7 lens is shown in figure 31(b) along with the test results for collimator B. A comparison shows that the collimator is slightly below diffraction-limited performance. However, it should be remembered that the collimator was tested at  $\lambda = 632.8$  nm which is outside of the wavelength range (510 nm to 610 nm) in which the supplier reported the collimator to be diffraction limited. The tangential and sagittal MTF's are nearly identical up to a spatial frequency of about 120 cycles/mm. Thus, even though the pupil function is primarily asymmetric, the magnitude of these asymmetrical aberrations is sufficiently small such that the MTF appears to be somewhat



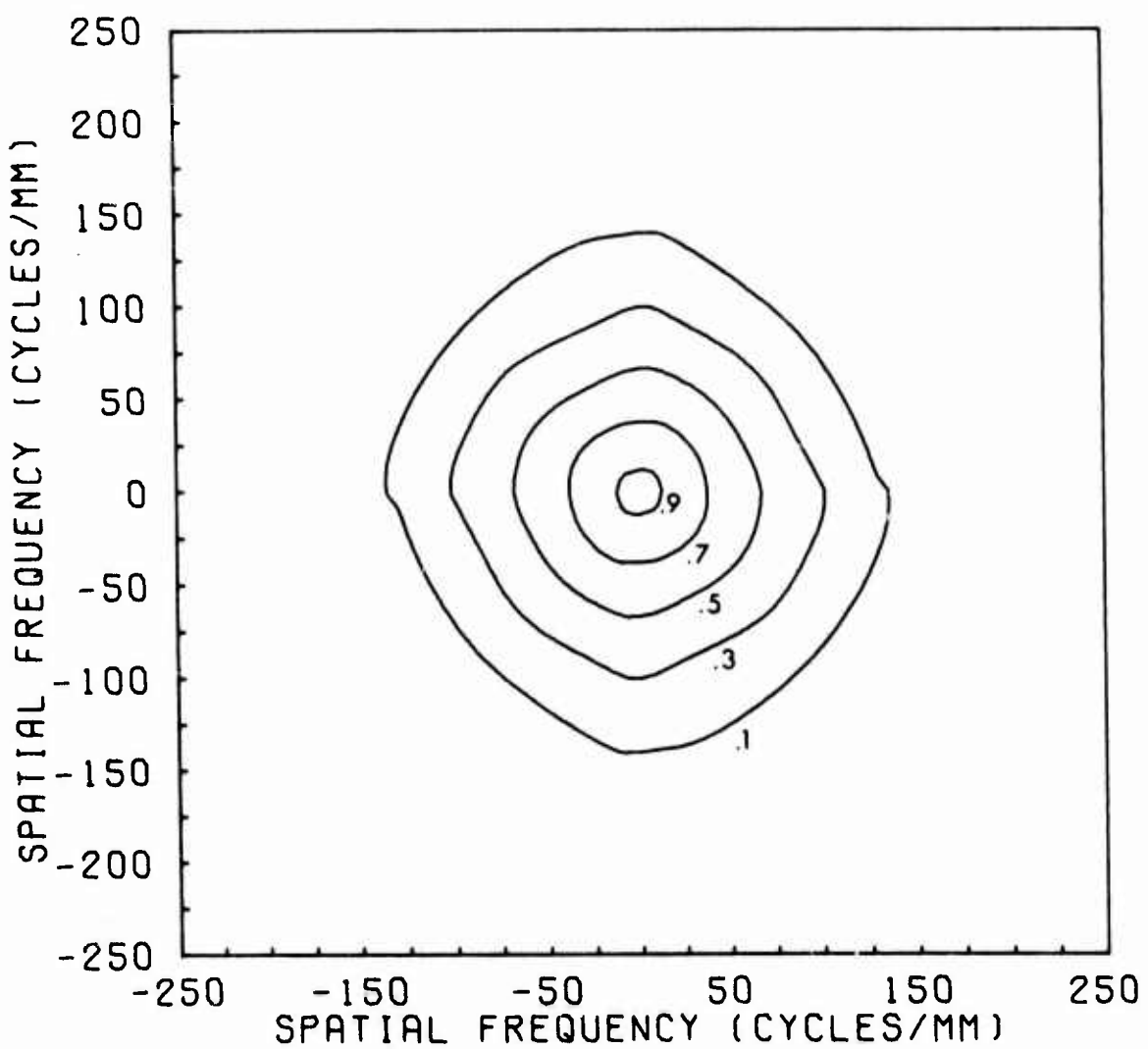
(a) Isocontours of pupil-function phase.

Figure 31.- On-axis WSI test results in plane of best focus for f/8.7 collimating doublet (collimator B);  $\lambda = 632.8$  nm.



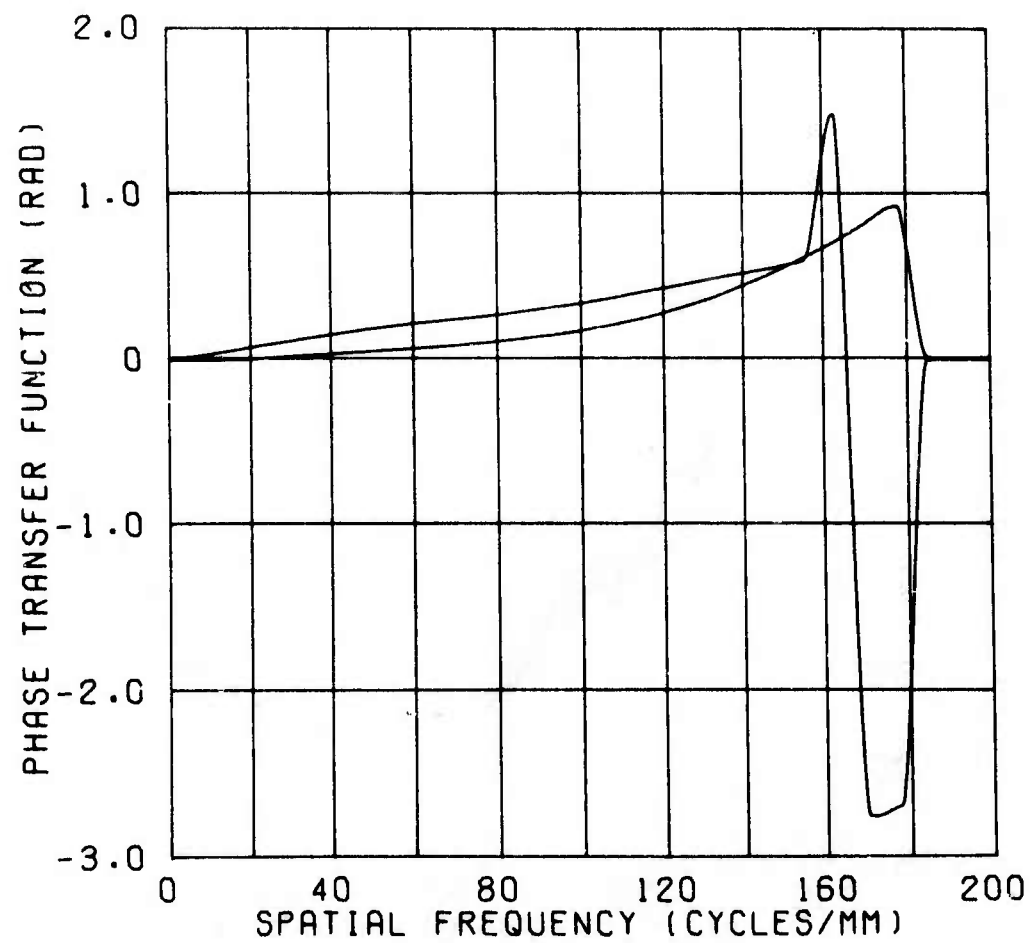
(b) Tangential and sagittal MTF.

Figure 31.- Continued.



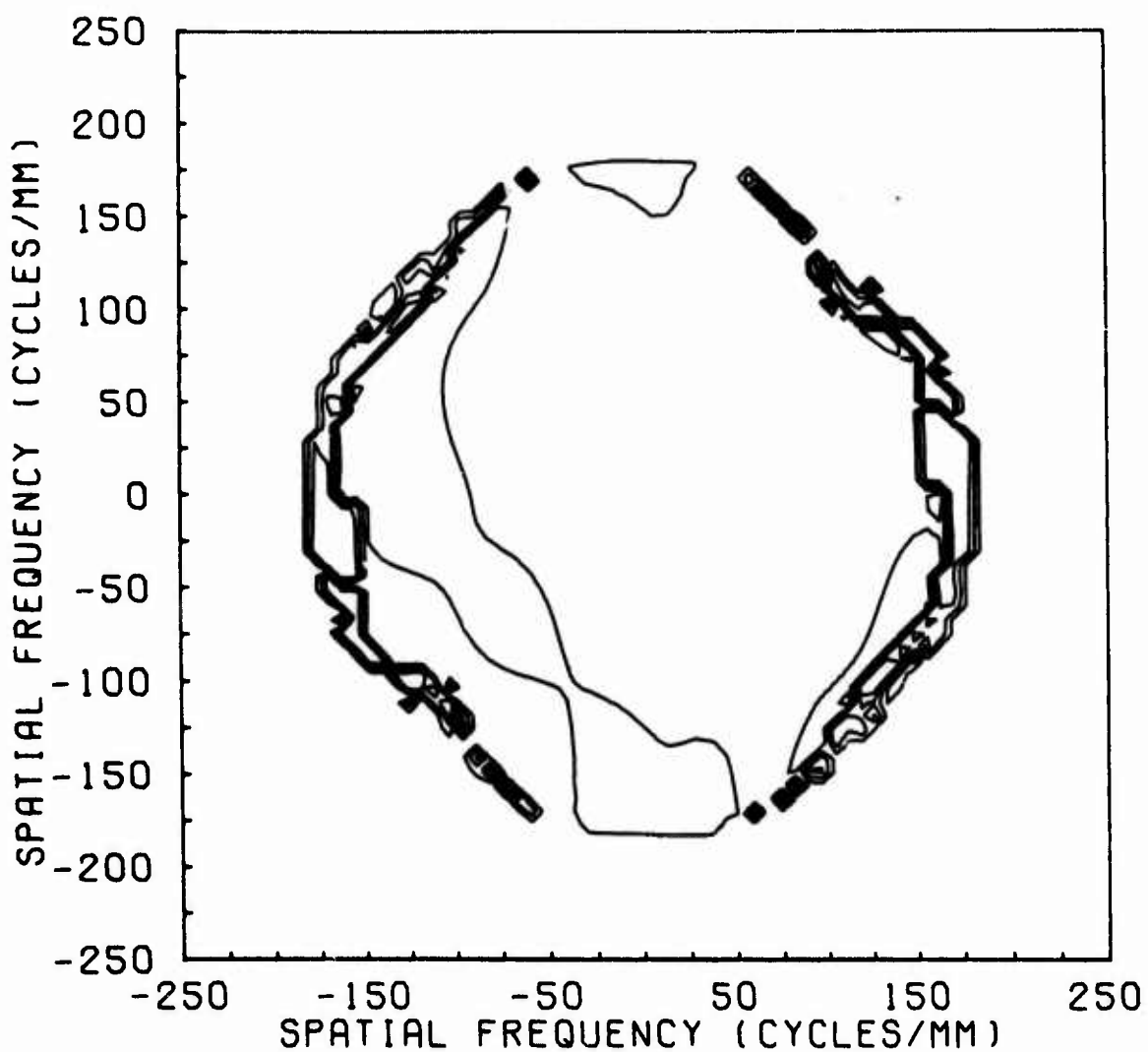
(c) Isocontours of MTF.

Figure 31.- Continued.



(d) Tangential and sagittal PTF.

Figure 31.- Continued.



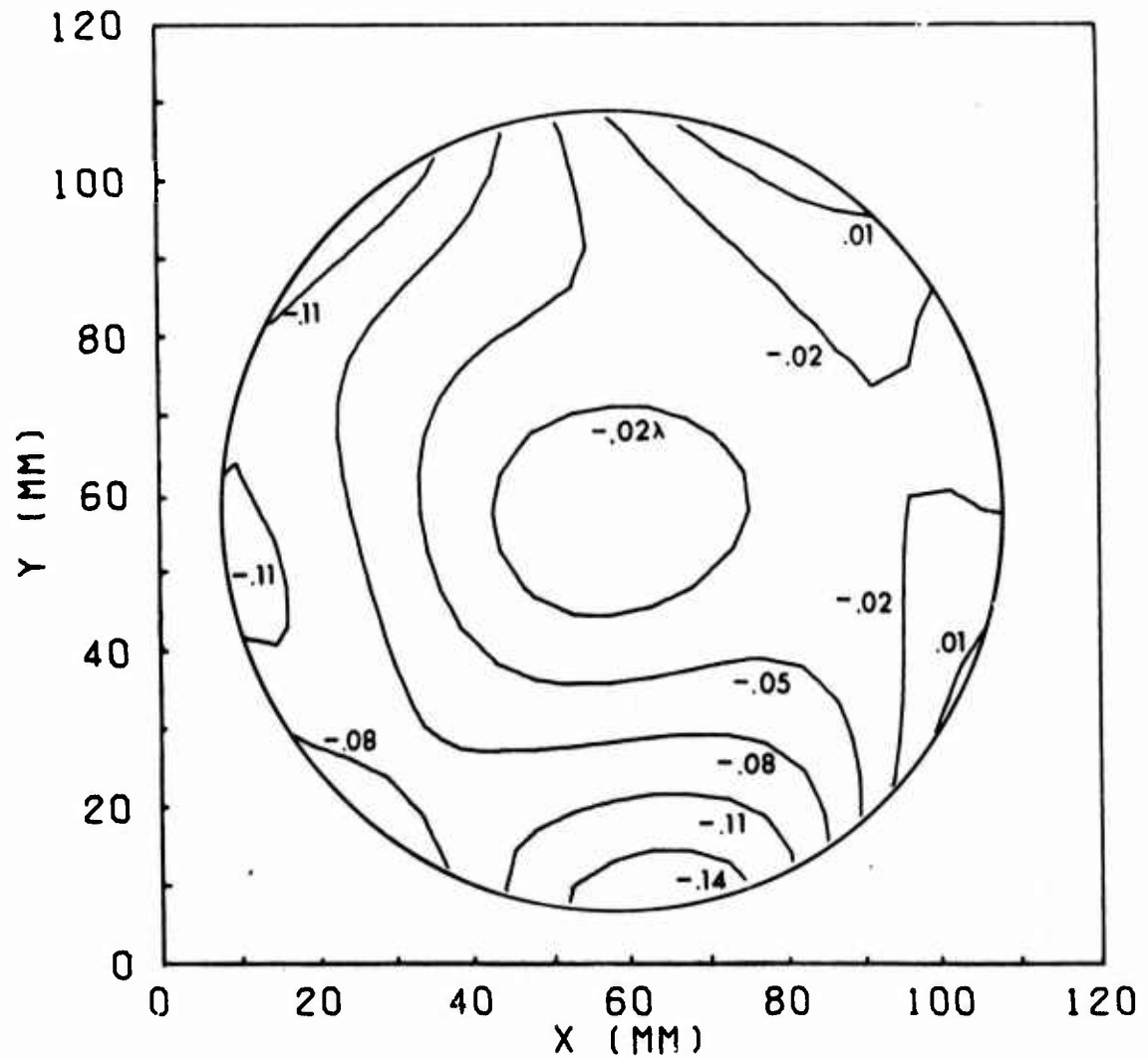
(e) Isocontours of PTF.

Figure 31.- Concluded.

TABLE 8. - MAXIMUM ABERRATIONS FOR f/8.7 COLLIMATING  
DOUBLET (COLLIMATOR B)<sup>a</sup>

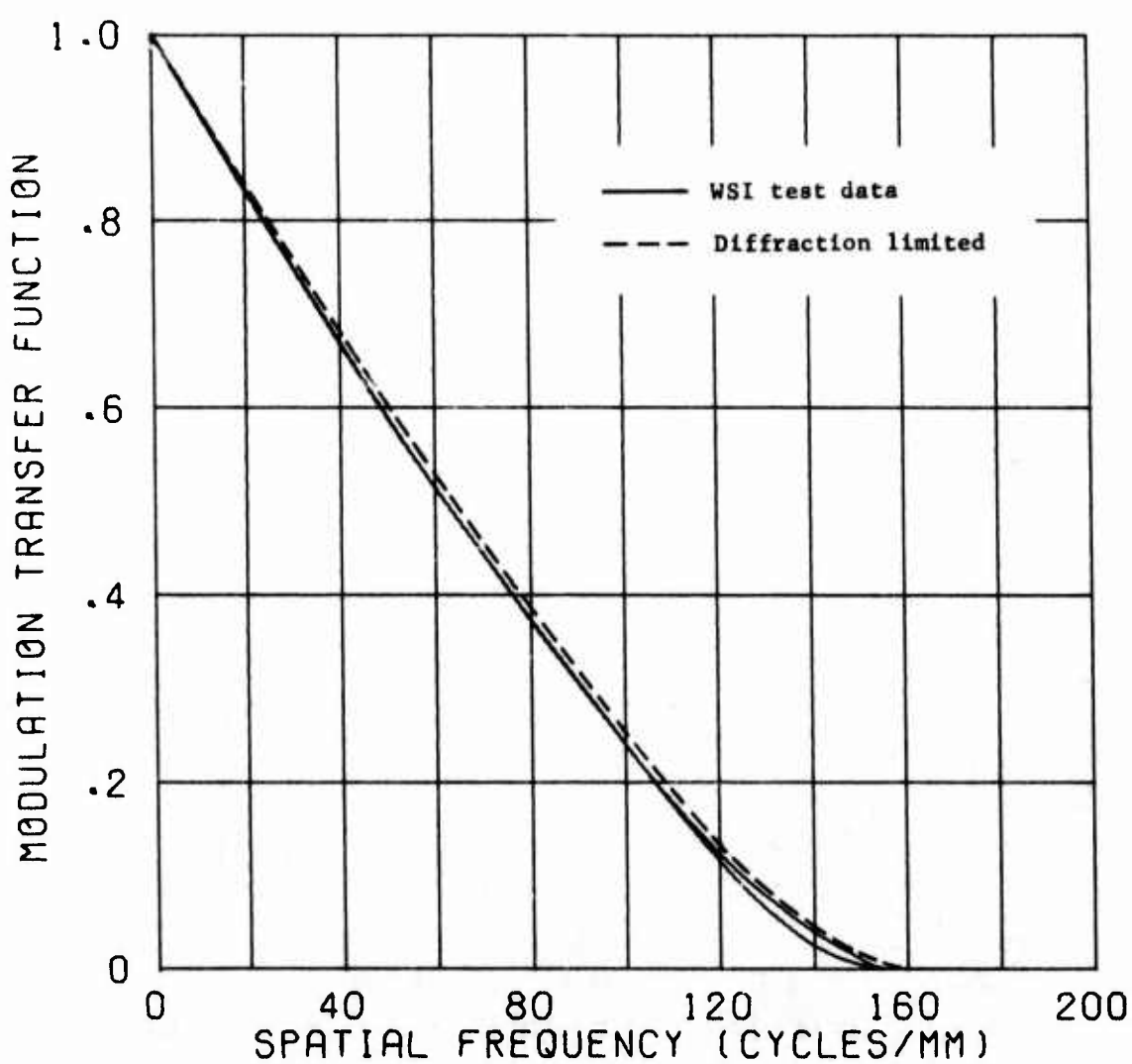
n	Maximum aberrations, units of $\lambda$	Type
4	- .395	
5	.0391	focus
6	.0097	0° astigmatism
7	.1796	45° astigmatism
8	.1781	x coma (3rd)
9	.0463	y coma (3rd)
10	.0111	x clover (3rd)
11	- .9927	y clover (3rd)
12	- .0304	3rd spherical
13	.0328	0° astigmatism (5th)
14	- .0265	45° astigmatism (5th)
15	- .0526	
16	- .1372	x coma (5th)
17	- .1907	y coma (5th)
18	- .0658	x clover (5th)
19	- .0877	y clover (5th)
20	- .0053	
21	.0165	
22	-1.2698	5th spherical
23	.6658	7th spherical

<sup>a</sup>In plane of best focus;  $\lambda = 632.8$  nm.



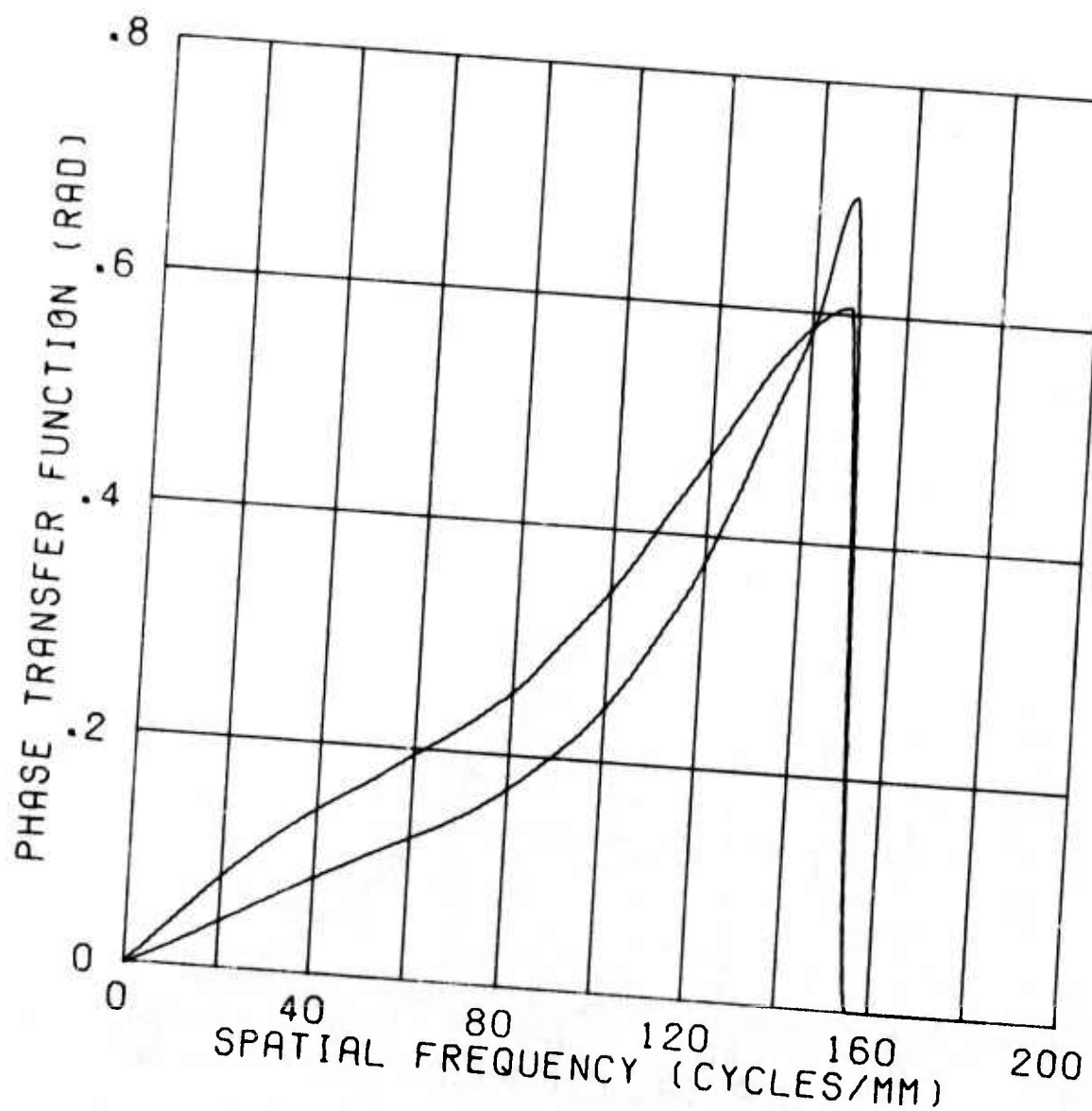
(a) Isocontours of pupil-function phase.

Figure 32.- On-axis WSI test results in plane of best focus for f/8.7 collimating doublet (collimator B) stopped down to f/10;  
 $\lambda = 632.8$  nm.



(b) Tangential and sagittal MTF.

Figure 32.- Continued.



(c) Tangential and sagittal PTF.

Figure 32.- Concluded.

TABLE 9. - MAXIMUM ABERRATIONS FOR f/8.7 COLIMATING  
DOUBLET (COLLIMATOR B) STOPPED DOWN TO f/10<sup>a</sup>

n	Maximum aberrations, units of $\lambda$	Type
4	- .237	focus
5	.0293	0° astigmatism
6	.0073	45° astigmatism
7	.1164	x coma (3rd)
8	.1154	y coma (3rd)
9	.0300	x clover (3rd)
10	.0072	y clover (3rd)
11	.5568	3rd spherical
12	- .0170	0° astigmatism (5th)
13	.0184	45° astigmatism (5th)
14	- .0149	
15	- .0295	
16	- .0666	x coma (5th)
17	- .0926	y coma (5th)
18	- .0320	x clover (5th)
19	- .0425	y clover (5th)
20	- .0026	
21	.0080	
22	- .5334	5th spherical
23	.2095	7th spherical

<sup>a</sup>In plane of best focus;  $\lambda = 632.8$  nm.

rotationally symmetric. This relative symmetry of the MTF is shown in the MTF isocontours plotted in figure 31(c).

The PTF for collimator B is given in figure 31(d). The differences in the tangential and sagittal PTF's are more pronounced than the differences in the corresponding MTF's. The isocontours of the PTF are plotted in figure 31(e).

Since collimator B was within a few percent of the diffraction-limited MTF, it was accepted. However, additional testing of the collimator on the WSI system to determine performance within the spectral region of 510 nm to 610 nm is planned. The collimator is used in the WSI test system to provide a collimated light beam for testing other lenses at infinite conjugates. Since the aberrations in the collimator are largest at the aperture edge, the full aperture is not used. In particular, the maximum aperture diameter used is about 10 cm or about 75 percent of the clear aperture; this is equivalent to stopping down the collimator from f/8.7 to f/10.

The performance of a lens at a greater f-number than that used in the WSI test system can be determined with the data-reduction computer program. (See appendix A.) The same test data, except for the original radius the test-lens aperture, is used as input data. The new value chosen for the radius corresponds to the modified f-number. In this case, the maximum value of the aberrations, the pupil function, and the OTF are for the stopped-down version of the test lens. For collimator B stopped down to f/10, the pupil function, MTF, PTF, and aberrations are shown in figures 32(a), 32(b), 32(c), and table 9, respectively. The resulting MTF is only about 1 percent below diffraction-limited performance up to 120 cycles/mm. The net sum of the symmetrical aberrations is  $-0.004\lambda$ , and the maximum value of the asymmetrical aberrations is about  $+0.1\lambda$ . The RMS of the wavefront is  $\lambda/29$ , and the effective focal length is 999.536 cm.

### XII.3. OTF Standard Test Lens

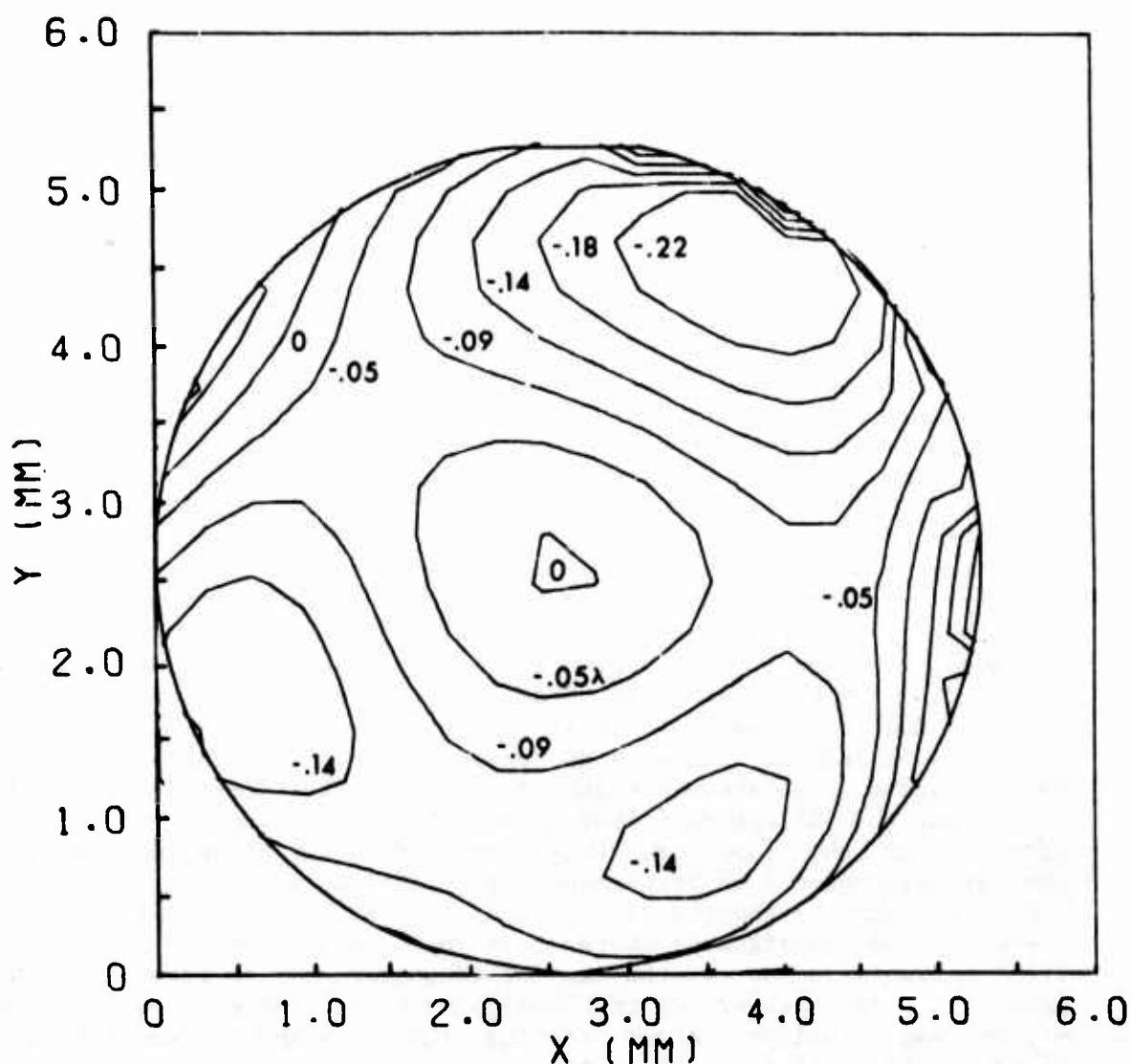
The OTF Standard Test Lens was designed and developed by SIRA, Chislehurst, Kent, England, as a test standard for OTF equipment. The results of OTF measurements on one of these lenses by various laboratories throughout the world are presented in reference 36. This lens is a simple planoconvex lens with a nominal thickness of 10 mm, a nominal diameter of 28 mm, and a nominal focal length of 50 mm. For the present tests, the lens was stopped down to f/8, thereby giving a lens diameter of  $5.30 \pm 0.025$  mm. With this stop plane located 1.0 mm behind the plane surface of the lens, the image distance  $z_2$  was 42.0 mm.

The OTF Standard Lens was tested at infinite conjugates by locating the light source about 4 m from the lens. This separation was accomplished by folding the optical path along the 2.75-m length test bench. The resulting test system was basically the system shown in figure 3 except that the test lens was located between the pellicle and interferometer cube; furthermore, the test system was single pass. A 100-W mercury-arc lamp with a monochromatic filter ( $\lambda = 546.1$  nm), condensing optics, and a nominally 100- $\mu\text{m}$ -diameter pinhole were used for the light source. A cube interferometer with  $\phi = 4.55$  mrad was used.

The first test results showed an MTF performance significantly below (as large as 25 percent) published values. Since this lens was particularly difficult to align using the Boys'-point method, it appeared that alignment errors may have been significant. The OTF Standard Lens is planoconvex with a relatively short focal length and, therefore, shows only one visible Boys'-point or subsidiary image. For this reason, a different alignment technique, which uses the one subsidiary image, a lens image of crosshairs, and a reflection from the front plane surface of the lens was devised. With this technique, the lens appeared to be centered when viewed through an alignment telescope; the supplier states that the lens optical axis is within 0.025 mm of the geometrical center of the lens aperture. However, the test-lens mount still did not have sufficient control for aligning the lens within the high degree of accuracy required for on-axis testing. An improved nodal slide for the test lens was obtained only after the OTF Standard Test Lens, which was on loan, had to be returned to the supplier; this improved nodal slide was used for testing collimator B as discussed in the previous section. Therefore, the test data presented in this section may contain slight errors stemming from misalignment of the test lens. Also, errors resulting from misregistration of the two interferograms may be present in the test data. An improved set of fiducial marks to reduce registration errors was developed after testing the OTF Standard Test Lens and prior to the testing of collimator B.

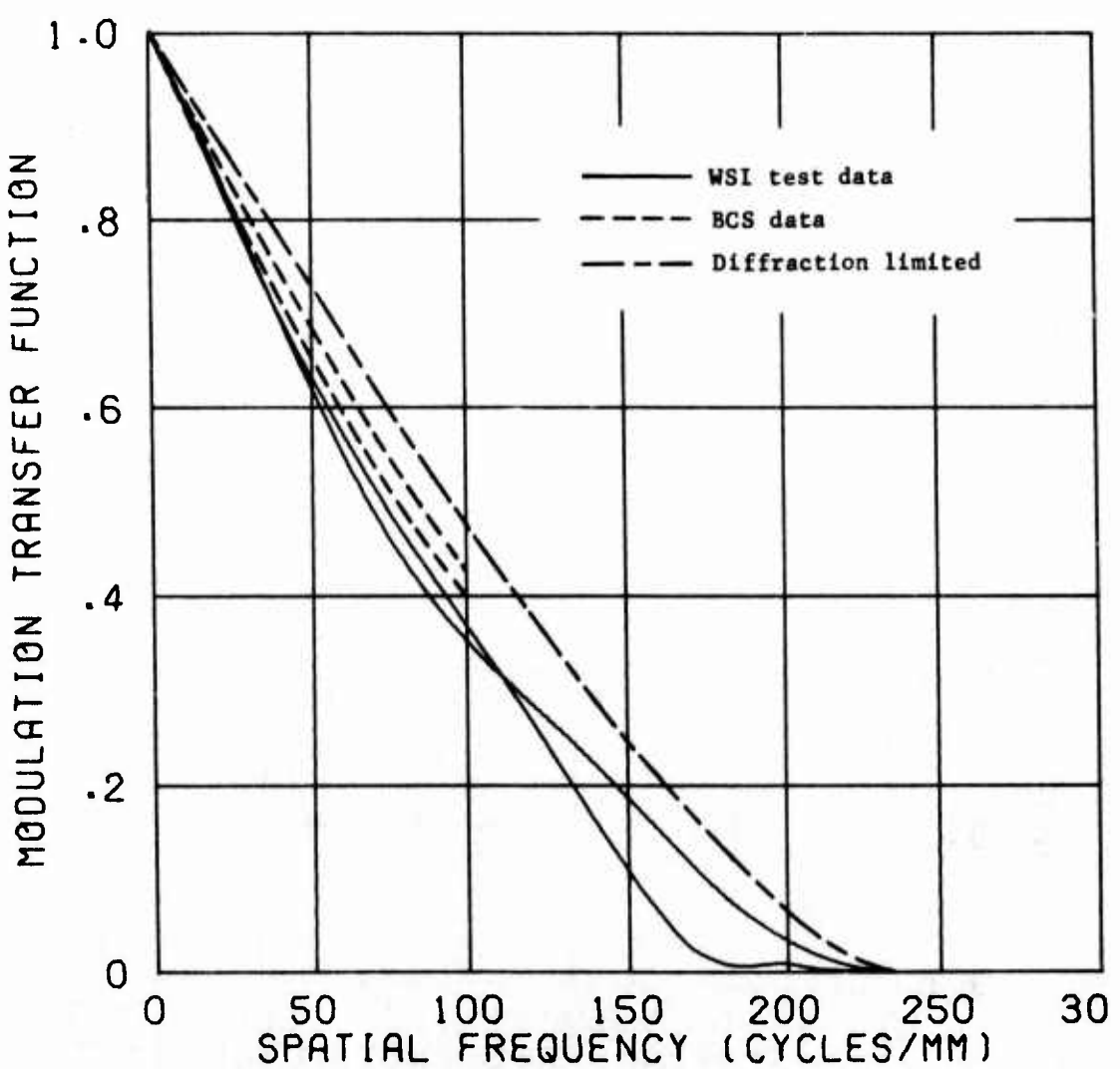
The resulting pupil function, MTF's, and PTF's for the plane of best focus are shown in figure 33. Table 10 lists the resulting maximum aberrations.

As shown in figure 33(a), the pupil function is asymmetric. The largest asymmetrical aberrations are x-coma (third and fifth-order) and x-clover (third and fifth-order); each of these aberrations has a maximum value of  $0.09 \lambda$  to  $0.17 \lambda$ . In reference 36, it is noted that with the stop positioned 1 mm from the plane surface of the OTF Standard Test Lens, coma is almost a minimum and, as a result, there is very little variation in the PTF as one goes off axis.



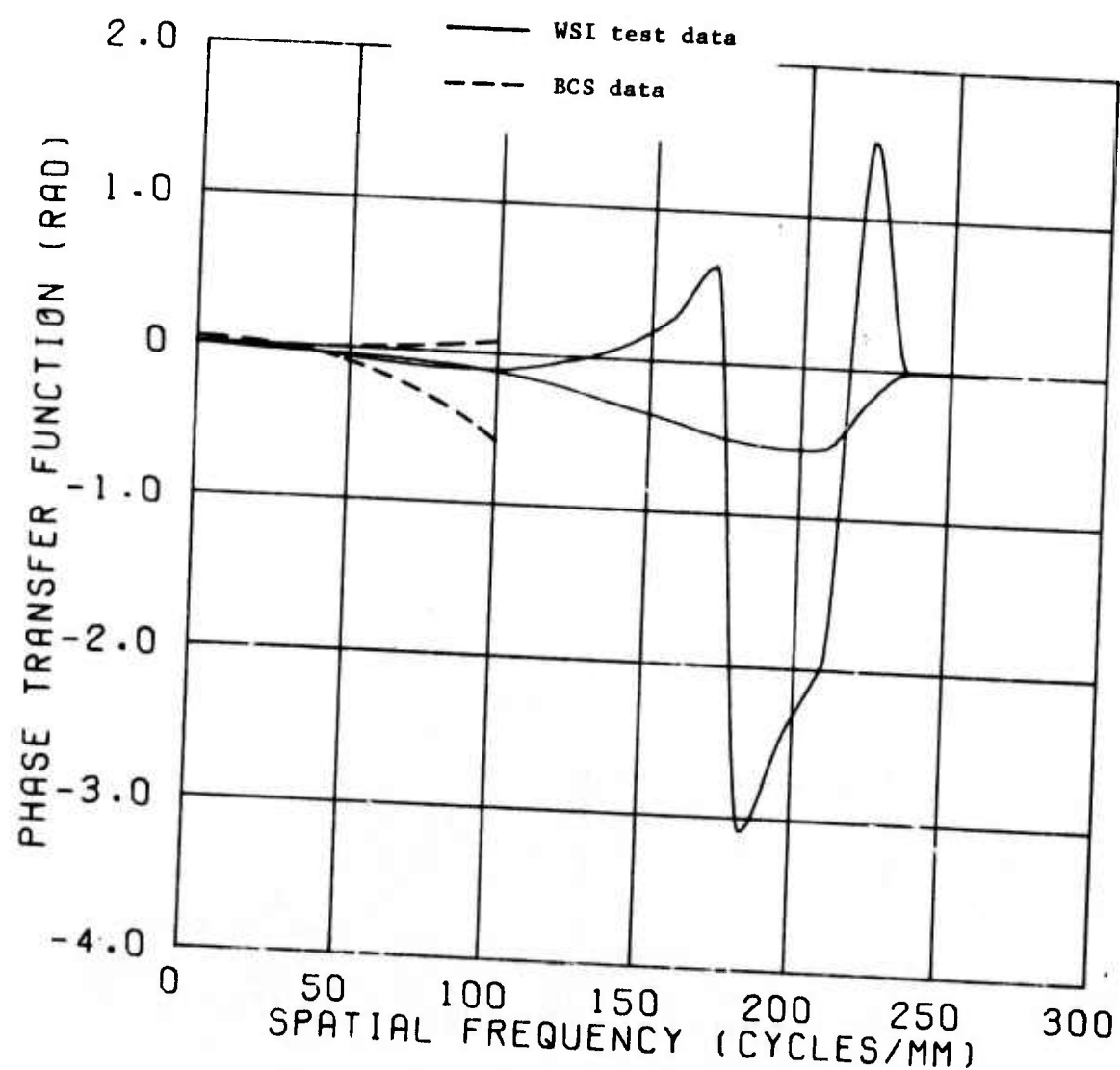
(a) Isocontours of pupil-function phase.

Figure 33.- On-axis WSI test results in plane of best focus for f/8  
OTF Standard Test Lens;  $\lambda = 546.1$  nm.



(b) Tangential and sagittal MTF.

Figure 33.- Continued.



(c) Tangential and sagittal PTF.

Figure 33.- Concluded.

TABLE 10. - MAXIMUM ABERRATIONS FOR f/8 OTF STANDARD TEST LENS<sup>a</sup>

n	Maximum aberrations, units of $\lambda$	Type
4	- .618	focus
5	.0119	0° astigmatism
6	.0092	45° astigmatism
7	- .1717	x coma (3rd)
8	.0403	y coma (3rd)
9	.1919	x clover (3rd)
10	.0500	y clover (3rd)
11	1.0444	3rd spherical
12	- .0178	0° astigmatism (5th)
13	.0581	45° astigmatism (5th)
14	.0314	
15	- .0839	
16	.2356	x coma (5th)
17	.0363	y coma (5th)
18	- .1485	x clover (5th)
19	- .0376	y clover (5th)
20	.0161	
21	.0273	
22	- .6480	5th spherical
23	.1919	7th spherical

<sup>a</sup>In plane of best focus;  $\lambda = 546.1$  nm.

Therefore, assuming that minimum coma should be well below the  $0.17 \lambda$  determined from the present test data and that coma does not increase significantly for slightly off-axis positions, the measured value of coma would not be expected from the possible lens misalignment discussed earlier. The maximum deviation of the wavefront is about  $0.3 \lambda$ , and the RMS of the wavefront is  $\lambda/14$ . The effective focal length, as measured from the stop plane rather than the second principal plane, is 41.658 mm.

In figure 33(b) the MTF for diffraction-limited performance of an f/8 lens and the MTF of the OTF Standard Test Lens as measured by the British Calibration Service (BCS) are given along with the MTF measured on the WSI test system. Both of the measured MTF's show that the lens is not diffraction limited. The differences between the tangential and sagittal MTF's are greater for the BCS data than the WSI data. Assuming that the MTF is not symmetric as these data show, these differences would be expected since the lens orientation about the optical axis was most likely not the same setting in the two test systems, i.e., the tangential and sagittal directions for the two sets of test data are not the same. The manufacturer of the OTF Standard Test Lens claims that the lens orientation about the test-system optical axis is unimportant since the lens has been constructed with a high degree of precision. However, as the measured MTF's show, the lens does exhibit asymmetry. It should be noted that the BCS test data does not extend beyond 100 cycles/mm, but the WSI test data continues out to the test-lens cut-off frequency. The WSI test system, unlike some other OTF-measurement systems, does not use an illuminated target of varying spatial frequency which is imaged by the test lens. Therefore, the WSI test system does not depend on the quality of the target or the degree of coherence of the target illumination; these factors can introduce OTF-measurement errors in the associated test systems, particularly at spatial frequencies beyond 100 cycles/mm [37]. The fairly large differences in the tangential and sagittal MTF's above 100 cycles/mm for the WSI test data may be due in part to lens misalignment or interferogram misregistration as discussed earlier.

The PTF's for the OTF Standards Lens as measured in the present tests and as measured by the BCS are given in figure 33(c). The closer agreement between tangential and sagittal values for the WSI test results as compared to the BCS test results is quite evident. The large differences in the tangential and sagittal PTF's in the vicinity of 100 cycles/mm for the WSI test data, like the MTF's, may in part result from lens misalignment or interferogram misregistration.

### XIII. COMPUTER PROGRAMS

The computer software for use with data from the WSI system consists of three programs to perform the following tasks: (1) reduction of fringe data to determine lens aberrations, pupil function, and OTF; (2) plotting of pupil function, MTF, and PTF; and (3) reduction of optical-density data from automatic fringe scanner to determine fringe-peak locations and lens aperture boundary. These programs are written in FORTRAN V for the Univac 1100 series computer systems. Some changes may be required to use these programs on other computer systems. A flow diagram of the complete data-reduction procedure for the WSI interferograms, including the computer programs, is given in figure 34.

An outline of the program operations, a tabulation of input and other variables, and a computational listing are presented for each of the three programs in appendices A, B, and C; sample printouts for the programs discussed in appendices A and B are also given. Other auxiliary program variables and parameters are also defined in these appendices, but no attempt has been made to define every alphanumeric quantity such as indexing parameters and dummy variables. The program listing contains comment cards which further define program variables and explain program operations.

Table 11 gives the approximate computer words required to execute the latest versions of the data reduction and plotting programs on the Univac 1108/Exec 8 computer system at the National Bureau of Standards, Washington, D.C. Also, included in this table are typical central-processor times for the programs at the NBS facility. The central-processor time for the data-reduction program is dependent on the size of the input data array (fringe-peak locations); the value given in table 11 is for an average array size of 25 (fringes) by 25 (scans) for each interferogram.

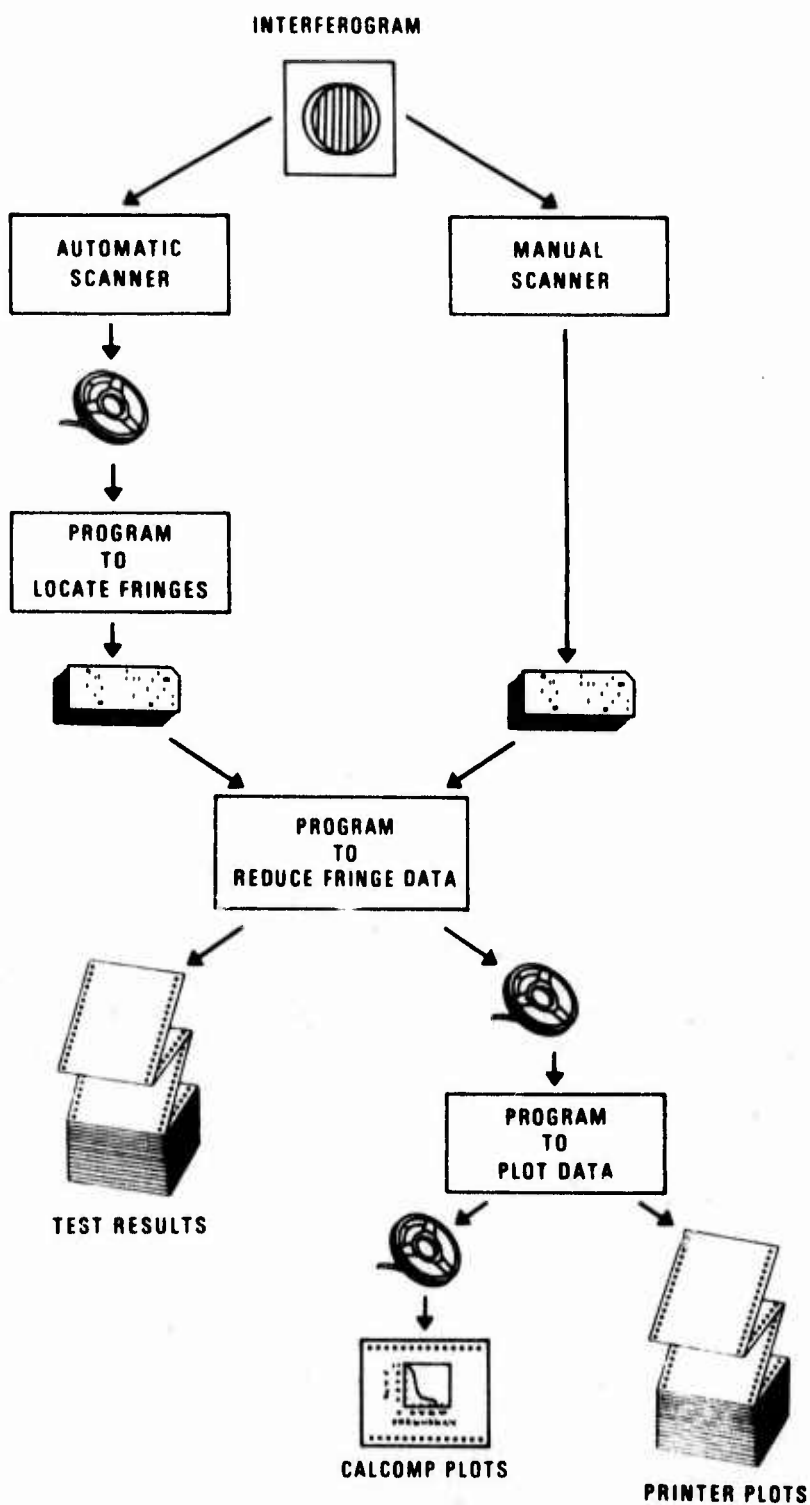


Figure 34.- Flow diagram of complete data-reduction procedures for WSI interferogram.

TABLE 11. - EXECUTION TIME AND STORAGE REQUIREMENT FOR  
WSI COMPUTER PROGRAMS

Computer program	Central processor time (CPU), sec.	Computer words <sup>b</sup>
Data reduction	180 <sup>a</sup>	40,200
Plotting	50	55,900

<sup>a</sup>For highly aberrated test lenses, the time required to search for plane of best focus may significantly increase CPU time.

<sup>b</sup>1 word is 36 bits for Univac computer system.

#### XIV. CONCLUSIONS

The present study was directed towards developing, evaluating, and installing an interferometric lens-testing system that would fit the test requirements of the sponsor. A wavefront shearing interferometer (WSI) system was developed and used to test several lenses on axis at the National Bureau of Standards. Several computer programs were also developed to automate reduction of the WSI test data.

A set of eight WSI cubes, which permits lens testing over a wide range of f-numbers, was fabricated and delivered to the sponsor. The computer programs for reducing both the WSI test data and the interferogram scan data from an automatic scanner were also presented to the sponsor. An automatic scanner purchased by the sponsor was tested and used at NBS for scanning some WSI interferograms; this scanner was later installed at the sponsor's facilities and subsequently interfaced to a minicomputer to permit controlled scanning. Therefore, a viable WSI test system is currently available to the sponsor at the sponsor's facilities.

Lens testing with the WSI at the NBS demonstrated the following:

- 1) the WSI is a versatile, inexpensive, and simple alternative for interferometric testing of lenses; lenses may be tested at infinite or finite conjugates;
- 2) the major effort required in testing with the WSI is data reduction; with the available computer programs and an automatic scanner, this task is greatly simplified;
- 3) asymmetric aberrations introduced by the WSI cube, which acts as a glass plate, can be kept to less than 0.05 wavelength by careful alignment procedures; spherical aberration is automatically removed in the data-reduction program and defect of focus is compensated during testing;
- 4) the major source of error in WSI testing is generally misalignment of the test lens; a nodal slide with translational and rotational controls is necessary to reduce alignment errors;
- 5) present testing techniques have resulted in root-mean-square differences of less than 0.04 wavelength; these differences could be further reduced with improvements in the technique to register the x and y-sheared interferograms;
- 6) recommendations for further testing with the WSI include extension to off-axis testing, improvement of the efficiency

and accuracy of data-reduction computer programs and extension of these programs to partially obscured and non-circular lens apertures, development of alternate techniques for locating the aperture boundary with the automatic scanner, and development of a real-time test system in which an aerial image of the fringe pattern is scanned, the results fed directly into a computer, and the lens performance automatically displayed on a viewing screen.

## XV. RECOMMENDATIONS

Although the WSI test system and data reduction procedures developed in the present study meet the requirements of the sponsor for a viable lens and mirror test system, there are modifications, extensions, and alternatives to be recommended. The implementation of these recommendations will depend, in part, on the specific needs of the user and the computer and scanning facilities available to the user.

A very desirable WSI test system would be one that performs essentially real-time testing. For such a system, the aerial image of the interference pattern would be scanned, rather than scanning a photographic record. The scan information would be input directly into a computer which, in turn, would reduce the test data. The resulting pupil function, MTF, PTF, and aberrations would be displayed on a viewing screen. With this system, the effect of lens alignment and other test-system parameters on the lens performance could be noted almost immediately. Thus, the systematic errors could be minimized. In addition, the time required for testing would be greatly reduced.

The WSI test system should be extended to off-axis testing. Lenses and mirrors are generally used to image an extended object, rather than a point source, and, therefore, the performance of the lens or mirror for off-axis imaging should be measured. With any of the various techniques currently used for off-axis testing, the primary difficulty is a very accurate measurement of the field position. For the WSI test system, this specification of field position means that the location and orientation of both the cube interferometer and the test lens with respect to the test-system optical axis must be measured accurately. In addition, the data-reduction computer program would have to be modified to process non-circular (elliptical) apertures.

Fiducial marks that can be correctly identified from the automatic-scanner data should be developed in order to reduce the interferogram-registration errors for automatic scanning. The current approach for registration of the x and y-sheared interferograms is designed primarily for a manual scanner. The image analysis for fiducial marks to be used with an automatic scanner should include the following: (1) distinguish fiducial marks from fringe locations, aperture boundary, and film defects; (2) identification of the x and y axes; and (3) distinguish between the x and y-sheared interferograms.

For automatic scanning, it is also recommended that other techniques for locating the edge of the test-lens aperture be investigated. The present approach of manually punching holes at the fringe terminals preparatory to scanning is subject to errors in visual judgment.

The computer programs for reducing data from the automatic scanner and for determining the pupil function, OTF, and aberrations should be extended to include data from a partially obscured aperture, and a non-circular aperture. In addition, these computer programs should be optimized in terms of efficiency and accuracy. Alternate computational techniques for such quantities as the pupil function and OTF should be studied.

## APPENDIX A

### COMPUTER PROGRAM TO REDUCE WSI FRINGE DATA

The computer program used to determine lens performance from the WSI fringe data is presented. An outline of program operation is given together with a detailed input description, auxiliary definitions of program variables, listing of subroutines, computation program listing, and a sample printout.

#### Outline of Program Operation

The outline of the program is presented with references to sections of this report that contain detailed information on the particular topic. The present program assumes the following: (1) input fringe data will be no longer than a 29 x 29 array; (2) lens aperture is circular and unobscured; (3) data from one scan does not contain more than one pair of coordinates for the same fringe, i.e., closed or looped fringe data is not treated; and (4) amplitude of pupil function is constant and assumed to be unity over the lens aperture.

#### A. Input data

1. Test-lens and experimental parameters
2. Fringe-peak coordinates and fringe orders from either manual or automatic scanner

#### B. Calculations

1. Register fringe data from x and y-sheared interferograms in common coordinate system (See appendix D.)
2. Convert fringe-coordinate data to normalized values using shear distance (See section IV.)
3. Use spline fit to interpolate fringe orders at grid points of rectangular normalized grid (See section IV.)
4. Determine pupil function to within a constant at grid points (See section IV.)
5. Perform least-squares fit of pupil function to twenty-three term polynomial representing aberration (See section IV.)

6. Remove symmetrical aberrations introduced by WSI cube from pupil function (See section VI.2.)
7. Remove constant and x and y tilt terms from pupil function
8. Calculate root mean square (RMS) of initial solution of pupil function, RMS of polynomial describing pupil function, and RMS of difference in these two solutions of the pupil function
  - o Calculate maximum values of aberrations at edge of lens aperture
10. Determine from polynomial representation values of pupil function in areas (lunes) of aperture for which fringe data could not be interpolated
11. Determine focal plane for which RMS of pupil function is a minimum by adjusting defocus term (See section V.2.)
12. Calculate pupil function (complex quantity) where amplitude is assumed to be constant with a value of 1.0
13. Calculate OTF by auto-correlation of pupil function (See section V.1.)
14. Determine MTF and PTF

C. Output data

1. Paper printout (See sample printout.)
  - a. Test-lens experimental parameters
  - b. Fringe-peak coordinates from scanner for x and y-sheared interferograms
  - c. Normalized fringe-peak coordinates for x and y-sheared interferograms
  - d. List of grid coordinates which lie inside lens aperture but outside region of interpolation

- e. Incidence matrix for x and y-sheared interferograms to show grid points at which fringe orders were interpolated
  - f. Fringe-order deviations determined at grid points by interpolation for x and y-sheared interferograms
  - g. Values of the pupil function to within a constant
  - h. Symmetrical aberrations introduced by WSI cube
  - i. Differences between initial solution and polynomial representation of pupil function
  - j. RMS of initial solution, RMS of polynomial representation of pupil function, and RMS of difference between these two solutions
  - k. Listing of aberration coefficients and maximum values of aberrations
  - l. Incidence matrix for grid points to indicate whether fringe order was interpolated, extrapolated, or outside of lens aperture
  - m. Pupil-function phase values corresponding to the focal plane specified by input value
  - n. Defocus coefficient, focal distance, and RMS or wavefront for different focal planes separated by increments of Rayleigh depth-of-focus tolerance
  - o. Pupil-function phase values corresponding to optimum focal plane
  - p. Coordinates of grid points
  - q. Values of complex pupil function
  - r. OTF values
  - s. MTF and PTF values
  - t. List of parameters written on tape for plotting program
2. Magnetic tape with values of parameters, pupil function, and OTF to be used by plotting program.

### Auxiliary Definitions

Several quantities appear in the final printout. In addition, some of these and other quantities can be useful in evaluating the sequence of operations in the program listing. Those quantities which have not been defined elsewhere are defined as follows:

<u>FORTRAN Variable</u>	<u>Description</u>
B(I)	Aberration coefficient in polynomial describing wavefront, $b$
B4CUB	Coefficient of defocus introduced by cube, $a_2$
B4MAX	Maximum value of defocus introduced by cube, $a_2$
B11CUB	Coefficient of third-order spherical aberration introduced by cube, $a_3$
B11MAX	Maximum value of third-order spherical aberration introduced by cube, $a_3 (RADIUS/z_2)^4$
B22CUB	Coefficient of fifth-order spherical aberration introduced by cube, $a_4$
B22MAX	Maximum value of fifth-order spherical aberration introduced by cube, $a_4 (RADIUS/z_2)^6$
B23CUB	Coefficient of seventh-order spherical aberration introduced by cube, $a_5$
B23MAX	Maximum value of seventh-order spherical aberration introduced by cube, $a_5 (RADIUS/z_2)^8$
B4BEST(M)	Coefficient of residual defocus for plane of best focus
DE(I,K)	Phase of pupil function or deviation of wavefront from reference sphere, $\phi(x,y)$
DEFFOC	Maximum value of residual defocus for plane of best focus
DEL(I,K)	Phase of pupil function with constant $b_1$ and tilt terms $b_2x$ , and $b_3y$ present
DELTA	Shear distance, $\Delta x$ or $\Delta y$
DELTXY	Spatial-frequency increment, $\Delta \mu_x$ or $\Delta \mu_y$

<u>FORTRAN Variable</u>	<u>Description</u>
DEVMAX	Maximum value of pupil-function phase
DEVMIN	Minimum value of pupil-function phase
F(L)	Terms of polynominal describing wavefront, F(x,y)
FNO	f-number of test lens, $z_2/2(\text{RADIUS})$
FNOBST	f-number of test lens for plane of best focus
FRACT	Multiplicative factor by which focal plane is shifted along optical axis in units of Rayleigh tolerance on depth of focus
FRSPAC	Fringe spacing in interferogram of perfect lens, $(\lambda z_2)/(\ell \Phi)$
HD(J,K)	Interpolated fringe-order deviation for x-sheared interferogram, P(J, K, N) or Q <sub>m,n</sub>
ISUMA	Total number of grid points for which fringe-order values were interpolated
ISUMB	Total number of grid points for which fringe-order values were extrapolated
ISUM	ISUMA + ISUMB
KX	Reduced spatial-frequency increment along x-axis, k <sub>x</sub>
KY	Reduced spatial-frequency increment along y-axis, k <sub>y</sub>
MI(I,K)	Incidence matrix for test-lens aperture; MI = 1 indicates that fringe-order value was interpolated at grid point (I,K); MI = 2 indicates that fringe-order value was extrapolated at grid point (I,K); MI = 0 indicates that grid point lies outside aperture
MI1(I,K)	Incidence matrix for x-sheared interferogram; MI1(I,K) = 1 indicates that fringe-order value was interpolated at grid point (I+2, K+2); MI1(I,K) = 0 indicates that no interpolation was made or grid point lies outside aperture

<u>FORTRAN Variable</u>	<u>Description</u>
MI2(I,K)	Incidence matrix for y-sheared interferogram; MI2 (I,K) = 0 indicates that fringe-order value was interpolated at grid point (K+2, I+2); MI2 (I,K) = 0 indicates that no interpolation was made or grid point lies outside aperture
N	Trigger or subscript to identify interferogram or frame  N = 1 for x-sheared interferogram N = 2 for y-sheared interferogram
NS	Maximum number of scans for either x or y-sheared interferogram
OTF(I,K)	Optical transfer function
P(J,K,N)	Interpolated fringe-order deviation for x or y-sheared interferogram, Q <sub>m,n</sub> or S <sub>m,n</sub>
POLYMX(I)	Maximum value of aberration term; b <sub>n</sub> F <sub>n</sub> (x,y) where x <sup>2</sup> + y <sup>2</sup> = (RADIUS) <sup>2</sup> and n = 1,2,...23
RAYLGH	Rayleigh tolerance on depth of focus, $\pm 3.2 (\lambda/2\pi) (z_2/\text{RADIUS})^2$
RMS	Root mean square of DEL values after removing cube aberrations and b <sub>1</sub> , b <sub>2</sub> x, and b <sub>3</sub> y
RMSDE	Root mean square of DE values, including extrapolated values, after removing cube aberrations and b <sub>1</sub> , b <sub>2</sub> x, and b <sub>3</sub> y
RMSMAX	RMSDE for plane of best focus
RMSR	Root mean square of DE value (interpolated) after removing cube aberrations and b <sub>1</sub> , b <sub>2</sub> x, and b <sub>3</sub> y
RMSS	Root mean square of V(I,K)
SIGN	Sign of Rayleigh tolerance on depth of focus; SIGN = 1.0 for focal plane shifted away from test lens; SIGN = -1.0 for focal plane shifted towards test lens

<u>FORTRAN Variable</u>	<u>Description</u>
TRANS(I,K)	Pupil function
VD(J,K)	Interpolated fringe-order deviation for y-sheared interferogram, P(J,K,2) or $S_{m,n}$
V(I,K)	Residual wavefront, DEL(I,K) - DE(I,K)
X	x-coordinate of grid point, $X_m$
X(J,K,N)	x-coordinate of fringe-peak location, $x_{i,j}$
XCEN	x-coordinate of center of aperture, XCEN = RADIUS
XGRID(I,K)	x-coordinate of grid point, $X_m$
XINT	Coordinate of grid point at which fringe order is interpolated in x or y-sheared interferogram, $X_m$ or $Y_n$
X1(K)	x-coordinate of left-hand boundary of aperture along Kth scan
X2(K)	x-coordinate of right-had boundary of aperture along Kth scan
Y	y-coordinate of grid point, $Y_n$
YBOUN1	y-coordinate of upper boundary of aperture, YCEN - RADIUS
YBOUN2	y-coordinate of lower boundary of aperture, YCEN + RADIUS
YCEN	y-coordinate of center of aperture, YCEN = RADIUS
YGRID(K)	y-coordinate of grid point, $Y_n$
YINT	Interpolated fringe order for x or y-sheared interferogram, $p(X_m)$ or $p(Y_n)$
ZZ2(M)	Focal-plane position along z-axis
Z2BEST	Optimum focal-plane position along z-axis

### Subroutines

A list of the subroutines used in this program is presented

<u>FORTRAN Name</u>	<u>Called by</u>	<u>Function</u>
SPLICO	MAIN	Determination of coefficients for spline-fitting interpolation (See reference 16).
SPLINE	MAIN	Interpolation of fringe order by method of spline fitting (See reference 16.)
SPECSP	MAIN	Interpolation of fringe order by method of spline fitting in special case of only two fringe-peak data for a scan
DEV	MAIN	Determination of pupil function, aberrations, and plane of best focus
INVERT	DEV	Perform matrix inversion by method of Gauss-Jordan Elimination (See reference 39.)
CORREL	MAIN	Compute optical transfer function by auto-correlation of pupil function

### Input Description

The following list contains the program input variables which are arranged according to order of presentation in the program.

Frame 1 is the x-sheared interferogram and frame 2 is the y-sheared interferogram. All variables that represent distances or coordinates in the lens aperture are measured from the interferograms as shown in figure 35.

<u>Input Card</u>	<u>FORTRAN Variable</u>	<u>Description</u>
1	TEST	Identifies test lens and test number or date
2	FOCUS	Trigger for determining focal plane in which OTF is calculated FOCUS = 1 nominal focal plane at distance Z2 FOCUS = 2 for optimum focal plane where RMS of wavefront is minimum
3	CUBE	Trigger for determining and removing defocus introduced by cube by interferometer CUBE = 1 for experimental case of measuring ZL from null fringe position; only corrections for spherical aberration are made CUBE = 2 for experimental case of measuring ZL from nominal focal plane at Z2; correction for defect of focus and spherical aberration are made
	THICK	Cube thickness, t, mm
4	ZL*	Distance along optical axis from nominal focal point or null-fringe position to back of cube, l, mm (See figure 4.)
	Z2	Nominal focal length, Z2, mm (See figure 4.)

---

\*This value is positive if cube is located between focal point and auxiliary lens and negative if cube is located between test lens and focal point.

<u>Input Card</u>	<u>FORTRAN Variable</u>	<u>Description</u>
	XMAG	Magnification of interferogram; ratio of diameter of test-lens aperture as measured on interferogram to nominal diameter of test-lens aperture
	PHI	Cube shear angle, $\phi$ , rad
	WAVEL	Wavelength of light used to illuminate test lens, $\lambda$ , mm
5	PASS	Trigger for double-pass tests PASS = 1 for single-pass test PASS = 2 for double-pass test
6	INPUT	Trigger to indicate method used for scanning interferogram INPUT = 1 for fringe data from manual scanner INPUT = 2 for fringe data from automatic scanner
7	CX	Distance along x axis of scanner from coordinate origin to left side of unsheared aperture for frame 1; mm (See figure 35.)
	CY	Distance along y axis of scanner from coordinate origin to right side of unsheared aperture for frame 2; mm (See figure 35.)
	POSX*	Distance along y axis of scanner from aperture edge to first scan for frame 1; mm (See figure 35.)
	POSY*	Distance along y axis of scanner from aperture edge to first scan for frame 2; mm (See figure 35.)

\*The values selected should be less than the shear distance DELTA; recommended values are DELTA/2.

<u>Input Card</u>	<u>FORTRAN Variable</u>	<u>Description</u>
	RADIUS	Radius of test-lens aperture as measured from interferogram; mm
8	NSX	Number of scans in frame 1
	NF1	Number of fringes in frame 1
9	NSY	Number of scans in frame 2
	NF2	Number of fringes in frame 2

The remaining input cards contain scan parameters and fringe-peak locations. The order of these cards depends upon the type of fringe scanning (manual or automatic), and the total number of cards depends upon the number of fringes and scans. The arrangement of these input cards is outlined for both methods of fringe scanning.

#### Manual Scanning:

<u>Input Card</u>	<u>FORTRAN Variable</u>	<u>Description</u>
10	K	Scan number; K = 1
	J1	Order number for first fringe of Kth scan; K = 1
	J2	Order number for last fringe of Kth scan; K = 1
11	X(J,K,N)	Fringe-peak location of Jth-order fringe of first scan of frame 1; mm
.	.	J = J1; K = 1; N = 1
.	.	.
.	.	.
.	X(J,K,N)	J = J2; K = 1; N = 1
.	K,J1,J2	Scan parameters for scan 2
.	X(J,K,N)	J = J1; K = 2; N = 1
.	X(J,K,N)	J = J2; K = 2; N = 1
.	.	.
.	.	.

The input data cards are continued in the above manner from all scans and fringe-peak locations for frames 1 and 2; data from frame 2 follow the data of frame 1 and are arranged in the same format.

Automatic Scanning:

Note: These input cards contain a rectangular array of values of  $X(J,K,N)$  for each frame; since the test lens aperture is circular,  $X(J,K,N) = 0.0$  for some values of  $J$  and  $K$ .

Input  
Card

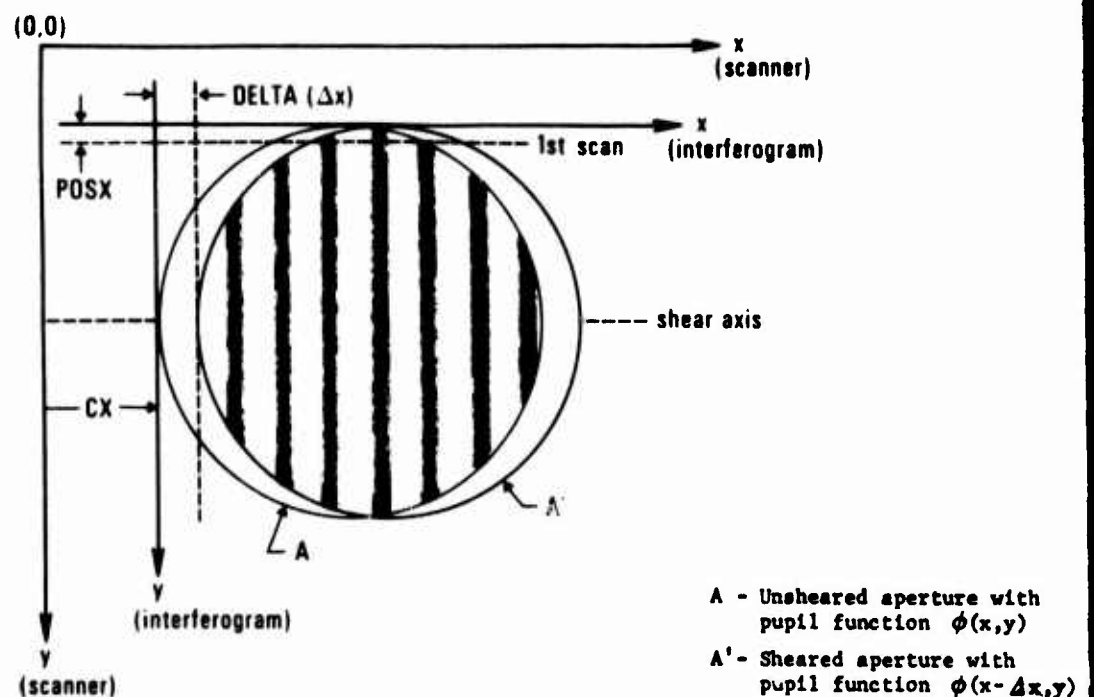
12

$X(J,K,N)$

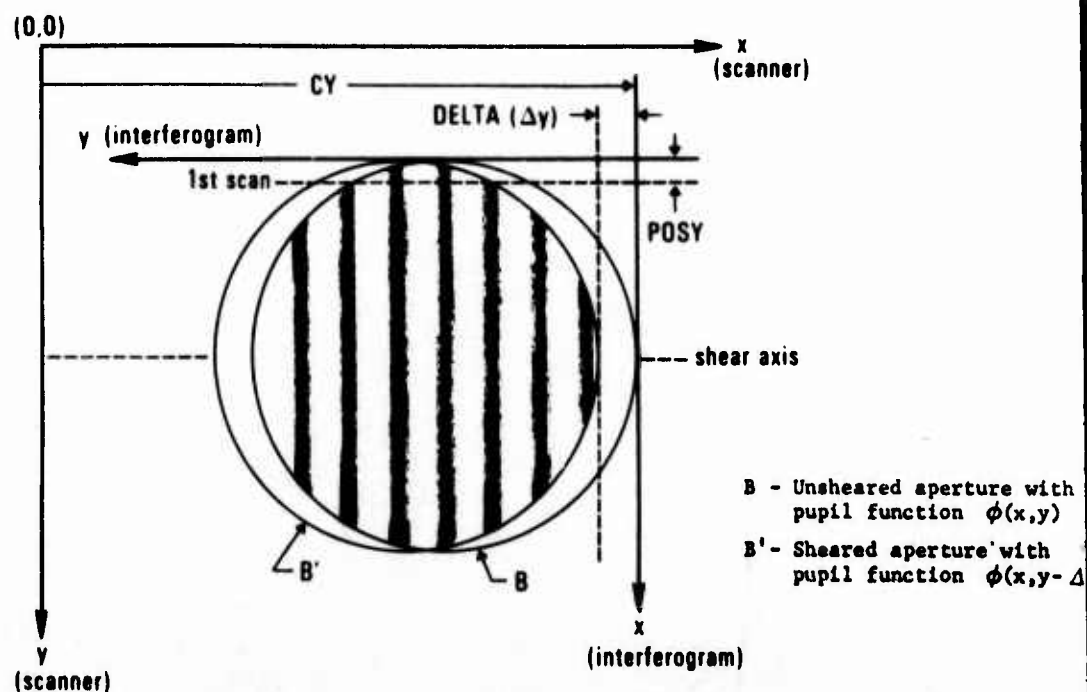
The order of these input cards is best described by giving the READ and FORMAT statements from the program:

```
READ (5,215)((X(J,K,N),J=1,7),K=1,NS)
READ (5,219)((X(J,K,N), J=8,15),K=1,NS)
READ (5,219)((X(J,K,N),J=16,23),K=1,NS)
READ (5,219)((X(J,K,N),J=24,29), K=1,NS)
215 FORMAT (7X,7F7.2)
219 FORMAT (8F7.2)
(See auxiliary definitions for NS.)
```

The input data cards are repeated in the above manner for frame 2 ( $N=2$ ).



(a) x-sheared interferogram.



(b) y-sheared interferogram.

Figure 35.- Schematic of x and y-sheared WSI interferograms showing measured parameters for input to data-reduction computer program.

Computation Program Listing

C THE FOLLOWING PROGRAM PERFORMS THE DATA REDUCTION OF WSI  
C INTERFEROGRAMS TO OBTAIN PUPIL FUNCTION, OTF, MTF, AND PTP  
C FOR TEST LENS  
C INPUT DATA ARE FRINGE-PEAK POSITIONS FROM EITHER -  
C (1) MANUAL SCANNER OR (2) AUTOMATIC SCANNER

DIMENSION B(23),C(4,32),DE(32,32),DU(32),DUMMY(2),HD(32,32),  
1MI(32,32),M11(32,32),M12(32,32),P(32,32,2),VD(32,32),X(32,32,2),  
2XDUM(32)  
DIMENSION TEST(6)  
COMPLEX TRANS(32,32),OTF(65,65)  
REAL JDUM(32)  
INTEGER PASS,CUBE,FOCUS  
EQUIVALENCE (HD(1,1),P(1,1,1)),(VD(1,1),P(1,1,2))

C THE FOLLOWING PARAMETER IS READ AS INPUT TO IDENTIFY TEST LENS  
READ(5,3) (TEST(I),I=1,6)  
3 FORMAT(6A6)

C THE FOLLOWING PARAMETER IS READ AS INPUT TO PERMIT DETERMINATION  
C OF PUPIL-FUNCTION PHASE IN PLANE OF BEST FOCUS  
READ(5,10)FOCUS

C THE FOLLOWING PARAMETERS ARE READ AS INPUT TO PERMIT DETERMINATION  
C OF THE EFFECT OF THE CUBE INTERFEROMETER ON TEST-LENS WAVEFRONT  
READ(5,11)CUBE,THICK  
11 FORMAT(12,F10.3)

C THE FOLLOWING PARAMETERS ARE READ AS INPUT DATA IN ORDER TO  
C CALCULATE SHEAR DISTANCE (DELTA) AND SPATIAL FREQUENCY (DELTXY)  
READ(5,15)ZL,22,XMAG,PHI,WAVEL  
15 FORMAT(3F10.3,2E10.3)

C THE FOLLOWING PARAMETER IS READ AS INPUT TO ALLOW PROGRAM TO  
C HANDLE DATA FROM DOUBLE-PASS SYSTEM  
READ(5,10)PASS  
10 FORMAT(12)

C THE FOLLOWING PARAMETER IS READ AS INPUT TO INDICATE IF  
C INTERFEROGRAMS WERE SCANNED MANUALLY OR AUTOMATICALLY  
READ(5,10)INPUT  
IP(INPUT.EQ.1) GO TO 100  
IP(INPUT.EQ.2) GO TO 200

C THE FOLLOWING PARAMETERS ARE READ AS INPUT DATA IF THE  
C INTERFEROGRAMS ARE SCANNED MANUALLY  
100 READ(5,16)CX,CY,POSX,POSY,RADIUS  
16 FORMAT(5F10.3)  
READ(5,12)NSX,NF1  
12 FORMAT(3I2)  
READ(5,12)NSY,NF2  
C FRINGE-PEAK POSITIONS ARE READ FOR A GIVEN SCAN  
C MAXIMUM NO. OF FRINGES ALLOWED PER FRAME IS 29  
N=1  
NSS=NSX  
201 READ(5,12)K,J1,J2  
READ(5,14)(X(J,K,N),J=J1,J2)



```

      IF(N.EQ.2) GO TO 35
      N=2
      NS=NSY
      GO TO 210
215 FORMAT(7X,7F7.2)
219 FORMAT(8F7.2)

      35 NS=MAX0(NSX,NSY)
      WRITE(6,31)CX,CY,POSX,POSY,RADIUS,NF1,NF2,NSX,NSY,NS
      34 WRITE(6,38)ZL,Z2,PHI,WAVEL,XMAG,THICK
      38 FORMAT(/1H ' ZL = 'F8.3,5X
1'DISTANCE ALONG OPTICAL AXIS BETWEEN BACK FACE OF CUBE INTERFEROME
2TER AND TEST-LENS FOCUS'//1H ' Z2 = 'F8.3,5X'IMAGE DISTANCE OF T
3EST LENS' //1H ' PHI = ' E9.4,2X'RAD' 5X'SHEAR ANGLE OF C
4UBE INTERFEROMETER'//1H ' WAVEL = ' E9.4,2X'MM'5X'WAVELENGTH OF
5LIGHT SOURCE'//1H ' XMAG = ' F6.3,5X'MAGNIFICATION OF INTERFERENC
6E PATTERN OCCURRING IN SCANNED INTERFEROGRAM'//1H ' THICK = 'F7.
73,2X'MM'5X'WSI CUBE THICKNESS'/')

C   COMPUTE SHEAR DISTANCE IN INTERFEROGRAM FOR COORDINATE
C   NORMALIZATION
      DELTA=(ZL*Z2)*PHI*Xmag
      WRITE(6,39)DELTA
      39 FORMAT(1H ' DELTA = 'F6.3,5X'COMPUTED SHEAR DISTANCE'/')

C   COMPUTE FRINGE SPACING IN INTERFEROGRAM FOR IDEAL LENS
      ZL=ABS(ZL)
      FRSPAC=((WAVEL*Z2)/(ZL*PHI))*XMAG
      WRITE(6,40)FRSPAC
      40 FORMAT(1H ' FRSPAC = 'F8.3,5X'FRINGE SPACING FOR IDEAL LENS'/')

      WRITE(6,42)
      42 FORMAT(1H1'FRINGE-PEAK POSITIONS X(J,K,N) AS SCANNED (INPUT DATA)
1ARE PRINTED BELOW - 1/1 J = FRINGE NO. 5X'K = SCAN NO. 1//1 VALUES
2 OF X(J,K,N) ARE PRINTED IN 2 BLOCKS FOR EACH FRAME 1//1 MAXIMUM N
3NUMBER OF FRINGES AND SCANS ALLOWED PER FRAME IS 29')
      DD 49 N=1,2
      WRITE(6,191)N
      WRITE(6,43)
      43 FORMAT(1H 3X'J'3X'1'7X'2'7X'3'7X'4'7X'5'7X'6'7X'7'7X'8'7X'9'6X'10'
16X'11'6X'12'6X'13'6X'14'6X'15'6X'16'/' K')
      DD 44 K=1,30
      44 WRITE(6,45)K,(X(J,K,N),J=1,16)
      45 FORMAT(1H 12,1X16F8.3)
      .  WRITE(6,46)
      46 FORMAT(//1H 3X'J'2X'17'6X'18'6X'19'6X'20'6X'21'6X'22'6X'23'6X'24'6
1X'25'6X'26'6X'27'6X'28'6X'29'/' K')
      DD 47 K=1,30
      47 WRITE(6,45)K,(X(J,K,N),J=17,29)
      49 CONTINUE

C   REVERSE ORDER OF DATA IN EACH SCAN OF SECOND INTERFEROGRAM TO
C   PERMIT LATER REGISTRATION OF DATA FROM TWO INTERFEROGRAMS
C   THIS CORRECTION ASSUMES A 90 DEGREE ROTATION CLOCKWISE BETWEEN FIRST
C   AND SECOND INTERFEROGRAM
C   DATA IS SIMULTANEOUSLY SHIFTED TO ALLOW TWO COLUMNS OF ZEROS
      K=1
      302 DD 303 J=1,NF2

```

303 DU(J)=X(J,K,2)  
 DD 305 J=1,NF2  
 305 X(J+2,K,2)=DU(NF2+1-J)  
 IF(K.GE.NS) GO TO 310  
 K=K+1  
 GO TO 302

C DATA FROM FIRST FRAME IS SHIFTED TO ALLOW FOR TWO COLUMNS OF ZEROS  
 310 K=1  
 301 DD 304 J=1,NF1  
 304 DU(J)=X(J,K,1)  
 DD 306 J=1,NF1  
 306 X(J+2,K,1)=DU(J)  
 IF(K.GE.NS) GO TO 311  
 K=K+1  
 GO TO 301  
 311 DD 312 K=1,NS  
 DD 312 J=1,2  
 X(J,K,2)=0.  
 312 X(J,K,1)=0.

C CONVERT FRINGE-PEAK POSITIONS TO NORMALIZED COORDINATES USING  
 C DELTA AND MOVE ORIGIN OF COORDINATE SYSTEM UNTIL AXES ARE TANGENT  
 C TO LENS APERTURE  
 NF1A=NF1\*2  
 NF2A=NF2\*2  
 N=1  
 DD 315 K=1,NS  
 DD 315 J=1,NF1A  
 IF(X(J,K,N).LT. 0.001) GO TO 315  
 X(J,K,N)=ABS((CX-X(J,K,N))/DELTA)  
 315 CONTINUE  
 N=2  
 DD 320 K=1,NS  
 DD 320 J=1,NF2A  
 IF(X(J,K,N).LT. 0.001) GO TO 320  
 X(J,K,N)=ABS((CY-X(J,K,N))/DELTA)  
 320 CONTINUE

WRITE(6,190)  
 190 FORMAT(1H1,'NORMALIZED FRINGE POSITIONS X(J,K,N) ARE PRINTED BELOW  
 1 - 1// J = FRINGE NO. K = SCAN NO. 1// VALUES OF X(J,K,N) ARE  
 2 PRINTED IN 2 BLOCKS OF 32(ROWS) BY 16(COLUMNS) FOR EACH FRAME 1//  
 3 NOTE - THE FIRST FRINGE WAS ASSIGNED J=3 AS INPUT DATA, THE SECOND  
 4 FRINGE J=4, ETC. 1)  
 406 DD 199 N=1,2  
 WRITE(6,191)N  
 191 FORMAT(1H 62X'FRAME 'I2//)  
 WRITE(6,192)  
 192 FORMAT(1H 3X'J'3X'2'7X'3'7X'4'7X'5'7X'6'7X'7'7X'8'7X'9'6X'10'6X'11  
 1'6X'12'6X'13'6X'14'6X'15'6X'16'6X'17'/' K')  
 DD 193 K=1,32  
 193 WRITE(6,194)K,(X(J,K,N),J=2,17)  
 194 FORMAT(1H I2,1X16F8.3/)  
 WRITE(6,196)  
 196 FORMAT(1H 3X'J'2X'18'6X'19'6X'20'6X'21'6X'22'6X'23'6X'24'6X'25'6  
 1X'26'6X'27'6X'28'6X'29'6X'30'6X'31'6X'32'6X'33'/' K')

197 WRITE(6,194)K,(X(J,K,N),J=16,33)  
199 CONTINUE

C INTERPOLATE FRINGE-ORDER VALUES AT GRID POINTS COMMON //  
C FRAME 1 AND FRAME 2  
POSX=POSX/DELTA  
POSY=POSY/DELTA  
U=POSY  
JMIN=0  
JMAX=0  
N=1  
NS=NSX  
WRITE(6,349)  
349 FORMAT(1H1 'THE FOLLOWING GRID POINTS XINT, IF ANY, LIE INSIDE LENS  
1 APERTURE BUT OUTSIDE REGION OF INTERPOLATION'///)  
350 DO 340 K=1,NS  
DO 323 J=3,31  
IF(JMIN.GT.0) GO TO 321  
IF(X(J,K,N).LT.0.0001) GO TO 323  
JMIN=J  
321 IF(X(J,K,N).LT.0.0001) GO TO 322  
GO TO 323  
322 JMAX=J-1  
GO TO 326  
323 CONTINUE  
326 N=JMAX-JMIN+1  
DO 329 J=JMIN,JMAX  
XDUM(J-JMIN+1)=X(J,K,N)  
JDUM(J-JMIN+1)=J  
IF(N.LE.2) GO TO 800  
329 CONTINUE  
C USE SUBROUTINES TO INTERPOLATE FRINGE DEVIATION AT GRID POINTS BY  
C SPLINE-FITTING TECHNIQUE  
C REFERENCE - R.H. PENNINGTON, INTRODUCTORY COMPUTER METHODS AND  
C NUMERICAL ANALYSIS, 2ND ED. (THE MACMILLAN COMPANY, U.S.A., 1970)  
330 CALL SPLICC(XDUM,JDUM,M,C)  
MM=XDUM(M)+1.00  
JM=XDUM(1)-1.00  
IF(JM.LT.1)JM=1  
DO 335 J=JM,MM  
XINT=0+J  
KDUM=K  
CALL SPLINE(XDUM,JDUM,M,C,XINT,YINT,8335,N,KDUM)  
C SUBTRACT INTEGER ORDER NUMBER MULTIPLIED BY RATIO OF SHEAR  
C DISTANCE TO IDEAL FRINGE SPACING FROM INTERPOLATED VALUE TO GIVE  
C DEVIATION OF FRINGE FROM IDEAL FRINGE  
P(J+2,K+2,N)=YINT-J\*(DELTA/FRSPAC)  
IF(N.EQ.1) MI1(J+2,K+2)=1  
IF(N.EQ.2) MI2(K+2,J+2)=1  
C ALL INTERPOLATED FRINGE-ORDER VALUES HAVE ALSO BEEN SHIFTED TO  
C ALLOW FOR TWO ROWS OF ZEROS  
335 CONTINUE  
JMIN=0  
JMAX=0  
GO TO 340  
C SPECIAL EXTRAPOLATION FOR SCAN WITH ONLY TWO FRINGE-PEAK LOCATIONS  
800 IF(K+4.GT.NS) GO TO 850  
XDUM(1)=2.0

```

XDUM(2)=3.0
XDUM(3)=4.0
XDUM(4)=5.0
JDUM(1)=X(JMIN-1,K*1,N)
JDUM(2)=X(JMIN-1,K*2,N)
JDUM(3)=X(JMIN-1,K*3,N)
JDUM(4)=X(JMIN-1,K*4,N)
M=4
XINT=1.0
KDUM=K
CALL SPLICG(XDUM,JDUM,M,C)
CALL SPECSP(XDUM,JDUM,M,C,XINT,YINT,N,KDUM)
YONE=YINT
JDUM(1)=X(JMAX+1,K*1,N)
JDUM(2)=X(JMAX+1,K*2,N)
JDUM(3)=X(JMAX+1,K*3,N)
JDUM(4)=X(JMAX+1,K*4,N)
CALL SPLICG(XDUM,JDUM,M,C)
CALL SPECSP(XDUM,JDUM,M,C,XINT,YINT,N,KDUM)
XDUM(1)=YONE
XDUM(2)=X(JMIN,K,N)
XDUM(3)=X(JMAX,K,N)
XDUM(4)=YINT
JDUM(1)=JMIN-1
JDUM(2)=JMIN
JDUM(3)=JMAX
JDUM(4)=JMAX+1
GO TO 330
650 XDUM(1)=1.0
XDUM(2)=2.0
XDUM(3)=3.0
XDUM(4)=4.0
JDUM(1)=X(JMIN-1,K-4,N)
JDUM(2)=X(JMIN-1,K-3,N)
JDUM(3)=X(JMIN-1,K-2,N)
JDUM(4)=X(JMIN-1,K-1,N)
M=4
XINT=5.0
KDUM=K
CALL SPLICG(XDUM,JDUM,M,C)
CALL SPECSP(XDUM,JDUM,M,C,XINT,YINT,N,KDUM)
YONE=YINT
JDUM(1)=X(JMAX+1,K-4,N)
JDUM(2)=X(JMAX+1,K-3,N)
JDUM(3)=X(JMAX+1,K-2,N)
JDUM(4)=X(JMAX+1,K-1,N)
CALL SPLICG(XDUM,JDUM,M,C)
CALL SPECSP(XDUM,JDUM,M,C,XINT,YINT,N,KDUM)
XDUM(1)=YONE
XDUM(2)=X(JMIN,K,N)
XDUM(3)=X(JMAX,K,N)
XDUM(4)=YINT
JDUM(1)=JMIN-1
JDUM(2)=JMIN
JDUM(3)=JMAX
JDUM(4)=JMAX+1
GO TO 330
340 CONTINUE

```

```

IF(N.EQ.2) GO TO 360
N=2
NS=NSY
U=PGSX
VAR2=PGSY
GO TO 350
C P(J,K,N)'S ARE NOW INTERPOLATED TO SAME GRID
C RESET NS TO PREVIOUS VALUE
360 NS=MAX0(NSX,NSY)

300 WRITE(6,600)
600 FORMAT(1H1 'VALUES OF MI1(I,K) ARE PRINTED BELOW -'//'
          1ICATES THAT A VALUE OF FRINGE ORDER P(J,K,N) WAS INTERPOLATED AT G
          2RID POINT (I*2,K*2) IN X-SHEARED INTERFEROGRAM'//'
          NOTE - FOR CASE
          3E OF TWO INPUT FRINGE PEAKS IN A SCAN, ONE VALUE OF P(J,K,N) IS IN
          4TERPOLATED AND TWO VALUES MAY BE EXTRAPOLATED'//')
          WRITE(6,601)MI1
601 FORMAT(1H0,3213)
          WRITE(6,602)
602 FORMAT(1H1 'VALUES OF MI2(I,K) ARE PRINTED BELOW -'//'
          1ICATES THAT A VALUE OF FRINGE ORDER P(J,K,N) WAS INTERPOLATED AT G
          2RID POINT (K*2,I*2) IN Y-SHEARED INTERFEROGRAM'//'
          NOTE - FOR CASE
          3E OF TWO INPUT FRINGE PEAKS IN A SCAN, ONE VALUE OF P(J,K,N) IS IN
          4TERPOLATED AND TWO VALUES MAY BE EXTRAPOLATED'//')
          WRITE(6,601)MI2

C PRINGE-ORDER DEVIATIONS ARE DIVIDED BY 2 IF THE WSI SYSTEM IS
C DOUBLE PASS
500 IF(PASS.EQ.1) GO TO 550
DO 501 N=1,2
DO 501 K=1,31
DO 501 J=1,31
P(J,K,N)=P(J,K,N)/2.0
501 CONTINUE

550 WRITE(6,370)
370 FORMAT(1H1
          'FRINGE-ORDER DEVIATIONS P(J,K,N) DETERMINED
          AT GRID POINTS BY INTERPOLATION FROM ADJACENT ORDER VALUES ARE PRI
          NTED BELOW'//'
          J = COLUMN NO. OF GRID POINT   K = ROW NO. OF GR
          ID POINT'//'
          VALUES OF P(J,K,N) ARE PRINTED IN 2 BLOCKS OF 32(ROWS
          4) BY 16(COLUMNS) FOR EACH FRAME'//'
          NOTE - VALUES AT GRID POINTS F
          OR WHICH J=1 (NOT PRINTED), J=2, AND AT GRID POINTS FOR WHICH K=1,
          6 K=2, HAVE BEEN SET EQUAL TO 0.0'')
          DO 299 N=1,2
          WRITE(6,191)N
          WRITE(6,192)
          DO 293 K=1,32
293 WRITE(6,194)K,(P(J,K,N),J=2,17)
          WRITE(6,196)
          DO 295 K=1,32
295 WRITE(6,194)K,(P(J,K,N),J=18,33)
299 CONTINUE

C CALL SUBROUTINE TO DETERMINE PHASE OF PUPIL FUNCTION

```

```

NSA=NS*2
DEVMAX=0
DEVMIN=0
C   CONVERT FOLLOWING PARAMETERS TO ACTUAL COORDINATE SYSTEM OF LENS
C   APERTURE
XCEN=RADIUS
YCEN=RADIUS
RADIUS=RADIUS/XMAG
DELTA=DELTA/XMAG
XCEN=XCEN/XMAG
YCEN=YCEN/XMAG
POSX=POSX*DELTA
POSY=POSY*DELTA
C   COMPUTE F/NUMBER OF TEST LENS
FNO=0.5*Z2/RADIUS
CALL DEV(MI,DE,NSA,MI1,MI2,DEVMAX,DEVMIN,RADIUS,DELTA,HD,VD,POSX,
1 POSY,XCEN,YCEN,B,WAVEL,FOCUS,THICK,Z2,SUM,PASS,CUBE,Z2BEST,FNO,
2 RMSMAX)

C   DETERMINE PUPIL FUNCTION OR COMPLEX TRANSMITTANCE MATRIX
DO 400 K=2,NSA
DO 400 J=2,NSA
IF(MI(J,K).EQ.C) TRANS(J,K)=(0.0,0.0)
IF(MI(J,K).EQ.0) GO TO 400
IF(MI(J,K).EQ.2) MI(J,K)=1
A=COS(6.2831852*DE(J,K))+MI(J,K)
D=SIN(6.2831852*DE(J,K))+MI(J,K)
TRANS(J,K)=CMPLX(A,D)
400 CONTINUE
WRITE(6,390)
390 FORMAT(1H1'VALUES OF THE PUPIL FUNCTION TRANS(I,K) ARE PRINTED BEL
1OW -'//') THE PUPIL FUNCTION IS A COMPLEX QUANTITY AND, THEREFORE
2, EACH VALUE IS A PAIR OF NUMBERS'/' VALUES OF TRANS(I,K) ARE PRI
3NTED IN 4 BLOCKS OF 32(ROWS) BY 8(COLUMNS)'//')
WRITE(6,391)
391 FORMAT(1H 2X'I'8X'1'15X'2'15X'3'15X'4'15X'5'15X'6'15X'7'15X'8'/
1 K')
DO 700 K=1,32
700 WRITE(6,392)K,(TRANS(I,K),I=1,8)
392 FORMAT(1H I2,1X16E8.3)
WRITE(6,393)
393 FORMAT(1H12X'I'8X'9'15X'10'14X'11'14X'12'14X'13'14X'14'14X'15'14X'
116'/' K')
DO 701 K=1,32
701 WRITE(6,392)K,(TRANS(I,K),I=9,16)
WRITE(6,394)
394 FORMAT(//1H12X'I'7X'17'14X'18'14X'19'14X'20'14X'21'14X'22'14X'23'1
14X'24'/' K')
DO 702 K=1,32
702 WRITE(6,392)K,(TRANS(I,K),I=17,24)
WRITE(6,395)
395 FORMAT(//1H12X'I'7X'25'14X'26'14X'27'14X'28'14X'29'14X'30'14X'31'1
14X'32'/' K')
DO 703 K=1,32
703 WRITE(6,392)K,(TRANS(I,K),I=25,32)

C   COMPUTE ACTUAL SPATIAL FREQUENCY INCREMENT (REDUCED INCREMENT IS
C   USED IN COMPUTATION OF OTF)

```

```

DELTXY=DELTA/(WAVELENGTH*Z2)

C IF(FOCUS.EQ.1) GO TO 705
C IF PLANE OF BEST FOCUS WAS DETERMINED, THEN DELTA, DELTXY, AND FNO
C MUST BE RECOMPUTED USING DISTANCE FROM EXIT PUPIL TO PLANE OF BEST
C FOCUS
C DELTA=(ZL+Z2BEST)*PHI
C DELTXY=DELTA/(WAVELENGTH*Z2BEST)
C FNOBEST=0.5*Z2BEST/RADIUS
C FNO=FNOBEST.

C USE SUBROUTINE TO DETERMINE OPTICAL TRANSFER FUNCTION
705 CALL CORREL(M1,B,DELTA,OTF,DE,SUM)
INDEX=1
WRITE(6,740)
740 FORMAT(1H1'VALUES OF THE OPTICAL TRANSFER FUNCTION, OTF, ARE PRINT
1ED BELOW -'//') THE OTF IS A COMPLEX QUANTITY AND, THEREFORE, EACH
2H VALUE IS A PAIR OF NUMBERS'/' VALUES OF OTF(I,K) ARE PRINTED IN
3 8 BLOCKS OF 65(ROWS) BY 8(COLUMNS)'//')
741 WRITE(6,391)
DO 745 K=1,65
745 WRITE(6,392)K,(OTF(I,K),I=1,8)
WRITE(6,393)
DO 746 K=1,65
746 WRITE(6,392)K,(OTF(I,K),I=9,16)
WRITE(6,394)
DO 747 K=1,65
747 WRITE(6,392)K,(OTF(I,K),I=17,24)
WRITE(6,395)
DO 748 K=1,65
748 WRITE(6,392)K,(OTF(I,K),I=25,32)
WRITE(6,396)
396 FORMAT(//1H12X'1'7X'33'14X'34'14X'35'14X'36'14X'37'14X'38'14X'39'1
14X'40'/' K')
DO 749 K=1,65
749 WRITE(6,392)K,(OTF(I,K),I=33,40)
WRITE(6,397)
397 FORMAT(//1H12X'1'7X'41'14X'42'14X'43'14X'44'14X'45'14X'46'14X'47'1
14X'48'/' K')
DO 750 K=1,65
750 WRITE(6,392)K,(OTF(I,K),I=41,48)
WRITE(6,398)
398 FORMAT(//1H12X'1'7X'49'14X'50'14X'51'14X'52'14X'53'14X'54'14X'55'1
14X'56'/' K')
DO 751 K=1,65
751 WRITE(6,392)K,(OTF(I,K),I=49,56)
WRITE(6,399)
399 FORMAT(//1H12X'1'7X'57'14X'58'14X'59'14X'60'14X'61'14X'62'14X'63'1
14X'64'/' K')
DO 752 K=1,65
752 WRITE(6,392)K,(OTF(I,K),I=57,64)
IF(INDEX.EQ.2) GO TO 765

C DETERMINE MODULUS (MTF) AND PHASE (PTF) OF OPTICAL TRANSFER
C FUNCTION (OTF)
C SAME VARIABLE, OTF, IS USED FOR COMPLEX NUMBER WHOSE REAL PART IS
C THE MTF AND THE IMAGINARY PART IS THE PTF - THIS SAVES STORAGE
DO 405 K=1,65

```

```

DO 405 J=1,65
DUMMY(1)=CABS(GTF(J,K))
DUMMY(2)=0.0
DUM=REAL(GTF(J,K))
DUM=ABS(DUM)
IF(DUM.LT.10.E-6) GO TO 405
DUMMY(2)=ATAN2(AIMAG(GTF(J,K)), REAL(GTF(J,K)))
405 GTF(J,K)=CMPLX(DUMMY(1),DUMMY(2))
INDEX=2
WRITE(6,760)
760 FORMAT(1H1'VALUES OF THE MODULUS (MTF) AND PHASE (PTF) OF THE OPTICAL TRANSFER FUNCTION ARE PRINTED BELOW -'//-' THE MTF AND PTF VALUES ARE PRINTED AS A PAIR IN 8 BLOCKS OF 65(ROWS) BY 8(COLUMNS)'//')
3//)
GO TO 741

765 CONTINUE

C   SEARCH MI(I,K) VALUES TO DETERMINE PARAMETERS NS1 AND NS2 FOR
C   PLOTTING PROGRAM
NS1=0
NS2=0
DO 435 K=1,32
DO 435 I=1,32
IF(MI(I,K).EQ.0) GO TO 435
IF(I.LE.NS1) GO TO 430
NS1=I
430 NS2=K
435 CONTINUE

C   WRITE INFORMATION GENERATED BY THIS PROGRAM ON TAPE FOR USE WITH
C   PLOTTING PROGRAM
WRITE TAPE 7, DEVMIN, DEVMAX, RADIUS, WAVELENGTH, DELTA, DELTXY, DE, GTF, NS1,
1 NS2, FNG, RMSMAX
ENDFILE 7
WRITE(6,440)DELTA,DELTXY,RADIUS,WAVELENGTH,DEVMIN,DEVMAX,NS1,NS2,FNG,-
1 RMSMAX
440 FORMAT(1H1'THE FOLLOWING PARAMETERS, IN ADDITION TO THE DE AND GTF VALUES, ARE WRITTEN ON TAPE WHICH BECOMES INPUT TO THE PLOTTING PROGRAM'//'
1 THIS LISTING SHOULD BE CHECKED BEFORE RUNNING PLOTTING
3 PROGRAM'//'
1 DELTA = 'F8.3,10X'DELTXY = 'F8.3//'
1 RADIUS = 'F8.3,9
4 X'WAVELLENGTH = 'E9.4//'
1 DEVMIN = 'F8.3,9X'DEVMAX = 'F8.3//'
1 NS1 =
5 'I2,18X'NS2 = 'I2//'
1 F/NUMBER = 'F8.3//'
1 RMSMAX = LAMBDA'F8.3)
STOP
END

```

```

SUBROUTINE DEV( MI, DE, NSA, M11, M12, DEVMAX, DEVMIN, RADIUS, DELTA, HD, VD,
1 PCSX, PCSY, XCEN, YCEN, B, WAVEI, FOCUS, THICK, Z2, SUM, PASS, CUBE, Z2BEST,
2 PNO, RMSMAX )
      DIMENSION B( 23 ), B4BEST( 250 ), C( 23, 23 ), DE( 32, 32 ), DEL( 32, 32 ),
1 DERM8( 32, 32 ), DUL( 32 ), F( 24 ), HD( 32, 32 ), MI( 32, 32 ), M11( 32, 32 ),
2 M12( 32, 32 ), NAME1( 23 ), NAME2( 23 ), NAME3( 23 ), NAME4( 46 ), NAMES( 46 ),
3 NAME6( 46 ), POLYMX( 23 ), Q( 23 ), RMSDE( 250 ), V( 32, 32 ), VD( 32, 32 ),
4 XGRID( 33, 33 ), X1( 33 ), X2( 33 ), YGRID( 33 ), ZZ2( 250 )
      INTEGER PASS, CUBE, FOCUS
      DATA NAME1/6HC0NSTA, 6HX-TILT, 6HY-TILT, 6HFCCUS, 6H0 DEG, 6H45 DEG, 6
1 1HX-COMA, 6HY-COMA, 6HX-CLOV, 6HY-CLOV, 6HSPHERI, 6H0 DEG, 6H45 DEG, 6H
2 2, 6H, 6HX-COMA, 6HY-COMA, 6HX-CLOV, 6HY-CLOV, 6H, 6H
3 , 6HSPHERI, 6HSPHERI/
      DATA NAME2/6HNT, 6H, 6H, 6HDEPCT, 6HASTIG, 6H ASTIG, 6
1 1H( 3RD ), 6H( 3RD ), 6HER( 3RD ), 6HER( 3RD ), 6ECAL( 3R, 6HASTIG, 6H ASTIG, 6H
2 2, 6H, 6H( 5TH ), 6H( 5TH ), 6HER( 5TH ), 6HER( 5TH, 6H, 6H
3 , 6HCAL( 5T, 6HCAL( 7T/
      DATA NAME3/6H, 6H, 6H, 6H, 6H( 3RD ), 6H.( 3RD ), 6
1 H, 6H, 6H, 6H, 6HD, 6H( 5TH ), 6H.( 5TH ), 6H
2 , 6H, 6H, 6H, 6H, 6H, 6H, 6H
3 , 6HH), 6HH) /
      DATA NAME4/6HC0NSTA, 6H, 6HX, 6H, 6HY, 6H 2, 6
1 HX * Y, 6H 2, 6HX - Y, 6H, 6H2 XY, 6H 2, 6HX(X *, 6H
2 2, 6HY(X *, 6H 2, 6HX(X -, 6H 2, 6HY( 3X, 6H 2, 6F(X *
3 , 6H 4, 6HX - Y, 6H, 6H2 XY, 6H 4, 6HX - 6, 6H
4 H4 XY, 6H 2, 6HX(X *, 6H 2, 6HY(X *, 6H 5, 6HX - 2, 6H
5 4, 6H3X Y *, 6H 5, 6HX - 1, 6H 4, 6H5X Y -, 6H 2, 6H(X *
6 , 6H 2, 6H(X *, 6H, 6H, 6H, 6H, 6H2, 6
DATA NAMES/6HNT, 6H, 6H, 6H, 6H, 6H, 6H2, 6
1 H, 6H2, 6H, 6H, 6H, 6H, 6H, 6H Y, 6H
2 2, 6H Y, 6H, 6H, 6H, 6H, 6H, 6H, 6H Y, 6H
3 , 6H4, 6H, 6H, 6H, 6H, 6H, 6H, 6H, 6H Y, 6H
4 HX - Y, 6H 2, 6H Y, 6H, 6H, 6H, 6H, 6H, 6H Y, 6H
5 2 3, 6H 2X Y, 6H, 6H, 6H, 6H, 6H, 6H, 6H, 6H Y, 6H
6 , 6H 2, 6H, 6H, 6H, 6H, 6H, 6H, 6H, 6H
      DATA NAME6/6H, 6H, 6H, 6H, 6H, 6H, 6H, 6
1 H, 6H, 6H, 6H, 6H, 6H, 6H, 6H, 6H
2 , 6H, 6H, 6H, 6H, 6H, 6H, 6H, 6H
3 , 6H, 6H, 6H2, 6H, 6H, 6H, 6H, 6H
4 H, 6H, 6H, 6H, 6H, 6H, 6H, 6H, 6H2
5 5, 6H - Y, 6H, 6H, 6H, 6H, 6H, 6H, 6H, 6H3XY, 6H3
6 , 6H, 6H, 6H, 6H, 6H, 6H, 6H, 6H

```

C THE PUPIL-FUNCTION PHASE IS FIRST DETERMINED TO WITHIN A CONSTANT  
C SELECT A GRID POINT ( K1, K2 ) AT, OR NEAR, THE CENTER OF THE LENS  
C APERTURE AND SET DEL = 0.0  
C THEN SOLVE FOR DEL AT ADJACENT GRID POINTS FOR WHICH INTERPOLATED  
C PRINGE DEVIATIONS ARE KNOWN

```

K1=(NSA*1)/2
K2=(NSA*1)/2
ASSIGN 145 TO M
DEL(K1, K2)=0.0
MI(K1, K2)=1
J=K1
K=K2
142 J=J+1
IF( K.GT. K2 ) GO TO 160

```

161 IF(K.LT.K2)GO TO 165  
 161 IF(MI1(J,K).EQ.0) GO TO 143  
 IF(MI(J-1,K).EQ.0) GO TO 143  
 DEL(J,K)=HD(J,K)+DEL(J-1,K)  
 MI(J,K)=1  
 GO TO 142  
 160 IF(MI2(J,K).EQ.0)GO TO 161  
 IF(MI1(J,K).EQ.0)GO TO 162  
 IF(MI(J-1,K).EQ.0) GO TO 162  
 IF(MI(J,K+1).EQ.0) GO TO 161  
 DEL(J,K)=.5\*(DEL(J-1,K)+DEL(J,K-1)+HD(J,K)+VD(K,J))  
 MI(J,K)=1  
 GO TO 142  
 162 IF(MI(J,K-1).EQ.0) GO TO 142  
 DEL(J,K)=DEL(J,K-1)+VD(K,J)  
 MI(J,K)=1  
 GO TO 142  
 165 IF(MI2(J,K+1).EQ.0)GO TO 161  
 IF(MI1(J,K).EQ.0)GO TO 166  
 IF(MI(J-1,K).EQ.0) GO TO 166  
 IF(MI(J,K+1).EQ.0) GO TO 161  
 DEL(J,K)=.5\*(DEL(J-1,K)+DEL(J,K+1)+HD(J,K)-VD(K+1,J))  
 MI(J,K)=1  
 GO TO 142  
 166 IF(MI(J,K+1).EQ.0) GO TO 142  
 DEL(J,K)=DEL(J,K+1)-VD(K+1,J)  
 MI(J,K)=1  
 GO TO 142  
 143 J=K1  
 144 J=J-1  
 IF(K.GT.K2)GO TO 170  
 IF(K.LT.K2)GO TO 175  
 167 IF(MI1(J+1,K).EQ.0)GO TO M,(145,147)  
 IF(MI(J+1,K).EQ.0) GO TO M,(145,147)  
 DEL(J,K)=DEL(J+1,K)-HD(J+1,K)  
 MI(J,K)=1  
 IF(MI1(J,K).EQ.0) MI(J,K)=2  
 GO TO 144  
 170 IF(MI2(J,K).EQ.0)GO TO 167  
 IF(MI1(J+1,K).EQ.0)GO TO 171  
 IF(MI(J+1,K).EQ.0) GO TO 171  
 IF(MI(J,K-1).EQ.0) GO TO 167  
 DEL(J,K)=(DEL(J+1,K)+DEL(J,K-1)+VD(K,J)-HD(J+1,K))/2  
 MI(J,K)=1  
 GO TO 144  
 171 IF(MI(J,K-1).EQ.0) GO TO 144  
 DEL(J,K)=DEL(J,K-1)+VD(K,J)  
 MI(J,K)=1  
 GO TO 144  
 175 IF(MI2(J,K+1).EQ.0)GO TO 167  
 IF(MI1(J+1,K).EQ.0)GO TO 176  
 IF(MI(J+1,K).EQ.0) GO TO 176  
 IF(MI(J,K+1).EQ.0) GO TO 167  
 DEL(J,K)=(DEL(J+1,K)+DEL(J,K+1)-HD(J+1,K)-VD(K+1,J))/2  
 MI(J,K)=1  
 GO TO 144  
 176 IF(MI(J,K+1).EQ.0) GO TO 144  
 DEL(J,K)=DEL(J,K+1)-VD(K+1,J)

```

      MI(J,K)=1
      GO TO 144
145 K=K+1
      J=K1
      IF(MI2(J,K) .EQ. 0) GO TO 146
      IF(MI(J,K-1).EQ.0) GO TO 146
      DEL(J,K)=DEL(J,K-1)+VD(K,J)
      MI(J,K)=1
      GO TO 142
146 K=K2
      ASSIGN 147 TO M
147 J=K1
      IF(MI2(J,K) .EQ. 0) GO TO 150
      IF(MI(J,K).EQ.0) GO TO 150
      DEL(J,K-1)=DEL(J,K)-VD(K,J)
      MI(J,K-1)=1
      IF(MI2(J,K) .EQ. 0) MI(J,K-1)=2
      K=K-1
      GO TO 142
150 CONTINUE
      WRITE(6,499),K1,K2
499 FORMAT(1H1 'VALUES OF DEL(I,K) ARE PRINTED BELOW -'//'
1I2,'') WAS SET EQUAL TO ZERO'//'
2 THE EXPERIMENTAL CONSTANTS B1,B2(X
3 HAVE NOT BEEN REMOVED FROM THE COMPUTED DEL VALUES'//')
      WRITE(6,66)
      DO 500 K=1,32
500 WRITE(6,68)K,(DEL(J,K),J=2,17)
      WRITE(6,69)
      DO 501 K=1,32
501 WRITE(6,68)K,(DEL(J,K),J=18,33)

C      SOLVE FOR ABERRATION COEFFICIENTS IN ACTUAL LENS COORDINATES WHERE
C      Y=0 AND X=0 AT LENS CENTER (XCEN,YCEN).
C      THIS CHOICE OF COORDINATE-SYSTEM ORIGIN INSURES THAT THE PUPIL
C      FUNCTION IS CENTERED AT LENS CENTER, THEREBY EQUAL TO ZERO AFTER.
C      SUBTRACTING THE WAVEFRONT CONSTANT B(1).
      DO 40 MM=1,23
      DO 40 L=1,23
40  C(MM,L)=0.0
      DO 20 K=2,NSA
      DO 20 I=2,NSA
      IF(MI(I,K).EQ.0) GO TO 20
      Y=(K-2)*DELTA*POSX - YCEN
      X=(I-2)*DELTA * POSY - XCEN
      F(1)=1.0
      F(2)=X
      F(3)=Y
      F(4)=F(2)*F(2)*F(3)*F(3)
      F(5)=F(2)*F(2)-F(3)*F(3)
      F(6)=F(2)*F(3)*2
      F(7)=F(2)*F(4)
      F(8)=F(3)*F(4)
      F(9)=F(2)*(2*F(5)-F(4))
      F(10)=F(3)*(2*F(5)+F(4))
      F(11)=F(4)*F(4)
      F(12)=F(4)*F(5)
      F(13)=F(4)*F(6)

```

```

P(14)=P(5)*P(5)-P(6)*P(6)
P(15)=2*P(6)*P(5)
P(16)=P(2)*P(11)
P(17)=P(3)*P(11)
P(18)=P(4)*P(9)
P(19)=P(4)*P(10)
P(20)=P(2)*(P(11)-2*P(12)+2*P(14))
P(21)=P(3)*(P(11)+2*P(12)+2*P(14))
P(22)=P(4)*P(11)
P(23)=P(11)*P(11)
DUL(I)=DEL(I,K)
P(24)=DUL(I)
      DO 151 L=1,23
Q(L)=Q(L)*F(L)*P(24)
DO 151 MM=L,23
C(MM,L)=C(MM,L)*P(L)*P(MM)
151 C(L,MM)=C(MM,L)
20 CONTINUE
C CALL SUBROUTINE TO INVERT MATRIX C(L,M)
CALL INVERT(C,23)
DO 60 I=1,23
B(I)=0.
DO 61 K=1,23
61 B(I)=B(I)+C(I,K)*Q(K)
60 CONTINUE

IF(CUBE .EQ. 1) GO TO 62
C DETERMINE VALUES OF ABERRATION COEFFICIENTS INTRODUCED BY CUBE
C THESE ABERRATIONS ARE SYMMETRICAL AND DO NOT INCLUDE THOSE
C INTRODUCED BY TILTING THE CUBE - ALSO, THESE ABERRATIONS ARE
C COMPUTED FOR THE INDEX OF REFRACTION OF THE CUBE EQUAL TO 1.46008
C FOR DOUBLE-PASS SYSTEMS, ONLY 1/2 OF CUBE ABERRATIONS ARE
C COMPUTED BECAUSE THE EARLIER DIVISION OF FRINGE DEVIATIONS (WHICH
C INCLUDE CUBE ABERRATIONS) BY 2 HAS ELIMINATED THE OTHER HALF
B4CUB=665.534*(THICK/WAVEL)*((1.0/Z2)**2)*0.5461E-3
GO TO 395
62 B4CUB = 0.0
395 B11CUB = -425.550*(THICK/WAVEL)*((1.0/Z2)**4)*0.5461E-3
B22CUB=252.000*(THICK/WAVEL)*((1.0/Z2)**6)*0.5461E-3
B23CUB=94.600*(THICK/WAVEL)*((1.0/Z2)**8)*0.5461E-3
B4MAX=B4CUB*RADIUS**2
B11MAX=B11CUB*RADIUS**4
B22MAX=B22CUB*RADIUS**6
B23MAX=B23CUB*RADIUS**8
WRITE(6,400)B4CUB,B4MAX,B11CUB,B11MAX,B22CUB,B22MAX,B23CUB,B23MAX
400 FORMAT(1H1 'THE COEFFICIENTS AND MAXIMUM VALUES OF THE ABERRATIONS
1 INTRODUCED BY THE CUBE INTERFEROMETER ARE LISTED BELOW! // / 14X'COE
2 FFICIENT'8X'MAX. VALUE'12X'TYPE'//2X'B(4)'7XE11.6,7XF12.7,7X'DEFEC
4 T OF FOCUS'//2X'B(11)'6XE11.6,7XF12.7,7X'3RD ORDER SPHERICAL'//2X'
5B(22)'6XE11.6,7XF12.7,7X'5TH ORDER SPHERICAL'//2X'B(23)'6XE11.6,7X
6F12.7,7X'7TH ORDER SPHERICAL'//.)
WRITE(6,401)FNG,THICK,WAVEL
401 FORMAT(1H 'TEST-LENS F/NO. = 'F5.2,15X'CUBE THICKNESS = 'F7.3,' MM
1 '15X'TEST-LIGHT WAVELENGTH = 'E10.4,' MM')
WRITE(6,402)
402 FORMAT(//1H 'NOTE - ONLY ONE-HALF OF EACH OF THE ABOVE ABERRATIONS
1 IS REMOVED IF THE TEST SYSTEM IS DOUBLE PASS!')

```

C IF THE CHOSEN VALUE OF RADIUS IS SMALLER THAN THE FULL TEST  
 C APERTURE, THEN THE EFFECTIVE F/NO. IS INCREASED.  
 C THE M(I,K) MATRIX IS CHANGED TO CORRESPOND TO THE SMALLER  
 C APERTURE BY CHOOSING A SMALLER RADIUS IN THE EXIT PUPIL PLANE  
 C WHERE CENTERING OF THE APERTURE IS AT (XCEN,YCEN).  
 C ABERRATION COEFFICIENTS DETERMINED FOR FULL APERTURE ARE USED FOR  
 C CONSTRUCTING THE WAVEFRONT FROM THE SMALLER APERTURE.  
 DO 700 I=2,NSA  
 DO 700 I=2,NSA  
 IF(MI(I,K).EQ.0) GO TO 700  
 X=(I-2)\*DELTA+POSY-XCEN  
 Y=(K-2)\*DELTA+POSX-YCEN  
 XX=X\*X  
 YY=Y\*Y  
 R=XX+YY  
 RR=SQRT(R)  
 IF(RR.GE.RADIUS) MI(I,K)=0  
 700 CONTINUE

C CALCULATE PUPIL-FUNCTION PHASE (DE) USING ABERRATION COEFFICIENTS  
 TT=0.0  
 AV=0.0  
 TT1=0.0  
 AV1=0.0  
 TT2=0.0  
 AV2=0.0  
 SUMA=0.0  
 DO 70 K=2,NSA  
 DO 70 I=2,NSA  
 DE(I,K)=0.0  
 IF(MI(I,K).EQ.0) GO TO 70  
 X=(I-2)\*DELTA+POSY-XCEN  
 Y=(K-2)\*DELTA+POSX-YCEN  
 XX=X\*X  
 YY=Y\*Y  
 R=XX+YY  
 DE(I,K)=B(4)\*R\*B(5)\*(XX-YY)\*B(6)\*  
 1 2\*X\*Y\*B(7)\*X\*R\*B(8)\*Y\*R\*B(9)\*X\*(XX-3\*YY)  
 2 \*B(10)\*Y\*(3\*XX-YY)\*B(11)\*R\*R\*B(12)\*(XX-YY)\*R\*B(13)\*  
 3 2\*X\*Y\*R\*B(14)\*(XX\*XX-6\*XX\*YY\*YY\*YY)\*B(15)\*4\*X\*  
 4 Y\*(XX-YY)\*B(16)\*X\*R\*B(17)\*Y\*R\*R  
 5\*B(18)\*X\*R\*(XX-3\*YY)\*B(19)\*Y\*R\*(3\*XX-YY)  
 6\*B(20)\*X\*(XX\*XX-10\*XX\*YY\*5\*YY\*YY)\*B(21)\*Y\*(5\*XX\*XX  
 7-10\*XX\*YY\*YY\*YY)\*B(22)\*R\*R\*R\*B(23)\*R\*\*4

C REMOVE SYMMETRICAL CUBE ABERRATIONS FROM DE AND DEL VALUES  
 DE(I,K)=DE(I,K)-(1./PASS)\*(B4CUB\*R\*B11CUB\*R\*R\*B22CUB\*R\*R\*R\*B23CUB\*  
 1 R\*\*4)  
 DEL(I,K)=DEL(I,K)-(1./PASS)\*(B4CUB\*R\*B11CUB\*R\*R\*B22CUB\*R\*R\*R\*B23CU  
 1 B\*R\*\*4)  
 TT1=TT1+DE(I,K)\*DE(I,K)  
 AV1=AV1+DE(I,K)

C REMOVE CONSTANT AND X AND Y TILTS FROM DEL VALUES  
 DEL(I,K)=DEL(I,K)-B(1)-B(2)\*X-B(3)\*Y  
 AV2=AV2+DEL(I,K)  
 TT2=TT2+DEL(I,K)\*DEL(I,K)

C CALCULATE DIFFERENCE BETWEEN INPUT AND OUTPUT WAVEFRONTS  
 V(I,K)=DEL(I,K)-DE(I,K)  
 TT=TT+V(I,K)\*V(I,K)

```

AV=AV+V( I,K )
SUMA=SUMA+1.
70 CONTINUE

      WRITE( 6,300 )
300 FORMAT(1H1 'RESIDUAL VALUES ( V(I,K) ), THAT IS, THE DIFFERENCES BETW
1EEN THE INPUT WAVEFRONT ( DEL VALUES ) AND OUTPUT WAVEFRONT ( DE VALU
2ES ) // ARE PRINTED BELOW - // SYMMETRICAL ABERRATIONS INTRODUCED
3BY CUBE HAVE BEEN REMOVED // )
      WRITE( 6,66 )
      DO 301 K=1,32
301 WRITE( 6,68 )K,( V(I,K),I=2,17 )
      WRITE( 6,69 )
      DO 302 K=1,32
302 WRITE( 6,68 )K,( V(I,K),I=18,33 )
      RMSS=SQRT(( TT2/SUMA)-( AV2*AV2)/( SUMA*SUMA ))
      RMSS=1.0/RMSS
      WRITE( 6,112 )RMSS
112 FORMAT(//1H 'RMS OF INPUT WAVEFRONT ( DEL VALUES ) WITH B(1),B(2),
1B(3), AND CUBE ABERRATIONS, IF ANY, REMOVED = LAMBDA//F8.5//)
      RMS=SQRT(( TT1/SUMA)-( AV1*AV1)/( SUMA*SUMA ))
      RMS=1.0/RMS
      WRITE( 6,114 )RMS
114 FORMAT(1H 'RMS OF ANALYTIC WAVEFRONT ( DE VALUES ) WITH B(1),B(2),B(
13), AND CUBE ABERRATIONS, IF ANY, REMOVED = LAMBDA//F8.5//)
      RMSR=SQRT(( TT/SUMA)-( AV*AV)/( SUMA*SUMA ))
      RMSR=1.0/RMSR
      WRITE( 6,113 )RMSR,WAVEL
113 FORMAT(1H 'RMS OF RESIDUAL WAVEFRONT ( DEL-DE ) = LAMBDA//F8.3// /30
1X'WHERE LAMBDA = 'E9.4,2X'MM')

C      CALCULATE ABERRATION TERMS AT EDGE OF LENS APERTURE

C      FIRST, REMOVE EFFECT OF CUBE FROM APPROPRIATE ABERRATIONS
      IF(CUBE .EQ. 1) GO TO 79
      B(4)=B(4)-(1./PASS)*B4CUB
79    B(11)=B(11)-(1./PASS)*B11CUB
      B(22)=B(22)-(1./PASS)*B22CUB
      B(23)=B(23)-(1./PASS)*B23CUB

      R1=RADIUS
      POLYMX(1)=B(1)
      POLYMX(2)=B(2)*R1
      POLYMX(3)=B(3)*R1
      POLYMX(4)=B(4)*R1**2
      POLYMX(5)=B(5)*R1**2
      POLYMX(6)=B(6)*R1**2
      POLYMX(7)=B(7)*R1**3
      POLYMX(8)=B(8)*R1**3
      POLYMX(9)=B(9)*R1**3
      POLYMX(10)=B(10)*R1**3
      POLYMX(11)=B(11)*R1**4
      POLYMX(12)=B(12)*R1**4
      POLYMX(13)=B(13)*R1**4
      POLYMX(14)=B(14)*R1**4
      POLYMX(15)=B(15)*R1**4
      POLYMX(16)=B(16)*R1**5

```

```

POLYMX(17)=B(17)*R1**5
POLYMX(18)=B(18)*R1**5
POLYMX(19)=B(19)*R1**5
POLYMX(20)=B(20)*R1**5
POLYMX(21)=B(21)*R1**5
POLYMX(22)=B(22)*R1**6
POLYMX(23)=B(23)*R1**8
WRITE(6,80)
D6 82 I=1,23
80 FORMAT(1H1 'THE COEFFICIENTS B(I) FOR THE SET OF 23 POLYNOMIALS WHICH DESCRIBE LENS ABERRATIONS ARE LISTED BELOW-// CUBE ABERRATION 28, IF ANY, HAVE BEEN REMOVED FROM BOTH THE COEFFICIENTS AND THE MAX VALUES',//12X'B(I)'7X'MAX VALUE OF ABERRATION'14X'ABERRATION'29 4X'POLYNOMIAL'1 I'1GX'( B(I)*RADIUS**N N=1,...,8)//)
WRITE(6,83)I,B(I),POLYMX(I),NAME1(I),NAME2(I),NAME3(I),NAME4(I+I-1),NAME5(I+I-1),NAME6(I+I-1)
83 FORMAT(1H I2,2XE14.6,7XF9.4,26X3A6,20X3A6)
82 WRITE(6,84)NAME4(2*I),NAME5(2*I),NAME6(2*I)
84 FORMAT(1H 98X3A6)

C EXTRAPOLATE DE VALUES
C EFFECT OF CUBE HAS ALREADY BEEN REMOVED BY PREVIOUS ADJUSTMENT OF
C APPROPRIATE COEFFICIENTS
C COORDINATES OF GRID POINTS ARE DETERMINED IN A COORDINATE SYSTEM
C WITH AXES TANGENT TO THE FULL CIRCULAR APERTURE
YBGUN1=YCEN-RADIUS
YBGUN2=YCEN+RADIUS
D6 420 K=2,NSA
    YGRID(K)=PGSX*(K-2.0)*DELTA
D6 420 I=2,NSA
    IF(YGRID(K).LT.YBGUN1) G6 TO 418
    IF(YGRID(K).GT.YBGUN2) G6 TO 418
    X1(K)=XCEN-SQRT(RADIUS**2 + 2.*YGRID(K)*YCEN -YCEN**2 -YGRID(K)**2)
    X2(K)=XCEN+SQRT(RADIUS**2 + 2.*YGRID(K)*YCEN -YCEN**2 -YGRID(K)**2)
    XGRID(I,K)=PGSY*(I-2)*DELTA
    IF(XGRID(I,K).LE.X1(K)) G6 TO 418
    IF(XGRID(I,K).GE.X2(K)) G6 TO 418
    IF(MI(I,K).EQ.1 .OR. MI(I,K).EQ.2) G6 TO 420
    Y=(K-2)*DELTA*PGSX - YCEN
    X= (I-2)*DELTA + PGSY - XCEN
    YY=Y*Y
    XX =X*X
    R = XX + YY
    DE(I,K)=B(4)*R*B(5)*(XX-YY)*B(6)*
1 2*X*Y*B(7)*X*R*B(8)*Y*R*B(9)*X*(XX-3*YY)
2 *B(10)*Y*(3*XX-YY)*B(11)*R*R*B(12)*(XX-YY)*R*B(13)*
3 2*X*Y*R*B(14)*(XX*XX-6*XX*YY*YY*YY)*B(15)*4*X*
4 Y*(XX-YY)*B(16)*X*R*R*B(17)*Y*R*R
5 *B(18)*X*R*(XX-3*YY)*B(19)*Y*R*(3*XX-YY)
6 *B(20)*X*(XX*XX-10*XX*YY*5*YY*YY)*B(21)*Y*(5*XX*XX
7 -10*XX*YY*YY*YY)*B(22)*R*R*R*B(23)*R**4
    MI(I,K)=2
    G6 TO 420
418 DE(I,K)=0.0
    MI(I,K)=0.0
419 IF(MI(I,K).EQ.0) XGRID(I,K)=0.0
420 CONTINUE
360 WRITE(6,396)

```

```

396 FORMAT(1H1,'COORDINATE VALUES DEFINING LENS APERTURE ARE PRINTED B
1 BELOW -//! X1 AND X2 ARE APERTURE BOUNDARIES FOR A PARTICULAR Y OR
2 SCAN VALUE'//)
DO 398 K=1,NSA
398 WRITE(6,399)K,YGRID(K),X1(K),X2(K)
399 FORMAT(1H0'SCAN 'I2,7X 'Y - 'F8.3,7X 'X1 - 'F8.3,7X 'X2 - 'F8.3)

SUMA=0.0
SUMB=0.0
DO 25 K=1,32
DO 25 J=1,32
IF(MI(J,K).EQ.0) GO TO 25
IF(MI(J,K).EQ.1) GO TO 18
SUMB=SUMB+1.0
GO TO 25
18 SUMA=SUMA+1.0
25 CONTINUE
SUM=SUMA+SUMB
ISUM=SUM
ISUMA=SUMA
ISUMB=SUMB
WRITE(6,890),
890 FORMAT(1H1'VALUES OF MI(I,K) ARE PRINTED BELOW -//! MI = 1 INDIC
1ATES THAT A VALUE OF FRINGE ORDER P(J,K,N) WAS INTERPOLATED AT GRI
2D POINT(I,K) //! MI = 2'79K //! //! //! //! //!
3!! !! !! EXTRAPOLATED !! !! !! //)
WRITE(6,891)MI
891 FORMAT(1H0,32I3)
WRITE(6,50)ISUM,ISUMA,ISUMB
50 FORMAT(//! TOTAL NUMBER OF GRID POINTS IN THE CLEAR LENS APERTURE
1IS 'IS,' OF WHICH'//10XIS,' WERE INTERPOLATED AND 'IS.' WERE
2EXTRAPOLATED')

WRITE(6,211)
211 FORMAT(1H1'VALUES OF THE PUPIL-FUNCTION PHASE ARE PRINTED BELOW -!
1/' TERMS INVOLVING B(1),B(2), AND B(3) HAVE BEEN SUBTRACTED FROM
2DE VALUES'! DE = 0.0 AT THE CENTER OF THE LENS APERTURE'! THES
3E VALUES OF DE DO NOT, GENERALLY, REPRESENT THE PUPIL FUNCTION IN
4THE PLANE OF BEST FOCUS'//)
WRITE(6,66)
66 FORMAT(1H 2X'I'4X'2'7X'3'7X'4'7X'5'7X'6'7X'7'7X'8'7X'9'6X'10'6X'11
1'6X'12'6X'13'6X'14'6X'15'6X'16'6X'17'//! K')
DO 761 K=1,32
761 WRITE(6,68)K,(DE(I,K),I=2,17)
* 68 FORMAT(1H I2,1X16F8.3/)
WRITE(6,69)
69 FORMAT(//1H 2X'J'3X'18'6X'19'6X'20'6X'21'6X'22'6X'23'6X'24'6X'25'6
1X'26'6X'27'6X'28'6X'29'6X'30'6X'31'6X'32'6X'33'//! K')
DO 762 K=1,32
762 WRITE(6,68)K,(DE(I,K),I=18,33)

IF(FOCUS.EQ.1) GO TO 430
C CALCULATE PUPIL-FUNCTION PHASE FOR PLANE OF BEST FOCUS
C FIRST, CALCULATE RMS OF DE VALUES, INCLUDING EXTRAPOLATED VALUES,
C FOR PREVIOUS VALUE OF B(4)
AV3=0.0
TT3=0.0
DO 250 K=2,32

```

```

DO 250 I=2,32
DERMS( I, K )=DE( I, K )
IF( MI( I, K ) .EQ. 0 ) GO TO 250
AV3=AV3+DE( I, K )
TT3=TT3+DE( I, K )+DE( I, K )
250 CONTINUE
RMSDE( 1 )=SQRT( ( TT3/SUM )-( AV3*AV3)/( SUM*SUM ) )
RMSDE( 1 )=1.0/RMSDE( 1 )
C THE FOCAL POSITION ALONG THE OPTICAL AXIS WILL BE CHANGED IN
C INCREMENTS OF THE RAYLEIGH TOLERANCE ON DEFOCUSING AND THE
C RESULTING CHANGE IN B(4) WILL BE CALCULATED
RAYLGH=3.2*( WAVEFL/6.283185)*( Z2/RADIUS)**2
FRACT=0.0
299 DO 298 K=2,32
DO 298 I=2,32
298 DE( I, K )=DERMS( I, K )
WRITE( 6, 254 )RAYLGH
254 FORMAT( 1H1 'RAYLEIGH TOLERANCE ON DEPTH OF FOCUS FOR TEST LENS IS '
1' GR - 'E9.3, ' MM'/// )
WRITE( 6, 255 )
255 FORMAT( 1H1 'COEFFICIENT FOR DEFECT OF FOCUS, CORRESPONDING DISTANCE
1 TO FOCAL PLANE, AND RMS OF RESULTING WAVEFRONT ARE LISTED BELOW -
2'///5X1 INDEX PARAMETER, M'11X'B(4)'13X'Z2(MM)'11X'RMS(LAMBDA/VALUE
3')'.' )
M=1
WRITE( 6, 256 )M,B(4),Z2,RMSDE( 1 )
256 FORMAT( 1H1 12XI3,16XE11.6,7XF8.3,12XF10.5/ )
B4BEST( 1 )=B( 4 )
SIGN=1.0
FRACT=FRACT + 0.10
ZZ2( 1 )=Z2
257 DO 270 M=2,250
ZZ2( M )=ZZ2( M-1 )-( SIGN+FRACT*RAYLGH )
B4BEST( M )=B4BEST( M-1 )+( SIGN+FRACT*RAYLGH )/( 2.0*ZZ2( M )*WAVEFL*
2*( ZZ2( M )+SIGN+FRACT*RAYLGH ) )
AV4=0.0
TT4=0.0
DO 260 K=2,32
DO 260 I=2,32
IF( MI( I, K ) .EQ. 0 ) GO TO 260
X = ( I-2)*DELTA + PCSY - XCEN
Y=( K-2)*DELTA+PCSX - YCEN
YY=Y*Y
XX = X*X
R = YY*XX
DE( I, K )=DE( I, K )+( B4BEST( M )-B4BEST( M-1 ))*R
AV4=AV4+DE( I, K )
TT4=TT4+DE( I, K )+DE( I, K )
260 CONTINUE
RMSDE( M )=SQRT( ( TT4/SUM )-( AV4*AV4)/( SUM*SUM ) )
RMSDE( M )=1.0/RMSDE( M )
WRITE( 6, 256 )M,B4BEST( M ),ZZ2( M ),RMSDE( M )
IF( M .NE. 125 ) GO TO 270
258 SIGN=-1.0
B4BEST( 125 )=B4BEST( 1 )
ZZ2( 125 )=ZZ2( 1 )
DO 259 K=2,32
DO 259 I=2,32

```

```

259 DE(I,K)=DERMS(I,K)
      WRITE(6,263)
263 FORMAT(1H 'FOCUS SHIFT IS SUBSEQUENTLY MADE TO OPPOSITE SIDE OF T
1EST FOCUS POSITION')
270 CONTINUE
      MMAX=1
      RMSMAX=RMSDE(1)
      DO 265 M=2,250
      RMSMAX=AMAX1(RMSMAX,RMSDE(M))
      IRMSMX=RMSMAX*1.0E6
      IRMSDE=RMSDE(M)*1.0E6
      IF(IRMSDE .GE. IRMSMX) MMAX=M
265 CONTINUE
      WRITE(6,266)RMSMAX,MMAX,FRACT
266 FORMAT(///1H 'THE MINIMUM RMS FROM THE VALUES LISTED ABOVE IS LAMB
1DA/'F8.3.' FOR M = 'I3///1H 'THE FOCAL POSITION, Z2, ALONG THE OP
2TICAL AXIS WAS CHANGED IN INCREMENTS OF 'F5.2.' OF THE RAYLEIGH TO
3LERANCE ON DEPTH OF FOCUS'//1H 'HOWEVER, IF M = 125 OR 250, THE INC
4REMENT WILL BE DOUBLED AND THE SEARCH FOR MAXIMUM LAMBDA/RMS REPEA
5TED')
      IF(MMAX.EQ.125 .OR. MMAX.EQ.250) GO TO 299
      AV4=0.0
      TT4=0.0
      DO 269 K=2,32
      DO 269 I=2,32
      IF(MI(I,K) .EQ. 0) GO TO 269
      X=(I-2)*DELTA + POSY - XCEN
      Y=(K-2)*DELTA*POSX - YCEN
      YY=Y*Y
      XX=X*X
      R=YY+XX
      DE(I,K)=DERMS(I,K)*(B4BEST(MMAX)-B4BEST(1))*R
      AV4=AV4+DE(I,K)
      TT4=TT4+DE(I,K)*DE(I,K)
269 CONTINUE
      RMSMAX=SQRT((TT4/SUM)-(AV4*AV4)/(SUM*SUM))
      RMSMAX=1.0/RMSMAX
      DEFFOC=B4BEST(MMAX)*RADIUS**2
      WRITE(6,440)RMSMAX,DEFFOC
440 FORMAT(1H1 'VALUES OF THE PUPIL-FUNCTION PHASE FOR PLANE OF BEST FO
CUS ARE PRINTED BELOW - 1/1 TERMS INVOLVING B(2) AND B(3) AND CUBE
2ABERRATIONS, IF ANY, HAVE BEEN SUBTRACTED FROM DE VALUES AND 1/1 DE
3=0 AT THE CENTER OF THE LENS APERTURE'//1 'THE RMS OF THIS WAVEFRON
4T IS LAMBDA/'F8.3.' WITH A REMAINING MAXIMUM FOCUS DEFECT OF 'F9.3
5//)
      WRITE(6,66)
      DO 441 K=1,32
441 WRITE(6,68)K,(DE(I,K),I=2,17)
      WRITE(6,69)
      DO 442 K=1,32
442 WRITE(6,68)K,(DE(I,K),I=18,33)
C      SET DEFECT OF FOCUS COEFFICIENT EQUAL TO VALUE OBTAINED FOR
C      WAVEFRONT WITH MINIMUM RMS SO THAT GTF WILL BE CALCULATED IN PLANE
C      OF BEST FOCUS
      B(4)=B4BEST(MMAX)
C      SET FOCAL DISTANCE EQUAL TO DISTANCE TO PLANE OF BEST FOCUS
      ZZBEST=ZZZ(MMAX)

```

```

430 WRITE(6,421)
421 FORMAT(1H1 'COORDINATES OF THE GRID POINTS AT WHICH DE(I,K) WAS DET
    1ERMINED ARE PRINTED BELOW -'///' NOTE - COORDINATE VALUES OF 0.0 I
    2NDICATE THAT THE GRID POINT WAS OUTSIDE THE LENS APERTURE'///')
    WRITE(6,422)
422 FORMAT(6X'X-VALUE'/13X'I'5X'2'6X'3'6X'4'6X'5'6X'6'6X'7'6X'8'6X'9'
    15X'10'5X'11'5X'12'5X'13'5X'14'5X'15'5X'16'5X'17'/2X'K'2X'Y-VALUE')
    DO 423 K=2,17
423 WRITE(6,424)K,YGRID(K), (XGRID(I,K),I=2,17)
424 FORMAT(1XI2,F8.2,4X16F7.2/) "
    DO 425 K=18,33
425 WRITE(6,424)K,YGRID(K), (XGRID(I,K),I=2,17)
    WRITE(6,426)
426 FORMAT(//63X'X-VALUE'/13X'I'5X'18'5X'19'5X'20'5X'21'5X'22'5X'23'5X
    1'24'5X'25'5X'26'5X'27'5X'28'5X'29'5X'30'5X'31'5X'32'5X'33'      /2
    2X'K'2X'Y-VALUE')
    DO 427 K=2,17
427 WRITE(6,424)K,YGRID(K), (XGRID(I,K),I=18,33)
    DO 428 K=18,33
428 WRITE(6,424)K,YGRID(K), (XGRID(I,K),I=18,33)

C      DETERMINE MAXIMUM AND MINIMUM VALUES OF DE TO BE USED IN
C      SUBSEQUENT PLOTTING PROGRAMS
    DO 450 I=2,NSA
    DO 450 J=2,NSA
    DEVMAX=AMAX1(DEVMAX,DE(I,J))
450 DEVMIN=AMIN1(DEVMIN,DE(I,J))

560 RETURN
END

```

```

C      SUBROUTINE CORREL( MI,B,DELTA,STF,DE,SUM)
C      THIS SUBROUTINE CALCULATES THE GTF BY PERFORMING THE
C      AUTOCORRELATION OF THE PUPIL FUNCTION
C      DIMENSION B( 23 ), DE( 32,32 ), MI( 32,32 )
C      COMPLEX V, GTF( 65,65 )
C      REAL KX, KY, KXY

SUM6=B( 17 ) + 3.*B( 19 ) + 5.*B( 21 )
SUM7=B( 16 ) - 3.*B( 18 ) + 5.*B( 20 )
SUM8=B( 16 ) - B( 18 ) - 5.*B( 20 )
SUM9=B( 17 ) + B( 19 ) - 5.*B( 21 )
DIF4=B( 13 ) - 2.*B( 15 )
DIF5=B( 11 ) - 3.*B( 14 )

DO 10 L=1,65
KX=DELTA*( L-33 )
A2=KX**2
A3=A2*KX
A4=A3*KX
A5=A4*KX
A6=A5*KX
A7=A6*KX
A8=A7*KX
TERM1=B( 22 )*6.*KX
TERM3=B( 23 )*8.*KX
DO 10 M=1,33
KY=DELTA*( M-33 )
B2=KY**2
B3=B2*KY
B4=B3*KY
B5=B4*KY
B6=B5*KY
B7=B6*KY
B8=B7*KY
KXY=KX*KY
B2X=B2*KX
B3X=B3*KX
B4X=B4*KX
B2Y=B2*KY
B3Y=B3*KY
B4Y=B4*KY
A2B2=A2*B2
A3B2=A3*B2
A4B2=A4*B2
A2B3=A2*B3
A2B4=A2*B4
DIF1=A2-B2
SUM1=A2*B2
A2Y=A2*KY
A3Y=A3*KY
A4Y=A4*KY
DIF2=B2-A2
SUM2=5.*A2 + B2
SUM3=A2 + 5.*B2
SUM4=A3 + 3.*B2X
SUM5=3.*A2Y + B3
DIF3=A3 - 3.*B2X

```

TERM2=B(22)\*6.\*KY  
 TERM4=B(23)\*8.\*KY  
 TERM5=24.\*B(22)\*KXY

C2 = 2.\*KX\*(B(4) + B(5)) + B(6)\*2.\*KY + 2.\*KXY\*(B(8) + 3.\*B(10))  
 1 • B(7)\*(3.\*A2 + B2) + B(9)\*3.\*DIF1 + B(11)\*4.\*(A3 + B2X)  
 2 • B(12)\*4.\*A3 + B(13)\*2.\*SUM5 + B(14)\*4.\*DIF3  
 3 • B(15)\*(12.\*A2Y - 4.\*B3) + B(16)\*(5.\*A4 + 6.\*A2B2 + B4)  
 4 • B(17)\*4.\*(A3Y + B3X) + B(18)\*(5.\*A4 - 6.\*A2B2 - 3.\*B4)  
 5 • B(19)\*(12.\*A3Y + 4.\*B3X) + B(20)\*5.\*A4 - 6.\*A2B2 + B4)  
 6 • B(21)\*20.\*A3Y - B3X) + B(22)\*6.\*A5 + 2.\*A3B2 + B4X)  
 7 • B(23)\*8.\*A7 + 3.\*A5\*B2 + 3.\*A3\*B4 + KX\*B6)

C3 = B(6)\*2.\*KX + 2.\*KY\*(B(4) - B(5)) + 2.\*KXY\*(B(7) - 3.\*B(9))  
 1 • B(8)\*(A2 + 3.\*B2) + B(10)\*3.\*DIF1 + B(11)\*4.\*(A2Y + B3)  
 2 • B(12)\*4.\*B3 + B(13)\*2.\*SUM4 + B(14)\*4.\*(B3 - 3.\*A2Y)  
 3 • B(15)\*4.\*DIF3 + B(16)\*4.\*(B3X + A3Y)  
 4 • B(17)\*(A4 + 6.\*A2B2 + 5.\*B4) - B(18)\*4.\*A3 + 3.\*B3X + A3Y)  
 5 • B(19)\*(3.\*A4 + 6.\*A2B2 - 5.\*B4) + B(20)\*20.\*B3X - A3Y)  
 6 • B(21)\*5.\*A4 - 6.\*A2B2 + B4) + B(22)\*6.\*A4\*KY + 2.\*A2B3 + B5)  
 7 • B(23)\*8.\*A6\*KY + 3.\*A4\*B3 + 3.\*A2\*B5 + B7)

C4 = 2.\*KX\*(B(8) + 3.\*B(10)) + 2.\*KY\*(B(7) - 3.\*B(9))  
 1 • 6.\*KXY\*DIF5 + B(13)\*6.\*SUM1 + B(15)\*12.\*DIF1  
 2 • B(16)\*4.\*SUM5 + B(17)\*4.\*SUM4  
 3 • B(18)\*12.\*A2Y + B3) + B(19)\*12.\*A3 + B2X)  
 4 • B(20)\*20.\*B3 - 3.\*A2Y) + B(21)\*20.\*DIF3  
 5 • B(22)\*24.\*A3Y + B3X) + B(23)\*48.\*A5\*KY + 2.\*A3\*B3 + KX\*B5)

C5 = 3.\*KX\*(B(7) + B(9)) + KY\*(B(8) + 3.\*B(10))  
 1 • 6.\*KXY\*(B(13) + 2.\*B(15)) + B(11)\*2.\*A2 + B2)  
 2 • B(12)\*6.\*A2 + B(14)\*6.\*DIF1 + B(16)\*(6.\*B2X + 10.\*B3)  
 3 • B(17)\*2.\*SUM5 + B(18)\*(10.\*A3 - 6.\*B2X)  
 4 • B(19)\*2.\*A2Y + B3) + B(20)\*10.\*A3 - 3.\*KXY)  
 5 • B(21)\*10.\*A2Y - B3) + B(22)\*3.\*A4 + 6.\*A2B2 + B4)  
 6 • B(23)\*4.\*A6 + 15.\*A4B2 + 9.\*A2B4 + B6)

C6 = KX\*(B(7) - 3.\*B(9)) + 3.\*KY\*(B(8) - B(10))  
 1 • 6.\*KXY\*DIF4 + B(11)\*2.\*A2 + 3.\*B2)  
 2 • B(12)\*6.\*B2 + B(14)\*6.\*DIF2 + B(16)\*2.\*SUM4  
 3 • B(17)\*(6.\*A2Y + 10.\*B3) - B(18)\*2.\*A2Y + 9.\*B2X + A3)  
 4 • B(19)\*(6.\*A2Y - 10.\*B3) + B(20)\*10.\*A3 - 3.\*KXY)  
 5 • B(21)\*10.\*B3 - 3.\*A2Y) + B(22)\*3.\*A4 + 6.\*A2B2 + 5.\*B4)  
 6 • B(23)\*4.\*A6 + 9.\*A4B2 + 15.\*A2B4 + 7.\*B6)

C7 = 4.\*KX\*(B(11) + B(12) + B(14)) + 2.\*KY\*(B(13) + 2.\*B(15))  
 1 • 4.\*KXY\*SUM6 + B(16)\*2.\*SUM2  
 2 • B(18)\*2.\*A2 - B2) + B(20)\*10.\*DIF1  
 3 • B(22)\*(20.\*A3 + 12.\*B2X) + B(23)\*(56.\*A5 + 80.\*A3B2 + 24.\*B4X)

C8 = 2.\*KX\*DIF4 + 4.\*KY\*(B(11) - B(12) + B(14))  
 1 • 4.\*KXY\*SUM7 + B(17)\*2.\*SUM3  
 2 • B(19)\*2.\*A2 - 5.\*B2) + B(21)\*10.\*DIF2  
 3 • B(22)\*(12.\*A2Y + 20.\*B3) + B(23)\*(24.\*A4Y + 80.\*A2B3 + 56.\*B5)

C9 = 6.\*KX\*(B(13) + 2.\*B(15)) + 4.\*KY\*DIF5  
 1 • 12.\*KXY\*SUM8 + B(17)\*6.\*SUM1  
 2 • B(19)\*3.\*A2 + B2) + B(21)\*30.\*DIF1

3       $B(22)*12.*(3.*A2Y + B3) + B(23)*24.*(5.*A4Y + 6.*A2B3 + B5)$   
 C10     $4.*KX*DIF5 + 6.*KY*(B(13) - 2.*B(15))$   
 1       $12.*KXY*SUM9 + B(16)*6.*SUM1$   
 2       $B(18)*6.*(A2 + 3.*B2) + B(20)*30.*DIF2$   
 3       $B(22)*12.*(A3 + 3.*B2X) + B(23)*24.*(A5 + 6.*A3B2 + 5.*B4X)$   
 C11     $6.*KX*SUM8 + KY*SUM9 + B(22)*18.*SUM1$   
 1       $B(23)*(60.*A4 + 216.*A2B2 + 60.*B4)$   
 C12     $5.*KX*(B(16) + B(18) + B(20)) + KY*SUM6 + B(22)*3.*SUM2$   
 1       $B(23)*(70.*A4 + 60.*A2B2 + 6.*B4)$   
 C13     $KX*SUM7 + 5.*KY*(B(17) - B(19) + B(21)) + B(22)*3.*SUM3$   
 1       $B(23)*(6.*A4 + 60.*A2B2 + 70.*B4)$   
 C14     $4.*KX*SUM6 + KY*SUM8 + B(23)*(96.*B3X + 160.*A3Y) + TERM5$   
 C15     $4.*KX*SUM9 + KY*SUM7 + B(23)*(160.*B3X + 96.*A3Y) + TERM5$   
 C16     $TERM1 + B(23)*(56.*A3 + 24.*B2X)$   
 C17     $TERM2 + B(23)*(24.*A2Y + 56.*B3)$   
 C18     $2.*TERM1 + B(23)*(80.*A3 + 144.*B2X)$   
 C19     $2.*TERM2 + B(23)*(144.*A2Y + 80.*B3)$   
 C20     $TERM2 + B(23)*24.*(5.*A2Y + B3)$   
 C21     $TERM1 + B(23)*24.*(A3 + 5.*B2X)$   
 C22     $B(23)*4.*(7.*A2 + B2)$   
 C23     $B(23)*4.*(A2 + 7.*B2)$   
 C24     $B(23)*48.*KXY$   
 C25     $C24$   
 C26     $B(23)*(60.*A2 + 36.*B2)$   
 C27     $B(23)*(36.*A2 + 60.*B2)$   
 C28     $TERM3$   
 C29     $TERM4$   
 C30     $C29$   
 C31     $C28$   
 C32     $3.*C28$   
 C33     $3.*C29$   
 C34     $C33$   
 C35     $C32$

100 CONTINUE

```

DG 10 J=1,32
X=DELTA*(J-13)
X2=X*X
X3=X2*X
X4=X3*X
X5=X4*X
X6=X5*X
X7=X6*X
DG 10 K=1,32
IF(MI(J,K).EQ.0) GO TO 10
IN=J+L-33
IF(IN.GT.32 .OR. IN.LT.1) GO TO 10
IM=K+M-33
IF(IM.GT.32 .OR. IM.LT.1) GO TO 10
IF(MI(IN,IM).EQ.0) GO TO 10
Y=DELTA*(K-13)
Y2=Y*Y
Y3=Y2*Y

```

```

Y4=Y3+Y
Y5=Y4+Y
Y6=Y5+Y
Y7=Y6+Y
XY=X+Y
YY2=Y+X2
XY2=X+Y2
X2Y2=X2+Y2
YX3=Y+X3
XY3=X+Y3
X3Y2=X3+Y2
X2Y3=X2+Y3
XY4=X+Y4
X4Y=X4+Y
X2Y4=X2+Y4
X4Y2=X4+Y2
X3Y3=X3+Y3
XY5=X+Y5
X5Y=X5+Y
X2Y5=X2+Y5
X5Y2=X5+Y2
XY6=X+Y6
X6Y=X6+Y
VV = 6.283185*(DE( IN, IM ) - DE( J, K ))
A=CGS(VV)
D=SIN(VV)
V=CMPLX(A,D)
V1 = 6.283185*(C2 + C4*Y + C10*Y2 + C15*Y3 + C21*Y4 + C25*Y5 + C31*Y6
1   + 2.*(C5*X + C9*XY + C11*XY2 + C19*XY3 + C27*XY4 + C33*XY5 )
2   + 3.*(C7*X2 + C14*XY2 + C18*X2Y2 + C35*X2Y4 )
3   + 4.*(C12*X3 + C20*XY3 + C26*X3Y2 + C34*X3Y3 )
4   + 5.*(C16*X4 + C24*X4Y + C32*X4Y2 )
5   + 6.*(C22*X5 + C30*XY5) + 7.*C28*X6 )
D1=V1+DELTA/2.0
D1 ABS=ARS(D1)
IF(D1ABS .LE. .001) GO TO 6
IF(D1ABS .GE. 1.0E+3) GO TO 10
SINC1=SIN(D1)/D1
GO TO 7
6 SINC1=1.00
GO TO 7
7 V2 = 6.283185*(C3 + C4*X + C9*X2 + C14*X3 + C20*X4 + C24*X5 + C30*X6
1   + 2.*(C6*Y + C10*XY + C11*YY2 + C18*YX3 + C26*X4Y + C32*X5Y )
2   + 3.*(C8*Y2 + C15*XY2 + C19*X2Y2 + C34*X4Y2 )
3   + 4.*(C13*Y3 + C21*XY3 + C27*X2Y3 + C35*X3Y3 )
4   + 5.*(C17*Y4 + C25*XY4 + C33*X2Y4 )
5   + 6.*(C23*Y5 + C31*XY5) + 7.*C29*Y6 )
D2=V2+DELTA/2.0
D2 ABS=ARS(D2)
IF(D2ABS .LE. .001) GO TO 8
IF(D2ABS .GE. 1.0E+3) GO TO 10
SINC2=SIN(D2)/D2
GO TO 9
8 SINC2=1.00
GO TO 9
9 GTF(L,M)=GTF(L,M) + V*SINC1*SINC2
10 CONTINUE

```

C USE SYMMETRY OF MTF ABOUT L=33, M=33 TO DETERMINE OTHER HALF OF  
C GTF VALUES  
D6 60 J=1,33  
D6 60 I=1,65  
F=REAL(GTF(65-I+1,33-J+1))  
G=-AIMAG(GTF(65-I+1,33-J+1))  
60 GTF(I,33+J-1)=CMPLX(F,G)  
D6 40 M=1,65  
D6 40 L=1,65  
40 GTF(L,M)=GTF(L,M)/SUM  
RETURN  
END

```

SUBROUTINE INVERT (A,N)
C      MATRIX INVERSION BY GAUSS-JORDAN ELIMINATION
      DIMENSION A(23,23),B(23),C(23),LZ(23)
      DO 10 J = 1,N
10 LZ(J) = J
      DO 20 I = 1,N
      K = I
      Y = A(I,I)
      LP = I + 1
      IF (N - LP) 14,11,11
11 DO 13 J = LP,N
      W = A(I,J)
      IF (ABS(W) - ABS(Y)) 13,13,12
12 K = J
      Y = W
13 CONTINUE
14 DO 15 J = 1,N
      C(J) = A(J,K)
      A(J,K) = A(J,I)
      A(J,I) = -C(J) / Y
      A(I,J) = A(I,J) / Y
15 B(J) = A(I,J)
      A(I,I) = 1.0 / Y
      J = LZ(I)
      LZ(I) = LZ(K)
      LZ(K) = J
      DO 19 K = 1,N
      IF (I - K) 16,19,16
16 DO 18 J = 1,N
      IF (I - J) 17,18,17
17 A(K,J) = A(K,J) - B(J) * C(K)
18 CONTINUE
19 CONTINUE
20 CONTINUE
      DO 200 I = 1,N
      IF (I - LZ(I)) 100,200,100
100 K = I + 1
      DO 500 J = K,N
      IF (I - LZ(J)) 500,600,500
500 M = LZ(I)
      LZ(I) = LZ(J)
      LZ(J) = M
      DO 700 L = 1,N
      C(L) = A(I,L)
      A(I,L) = A(J,L)
700 A(J,L) = C(L)
500 CONTINUE
200 CONTINUE
      RETURN
      END

```

```

      SUBROUTINE SPLICE(X,Y,M,C)
C THIS SUBROUTINE DETERMINES CONSTANT COEFFICIENTS C(I,K) OF SPLINE-
C FITTED CURVE WHICH PASSES THROUGH DATA POINTS
C DIMENSION X(32),Y(32),D(32),P(32),E(32),C(4,32),A(32,3),B(32),
1Z(32)
      MM=M-1
      DO 2 K=1,MM
      D(K)=X(K+1)-X(K)
      P(K)=D(K)/6.
2     E(K)=(Y(K+1)-Y(K))/D(K)
      DO 3 K=2,MM
3     B(K)=E(K)-E(K-1)
      A(1,2)=-1.-D(1)/D(2)
      A(1,3)=D(1)/D(2)
      A(2,3)=P(2)-P(1)*A(1,3)
      A(2,2)=2.*(P(1)*P(2))-P(1)*A(1,2)
      A(2,3)=A(2,3)/A(2,2)
      B(2)=B(2)/A(2,2)
      DO 4 K=3,MM
      A(K,2)=2.*(P(K-1)*P(K))-P(K-1)*A(K-1,3)
      B(K)=B(K)-P(K-1)*B(K-1)
      A(K,3)=P(K)/A(K,2)
4     B(K)=B(K)/A(K,2)
      Q=D(M-2)/D(M-1)
      A(M,1)=1.+Q*A(M-2,3)
      A(M,2)=-Q-A(M,1)*A(M-1,3)
      B(M)=B(M-2)-A(M,1)*B(M-1)
      Z(M)=B(M)/A(M,2)
      MN=M-2
      DO 6 I=1,MN
      K=M-I
6     Z(K)=B(K)-A(K,3)*Z(K+1)
      Z(1)=-A(1,2)*Z(2)-A(1,3)*Z(3)
      DO 7 K=1,MM
      Q=1./((6.*D(K)))
      C(1,K)=Z(1)*Q
      C(2,K)=Z(K+1)*Q
      C(3,K)=Y(K)/D(K)-Z(K)*P(K)
7     C(4,K)=Y(K+1)/D(K)-Z(K+1)*P(K)
      RETURN
101    FORMAT(2E12.4)
      END

```

C SUBROUTINE SPLINE(X,Y,M,C,XINT,YINT,4,N,KDUM)  
C THIS SUBROUTINE USES COEFFICIENTS FROM SUBROUTINE SPLICE TO  
C CONSTRUCT CURVE THROUGH DATA AND THEREFROM TO INTERPOLATE FRINGE  
C DEVIATIONS AT SELECTED GRID POINTS  
C DIMENSION X(32),Y(32),C(4,32)  
C KK=KDUM  
C IF(XINT-X(1))7,1,2  
1 YINT=Y(1)  
C RETURN  
2 K=1  
3 IF(XINT-X(K+1))6,4,5  
4 YINT=Y(K+1)  
C RETURN  
5 K=K+1  
6 IF(XINT-X(M))3,8,7  
6 YINT=(X(K+1)-XINT)\*(C(1,K)\*(X(K+1)-XINT)\*\*2+C(3,K))  
YINT=YINT+(XINT-X(K))\*(C(2,K)\*(XINT-X(K)\*\*2+C(4,K)))  
C RETURN  
8 YINT=Y@M)  
C RETURN  
7 WRITE(6,101)XINT,KK,N  
101 FORMAT(1H 'XINT = 'F7.3,5X'FOR SCAN 'I2,' AND FRAME'I2/)  
C RETURN 7  
C END

C  
C  
C  
C

SUBROUTINE SPECSP(X,Y,M,C,XINT,YINT,N,EDUM)  
THIS SUBROUTINE USES COEFFICIENTS FROM SUBROUTINE SPLICE TO  
CONSTRUCT CURVE THROUGH DATA FOR SPECIAL CASE IN WHICH ONLY TWO  
FRINGE-PEAK LOCATIONS EXIST FOR A SCAN AND THEREFROM TO  
INTERPOLATE FRINGE DEVIATIONS AT SELECTED GRID POINTS  
DIMENSION X(32),Y(32),C(4,32)

KK=EDUM  
IF(XINT-X(1))7,1,2  
1 YINT=Y(1)  
RETURN  
2 K=1  
3 IF(XINT-X(K+1))6,4,5  
4 YINT=Y(K+1)  
RETURN  
5 K=K+1  
IF(K .LT. M) GO TO 3  
K=K-1  
6 YINT=(X(K+1)-XINT)\*(C(1,K)\*(X(K+1)-XINT)\*\*2+C(3,K))  
YINT=YINT\*(XINT-X(K))\*(C(2,K)\*(XINT-X(K))\*\*2+C(4,K))  
RETURN  
7 K=1  
GO TO 6  
END

### Sample Printout

THE INFLUENCE OF COMPUTER PROGRAMS ON THE TEST-ITEM-TEST-TAKING RELATIONSHIP

CALIBRATION P/0.7 UTEST 31

ON THE WAVEFRONT SHEARING INTERFEROMETER TEST SYSTEM

VALUES AND DEFINITIONS OF PHOTOGAN PANAMETERS ARE PRINTED BELOW -  
NOTES (1) X AND Y AXES ARE COORDINATE SYSTEM OF SCANNER  
(2) DISTANCE VALUES ARE IN MM UNLESS SPECIFIED OTHERWISE

INPUT = 1 INDICATES THAT INPUT DATA WAS FRINGE-PEAK POSITIONS OBTAINED FROM MANUAL SCAN  
INPUT = 2 INDICATES THAT TEST SYSTEM HAS DOUBLE PASS

FIGURE 1 IS X-SHEARED INTERFEROGRAM AND FRAME 2 IS Y-SMEARED INTERFEROGRAM

FRINGE-PEAK POSITIONS  $(J, J, K, N)$  AS SCANNED (INPUT DATA) ARE PRINTED BELOW -

$J$  = FRINGE NO.  
 $K$  = SCAN NO.

VALUES OF  $X(J, J, K, N)$  ARE PRINTED IN 2 BLOCKS FOR EACH FRAME

MAXIMUM NUMBER OF FRINGES AND SCANS ALLOWED PER FRAME IS 29

FRAME 1

$J$	1	2	3	4	5	6	7	8	9	10	11	12	13	14	15	16
$K$																
1	-0.00	.000	.000	.000	.000	.000	.000	.000	.000	.000	.000	.000	.000	.000	.000	.000
2	.000	.000	.000	.000	.000	.000	.000	.000	.000	.000	.000	.000	.000	.000	.000	.000
3	.000	.000	.000	.000	.000	.000	.000	.000	.000	.000	.000	.000	.000	.000	.000	.000
4	.000	.000	.000	.000	.000	.000	.000	.000	.000	.000	.000	.000	.000	.000	.000	.000
5	.000	.000	.000	.000	.000	.000	.000	.000	.000	.000	.000	.000	.000	.000	.000	.000
6	.000	.000	.000	.000	.000	.000	.000	.000	.000	.000	.000	.000	.000	.000	.000	.000
7	.000	.000	.000	.000	.000	.000	.000	.000	.000	.000	.000	.000	.000	.000	.000	.000
8	.000	.000	.000	.000	.000	.000	.000	.000	.000	.000	.000	.000	.000	.000	.000	.000
9	.000	.000	.000	.000	.000	.000	.000	.000	.000	.000	.000	.000	.000	.000	.000	.000
10	.000	.000	.000	.000	.000	.000	.000	.000	.000	.000	.000	.000	.000	.000	.000	.000
11	.000	.000	.000	.000	.000	.000	.000	.000	.000	.000	.000	.000	.000	.000	.000	.000
12	.000	.000	.000	.000	.000	.000	.000	.000	.000	.000	.000	.000	.000	.000	.000	.000
13	.000	.000	.000	.000	.000	.000	.000	.000	.000	.000	.000	.000	.000	.000	.000	.000
14	.000	.000	.000	.000	.000	.000	.000	.000	.000	.000	.000	.000	.000	.000	.000	.000
15	.000	.000	.000	.000	.000	.000	.000	.000	.000	.000	.000	.000	.000	.000	.000	.000
16	.000	.000	.000	.000	.000	.000	.000	.000	.000	.000	.000	.000	.000	.000	.000	.000
17	.000	.000	.000	.000	.000	.000	.000	.000	.000	.000	.000	.000	.000	.000	.000	.000
18	.000	.000	.000	.000	.000	.000	.000	.000	.000	.000	.000	.000	.000	.000	.000	.000
19	.000	.000	.000	.000	.000	.000	.000	.000	.000	.000	.000	.000	.000	.000	.000	.000
20	.000	.000	.000	.000	.000	.000	.000	.000	.000	.000	.000	.000	.000	.000	.000	.000
21	.000	.000	.000	.000	.000	.000	.000	.000	.000	.000	.000	.000	.000	.000	.000	.000
22	.000	.000	.000	.000	.000	.000	.000	.000	.000	.000	.000	.000	.000	.000	.000	.000
23	.000	.000	.000	.000	.000	.000	.000	.000	.000	.000	.000	.000	.000	.000	.000	.000
24	.000	.000	.000	.000	.000	.000	.000	.000	.000	.000	.000	.000	.000	.000	.000	.000
25	.000	.000	.000	.000	.000	.000	.000	.000	.000	.000	.000	.000	.000	.000	.000	.000
26	.000	.000	.000	.000	.000	.000	.000	.000	.000	.000	.000	.000	.000	.000	.000	.000
27	.000	.000	.000	.000	.000	.000	.000	.000	.000	.000	.000	.000	.000	.000	.000	.000
28	.000	.000	.000	.000	.000	.000	.000	.000	.000	.000	.000	.000	.000	.000	.000	.000
29	.000	.000	.000	.000	.000	.000	.000	.000	.000	.000	.000	.000	.000	.000	.000	.000
30	.000	.000	.000	.000	.000	.000	.000	.000	.000	.000	.000	.000	.000	.000	.000	.000





NORMALIZED PRINCE POSITIONS X(J,K,N) ARE PRINTED BELOW -

J = PRINCE NO.      K = SCAN NO.

VALUES OF X(J,K,N) ARE PRINTED IN 2 BLOCKS OF 32(ROWS) BY 16(COLUMNS) FOR EACH FRAME

NOTE - THE FIRST PRINCE WAS ASSIGNED J=3 AS INPUT DATA. THE SECOND PRINCE J=4, ETC.

FRAME 1

K	J	2	3	4	5	6	7	8	9	10	11	12	13	14	15	16	17
1	-.000	.000	.000	.000	.000	.000	.000	.000	.000	.000	9.840	10.917	11.999	12.982	14.059	15.074	16.169
2	-.000	.000	.000	.000	.000	.000	.000	.000	.000	.000	9.833	10.893	11.987	12.970	14.078	15.118	16.169
3	-.000	.000	.000	.000	.000	.000	.000	.000	.000	.000	9.836	10.897	11.972	12.981	14.055	15.113	16.138
4	-.000	.000	.000	.000	.000	.000	.000	.000	.000	.000	9.821	10.879	11.940	12.988	14.056	15.102	16.150
5	-.000	.000	.000	.000	.000	.000	.000	.000	.000	.000	9.827	10.874	11.929	12.982	14.030	15.098	16.104
6	-.000	.000	.000	.000	.000	.000	.000	.000	.000	.000	9.828	10.874	11.928	12.987	14.024	15.056	16.123
7	-.000	.000	.000	.000	.000	.000	.000	.000	.000	.000	9.809	10.867	11.919	12.988	14.020	15.094	16.156
8	-.000	.000	2.605	3.472	4.548	5.551	6.642	7.681	8.757	9.798	10.851	11.898	12.976	14.033	15.100	16.153	
9	-.000	.000	2.514	3.468	4.508	5.608	6.630	7.676	8.760	9.789	10.841	11.908	12.966	14.030	15.097	16.107	
10	-.000	1.650	2.683	3.441	4.505	5.505	6.613	7.678	8.741	9.776	10.857	11.925	12.981	14.042	15.097	16.177	
11	-.000	1.669	2.612	3.444	4.508	5.502	6.627	7.670	8.718	9.776	10.862	11.923	12.982	14.011	15.084	16.174	
12	-.000	1.569	2.425	3.437	4.508	5.543	6.613	7.668	8.705	9.767	10.862	11.921	12.976	14.034	15.110	16.192	
13	-.000	1.533	2.423	3.456	4.509	5.554	6.609	7.657	8.703	9.770	10.851	11.937	12.986	13.993	15.091	16.166	
14	-.000	1.533	2.416	3.444	4.498	5.548	6.600	7.670	8.719	9.768	10.868	11.918	12.987	14.029	15.096	16.186	
15	-.000	1.553	2.395	3.438	4.499	5.549	6.624	7.670	8.724	9.761	10.831	11.921	12.976	14.034	15.110	16.192	
16	-.000	2.416	3.415	4.485	5.540	6.601	7.669	8.727	9.789	10.837	11.900	12.967	14.052	15.115	16.174		
17	-.000	2.427	3.424	4.460	5.537	6.598	7.672	8.715	9.769	10.836	11.905	12.974	14.035	15.098	16.143		
18	-.000	2.495	3.439	4.460	5.521	6.643	7.655	8.729	9.761	10.861	11.908	12.963	14.029	15.079	16.126		
19	-.000	-	.000	3.494	4.474	5.520	6.600	7.665	8.712	9.759	10.824	11.895	12.944	14.003	15.052	16.105	
20	-.000	-	.000	-	4.519	5.521	6.600	7.643	8.712	9.758	10.805	11.873	12.938	13.981	15.039	16.097	
21	-.000	-	.000	-	4.614	5.501	6.597	7.626	8.692	9.750	10.814	11.873	12.941	13.976	15.060	16.089	
22	-.000	-	.000	-	-	5.564	6.586	7.541	8.692	9.727	10.803	11.866	12.934	13.960	15.038	16.089	

	<i>K</i>	<i>J</i>	18	19	20	21	22	23	24	25	26	27	28	29	30	31	32	33
1	-000	-000	-000	-000	-000	-000	-000	-000	-000	-000	-000	-000	-000	-000	-000	-000	-000	
2	17.211	-000	-000	-000	-000	-000	-000	-000	-000	-000	-000	-000	-000	-000	-000	-000	-000	
3	17.248	18.244	19.261	-000	-000	-000	-000	-000	-000	-000	-000	-000	-000	-000	-000	-000	-000	
4	17.248	18.255	19.349	20.287	-000	-000	-000	-000	-000	-000	-000	-000	-000	-000	-000	-000	-000	
5	17.225	18.292	19.331	20.376	21.366	-000	-000	-000	-000	-000	-000	-000	-000	-000	-000	-000	-000	
6	17.225	18.259	19.340	20.386	21.438	22.333	-000	-000	-000	-000	-000	-000	-000	-000	-000	-000	-000	
7	17.218	18.251	19.314	20.397	21.440	22.467	-000	-000	-000	-000	-000	-000	-000	-000	-000	-000	-000	
8	17.215	18.249	19.307	20.411	21.441	22.485	23.453	-000	-000	-000	-000	-000	-000	-000	-000	-000	-000	
9	17.222	18.237	19.329	20.377	21.440	22.491	23.509	-000	-000	-000	-000	-000	-000	-000	-000	-000	-000	
10	17.203	18.252	19.335	20.344	21.455	22.497	23.532	24.429	-000	-000	-000	-000	-000	-000	-000	-000	-000	
11	17.191	18.244	19.313	20.355	21.401	22.503	23.534	24.476	-000	-000	-000	-000	-000	-000	-000	-000	-000	
12	17.206	18.261	19.292	20.386	21.408	22.488	23.529	24.510	-000	-000	-000	-000	-000	-000	-000	-000	-000	
13	17.216	18.242	19.282	20.355	21.413	22.492	23.520	24.491	-000	-000	-000	-000	-000	-000	-000	-000	-000	
14	17.231	18.244	19.261	20.333	21.405	22.471	23.518	24.491	-000	-000	-000	-000	-000	-000	-000	-000	-000	
15	17.212	18.246	19.259	20.323	21.379	22.478	23.514	24.440	-000	-000	-000	-000	-000	-000	-000	-000	-000	
16	17.205	18.233	19.288	20.304	21.373	22.481	23.454	-000	-000	-000	-000	-000	-000	-000	-000	-000	-000	
17	17.184	18.240	19.301	20.362	21.370	22.438	23.429	-000	-000	-000	-000	-000	-000	-000	-000	-000	-000	

18	17.159	18.234	19.295	20.355	21.392	22.414	.000	.000	.000	.000	.000	.000	.000	.000	.000	.000	.000	.000
19	17.162	18.210	19.266	20.327	21.381	22.393	.000	.000	.000	.000	.000	.000	.000	.000	.000	.000	.000	.000
20	17.135	18.215	19.266	20.328	21.367	22.390	.000	.000	.000	.000	.000	.000	.000	.000	.000	.000	.000	.000
21	17.128	18.196	19.267	20.256	21.243	22.300	.000	.000	.000	.000	.000	.000	.000	.000	.000	.000	.000	.000
22	17.128	18.139	19.174	20.197	.000	.000	.000	.000	.000	.000	.000	.000	.000	.000	.000	.000	.000	.000
23	17.168	18.173	.000	.000	.000	.000	.000	.000	.000	.000	.000	.000	.000	.000	.000	.000	.000	.000
24	.000	.000	.000	.000	.000	.000	.000	.000	.000	.000	.000	.000	.000	.000	.000	.000	.000	.000
25	.000	.000	.000	.000	.000	.000	.000	.000	.000	.000	.000	.000	.000	.000	.000	.000	.000	.000
26	.000	.000	.000	.000	.000	.000	.000	.000	.000	.000	.000	.000	.000	.000	.000	.000	.000	.000
27	.000	.000	.000	.000	.000	.000	.000	.000	.000	.000	.000	.000	.000	.000	.000	.000	.000	.000
28	.000	.000	.000	.000	.000	.000	.000	.000	.000	.000	.000	.000	.000	.000	.000	.000	.000	.000
29	.000	.000	.000	.000	.000	.000	.000	.000	.000	.000	.000	.000	.000	.000	.000	.000	.000	.000
30	.000	.000	.000	.000	.000	.000	.000	.000	.000	.000	.000	.000	.000	.000	.000	.000	.000	.000
31	.000	.000	.000	.000	.000	.000	.000	.000	.000	.000	.000	.000	.000	.000	.000	.000	.000	.000
32	.000	.000	.000	.000	.000	.000	.000	.000	.000	.000	.000	.000	.000	.000	.000	.000	.000	.000

## FRAME 2

x	1	2	3	4	5	6	7	8	9	10	11	12	13	14	15	16	17	
1	.000	.000	.000	.000	.000	.000	.000	.000	.000	.000	11.425	12.508	13.464	14.543	.000	.000	.000	
2	.000	.000	.000	.000	.000	.000	.000	.000	.000	.000	10.324	11.367	12.440	13.510	14.574	15.559	16.639	
3	.000	.000	.000	.000	.000	.000	.000	.000	.000	.000	9.301	9.348	9.314	10.314	11.363	12.436	13.502	14.560
4	.000	.000	.000	.000	.000	.000	.000	.000	.000	.000	5.236	6.153	7.174	8.212	9.293	10.310	11.368	12.458
5	.000	.000	.000	.000	.000	.000	.000	.000	.000	.000	4.189	5.120	6.150	7.144	8.204	9.267	10.317	11.369
6	.000	.000	.000	.000	.000	.000	.000	.000	.000	.000	5.061	6.103	7.107	8.216	9.275	10.326	11.420	12.439
7	.000	.000	.039	.025	.039	.000	.000	.000	.000	.000	6.109	7.170	8.198	9.266	10.349	11.415	12.450	13.513
8	.000	.000	.000	.000	.000	.000	.000	.000	.000	.000	3.992	5.025	6.092	7.166	8.178	9.269	10.321	11.400
9	.000	.010	.000	.000	.000	.000	.000	.000	.000	.000	3.981	5.038	6.094	7.175	8.223	9.262	10.323	11.400
10	.000	.001	.000	.000	.000	.000	.000	.000	.000	.000	3.964	5.024	6.117	7.201	8.256	9.214	10.308	11.394





THE FOLLOWING GRID POINTS XINT, IF ANY, LIE INSIDE LENS APERTURE BUT OUTSIDE REGION OF INTERPOLATION

```
XINT = 9.500 FOR SCAN 1 AND FRAME 1  
XINT = 10.500 FOR SCAN 1 AND FRAME 1  
XINT = 15.500 FOR SCAN 1 AND FRAME 1  
XINT = 16.500 FOR SCAN 1 AND FRAME 1  
XINT = 7.500 FOR SCAN 2 AND FRAME 1  
XINT = 8.500 FOR SCAN 2 AND FRAME 1  
XINT = 17.500 FOR SCAN 2 AND FRAME 1  
XINT = 18.500 FOR SCAN 2 AND FRAME 1  
XINT = 5.500 FOR SCAN 3 AND FRAME 1  
XINT = 6.500 FOR SCAN 3 AND FRAME 1  
XINT = 19.500 FOR SCAN 3 AND FRAME 1  
XINT = 20.500 FOR SCAN 3 AND FRAME 1  
XINT = 4.500 FOR SCAN 4 AND FRAME 1  
XINT = 5.500 FOR SCAN 4 AND FRAME 1  
XINT = 20.500 FOR SCAN 4 AND FRAME 1  
XINT = 21.500 FOR SCAN 4 AND FRAME 1  
XINT = 3.500 FOR SCAN 5 AND FRAME 1  
XINT = 4.500 FOR SCAN 5 AND FRAME 1  
XINT = 21.500 FOR SCAN 5 AND FRAME 1  
XINT = 22.500 FOR SCAN 5 AND FRAME 1  
XINT = 2.500 FOR SCAN 6 AND FRAME 1  
XINT = 3.500 FOR SCAN 6 AND FRAME 1  
XINT = 22.500 FOR SCAN 6 AND FRAME 1  
XINT = 23.500 FOR SCAN 6 AND FRAME 1  
XINT = 2.500 FOR SCAN 7 AND FRAME 1  
XINT = 3.500 FOR SCAN 7 AND FRAME 1  
XINT = 22.500 FOR SCAN 7 AND FRAME 1
```

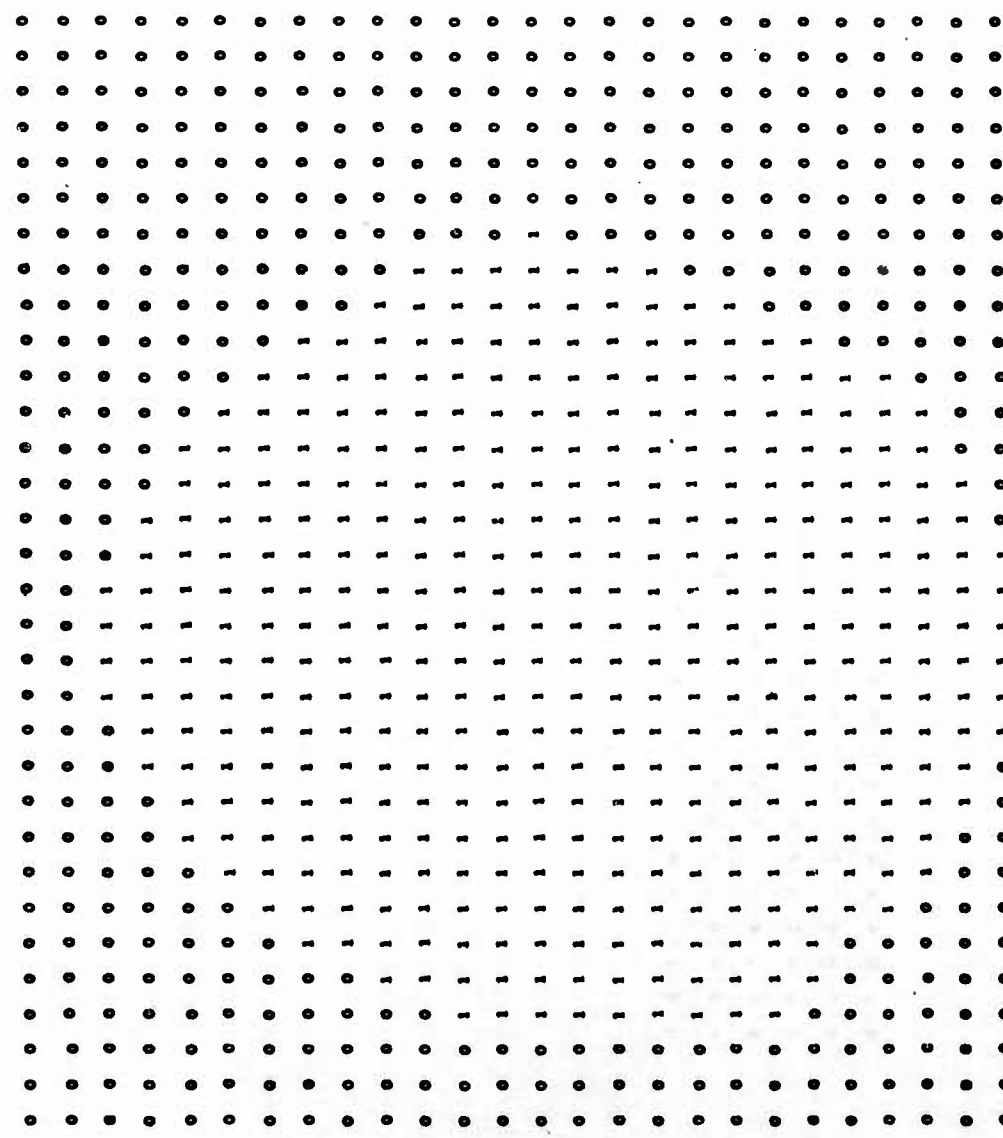
XINT = 23.500 FOR SCAN 7 AND FRAME 1  
XINT = 1.500 FOR SCAN 8 AND FRAME 1  
XINT = 2.500 FOR SCAN 9 AND FRAME 1  
XINT = 23.500 FOR SCAN 8 AND FRAME 1  
XINT = 24.500 FOR SCAN 9 AND FRAME 1  
XINT = 1.500 FOR SCAN 9 AND FRAME 1  
XINT = 2.500 FOR SCAN 9 AND FRAME 1  
XINT = 24.500 FOR SCAN 9 AND FRAME 1  
XINT = 1.500 FOR SCAN 10 AND FRAME 1  
XINT = 2.500 FOR SCAN 10 AND FRAME 1  
XINT = 25.500 FOR SCAN 10 AND FRAME 1  
XINT = 1.500 FOR SCAN 11 AND FRAME 1  
XINT = 2.500 FOR SCAN 11 AND FRAME 1  
XINT = 25.500 FOR SCAN 11 AND FRAME 1  
XINT = 1.500 FOR SCAN 12 AND FRAME 1  
XINT = 2.500 FOR SCAN 12 AND FRAME 1  
XINT = 1.500 FOR SCAN 13 AND FRAME 1  
XINT = 2.500 FOR SCAN 13 AND FRAME 1  
XINT = 23.500 FOR SCAN 13 AND FRAME 1  
XINT = 1.500 FOR SCAN 14 AND FRAME 1  
XINT = 2.500 FOR SCAN 14 AND FRAME 1  
XINT = 25.500 FOR SCAN 15 AND FRAME 1  
XINT = 1.500 FOR SCAN 16 AND FRAME 1  
XINT = 23.500 FOR SCAN 16 AND FRAME 1  
XINT = 24.500 FOR SCAN 16 AND FRAME 1  
XINT = 1.500 FOR SCAN 17 AND FRAME 1

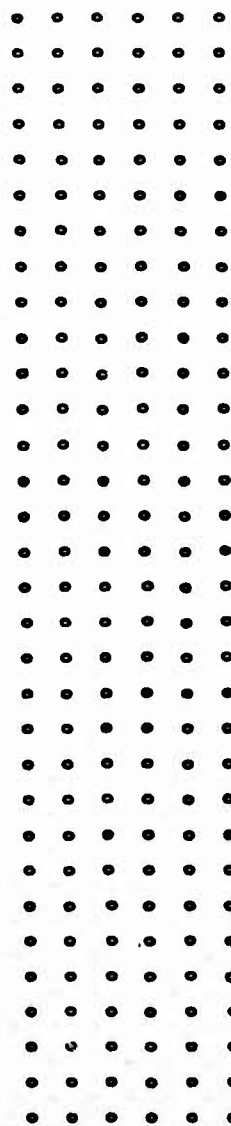
XINT =	23.500	FOR SCAN 17 AND FRAME 1
XINT =	24.500	FOR SCAN 17 AND FRAME 1
XINT =	1.500	FOR SCAN 18 AND FRAME 1
XINT =	22.500	FOR SCAN 18 AND FRAME 1
XINT =	23.500	FOR SCAN 18 AND FRAME 1
XINT =	2.500	FOR SCAN 19 AND FRAME 1
XINT =	22.500	FOR SCAN 19 AND FRAME 1
XINT =	23.500	FOR SCAN 19 AND FRAME 1
XINT =	3.500	FOR SCAN 20 AND FRAME 1
XINT =	4.500	FOR SCAN 20 AND FRAME 1
XINT =	21.500	FOR SCAN 20 AND FRAME 1
XINT =	22.500	FOR SCAN 20 AND FRAME 1
XINT =	3.500	FOR SCAN 21 AND FRAME 1
XINT =	4.500	FOR SCAN 21 AND FRAME 1
XINT =	21.500	FOR SCAN 21 AND FRAME 1
XINT =	22.500	FOR SCAN 21 AND FRAME 1
XINT =	4.500	FOR SCAN 22 AND FRAME 1
XINT =	5.500	FOR SCAN 22 AND FRAME 1
XINT =	20.500	FOR SCAN 22 AND FRAME 1
XINT =	21.500	FOR SCAN 22 AND FRAME 1
XINT =	6.500	FOR SCAN 23 AND FRAME 1
XINT =	7.500	FOR SCAN 23 AND FRAME 1
XINT =	18.500	FOR SCAN 23 AND FRAME 1
XINT =	19.500	FOR SCAN 23 AND FRAME 1
XINT =	8.500	FOR SCAN 24 AND FRAME 1
XINT =	9.500	FOR SCAN 24 AND FRAME 1
XINT =	16.500	FOR SCAN 24 AND FRAME 1
XINT =	17.500	FOR SCAN 24 AND FRAME 1
XINT =	18.500	FOR SCAN 1 AND FRAME 2

XINT = 15.500 FOR SCAN 1 AND FRAME 2  
XINT = 7.500 FOR SCAN 2 AND FRAME 2  
XINT = 18.500 FOR SCAN 2 AND FRAME 2  
XINT = 6.500 FOR SCAN 3 AND FRAME 2  
XINT = 19.500 FOR SCAN 3 AND FRAME 2  
XINT = 4.500 FOR SCAN 4 AND FRAME 2  
XINT = 20.500 FOR SCAN 4 AND FRAME 2  
XINT = 3.500 FOR SCAN 5 AND FRAME 2  
XINT = 21.500 FOR SCAN 5 AND FRAME 2  
XINT = 2.500 FOR SCAN 6 AND FRAME 2  
XINT = 22.500 FOR SCAN 6 AND FRAME 2  
XINT = 2.500 FOR SCAN 7 AND FRAME 2  
XINT = 23.500 FOR SCAN 7 AND FRAME 2  
XINT = 1.500 FOR SCAN 8 AND FRAME 2  
XINT = 2.500 FOR SCAN 8 AND FRAME 2  
XINT = 23.500 FOR SCAN 8 AND FRAME 2  
XINT = 1.500 FOR SCAN 9 AND FRAME 2  
XINT = 24.500 FOR SCAN 9 AND FRAME 2  
XINT = 1.500 FOR SCAN 10 AND FRAME 2  
XINT = 24.500 FOR SCAN 10 AND FRAME 2  
XINT = 1.500 FOR SCAN 11 AND FRAME 2  
XINT = 24.500 FOR SCAN 11 AND FRAME 2  
XINT = 25.500 FOR SCAN 11 AND FRAME 2  
XINT = 1.500 FOR SCAN 12 AND FRAME 2  
XINT = 24.500 FOR SCAN 12 AND FRAME 2  
XINT = 25.500 FOR SCAN 12 AND FRAME 2  
XINT = 1.500 FOR SCAN 13 AND FRAME 2  
XINT = 24.500 FOR SCAN 13 AND FRAME 2  
XINT = 25.500 FOR SCAN 13 AND FRAME 2

XINT = 1.500 FOR SCAN 14 AND FRAME 2  
XINT = 24.500 FOR SCAN 14 AND FRAME 2  
XINT = 25.500 FOR SCAN 14 AND FRAME 2  
XINT = 1.500 FOR SCAN 15 AND FRAME 2  
XINT = 24.500 FOR SCAN 15 AND FRAME 2  
XINT = 25.500 FOR SCAN 15 AND FRAME 2  
XINT = 1.500 FOR SCAN 16 AND FRAME 2  
XINT = 24.500 FOR SCAN 16 AND FRAME 2  
XINT = 2.500 FOR SCAN 17 AND FRAME 2  
XINT = 23.500 FOR SCAN 17 AND FRAME 2  
XINT = 24.500 FOR SCAN 17 AND FRAME 2  
XINT = 2.500 FOR SCAN 18 AND FRAME 2  
XINT = 23.500 FOR SCAN 18 AND FRAME 2  
XINT = 3.500 FOR SCAN 19 AND FRAME 2  
XINT = 23.500 FOR SCAN 19 AND FRAME 2  
XINT = 3.500 FOR SCAN 20 AND FRAME 2  
XINT = 22.500 FOR SCAN 20 AND FRAME 2  
XINT = 4.500 FOR SCAN 21 AND FRAME 2  
XINT = 21.500 FOR SCAN 21 AND FRAME 2  
XINT = 5.500 FOR SCAN 22 AND FRAME 2  
XINT = 20.500 FOR SCAN 22 AND FRAME 2  
XINT = 6.500 FOR SCAN 23 AND FRAME 2  
XINT = 19.500 FOR SCAN 23 AND FRAME 2  
XINT = 6.500 FOR SCAN 24 AND FRAME 2  
XINT = 17.500 FOR SCAN 24 AND FRAME 2

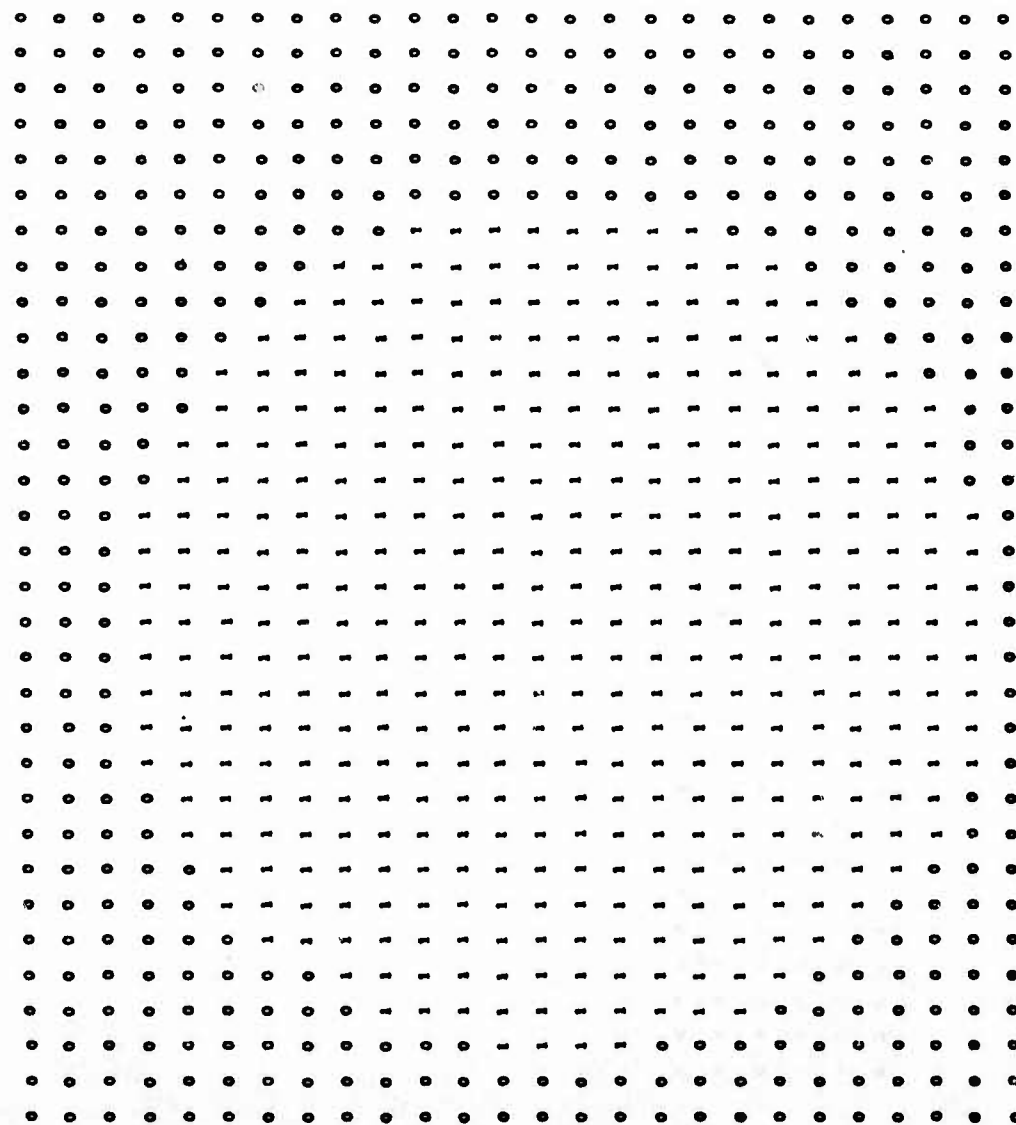
VALUES OF  $N_{IJK}$  ARE PRINTED BELOW -  
 $N_{IJK} = 1$  INDICATES THAT A VALUE OF PRIME ORDER  $P_{IJK}$  WAS INTERPOLATED AT GRID POINT  $(I+2, K+2)$  IN X-SHEARED INTERFEROGRAM

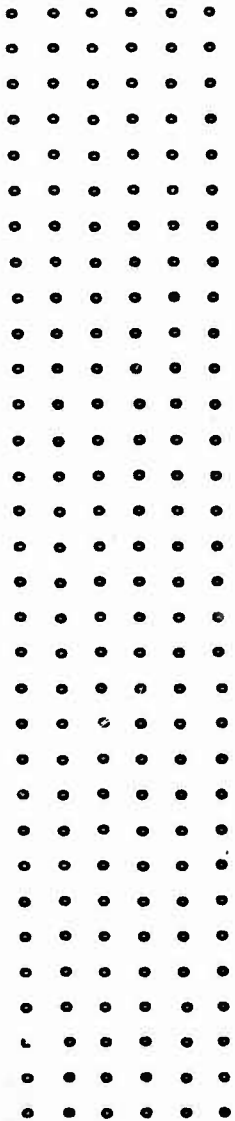




180

VALUES OF  $M_{12}(k)$  ARE PRINTED BELOW -  
 $M_{12} = 1$  INDICATES THAT A VALUE OF FADING ORDER  $m(j,k,n)$  WAS INTERPOLATED AT GRID POINT  $(k+2, l+2)$  IN  $\gamma$ -SHEARED INTERFEROGRAM





PRINC-E ORDER DEVIATIONS  $P(j,k,n)$  DETERMINED AT GRID POINTS BY INTERPOLATION FROM ADJACENT ORDER VALUES ARE PRINTED BELOW  
 $j$  = COLUMN NO. OF GRID POINT       $k$  = ROW NO. OF GRID POINT

VALUES OF  $P(j,k,n)$  ARE PRINTED IN 2 BLOCKS OF 32ROWS BY 16(COLUMNS) FOR EACH FRAME

NOTE - VALUES AT GRID POINTS FOR WHICH  $j=1$  (NOT PRINTED).  $j=2$ , AND AT GRID POINTS FOR WHICH  $k=1$ ,  $k=2$ , HAVE BEEN SET EQUAL TO 0.0

FRAME 1

$j$	2	3	4	5	6	7	8	9	10	11	12	13	14	15	16	17
$k$																
1	.000	.000	.000	.000	.000	.000	.000	.000	.000	.000	.000	.000	.000	.000	.000	.000
2	.000	.000	.000	.000	.000	.000	.000	.000	.000	.000	.000	.000	.000	.000	.000	.000
3	.000	.000	.000	.000	.000	.000	.000	.000	.000	.000	.000	.000	.000	.000	.000	.000
4	.000	.000	.000	.000	.000	.000	.000	.000	.000	.000	.000	.000	.000	.000	.000	.000
5	.000	.000	.000	.000	.000	.000	.000	.000	.000	.000	.000	.000	.000	.000	.000	.000
6	.000	.000	.000	.000	.000	.000	.000	.000	.000	.000	.000	.000	.000	.000	.000	.000
7	.000	.000	.000	.000	.000	.000	.000	.000	.000	.000	.000	.000	.000	.000	.000	.000
8	.000	.000	.000	.000	.000	.000	.000	.000	.000	.000	.000	.000	.000	.000	.000	.000
9	.000	.000	.000	.000	.000	.000	.000	.000	.000	.000	.000	.000	.000	.000	.000	.000
10	.000	.000	.000	.000	.000	.000	.000	.000	.000	.000	.000	.000	.000	.000	.000	.000
11	.000	.000	.000	.000	.000	.000	.000	.000	.000	.000	.000	.000	.000	.000	.000	.000
12	.000	.000	.000	.000	.000	.000	.000	.000	.000	.000	.000	.000	.000	.000	.000	.000
13	.000	.000	.000	.000	.000	.000	.000	.000	.000	.000	.000	.000	.000	.000	.000	.000
14	.000	.000	.000	.000	.000	.000	.000	.000	.000	.000	.000	.000	.000	.000	.000	.000
15	.000	.000	.000	.000	.000	.000	.000	.000	.000	.000	.000	.000	.000	.000	.000	.000
16	.000	.000	.000	.000	.000	.000	.000	.000	.000	.000	.000	.000	.000	.000	.000	.000
17	.000	.000	.000	.000	.000	.000	.000	.000	.000	.000	.000	.000	.000	.000	.000	.000
18	.000	.000	.000	.000	.000	.000	.000	.000	.000	.000	.000	.000	.000	.000	.000	.000
19	.000	.000	.000	.000	.000	.000	.000	.000	.000	.000	.000	.000	.000	.000	.000	.000
20	.000	.000	.000	.000	.000	.000	.000	.000	.000	.000	.000	.000	.000	.000	.000	.000
21	.000	.000	.000	.000	.000	.000	.000	.000	.000	.000	.000	.000	.000	.000	.000	.000
22	.000	.000	.000	.000	.000	.000	.000	.000	.000	.000	.000	.000	.000	.000	.000	.000



FRAME 2





VALUES OF DEL(1,1) ARE PRINTED BELOW -

DEL(13,12) WAS SET EQUAL TO ZERO

THE EXPERIMENTAL CONSTANTS  $B_1$ ,  $B_2$  (X TILT), AND  $B_3$  (Y TILT) ARE UNKNOWN AT THIS POINT AND, THEREFORE,  
HAVE NOT BEEN REMOVED FROM THE COMPUTED DEL VALUES

	1	2	3	4	5	6	7	8	9	10	11	12	13	14	15	16	17
K	.000	.000	.000	.000	.000	.000	.000	.000	.000	.000	.000	.000	.000	.000	.000	.000	
1	.000	.000	.000	.000	.000	.000	.000	.000	.000	.000	.000	.000	.000	.000	.000	.000	
2	.000	.000	.000	.000	.000	.000	.000	.000	.000	.000	.000	.000	.000	.000	.000	.000	
3	.000	.000	.000	.000	.000	.000	.000	.000	.000	.000	.000	.000	.000	.000	.000	.000	
4	.000	.000	.000	.000	.000	.000	.000	.000	.000	.000	.000	.000	.000	.000	.000	.000	
5	.000	.000	.000	.000	.000	.000	.000	.000	.000	.000	.000	.000	.000	.000	.000	.000	
6	.000	.000	.000	.000	.000	.000	.000	.000	.000	.000	.000	.000	.000	.000	.000	.000	
7	.000	.000	.000	.000	.000	.000	.000	.000	.000	.000	.000	.000	.000	.000	.000	.000	
8	.000	.000	.000	.000	.000	.000	.000	.000	.000	.000	.000	.000	.000	.000	.000	.000	
9	.000	.000	.000	.000	.000	.000	.000	.000	.000	.000	.000	.000	.000	.000	.000	.000	
10	.000	.000	.000	.000	.000	.000	.000	.000	.000	.000	.000	.000	.000	.000	.000	.000	
11	.000	.000	.000	.000	.000	.000	.000	.000	.000	.000	.000	.000	.000	.000	.000	.000	
12	.000	.000	.000	.000	.000	.000	.000	.000	.000	.000	.000	.000	.000	.000	.000	.000	
13	.000	.000	.000	.000	.000	.000	.000	.000	.000	.000	.000	.000	.000	.000	.000	.000	
14	.000	.000	.000	.000	.000	.000	.000	.000	.000	.000	.000	.000	.000	.000	.000	.000	
15	.000	.000	.000	.000	.000	.000	.000	.000	.000	.000	.000	.000	.000	.000	.000	.000	
16	.000	.000	.000	.000	.000	.000	.000	.000	.000	.000	.000	.000	.000	.000	.000	.000	
17	.000	.000	.000	.000	.000	.000	.000	.000	.000	.000	.000	.000	.000	.000	.000	.000	
18	.000	.000	.000	.000	.000	.000	.000	.000	.000	.000	.000	.000	.000	.000	.000	.000	
19	.000	.000	.000	.000	.000	.000	.000	.000	.000	.000	.000	.000	.000	.000	.000	.000	
20	.000	.000	.000	.000	.000	.000	.000	.000	.000	.000	.000	.000	.000	.000	.000	.000	
21	.000	.000	.000	.000	.000	.000	.000	.000	.000	.000	.000	.000	.000	.000	.000	.000	
22	.000	.000	.000	.000	.000	.000	.000	.000	.000	.000	.000	.000	.000	.000	.000	.000	
23	.000	.000	.000	.000	.000	.000	.000	.000	.000	.000	.000	.000	.000	.000	.000	.000	



19	8.027	8.864	9.686	10.494	11.290	12.069	12.817	13.479	.000	.000	.000	.000	.000	.000
20	8.193	9.433	10.250	11.050	11.842	12.626	13.365	14.057	.000	.000	.000	.000	.000	.000
21	9.148	9.989	10.807	11.610	12.399	13.177	13.921	.000	.000	.000	.000	.000	.000	.000
22	9.692	10.533	11.366	12.153	12.943	13.716	.000	.000	.000	.000	.000	.000	.000	.000
23	10.218	11.056	11.878	12.668	13.505	.003	.000	.000	.000	.000	.000	.000	.000	.000
24	10.724	11.571	12.422	13.251	.000	.000	.000	.000	.000	.000	.000	.000	.000	.000
25	11.244	12.123	.000	.000	.000	.000	.000	.000	.000	.000	.000	.000	.000	.000
26	.000	.000	.000	.000	.000	.000	.000	.000	.000	.000	.000	.000	.000	.000
27	.000	.000	.000	.000	.000	.000	.000	.000	.000	.000	.000	.000	.000	.000
28	.000	.000	.000	.000	.000	.000	.000	.000	.000	.000	.000	.000	.000	.000
29	.000	.000	.000	.000	.000	.000	.000	.000	.000	.000	.000	.000	.000	.000
30	.000	.000	.000	.000	.000	.000	.000	.000	.000	.000	.000	.000	.000	.000
31	.000	.000	.000	.000	.000	.000	.000	.000	.000	.000	.000	.000	.000	.000
32	.000	.000	.000	.000	.000	.000	.000	.000	.000	.000	.000	.000	.000	.000

THE COEFFICIENTS AND MAXIMUM VALUES OF THE ABBERRATIONS INTRODUCED BY THE CUBE INTERFEROMETER ARE LISTED BELOW

COEFFICIENT	MAX. VALUE	TYPE
B(0)	.0000000	DEFECT OF FOCUS
B(11)	-.477419-08	3RD ORDER SPHERICAL
B(22)	.282715-14	5TH ORDER SPHERICAL
E(23)	.106130-20	7TH ORDER SPHERICAL

TEST-LENS F/NO. = .65                    CUBE THICKNESS = 13.000 MM                    TEST-LIGHT WAVELENGTH = .6320-03 MM

NOTE - ONLY ONE-HALF OF EACH OF THE ABOVE ABBERRATIONS IS REMOVED IF THE TEST SYSTEM IS DOUBLE PASS

RESIDUAL VALUES (W11,K1). THAT IS, THE DIFFERENCES BETWEEN THE INPUT WAVEFRONT (DEL VALUES) AND OUTPUT WAVEFRONT (DE VALUES)  
 ARE PRINTED BELOW -  
 SYMMETRICAL ABERATIONS INTRODUCED BY CUBE HAVE BEEN REMOVED

	1	2	3	4	5	6	7	8	9	10	11	12	13	14	15	16	17
x	.000	.000	.000	.000	.000	.000	.000	.000	.000	.000	.000	.000	.000	.000	.000	.000	.000
1	.000	.000	.000	.000	.000	.000	.000	.000	.000	.000	.000	.000	.000	.000	.000	.000	.000
2	.000	.000	.000	.000	.000	.000	.000	.000	.000	.000	.000	.000	.000	.000	.000	.000	.000
3	.000	.000	.000	.000	.000	.000	.000	.000	.000	.007	.029	.005	.019	.013	.009	.037	
4	.000	.000	.000	.000	.000	.000	.000	.002	.016	.010	.004	.021	.008	.001	.012		
5	.000	.000	.000	.000	.026	.018	.001	.010	.003	.001	.013	.008	.007	.007	.016		
6	.000	.000	.000	.000	.009	.008	.003	.002	.006	.009	.004	.002	.013	.016	.025		
7	.000	.000	.000	.000	.017	.005	.006	.001	.006	.008	.003	.001	.003	.008	.019		
8	.000	.000	.000	.000	.004	.014	.013	.001	.002	.002	.003	.002	.010	.004	.004	.014	
9	.000	.000	.000	.012	.010	.003	.000	.007	.001	.009	.010	.015	.020	.023	.010	.006	
10	.000	.000	.000	.004	.008	.002	.007	.007	.004	.014	.025	.015	.010	.001	.004	.002	
11	.000	.000	.000	.018	.010	.005	.010	.012	.015	.001	.004	.008	.005	.011	.009	.002	
12	.000	.000	.004	.010	.001	.007	.013	.013	.009	.004	.003	.001	.003	.001	.001	.004	
13	.000	.014	.001	.004	.002	.009	.003	.001	.000	.004	.002	.005	.005	.009	.006	.008	
14	.000	.016	.005	.010	.004	.011	.006	.003	.003	.002	.002	.000	.003	.008	.003	.000	
15	.000	.009	.009	.010	.003	.003	.001	.006	.002	.003	.005	.000	.006	.005	.019	.012	
16	.000	.011	.002	.002	.010	.009	.005	.007	.005	.001	.004	.006	.001	.008	.021	.017	
17	.000	.015	.004	.002	.008	.004	.007	.005	.004	.004	.001	.007	.009	.006	.016	.020	.010
18	.000	.012	.001	.002	.010	.008	.006	.005	.004	.004	.007	.010	.006	.006	.001	.005	
19	.000	.011	.022	.003	.007	.008	.009	.008	.001	.001	.005	.007	.004	.004	.008	.012	
20	.000	.009	.004	.012	.001	.000	.006	.007	.011	.000	.009	.017	.014	.016	.006	.013	
21	.000	.000	.001	.004	.012	.004	.004	.013	.009	.003	.003	.004	.007	.003	.003	.010	
22	.000	.000	.000	.003	.000	.003	.019	.001	.001	.009	.005	.002	.013	.012	.009	.002	
23	.000	.000	.000	.000	.004	.007	.010	.003	.010	.001	.007	.017	.014	.016	.006	.008	
24	.000	.000	.000	.000	.008	.004	.012	.002	.005	.002	.007	.008	.007	.008	.002	.011	
25	.000	.000	.000	.000	.000	.000	.028	.008	.009	.004	.011	.009	.004	.004	.004	.004	
26	.000	.000	.000	.000	.000	.000	.000	.000	.000	.000	.000	.000	.000	.000	.000	.000	



22	-0.004	-0.001	-0.008	-0.002	-0.004	-0.005	-0.000	-0.000	-0.000	-0.000	-0.000	-0.000	-0.000	-0.000
23	-0.004	-0.006	-0.006	-0.002	-0.020	-0.000	-0.000	-0.000	-0.000	-0.000	-0.000	-0.000	-0.000	-0.000
24	-0.017	-0.014	-0.007	-0.000	-0.000	-0.000	-0.000	-0.000	-0.000	-0.000	-0.000	-0.000	-0.000	-0.000
25	-0.010	-0.005	-0.000	-0.000	-0.000	-0.000	-0.000	-0.000	-0.000	-0.000	-0.000	-0.000	-0.000	-0.000
26	-0.000	-0.000	-0.000	-0.000	-0.000	-0.000	-0.000	-0.000	-0.000	-0.000	-0.000	-0.000	-0.000	-0.000
27	-0.000	-0.000	-0.000	-0.000	-0.000	-0.000	-0.000	-0.000	-0.000	-0.000	-0.000	-0.000	-0.000	-0.000
28	-0.000	-0.000	-0.000	-0.000	-0.000	-0.000	-0.000	-0.000	-0.000	-0.000	-0.000	-0.000	-0.000	-0.000
29	-0.000	-0.000	-0.000	-0.000	-0.000	-0.000	-0.000	-0.000	-0.000	-0.000	-0.000	-0.000	-0.000	-0.000
30	-0.000	-0.000	-0.000	-0.000	-0.000	-0.000	-0.000	-0.000	-0.000	-0.000	-0.000	-0.000	-0.000	-0.000
31	-0.000	-0.000	-0.000	-0.000	-0.000	-0.000	-0.000	-0.000	-0.000	-0.000	-0.000	-0.000	-0.000	-0.000
32	-0.000	-0.000	-0.000	-0.000	-0.000	-0.000	-0.000	-0.000	-0.000	-0.000	-0.000	-0.000	-0.000	-0.000

RMS OF INPUT WAVEFRONT (DEL VALUES) WITH B(11),B(21),B(31). AND CUBE ABERRATIONS. IF ANY. REMOVED = LAMBDA/ 3.10505

RMS OF ANALYTIC WAVEFRONT (DE VALUES) WITH B(11),B(21),B(31). AND CUBE ABERRATIONS. IF ANY. REMOVED = LAMBDA/ 3.10436

RMS OF RESIDUAL WAVEFRONT (DEL-DE) = LAMBDA/ 94.048

MEAN LAMBDA = -0.328-0.3 MM

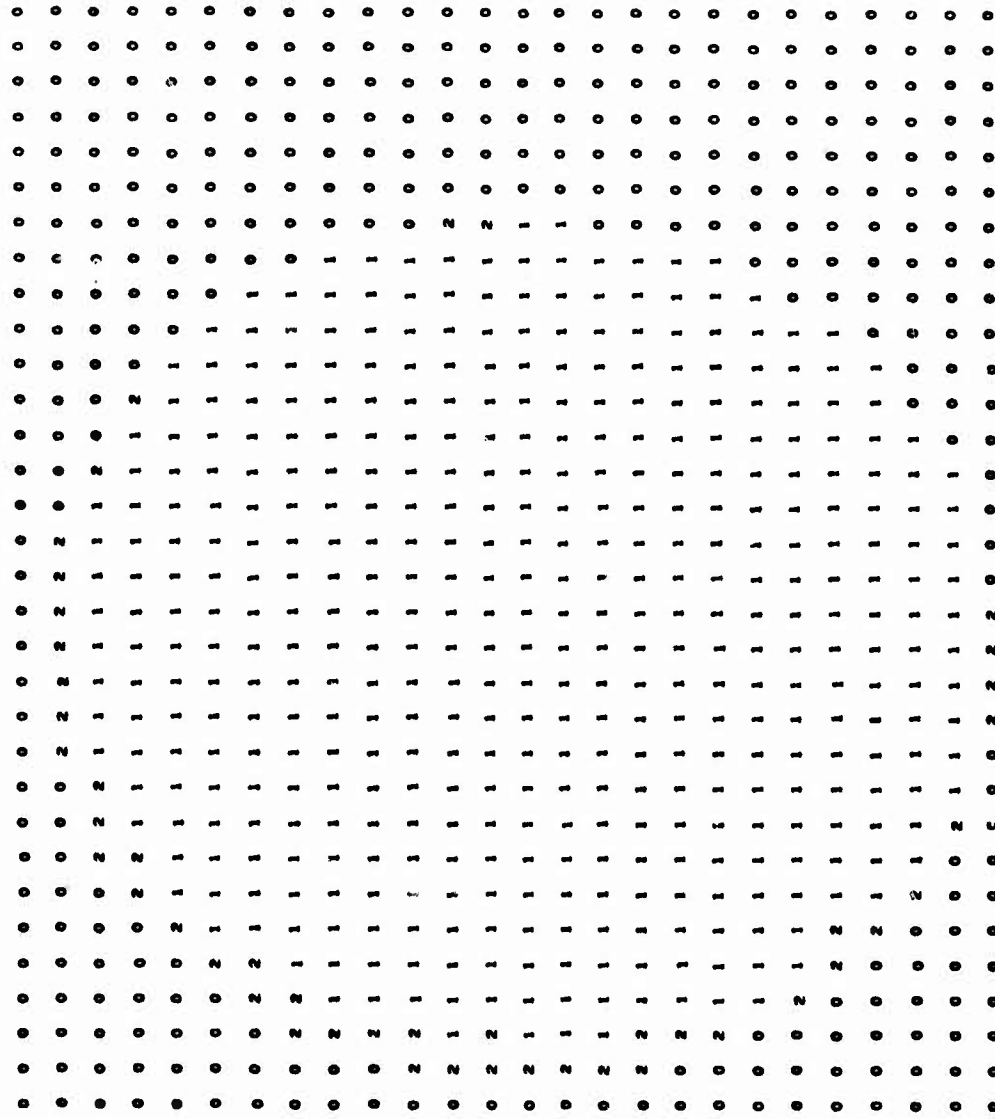
THE COEFFICIENTS USED FOR THE SET OF 23 POLYNOMIALS WHICH DESCRIBE LENS ABBERRATIONS ARE LISTED BELOW.  
CUBE ABBERRATIONS, IF ANY, HAVE BEEN REMOVED FROM BOTH THE COEFFICIENTS AND THE MAX VALUES

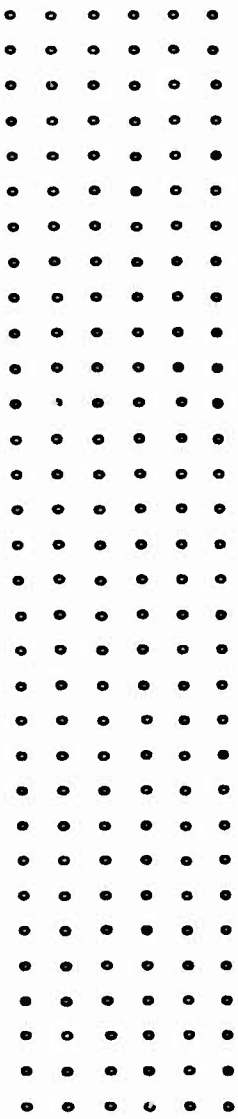
#	OBJ	MAX VALUE OF ABBERRATION (0.011 RADIUS IN MM)	ABBERRATION	POLYNOMIAL
1		1.3194	CONSTANT	
2		11.1408	X-TILT	$x$
3		7.5994	Y-TILT	$y$
4		-1.5609	FOCUS DEFECT	$x^2 - y^2$
5		-0.0391	0 DEG ASTIG.(3RD)	$x^2 + y^2$
6		-0.0997	45 DEG ASTIG.(3RD)	$x - y$
7		0.1706	X-COMA(3RD)	$x^2$
8		0.1781	Y-COMA(3RD)	$y^2$
9		0.0443	X-CLOVER(3RD)	$x(x - 3y)$
10		-0.578237-07	Y-CLOVER(3RD)	$y(3x - y)$
11		-0.006976-07	SPHERICAL(3RD)	$(x + y)^2$
12		-0.372394-08	0 DEG ASTIG.(5TH)	$x - y$
13		0.0328	45 DEG ASTIG.(5TH)	$2xy(x^2 - y^2)$
14		-0.0265		$x - 6xy^2 + y^4$
15		-0.0226		$4xy(x - y)$
16		-0.213378-09	X-COMA(15TH)	$x^2$
17		-0.220168-09	Y-COMA(15TH)	$y^2$
18		-0.00265-05	X-CLOVER(15TH)	$x^5 - 3x^3y^2 + 3xy^4$
19		-0.130140-09	Y-CLOVER(15TH)	$3x^4y - 2x^2y^3 - y^5$
20		-0.00026-11		$x^5 - 10x^3y^2 + 15xy^4$
21		-0.236568-10	Spherical(15TH)	$x^6 - 2x^4y^2 + 2x^2y^4 - y^6$
22		-0.301339-10		$(x + y)^4$
23		-0.636203-14	SPHERICAL(17TH)	$x^2 - 2x^4 + (x + y)^4$

COORDINATE VALUES DEFINING LENS APERTURE ARE PRINTED BELOW -  
X1 AND X2 ARE APERTURE ENDCAVES FOR A PARTICULAR Y OR SCAN VALUE

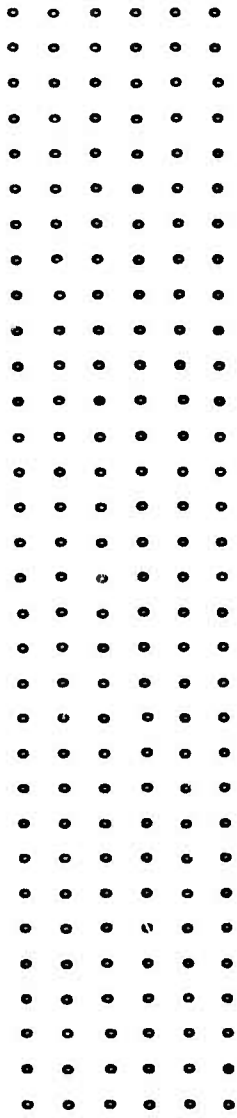
SCAN 1	y =	.000	x1 =	.000	x2 =	.000
SCAN 2	y =	2.361	x1 =	41.497	x2 =	74.057
SCAN 3	y =	7.023	x1 =	30.168	x2 =	25.385
SCAN 4	y =	11.705	x1 =	22.912	x2 =	92.642
SCAN 5	y =	16.387	x1 =	17.445	x2 =	98.089
SCAN 6	y =	21.070	x1 =	13.159	x2 =	102.395
SCAN 7	y =	25.752	x1 =	9.688	x2 =	105.866
SCAN 8	y =	30.434	x1 =	6.880	x2 =	108.674
SCAN 9	y =	35.116	x1 =	4.629	x2 =	110.924
SCAN 10	y =	39.798	x1 =	2.869	x2 =	112.685
SCAN 11	y =	44.480	x1 =	1.551	x2 =	114.003
SCAN 12	y =	49.162	x1 =	.646	x2 =	114.906
SCAN 13	y =	53.844	x1 =	.134	x2 =	115.420
SCAN 14	y =	58.527	x1 =	.005	x2 =	115.549
SCAN 15	y =	63.205	x1 =	-.256	x2 =	115.299
SCAN 16	y =	67.881	x1 =	-.892	x2 =	114.662
SCAN 17	y =	72.573	x1 =	1.927	x2 =	113.627
SCAN 18	y =	77.255	x1 =	3.382	x2 =	112.172
SCAN 19	y =	81.937	x1 =	5.294	x2 =	110.260
SCAN 20	y =	86.619	x1 =	7.714	x2 =	107.840
SCAN 21	y =	91.302	x1 =	10.721	x2 =	104.833
SCAN 22	y =	95.984	x1 =	14.436	x2 =	101.118
SCAN 23	y =	100.666	x1 =	19.064	x2 =	96.490
SCAN 24	y =	105.348	x1 =	24.987	x2 =	90.567
SCAN 25	y =	110.030	x1 =	33.124	x2 =	82.430
SCAN 26	y =	114.712	x1 =	37.951	x2 =	67.603

VALUES OF  $W(I,J,K)$  ARE PRINTED BELOW -  
 $P_1 = 1$  INDICATES THAT A VALUE OF PRINCE ORDER  $P(I,J,K,N)$  WAS INTERPOLATED AT GRID POINT  $(I,J,K)$   
 $P_1 = 0$  INDICATES THAT A VALUE OF PRINCE ORDER  $P(I,J,K,N)$  WAS EXTRAPOLATED AT GRID POINT  $(I,J,K)$   
 $P_1 = 2$





TOTAL NUMBER OF GRID POINTS IN THE CLEAR LENS APERTURE IS 463 OF WHICH  
437 WERE INTERPOLATED AND 26 WERE EXTRAPOLATED



TOTAL NUMBER OF GRID POINTS IN THE CLEAR LENS APERTURE IS 400 OF WHICH  
437 WERE INTERPOLATED AND 63 WERE EXTRAPOLATED

VALUES OF THE PUPIL FUNCTION PHASE ARE PRINTED BELOW -  
 TERMS INVOLVING B(11), B(12), AND B(13) HAVE BEEN SUBTRACTED FROM DE VALUES  
 DE = 0.0 AT THE CENTER OF THE LENS APERTURE  
 THESE VALUES OF DE DO NOT, GENERALLY, REPRESENT THE PUPIL FUNCTION IN THE PLANE OF BEST FOCUS

	1	2	3	4	5	6	7	8	9	10	11	12	13	14	15	16	17
x	.000	.000	.000	.000	.000	.000	.000	.000	.000	.000	.000	.000	.000	.000	.000	.000	.000
1	.000	.000	.000	.000	.000	.000	.000	.000	.000	.000	-1.167	-1.176	-1.187	-1.202	-1.220	-1.239	-1.256
2	.000	.000	.000	.000	.000	.000	.000	.000	.000	-1.051	-1.038	-1.032	-1.034	-1.043	-1.050	-1.054	-1.111
3	.000	.000	.000	.000	.000	.000	.000	.000	.000	-1.036	-1.032	-1.034	-1.034	-1.034	-1.034	-1.034	-1.034
4	.000	.000	.000	.000	.000	.000	.000	.000	.000	-1.036	-1.036	-1.036	-1.036	-1.036	-1.036	-1.036	-1.036
5	.000	.000	.000	.000	.000	.000	.000	.000	.000	-1.036	-1.036	-1.036	-1.036	-1.036	-1.036	-1.036	-1.036
6	.000	.000	.000	.000	.000	.000	.000	.000	.000	-1.036	-1.036	-1.036	-1.036	-1.036	-1.036	-1.036	-1.036
7	.000	.000	.000	.000	.000	.000	.000	.000	.000	-1.036	-1.036	-1.036	-1.036	-1.036	-1.036	-1.036	-1.036
8	.000	.000	.000	.000	.000	.000	.000	.000	.000	-1.036	-1.036	-1.036	-1.036	-1.036	-1.036	-1.036	-1.036
9	.000	.000	.000	.000	.000	.000	.000	.000	.000	-1.036	-1.036	-1.036	-1.036	-1.036	-1.036	-1.036	-1.036
10	.000	.000	.000	.000	.000	.000	.000	.000	.000	-1.036	-1.036	-1.036	-1.036	-1.036	-1.036	-1.036	-1.036
11	-1.156	-1.040	-1.001	-1.059	-1.025	-1.053	-1.034	-1.030	-1.021	-1.019	-1.015	-1.015	-1.009	-1.003	-1.000	-1.000	-1.000
12	-1.143	-1.015	-1.070	-1.024	-1.058	-1.064	-1.054	-1.058	-1.047	-1.041	-1.035	-1.035	-1.035	-1.035	-1.035	-1.035	-1.035
13	-1.134	-1.099	-1.049	-1.072	-1.055	-1.0440	-1.0329	-1.0233	-1.0152	-1.0087	-1.0014	-1.0014	-1.0008	-1.0021	-1.0052	-1.0099	-1.0099
14	-1.132	-1.093	-1.041	-1.053	-1.055	-1.031	-1.021	-1.0225	-1.0144	-1.0080	-1.0034	-1.0007	-1.001	-1.0013	-1.004	-1.004	-1.004
15	-1.140	-1.000	-1.067	-1.059	-1.052	-1.0438	-1.0329	-1.0234	-1.0155	-1.0092	-1.0067	-1.0021	-1.0014	-1.0026	-1.0056	-1.0102	-1.0126
16	-1.159	-1.021	-1.069	-1.071	-1.058	-1.0462	-1.0354	-1.0261	-1.0184	-1.0123	-1.0079	-1.0054	-1.0047	-1.0058	-1.0087	-1.0131	-1.0171
17	-1.161	-1.058	-1.008	-1.060	-1.024	-1.0503	-1.030	-1.020	-1.0114	-1.0068	-1.0042	-1.0014	-1.0008	-1.0021	-1.0052	-1.0099	-1.0099
18	.000	.000	.000	.000	.000	.000	.000	.000	.000	-1.036	-1.036	-1.036	-1.036	-1.036	-1.036	-1.036	-1.036
19	.000	.000	.000	.000	.000	.000	.000	.000	.000	-1.036	-1.036	-1.036	-1.036	-1.036	-1.036	-1.036	-1.036
20	.000	.000	.000	.000	.000	.000	.000	.000	.000	-1.036	-1.036	-1.036	-1.036	-1.036	-1.036	-1.036	-1.036
21	.000	.000	.000	.000	.000	.000	.000	.000	.000	-1.036	-1.036	-1.036	-1.036	-1.036	-1.036	-1.036	-1.036
22	.000	.000	.000	.000	.000	.000	.000	.000	.000	-1.036	-1.036	-1.036	-1.036	-1.036	-1.036	-1.036	-1.036
23	.000	.000	.000	.000	.000	.000	.000	.000	.000	-1.036	-1.036	-1.036	-1.036	-1.036	-1.036	-1.036	-1.036
24	.000	.000	.000	.000	.000	.000	.000	.000	.000	-1.036	-1.036	-1.036	-1.036	-1.036	-1.036	-1.036	-1.036
25	.000	.000	.000	.000	.000	.000	.000	.000	.000	-1.036	-1.036	-1.036	-1.036	-1.036	-1.036	-1.036	-1.036





RAYLEIGH TOLERANCE ON DEPTH OF FOCUS FOR TEST LENS IS + OR - .0005-01 MM

COEFFICIENT FOR DEFECT OF FOCUS, CORRESPONDING DISTANCE TO FOCAL PLANE, AND RMS OF RESULTING WAVEFRONT ARE LISTED BELOW -

INDEX PARAMETER, N	B(4)	22(MM)	RMS(LAMBDA/VALUE)
1	-0.461605-03	1000.000	2.93786
2	-0.453980-03	999.990	3.00264
3	-0.446351-03	999.981	3.07031
4	-0.438722-03	999.971	3.14106
5	-0.431054-03	999.961	3.21511
6	-0.423485-03	999.952	3.29269
7	-0.415835-03	999.942	3.37406
8	-0.408206-03	999.932	3.45949
9	-0.400577-03	999.923	3.54929
10	-0.392967-03	999.913	3.64381
11	-0.385317-03	999.903	3.74341
12	-0.377687-03	999.894	3.84851
13	-0.370057-03	999.884	3.95958
14	-0.362427-03	999.875	4.07711
15	-0.354797-03	999.865	4.20168
16	-0.347166-03	999.855	4.33392
17	-0.339536-03	999.846	4.47456
18	-0.331905-03	999.836	4.62438
19	-0.324274-03	999.826	4.78429
20	-0.316643-03	999.817	4.95531
21	-0.309012-03	999.807	5.13861
22	-0.301380-03	999.797	5.33548
23	-0.293749-03	999.788	5.54745
24	-0.286117-03	999.778	5.77622

25	- .278485-03	999.-64
26	- .270853-03	999.-759
27	- .283221-03	999.-749
28	- .285589-03	999.-739
29	- .287956-03	999.-730
30	- .290324-03	999.-720
31	- .292691-03	999.-710
32	- .295058-03	999.-701
33	- .297425-03	999.-691
34	- .299792-03	999.-682
35	- .302159-03	999.-672
36	- .304525-03	999.-662
37	- .306892-03	999.-653
38	- .309259-03	999.-643
39	- .311626-03	999.-633
40	- .313990-03	999.-624
41	- .3156356-03	999.-614
42	- .3168722-03	999.-604
43	- .3181087-03	999.-595
44	- .3193452-03	999.-585
45	- .3205816-03	999.-575
46	- .3218163-03	999.-566
47	- .3230488-03	999.-556
48	- .3242913-03	999.-546
49	- .3252772-04	999.-537
50	- .3276416-04	999.-527
51	- .3300660-04	999.-517
52	- .3237362-04	999.-508
53	- .3473942-04	999.-499

54	999.088	13.43456
55	999.479	12.46514
56	999.469	11.59238
57	999.469	10.80999
58	999.458	10.16979
59	999.449	9.48271
60	999.439	8.92004
61	999.421	8.41388
62	999.411	7.95718
63	999.402	7.54378
64	999.393	7.16834
65	999.382	6.82627
66	999.373	6.51360
67	999.363	6.22693
68	999.353	5.96731
69	999.344	5.72020
70	999.334	5.49540
71	999.324	5.28700
72	999.315	5.09333
73	999.305	4.91292
74	999.295	4.74451
75	999.286	4.58697
76	999.276	4.43931
77	999.267	4.30064
78	999.257	4.17020
79	999.247	4.04727
80	999.238	3.93126
81	999.228	3.82159
	999.218	3.71777

22

83	-164413-03	999.269	3.61935
84	-112053-03	999.199	3.52594
85	-179694-03	999.189	3.43715
86	-167335-03	999.160	3.35267
87	-194976-03	999.170	3.27218
88	-202617-03	999.160	3.19542
89	-210258-03	999.151	3.12214
90	-217900-03	999.141	3.05211
91	-225541-03	999.131	2.98511
92	-233163-03	999.122	2.92096
93	-240825-03	999.112	2.85549
94	-248467-03	999.102	2.80052
95	-256109-03	999.093	2.74391
96	-263751-03	999.083	2.68953
97	-271394-03	999.073	2.63724
98	-279036-03	999.064	2.58693
99	-286679-03	999.054	2.53669
100	-294322-03	999.045	2.49181
101	-301965-03	999.035	2.44661
102	-309608-03	999.025	2.40339
103	-317251-03	999.016	2.36147
104	-324895-03	999.006	2.32098
105	-332538-03	998.996	2.28185
106	-340182-03	998.987	2.24401
107	-347826-03	998.977	2.20739
108	-355470-03	998.967	2.17194
109	-363114-03	998.958	2.13761
110	-370759-03	998.948	2.10434
111	-378403-03	998.938	2.07208

112	.3860468-03	998.929	2.04079
113	.393693-03	998.919	2.01043
114	.401338-03	998.909	1.98095
115	.408983-03	998.900	1.95232
116	.416628-03	998.890	1.92450
117	.424273-03	998.880	1.89746
118	.431919-03	998.871	1.87117
119	.439565-03	998.861	1.84559
120	.447211-03	998.852	1.82070
121	.454857-03	998.842	1.79596
122	.462503-03	998.832	1.77285
123	.470149-03	998.823	1.74987
124	.477795-03	998.813	1.72747
125	.485442-03	998.803	1.70563

FOCUS SHIFT IS SUBSEQUENTLY MADE TO OPPOSITE SIDE OF TEST FOCUS POSITION

140	-0.576017-03	1000.165	2.21619
141	-0.583643-03	1000.154	2.16248
142	-0.591269-03	1000.164	2.14790
143	-0.598895-03	1000.174	2.11439
144	-0.606520-03	1000.163	2.06191
145	-0.614146-03	1000.193	2.05540
146	-0.621771-03	1000.203	2.01983
147	-0.629396-03	1000.212	1.99016
148	-0.637021-03	1000.222	1.96136
149	-0.644646-03	1000.232	1.93336
150	-0.652271-03	1000.241	1.90612
151	-0.659896-03	1000.251	1.87946
152	-0.667520-03	1000.261	1.85393
153	-0.675145-03	1000.270	1.82868
154	-0.682769-03	1000.280	1.80450
155	-0.690393-03	1000.290	1.78076
156	-0.698017-03	1000.299	1.75763
157	-0.705640-03	1000.309	1.73510
158	-0.713264-03	1000.318	1.71313
159	-0.720887-03	1000.328	1.69171
160	-0.728511-03	1000.338	1.67082
161	-0.736134-03	1000.347	1.65044
162	-0.743757-03	1000.357	1.63055
163	-0.751380-03	1000.367	1.61113
164	-0.759002-03	1000.376	1.59217
165	-0.766625-03	1000.386	1.57365
166	-0.774247-03	1000.396	1.55555
167	-0.781869-03	1000.405	1.53766
168	-0.789492-03	1000.415	1.52057

169	-0.797113-03	1000.425	1.20364
170	-0.604735-03	1000.434	1.48713
171	-0.812357-03	1000.444	1.47095
172	-0.819878-03	1000.454	1.45512
173	-0.827400-03	1000.463	1.43963
174	-0.835221-03	1000.473	1.42447
175	-0.842842-03	1000.483	1.40962
176	-0.850463-03	1000.492	1.39507
177	-0.858084-03	1000.502	1.38082
178	-0.865704-03	1000.512	1.36686
179	-0.873325-03	1000.521	1.35318
180	-0.880945-03	1000.531	1.33977
181	-0.888565-03	1000.540	1.32663
182	-0.896186-03	1000.550	1.31374
183	-0.903805-03	1000.560	1.30109
184	-0.911425-03	1000.569	1.28869
185	-0.919045-03	1000.579	1.27652
186	-0.926664-03	1000.589	1.26458
187	-0.934284-03	1000.598	1.25286
188	-0.941903-03	1000.608	1.24135
189	-0.949522-03	1000.618	1.23006
190	-0.957141-03	1000.627	1.21896
191	-0.964759-03	1000.637	1.20807
192	-0.972378-03	1000.647	1.19737
193	-0.979996-03	1000.656	1.18685
194	-0.987615-03	1000.666	1.17652
195	-0.995233-03	1000.676	1.16637
196	-0.102085-02	1000.685	1.15639
197	-0.101947-02	1000.695	1.14656

198	-+101809-02	1000-705	1-13694
199	-+102570-02	1000-714	1-12745
200	-+103332-02	1000-724	1-11913
201	-+104094-02	1000-733	1-10695
202	-+104856-02	1000-743	1-09493
203	-+105617-02	1000-753	1-08105
204	-+106379-02	1000-762	1-06231
205	-+107141-02	1000-772	1-05371
206	-+107902-02	1000-782	1-06525
207	-+108664-02	1000-791	1-05692
208	-+109426-02	1000-801	1-04872
209	-+110187-02	1000-811	1-04064
210	-+110949-02	1000-820	1-03269
211	-+111710-02	1000-830	1-02486
212	-+112472-02	1000-840	1-01715
213	-+113233-02	1000-850	1-00955
214	-+113955-02	1000-859	1-00207
215	-+114676-02	1000-869	0-99469
216	-+115518-02	1000-878	0-98743
217	-+116279-02	1000-888	0-98026
218	-+117041-02	1000-898	0-97321
219	-+117802-02	1000-907	0-96625
220	-+118564-02	1000-917	0-95939
221	-+119325-02	1000-927	0-95263
222	-+120087-02	1000-936	0-94596
223	-+120848-02	1000-946	0-93936
224	-+121609-02	1000-955	0-93290
225	-+122371-02	1000-955	0-92551
226	-+123132-02	1000-975	0-92026

227	-0.123899-0.02	1000.984	.91398
228	-0.124655-0.02	1000.994	.90784
229	-0.125416-0.02	1001.004	.90178
230	-0.126177-0.02	1001.013	.89569
231	-0.126939-0.02	1001.023	.88951
232	-0.127700-0.02	1001.033	.88339
233	-0.128461-0.02	1001.042	.87734
234	-0.129223-0.02	1001.052	.87127
235	-0.129984-0.02	1001.062	.86527
236	-0.130745-0.02	1001.071	.86195
237	-0.131506-0.02	1001.081	.85669
238	-0.132267-0.02	1001.091	.85070
239	-0.133029-0.02	1001.100	.84438
240	-0.133790-0.02	1001.110	.84013
241	-0.134551-0.02	1001.120	.83494
242	-0.135312-0.02	1001.129	.82881
243	-0.136073-0.02	1001.139	.82475
244	-0.136834-0.02	1001.148	.81975
245	-0.137595-0.02	1001.158	.81461
246	-0.138356-0.02	1001.168	.80953
247	-0.139117-0.02	1001.177	.80310
248	-0.139878-0.02	1001.187	.80034
249	-0.140639-0.02	1001.197	.79553
250	-0.141400-0.02	1001.206	.79097

THE MINIMUM RMS FROM THE VALUES LISTED ABOVE IS LAMBDA 20.625 FOR n = 46

THE FOCAL POSITION, 22, ALONG THE OPTICAL AXIS WAS CHANGED IN INCREMENTS OF .10 OF THE RAYLEIGH TOLERANCE ON DEPTH OF FOCUS  
HOWEVER, IF n = 125 OR 250, THE INCREMENT WILL BE DOUBLED AND THE SEARCH FOR MAXIMUM LAMBDA/HMS REPEATED

VALUES OF THE PUPIL-FUNCTION PHASE FOR PLANE OF BEST FOCUS ARE PRINTED BELOW  
 TERMS INVOLVING B(12) AND B(31) AND CUBE ABERATIONS, IF ANY, HAVE BEEN SUBTRACTED FROM OE VALUES AND  
 DEG AT THE CENTER OF THE LENS APERTURE

THE RPS OF THIS WAVEFRONT IS LAMBDA/ 20.625 WITH A REMAINING MAXIMUM FOCUS DEFECT OF -0.395

	1	2	3	4	5	6	7	8	9	10	11	12	13	14	15	16	17
K	.000	.000	.000	.000	.000	.000	.000	.000	.000	.000	.000	.000	.000	.000	.000	.000	
1	.000	.000	.000	.000	.000	.000	.000	.000	.000	.000	.000	.000	.000	.000	.000	.000	
2	.000	.000	.000	.000	.000	.000	.000	.000	.000	.000	.000	.000	.000	.000	.000	.000	
3	.000	.000	.000	.000	.000	.000	.000	.000	.000	.000	.000	.000	.000	.000	.000	.000	
4	.000	.000	.000	.000	.000	.000	.000	.000	.000	.000	.000	.000	.000	.000	.000	.000	
5	.000	.000	.000	.000	.000	.000	.000	.000	.000	.000	.000	.000	.000	.000	.000	.000	
6	.000	.000	.000	.000	.000	.000	.000	.000	.000	.000	.000	.000	.000	.000	.000	.000	
7	.000	.000	.016	.036	.062	.073	.079	.081	.083	.085	.086	.088	.091	.095	.097	.099	
8	.000	.026	.032	.072	.083	.085	.085	.085	.086	.086	.087	.087	.088	.089	.089	.089	
9	.000	.035	.078	.093	.095	.096	.096	.096	.096	.096	.096	.096	.096	.096	.096	.096	
10	.000	.072	.100	.105	.100	.091	.081	.069	.059	.049	.043	.039	.039	.041	.045	.049	
11	.039	.094	.111	.110	.102	.090	.076	.063	.049	.037	.026	.023	.022	.025	.030	.036	
12	.062	.105	.115	.111	.100	.086	.072	.056	.041	.027	.017	.011	.010	.013	.016	.025	
13	.074	.109	.115	.108	.097	.083	.067	.051	.035	.021	.010	.004	.002	.005	.011	.019	
14	.077	.108	.112	.104	.093	.079	.064	.048	.033	.019	.008	.002	.000	.003	.009	.016	
15	.074	.105	.108	.100	.089	.076	.062	.048	.034	.021	.011	.005	.004	.006	.011	.017	
16	.069	.101	.105	.098	.087	.075	.062	.050	.038	.027	.018	.013	.011	.013	.017	.021	
17	.060	.098	.104	.097	.086	.075	.064	.054	.044	.035	.026	.024	.022	.024	.026	.026	
18	.060	.096	.106	.103	.099	.089	.078	.066	.059	.051	.044	.038	.034	.032	.031	.030	
19	.060	.094	.100	.107	.107	.095	.084	.074	.064	.051	.047	.043	.040	.037	.035	.031	
20	.060	.090	.117	.117	.107	.095	.084	.074	.064	.056	.046	.044	.040	.035	.029	.026	
21	.060	.090	.121	.131	.123	.110	.096	.084	.074	.066	.058	.052	.045	.038	.031	.023	
22	.060	.090	.000	.161	.140	.128	.112	.097	.083	.072	.061	.051	.042	.032	.023	.013	
23	.060	.090	.000	.000	.152	.145	.129	.111	.094	.078	.063	.050	.037	.024	.011	.001	
24	.060	.090	.000	.000	.151	.141	.123	.103	.083	.064	.045	.028	.011	.005	.021	.021	
25	.060	.090	.000	.000	.000	.000	.000	.000	.000	.000	.000	.000	.000	.012	.034	.056	

	18	19	20	21	22	23	24	25	26	27	28	29	30	31	32	33
1	.000	.000	.000	.000	.000	.000	.000	.000	.000	.000	.000	.000	.000	.000	.000	.000
2	-.000	-.000	-.000	-.000	-.000	-.000	-.000	-.000	-.000	-.000	-.000	-.000	-.000	-.000	-.000	-.000
3	-.124	-.078	-.000	-.000	-.000	-.000	-.000	-.000	-.000	-.000	-.000	-.000	-.000	-.000	-.000	-.000
4	-.130	-.100	-.053	-.018	-.000	-.000	-.000	-.000	-.000	-.000	-.000	-.000	-.000	-.000	-.000	-.000
5	-.121	-.100	-.068	-.020	-.052	-.000	-.000	-.000	-.000	-.000	-.000	-.000	-.000	-.000	-.000	-.000
6	-.104	-.092	-.068	-.034	-.015	-.000	-.000	-.000	-.000	-.000	-.000	-.000	-.000	-.000	-.000	-.000
7	-.091	-.080	-.063	-.038	-.003	-.018	-.012	-.000	-.000	-.000	-.000	-.000	-.000	-.000	-.000	-.000
8	-.077	-.069	-.056	-.037	-.011	-.024	-.077	-.000	-.000	-.000	-.000	-.000	-.000	-.000	-.000	-.000
9	-.063	-.058	-.049	-.034	-.015	-.010	-.046	-.104	-.000	-.000	-.000	-.000	-.000	-.000	-.000	-.000
10	-.050	-.048	-.042	-.031	-.017	-.001	-.024	-.092	-.000	-.000	-.000	-.000	-.000	-.000	-.000	-.000
11	-.039	-.040	-.036	-.028	-.018	-.005	-.009	-.032	-.000	-.000	-.000	-.000	-.000	-.000	-.000	-.000
12	-.031	-.033	-.031	-.026	-.018	-.010	-.003	-.010	-.040	-.000	-.000	-.000	-.000	-.000	-.000	-.000
13	-.025	-.028	-.024	-.019	-.014	-.012	-.008	-.009	-.000	-.000	-.000	-.000	-.000	-.000	-.000	-.000
14	-.022	-.026	-.026	-.023	-.019	-.018	-.020	-.022	-.014	-.000	-.000	-.000	-.000	-.000	-.000	-.000
15	-.022	-.025	-.025	-.022	-.020	-.021	-.027	-.032	-.000	-.000	-.000	-.000	-.000	-.000	-.000	-.000
16	-.024	-.025	-.024	-.021	-.020	-.024	-.024	-.032	-.043	-.000	-.000	-.000	-.000	-.000	-.000	-.000
17	-.027	-.025	-.023	-.020	-.020	-.026	-.037	-.050	-.000	-.000	-.000	-.000	-.000	-.000	-.000	-.000
18	-.026	-.025	-.022	-.018	-.010	-.020	-.027	-.051	-.000	-.000	-.000	-.000	-.000	-.000	-.000	-.000
19	-.027	-.022	-.017	-.015	-.018	-.026	-.039	-.045	-.000	-.000	-.000	-.000	-.000	-.000	-.000	-.000
20	-.022	-.016	-.011	-.010	-.013	-.022	-.030	-.000	-.000	-.000	-.000	-.000	-.000	-.000	-.000	-.000



COORDINATES OF THE GRID POINTS AT WHICH DELTA(X) WAS DETERMINED ARE PRINTED BELOW -

NOTE - COORDINATE VALUES OF 0.0 INDICATE THAT THE GRID POINT WAS OUTSIDE THE LENS APERTURE

	X-VALUE	1	2	3	4	5	6	7	8	9	10	11	12	13	14	15	16	17
2	2.34	.00	.00	.00	.00	.00	.00	.00	.00	.00	.00	.00	.00	.00	.00	.00	.00	.00
3	7.02	.00	.00	.00	.00	.00	.00	.00	.00	.00	.00	.00	.00	.00	.00	.00	.00	.00
4	11.71	.00	.00	.00	.00	.00	.00	.00	.00	.00	.00	.00	.00	.00	.00	.00	.00	.00
5	16.39	.00	.00	.00	.00	.00	.00	.00	.00	.00	.00	.00	.00	.00	.00	.00	.00	.00
6	21.07	.00	.00	.00	.00	.00	.00	.00	.00	.00	.00	.00	.00	.00	.00	.00	.00	.00
7	25.75	.00	.00	.00	.00	.00	.00	.00	.00	.00	.00	.00	.00	.00	.00	.00	.00	.00
8	30.43	.00	.00	.00	.00	.00	.00	.00	.00	.00	.00	.00	.00	.00	.00	.00	.00	.00
9	35.12	.00	.00	.00	.00	.00	.00	.00	.00	.00	.00	.00	.00	.00	.00	.00	.00	.00
10	39.80	.00	.00	.00	.00	.00	.00	.00	.00	.00	.00	.00	.00	.00	.00	.00	.00	.00
11	44.48	2.34	7.02	11.71	16.39	21.07	25.75	30.43	35.12	39.80	44.48	49.16	53.84	58.53	63.21	67.89	72.57	72.57
12	49.16	2.36	7.02	11.71	16.39	21.07	25.75	30.43	35.12	39.80	44.48	49.16	53.84	58.53	63.21	67.89	72.57	72.57
13	53.86	2.34	7.02	11.71	16.39	21.07	25.75	30.43	35.12	39.80	44.48	49.16	53.84	58.53	63.21	67.89	72.57	72.57
14	58.53	2.34	7.02	11.71	16.39	21.07	25.75	30.43	35.12	39.80	44.48	49.16	53.84	58.53	63.21	67.89	72.57	72.57
15	63.21	2.34	7.02	11.71	16.39	21.07	25.75	30.43	35.12	39.80	44.48	49.16	53.84	58.53	63.21	67.89	72.57	72.57
16	67.89	2.34	7.02	11.71	16.39	21.07	25.75	30.43	35.12	39.80	44.48	49.16	53.84	58.53	63.21	67.89	72.57	72.57
17	72.57	2.34	7.02	11.71	16.39	21.07	25.75	30.43	35.12	39.80	44.48	49.16	53.84	58.53	63.21	67.89	72.57	72.57
18	77.26	.00	.00	.00	.00	.00	.00	.00	.00	.00	.00	.00	.00	.00	.00	.00	.00	.00
19	81.94	.00	.00	.00	.00	.00	.00	.00	.00	.00	.00	.00	.00	.00	.00	.00	.00	.00
20	86.62	.00	.00	.00	.00	.00	.00	.00	.00	.00	.00	.00	.00	.00	.00	.00	.00	.00
21	91.30	.00	.00	.00	.00	.00	.00	.00	.00	.00	.00	.00	.00	.00	.00	.00	.00	.00
22	95.98	.00	.00	.00	.00	.00	.00	.00	.00	.00	.00	.00	.00	.00	.00	.00	.00	.00
23	100.67	.00	.00	.00	.00	.00	.00	.00	.00	.00	.00	.00	.00	.00	.00	.00	.00	.00
24	105.35	.00	.00	.00	.00	.00	.00	.00	.00	.00	.00	.00	.00	.00	.00	.00	.00	.00
25	110.03	.00	.00	.00	.00	.00	.00	.00	.00	.00	.00	.00	.00	.00	.00	.00	.00	.00





VALUES OF THE PUPIL FUNCTION TRANSMISSION ARE PRINTED BELOW -

THE PUPIL FUNCTION IS A COMPLEX QUANTITY AND, THEREFORE, EACH VALUE IS A PAIR OF NUMBERS  
VALUES OF TRANSMISSION ARE PRINTED IN 4 BLOCKS OF 32 ROWS BY 8 COLUMNS

K	1	2	3	4	5	6	7
1	.000	.000	.000	.000	.000	.000	.000
2	.000	.000	.000	.000	.000	.000	.000
3	.000	.000	.000	.000	.000	.000	.000
4	.000	.000	.000	.000	.000	.000	.000
5	.000	.000	.000	.000	.000	.000	.000
6	.000	.000	.000	.000	.000	.000	.000
7	.000	.000	.000	.000	.000	.000	.000
8	.000	.000	.000	.000	.000	.000	.000
9	.000	.000	.000	.000	.000	.000	.000
10	.000	.000	.000	.000	.000	.000	.000
11	.000	.000	.000	.000	.000	.000	.000
12	.000	.000	.000	.000	.000	.000	.000
13	.000	.000	.000	.000	.000	.000	.000
14	.000	.000	.000	.000	.000	.000	.000
15	.000	.000	.000	.000	.000	.000	.000
16	.000	.000	.000	.000	.000	.000	.000
17	.000	.000	.000	.000	.000	.000	.000
18	.000	.000	.000	.000	.000	.000	.000
19	.000	.000	.000	.000	.000	.000	.000
20	.000	.000	.000	.000	.000	.000	.000
21	.000	.000	.000	.000	.000	.000	.000
22	.000	.000	.000	.000	.000	.000	.000
23	.000	.000	.000	.000	.000	.000	.000
24	.000	.000	.000	.000	.000	.000	.000
25	.000	.000	.000	.000	.000	.000	.000
26	.000	.000	.000	.000	.000	.000	.000
27	.000	.000	.000	.000	.000	.000	.000
28	.000	.000	.000	.000	.000	.000	.000
29	.000	.000	.000	.000	.000	.000	.000
30	.000	.000	.000	.000	.000	.000	.000
31	.000	.000	.000	.000	.000	.000	.000
32	.000	.000	.000	.000	.000	.000	.000

	9	10	11	12	13	14	15	16
1	.000	.000	.000	.000	.000	.000	.000	.000
2	.000	.000	.000	.949+00	-.315+00	.821+00	-.603+00	.699+00
3	.999+00	-.386+01	.940+00	-.532+00	.721+00	.620+00	-.715+00	-.797+00
4	.549+00	-.316+00	.874+00	-.456+00	.794+00	-.608+00	.620+00	.620+00
5	.902+00	-.433+00	.851+00	-.526+00	.802+00	-.598+00	.648+00	-.698+00
6	.879+00	-.478+00	.853+00	-.522+00	.828+00	-.561+00	.755+00	-.656+00
7	.872+00	-.489+00	.867+00	-.452+00	.820+00	-.510+00	.851+00	-.524+00
8	.878+00	-.479+00	.887+00	-.452+00	.893+00	-.450+00	.895+00	-.444+00
9	.890+00	-.456+00	.910+00	-.415+00	.925+00	-.383+00	.925+00	-.356+00
10	.907+00	-.422+00	.933+00	-.360+00	.952+00	-.305+00	.965+00	-.264+00
11	.924+00	-.383+00	.953+00	-.324+00	.973+00	-.232+00	.984+00	-.178+00
12	.939+00	-.345+00	.967+00	-.244+00	.985+00	-.172+00	.998+00	-.108+00
13	.549+00	-.315+00	.976+00	-.219+00	.991+00	-.132+00	.998+00	-.638+01
14	.955+00	-.298+00	.979+00	-.264+00	.993+00	-.119+00	.999+00	-.516+01
15	.955+00	-.296+00	.978+00	-.211+00	.991+00	-.133+00	.997+00	-.710+01
16	.551+00	-.309+00	.972+00	-.226+03	.986+00	-.165+03	.993+00	-.116+00
17	.543+00	-.333+00	.962+00	-.273+00	.976+00	-.219+00	.984+00	-.176+00
18	.931+00	-.365+00	.946+00	-.216+00	.962+00	-.273+00	.971+00	-.238+00
19	.915+00	-.3400	.933+00	-.360+00	.946+00	-.324+00	.956+00	-.293+00
20	.894+00	-.448+00	.915+00	-.464+00	.943+00	-.366+00	.943+00	-.331+00
21	.854+00	-.504+00	.894+00	-.499+00	.916+00	-.401+00	.933+00	-.358+00
22	.821+00	-.571+00	.866+00	-.566+00	.900+00	-.435+00	.927+00	-.375+00
23	.765+00	-.644+00	.821+00	-.537+00	.882+00	-.470+00	.922+00	-.387+00
24	.715+00	-.699+00	.797+00	-.603+00	.867+00	-.498+00	.921+00	-.369+00
25	.729+00	-.684+00	.765+00	-.533+00	.880+00	-.476+00	.939+00	-.363+00
26	.000	.000	.000	.000	.000	.000	.000	.000
27	.000	.000	.000	.000	.000	.000	.000	.000
28	.000	.000	.000	.000	.000	.000	.000	.000
29	.000	.000	.000	.000	.000	.000	.000	.000
30	.000	.000	.000	.000	.000	.000	.000	.000
31	.000	.000	.000	.000	.000	.000	.000	.000
32	.000	.000	.000	.000	.000	.000	.000	.000

	1	17	18	19	20	21	22	23	24
1	.000	.000	.000	.000	.000	.000	.000	.000	.000
2	.705+00- .709+00	.000	.000	.000	.000	.000	.000	.000	.000
3	.581+00- .614+00	.710+00- .704+00	.681+00- .679+00	.000	.000	.000	.000	.000	.000
4	.683+00- .709+00	.683+00- .703+00	.807+00- .598+00	.944+00- .329+00	.993+00- .114+00	.992+00- .124+00	.946+00- .324+00	.000	.000
5	.601+00- .740+00	.724+00- .684+00	.808+00- .589+00	.910+00- .415+00	.992+00- .213+00	.977+00- .162+00	.955+00- .846+00	.533+00	.000
6	.675+00- .740+00	.724+00- .684+00	.808+00- .589+00	.910+00- .416+00	.992+00- .213+00	.977+00- .162+00	.955+00- .846+00	.533+00	.000
7	.751+00- .660+00	.788+00- .620+00	.839+00- .544+00	.900+00- .303+00	.980+00- .185+00	.972+00- .225+00	.103+00- .162+00	.152+00	.701+00- .713+00
8	.819+00- .573+00	.875+00- .483+00	.983+00- .483+00	.923+00- .323+00	.973+00- .143+00	.973+00- .229+00	.998+00- .691+01	.988+00	.153+00- .684+00
9	.876+00- .483+00	.886+00- .464+00	.908+00- .420+00	.939+00- .343+00	.973+00- .143+00	.977+00- .213+00	.995+00- .934+01	.938+00	.60+01- .955+00
10	.920+00- .391+00	.922+00- .366+00	.934+00- .357+00	.954+00- .300+00	.970+00- .194+00	.995+00- .105+00	.100+00- .105+00	.100+01	.623+02- .968+00
11	.953+00- .302+00	.959+00- .312+00	.954+00- .299+00	.986+00- .260+00	.984+00- .194+00	.984+00- .174+00	.994+00- .110+00	.999+00- .31+01	.928+00- .573+01
12	.975+00- .222+00	.970+00- .245+00	.970+00- .247+00	.975+00- .222+00	.984+00- .174+00	.984+00- .174+00	.994+00- .110+00	.999+00- .31+01	.100+01- .157+01
13	.989+00- .152+00	.982+00- .191+00	.979+00- .205+00	.981+00- .195+00	.987+00- .161+00	.993+00- .114+00	.994+00- .046+01	.994+00- .046+01	.997+00- .74+01
14	.993+00- .116+00	.988+00- .155+00	.984+00- .155+00	.985+00- .174+00	.985+00- .151+00	.989+00- .118+00	.996+00- .020+01	.996+00- .020+01	.997+00- .112+00
15	.995+00- .099+01	.990+00- .128+00	.987+00- .160+00	.987+00- .160+00	.990+00- .160+00	.990+00- .160+00	.993+00- .122+00	.993+00- .122+00	.992+00- .124+00
16	.994+00- .107+00	.990+00- .139+00	.988+00- .155+00	.988+00- .153+00	.988+00- .153+00	.990+00- .139+00	.992+00- .125+00	.991+00- .121+00	.986+00- .166+00
17	.991+00- .121+00	.989+00- .151+00	.988+00- .157+00	.989+00- .149+00	.991+00- .149+00	.991+00- .134+00	.992+00- .128+00	.989+00- .147+00	.979+00- .202+00
18	.987+00- .161+00	.986+00- .166+00	.987+00- .159+00	.980+00- .143+00	.992+00- .130+00	.993+00- .114+00	.992+00- .122+00	.987+00- .160+00	.973+00- .230+00
19	.983+00- .186+00	.983+00- .174+00	.988+00- .154+00	.988+00- .154+00	.992+00- .130+00	.993+00- .114+00	.992+00- .122+00	.995+00- .168+00	.969+00- .247+00
20	.981+00- .154+00	.986+00- .167+00	.991+00- .135+00	.994+00- .106+00	.994+00- .106+00	.996+00- .631+01	.994+00- .110+00	.986+00- .184+00	.571+00- .240+00
21	.984+00- .180+00	.990+00- .140+00	.995+00- .140+00	.996+00- .698+01	.996+00- .698+01	.998+00- .611+01	.996+00- .644+01	.994+00- .137+00	.982+00- .189+00
22	.997+00- .759+01	.100+00- .216+01	.100+01- .269+01	.098+00- .592+01	.997+00- .592+01	.997+00- .321+01	.598+00- .629+01	.000	.000
23	.100+01- .549+02	.991+00- .749+01	.991+00- .749+01	.134+00- .913+00	.973+00- .973+00	.229+00	.954+00	.109+00	.000
24	.991+00- .131+00	.975+00- .223+00	.950+00- .311+00	.615+00- .403+00	.000	.000	.000	.000	.000
25	.938+00- .346+00	.878+00- .478+00	.788+00- .615+00	.000	.000	.000	.000	.000	.000
26	.000	.000	.000	.000	.000	.000	.000	.000	.000
27	.000	.000	.000	.000	.000	.000	.000	.000	.000
28	.000	.000	.000	.000	.000	.000	.000	.000	.000
29	.000	.000	.000	.000	.000	.000	.000	.000	.000
30	.000	.000	.000	.000	.000	.000	.000	.000	.000
31	.000	.000	.000	.000	.000	.000	.000	.000	.000
32	.000	.000	.000	.000	.000	.000	.000	.000	.000



VALUES OF THE OPTICAL TRANSFER FUNCTION. OTF. ARE PRINTED BELOW -

THE GTF IS A COMPLEX QUANTITY AND, THEREFORE, EACH VALUE IS A PAIR OF NUMBERS. VALUES OF  $O_{11}, \dots, O_{1N}$  ARE PRINTED IN 8 BLOCKS OF 65 (ROWS) BY 6 (COLUMNS).





100

— 10 —

100

— 1 —

— 10 —

• 8 •

100

○ ○ ○ ○ ○ ○ ○ ○

• • • • •

— 1 —

100

卷之三

A horizontal row of seven small black circles, evenly spaced, representing the number seven.

卷之三

	17	18	19	20	21	22	23	24
k -1	.000	.000	.000	.000	.000	.000	.000	.000
2	.000	.000	.000	.000	.000	.000	.000	.000
3	.000	.000	.000	.000	.000	.000	.000	.000
4	.000	.000	.000	.000	.000	.000	.000	.000
5	.000	.000	.000	.000	.000	.000	.000	.000
6	.000	.000	.000	.000	.000	.000	.000	.000
7	.000	.000	.000	.000	.000	.000	.000	.000
8	.000	.000	.000	.000	.000	.000	.000	.000
9	.000	.000	.000	.000	.000	.000	.000	.000
10	.000	.000	.000	.000	.000	.000	.000	.000
11	.000	.000	.000	.000	.000	.000	.000	.000
12	.000	.000	.000	.000	.000	.000	.000	.000
13	.000	.000	.000	.000	.000	.000	.000	.000
14	.000	.000	.000	.000	.000	.000	.000	.000
15	-.277-05--.379-06	.135-04-.936-07	-.301-05-.673-05	.211-04-.542-05	.493-03-.756-05	.950-04-.626-03	.436-02-.426-03	.592-01-.358-03
16	.770-05-.176-05	.371-05-.441-05	.150-04-.103-04	.263-03-.231-04	.201-02-.198-03	.102-01-.655-03	.132-01-.477-03	.252-01-.630-03
17	-.367-05	.470-05	.163-04-.414-04	.150-03-.163-02	.149-03-.160-03	.149-03-.164-03	.231-01-.114-02	.399-01-.297-02
18	.899-05-.333-06	.109-03-.382-03	.205-03-.485-03	.614-03-.102-01	.103-02-.309-01	.225-02-.547-01	.127-01-.902-02	.102-00-.275-01
19	-.625-04-.109-03	.138-02-.451-02	.411-02-.152-03	.990-02-.297-01	.175-02-.537-01	.154-01-.812-02	.613-01-.966-02	.103-00-.327-01
20	-.192-02--.451-04	.124-01-.172-02	.172-01-.289-01	.437-03-.537-02	.886-02-.812-01	.217-01-.109-02	.109-00-.339-01	.103-00-.435-01
21	.405-02	.125-02	.124-01-.172-02	.172-01-.289-01	.94-01-.760-01	.107-00-.355-01	.137-00-.516-01	.167-00-.779-01
22	.140-01	.182-02	.285-01-.780-04	.503-01-.663-02	.780-01-.663-02	.102-00-.718-01	.102-00-.718-01	.102-00-.718-01
23	.271-01	.60-0-04	.463-01-.530-02	.530-02-.628-04	.196-03-.162-01	.263-03-.334-01	.292-02-.292-02	.551-01-.154-01
24	.413-01	.122-01	.122-01-.122-01	.122-01-.122-01	.125-01-.125-01	.125-01-.125-01	.125-01-.125-01	.125-01-.125-01
25	.548-01-.107-01	.805-01-.206-01	.206-01-.112-00	.352-01-.112-00	.146-00-.525-01	.184-00-.712-01	.219-00-.887-01	.256-00-.103-00
26	.661-01	.882-01	.975-01-.297-01	.131-03-.441-01	.167-00-.609-01	.203-00-.792-01	.244-00-.952-01	.164-00-.608-01
27	.810-01	.261-01	.114-00-.384-01	.384-01-.149-00	.525-01-.187-00	.683-01-.227-00	.843-01-.100-00	.309-00-.114-00
28	.944-01-.362-01	.130-00-.467-01	.467-01-.164-00	.601-01-.164-00	.207-00-.741-01	.244-00-.885-01	.291-00-.103-00	.335-00-.116-00
29	.108-00-.411-01	.146-00-.54-3-01	.146-00-.54-3-01	.186-03-.669-01	.228-00-.802-01	.271-00-.934-01	.315-00-.102-00	.360-00-.118-00
30	.123-00-.455-01	.164-00-.623-01	.633-01-.252-00	.929-01-.352-01	.146-00-.525-01	.184-00-.712-01	.219-00-.887-01	.256-00-.103-00
31	.139-0-0-.57-01	.182-00-.709-01	.709-01-.226-00	.929-01-.226-00	.161-00-.525-01	.205-00-.792-01	.244-00-.952-01	.164-00-.608-01
32	.155-00-.65-01	.232-00-.806-01	.806-01-.248-00	.923-01-.248-00	.101-00-.525-01	.342-00-.110-00	.387-00-.117-00	.432-00-.124-00
33	.182-00-.835-01	.226-00-.942-01	.942-01-.271-00	.103-00-.271-00	.103-00-.315-00	.113-00-.355-00	.115-00-.403-00	.136-00-.127-00
34	.182-00-.889-01	.226-00-.942-01	.942-01-.271-00	.103-00-.271-00	.103-00-.315-00	.113-00-.355-00	.115-00-.403-00	.136-00-.127-00
35	.177-00-.926-01	.226-00-.942-01	.942-01-.271-00	.103-00-.271-00	.103-00-.315-00	.113-00-.355-00	.115-00-.403-00	.136-00-.127-00
36	.165-00-.76-01	.208-00-.84-3-01	.84-3-01-.252-00	.923-01-.252-00	.161-01-.493-01	.234-00-.789-01	.364-00-.113-00	.434-00-.125-00
37	.151-00-.65-01	.191-00-.76-3-01	.76-3-01-.236-00	.903-01-.236-00	.181-00-.525-01	.323-00-.789-01	.369-00-.115-00	.434-00-.125-00
38	.135-00-.628-01	.176-00-.585-01	.585-01-.219-00	.665-01-.219-00	.305-00-.673-01	.340-00-.673-01	.340-00-.673-01	.370-00-.501-01
39	.119-00-.558-01	.335-01-.208-01	.208-01-.618-01	.665-01-.618-01	.242-00-.608-01	.286-00-.558-01	.305-00-.558-01	.333-00-.422-01
40	.102-00-.488-01	.139-00-.530-01	.530-01-.179-00	.537-01-.179-00	.221-00-.510-01	.263-00-.459-01	.304-00-.393-01	.347-00-.258-01
41	.84-3-01-.418-01	.119-00-.458-01	.458-01-.157-00	.462-01-.157-00	.197-00-.432-01	.237-00-.378-01	.276-00-.309-01	.313-00-.237-01
42	.654-01-.352-01	.985-01-.392-01	.392-01-.134-00	.397-01-.134-00	.172-00-.368-01	.213-00-.491-01	.243-00-.578-01	.313-00-.419-01
43	.464-01-.280-01	.771-01-.353-01	.353-01-.110-00	.353-01-.110-00	.162-00-.327-01	.216-00-.427-01	.244-00-.502-01	.349-00-.377-01
44	.283-01-.157-01	.546-01-.274-01	.274-01-.865-01	.306-01-.865-01	.120-00-.291-01	.153-00-.421-01	.185-00-.571-01	.214-00-.403-01
45	.130-01-.116-01	.335-01-.208-01	.208-01-.618-01	.618-01-.618-01	.922-01-.465-01	.128-00-.231-01	.153-00-.465-01	.181-00-.323-01
46	.220-02-.406-02	.152-01-.134-01	.134-01-.384-01	.221-01-.384-01	.501-01-.658-01	.94-01-.231-01	.122-00-.171-01	.141-00-.101-01
47	.135-02-.192-03	.239-02-.563-02	.563-02-.180-01	.180-01-.183-01	.411-01-.228-01	.67-01-.222-01	.931-01-.186-01	.140-00-.121-02
48	.147-04	.216-03-.793-03	.613-03-.423-02	.888-02-.397-01	.204-01-.183-01	.426-01-.222-01	.669-01-.197-01	.110-00-.123-01
49	.164-04	.220-04-.580-04	.531-03-.813-03	.279-02-.911-02	.164-01-.184-01	.462-01-.186-01	.670-01-.132-01	.145-00-.127-02
50	.134-04	.245-04-.302-04	.302-04-.143-03	.251-03-.143-03	.120-00-.291-01	.153-00-.421-01	.185-00-.571-01	.214-00-.403-01
51	.148-05-.377-05	.19-05-.222-06	.353-04-.143-03	.377-03-.143-03	.201-03-.162-02	.557-02-.709-02	.166-01-.116-01	.318-01-.179-02
52	.000	.000	.000	.000	.000	.000	.000	.000
53	.000	.000	.000	.000	.000	.000	.000	.000
54	.000	.000	.000	.000	.000	.000	.000	.000
55	.000	.000	.000	.000	.000	.000	.000	.000
56	.000	.000	.000	.000	.000	.000	.000	.000



		25	26	27	28	29	30	31	32
1	x	1 .000	.000	.000	.000	.000	.000	.000	.000
2		2 .000	.000	.000	.000	.000	.000	.000	.000
3		3 .000	.000	.000	.000	.000	.000	.000	.000
4		4 .000	.000	.000	.000	.000	.000	.000	.000
5		5 .000	.000	.000	.000	.000	.000	.000	.000
6		6 .000	.000	.000	.000	.000	.000	.000	.000
7		7 .000	.000	.000	.000	.000	.000	.000	.000
8		8 .000	.000	.000	.000	.000	.000	.000	.000
9		9 .000	.000	.000	.000	.000	.000	.000	.000
10	-	10 .004-04	145-04	146-02	146-04	146-02	146-02	146-02	146-02
11	-	11 .166-02	795-04	569-02	143-03	104-01	156-02	157-01	147-02
12	-	12 .637-02	246-04	129-01	747-03	200-01	334-02	265-01	152-01
13	-	13 .142-01	246-02	319-01	659-02	397-01	125-01	459-01	208-01
14	-	14 .248-01	1119-02	356-01	484-02	461-01	102-01	554-01	179-01
15	-	15 .378-01	372-02	509-01	13-03	629-01	153-01	739-01	244-01
16	*	16 .543-01	737-02	689-01	138-01	624-01	233-01	957-01	319-01
17	*	17 .726-01	156-01	901-01	215-01	104-03	21-01	121-00	405-01
18	*	18 .964-01	234-01	115-00	322-01	133-03	414-01	150-00	50-01
19	*	19 .124-01	365-01	144-00	456-01	164-00	53-01	183-00	60-01
20	*	20 .135-03	524-01	177-00	604-00	199-00	665-01	220-00	7-01
21	*	21 .189-00	691-01	214-00	765-01	237-00	79-01	260-00	809-01
22	*	22 .225-00	856-01	253-00	502-01	278-00	51-01	304-00	897-01
23	*	23 .261-00	106-00	292-00	104-00	320-00	102-00	349-00	978-01
24	*	24 .292-00	113-00	332-00	115-00	363-00	112-00	395-00	105-00
25	*	25 .323-00	122-00	369-00	123-00	406-00	120-00	441-00	112-00
26	*	26 .365-00	124-00	406-00	129-00	441-00	126-00	485-00	127-00
27	*	27 .397-00	131-00	441-00	134-00	486-00	131-00	528-00	122-00
28	*	28 .427-00	134-00	473-00	137-00	522-00	135-00	570-00	127-00
29	*	29 .455-00	135-00	506-00	140-00	526-00	140-00	539-00	139-00
30	*	30 .483-00	136-00	534-00	141-00	554-00	141-00	561-00	134-00
31	*	31 .509-00	135-00	560-00	138-00	614-00	138-00	669-00	132-00
32	*	32 .529-00	129-00	580-00	129-00	633-00	127-00	659-00	101-00
33	*	33 .540-00	120-00	592-00	120-00	644-00	111-00	659-00	105-00
34	*	34 .541-00	103-00	592-00	982-01	646-00	91-01	702-00	808-01
35	*	35 .636-00	881-01	566-00	813-01	656-00	723-01	691-00	639-01
36	*	36 .524-00	723-01	573-00	640-01	588-00	641-00	664-00	647-01
37	*	37 .504-00	561-01	548-00	491-01	592-00	416-00	634-00	344-01
38	*	38 .478-00	426-01	518-00	369-01	557-00	122-01	594-00	265-01
39	*	39 .447-00	311-01	482-00	280-01	542-00	117-01	569-00	105-01
40	*	40 .413-00	227-01	444-00	198-01	473-00	17-01	502-00	151-01
41	*	41 .377-00	144-01	404-00	127-01	429-00	115-01	453-00	875-02
42	*	42 .339-00	836-02	362-00	586-02	461-02	40-02	452-00	979-02
43	*	43 .299-00	299-02	321-00	402-03	342-00	212-02	447-02	382-00
44	*	44 .262-00	167-02	282-00	608-02	302-00	847-02	526-01	645-02
45	*	45 .226-00	599-02	245-00	108-01	263-00	143-01	320-00	137-00
46	*	46 .191-00	737-02	209-00	147-01	226-00	195-01	242-00	231-01
47	*	47 .158-00	863-02	175-00	174-01	191-00	239-01	206-00	283-01
48	*	48 .122-00	792-02	117-00	186-01	187-01	150-00	256-01	173-01
49	*	49 .102-00	577-03	932-01	174-01	106-00	265-01	116-00	333-01
50	*	50 .798-01	631-02	518-00	369-01	557-00	122-01	594-00	265-01
51	*	51 .606-01	444-02	722-01	150-01	630-01	20-01	924-01	311-01
52	*	52 .440-01	268-02	542-01	120-01	629-01	2-01	710-01	276-01
53	*	53 .293-01	132-02	386-01	487-01	519-01	174-01	239-01	577-01
54	*	54 .167-01	577-03	244-01	599-02	387-01	125-01	182-01	401-01
55	*	55 .652-02	278-03	125-01	332-02	117-01	218-01	225-01	178-01
56	-	56 .-263-03	-712-05	-451-03	-704-02	-359-02	-104-01	-127-01	-117-01







	41	42	43	44	45	46	47	48
K								
1	.000	.003	.000	.000	.000	.000	.000	.000
2	.000	.000	.000	.000	.000	.000	.000	.000
3	.000	.000	.000	.000	.000	.000	.000	.000
4	.000	.000	.000	.000	.000	.000	.000	.000
5	.000	.000	.000	.000	.000	.000	.000	.000
6	.000	.000	.000	.000	.000	.000	.000	.000
7	.000	.000	.000	.000	.000	.000	.000	.000
8	.000	.000	.000	.000	.000	.000	.000	.000
9	.000	.000	.000	.000	.000	.000	.000	.000
10	-.203-.03	.712-.05	.000	.000	.000	.000	.000	.000
11	.652-.12	-.217-.03	.581-.03	-.885-.04	-.236-.04	.000	.000	.000
12	.167-.01	-.578-.03	.681-.02	.204-.02	.181-.02	-.114-.03	-.589-.04	-.320-.05
13	.293-.01	-.132-.02	.190-.01	.373-.02	.039-.02	.483-.02	.261-.02	.267-.02
14	.440-.01	-.269-.02	.319-.01	.488-.02	.193-.01	.647-.02	.845-.02	.720-.02
15	.606-.01	-.644-.02	.473-.01	.525-.02	.318-.01	.112-.01	.166-.01	.557-.02
16	.798-.01	-.611-.02	.650-.01	.473-.02	.478-.01	.128-.01	.296-.01	.159-.01
17	.102-.00	-.792-.02	.855-.01	.138-.02	.670-.01	.132-.01	.462-.01	.188-.01
18	.128+.00	-.873-.02	.110-.00	.204-.02	.301-.01	.669-.01	.197-.01	.026-.01
19	.158+.00	-.860-.02	.140-.00	.121-.02	.118+.00	.107-.01	.931-.01	.186-.01
20	.191+.00	-.737-.02	.171+.00	.101-.02	.165+.00	.932-.02	.122+.00	.171-.01
21	.226+.00	-.503-.02	.205+.00	.157-.02	.179-.02	.150+.00	.165+.01	.123+.00
22	.262+.00	-.157-.02	.240+.00	.388-.02	.216+.00	.101-.01	.185+.00	.171-.01
23	.299+.00	-.294-.02	.427+.00	.727-.02	.248+.00	.127-.01	.216+.00	.202-.01
24	.339+.00	-.636-.02	.313+.00	.119-.01	.282+.00	.170-.01	.247+.00	.210-.01
25	.377+.00	-.149-.01	.347+.00	.184-.01	.311+.00	.237+.00	.276+.00	.309-.01
26	.413+.00	-.227-.01	.379+.00	.268-.01	.333+.00	.322-.01	.304+.00	.393-.01
27	.447+.00	-.315-.01	.410+.00	.407-.01	.363+.00	.328+.00	.328+.00	.501-.01
28	.478+.00	-.426-.01	.436+.00	.496-.01	.393+.01	.564-.01	.349+.00	.624-.01
29	.504+.00	-.564-.01	.459+.00	.637-.01	.414+.00	.702-.01	.359+.00	.727-.01
30	.524+.00	-.723-.01	.477+.00	.791-.01	.435+.00	.844-.01	.584+.00	.874-.01
31	.536+.00	-.881-.01	.488+.00	.930-.01	.497-.00	.977-.01	.397+.00	.101+.00
32	.541+.00	-.103+.00	.493+.00	.107+.00	.447+.00	.110+.00	.403+.00	.109+.00
33	.540+.00	-.120+.00	.492+.00	.120+.00	.447+.00	.118+.00	.402+.00	.115+.00
34	.529+.00	-.139+.00	.479+.00	.127+.00	.435+.00	.123+.00	.374+.00	.117+.00
35	.505+.00	-.135+.00	.459+.00	.128+.00	.411+.00	.122+.00	.364+.00	.113+.00
36	.483+.00	-.136+.00	.434+.00	.128+.00	.386+.00	.119+.00	.340+.00	.109+.00
37	.455+.00	-.135+.00	.407+.00	.128+.00	.366+.00	.116+.00	.316+.00	.106+.00
38	.427+.00	-.134+.00	.380+.00	.127+.00	.335+.00	.116+.00	.291+.00	.103+.00
39	.397+.00	-.131+.00	.352+.00	.124+.00	.304+.00	.114+.00	.268+.00	.100+.00
40	.365+.00	-.128+.00	.325+.00	.121+.00	.281+.00	.110+.00	.244+.00	.962-.01
41	.332+.00	-.122+.00	.295+.00	.120+.00	.256+.00	.103+.00	.219+.00	.867-.01
42	.298+.00	-.113+.00	.262+.00	.105+.00	.226+.00	.102+.00	.193+.00	.791-.01
43	.261+.00	-.104+.00	.230+.00	.938-.01	.198+.00	.819+.01	.165+.00	.669+.01
44	.225+.00	-.854-.01	.197+.00	.779-.01	.167+.00	.661-.01	.137+.00	.516-.01
45	.189+.00	.691-.01	.164+.00	.608-.01	.137+.00	.494-.01	.109+.00	.359-.01
46	.155+.00	.522-.01	.132+.00	.435-.01	.104+.00	.327-.01	.813-.01	.209-.01
47	.124+.00	.369-.01	.102+.00	.276-.01	.796-.01	.179-.01	.547-.01	.902-.02
48	.964-.01	.234-.01	.760-.01	.154-.01	.555-.01	.612-.02	.234-.01	.292-.02
49	.736-.01	.156-.01	.558-.01	.748-.02	.367-.01	.319-.02	.167-.01	.973-.03
50	.543-.01	.737-.02	.389-.01	.297-.02	.231-.01	.114-.02	.102-.01	.655-.03
51	.378-.01	.372-.02	.252-.01	.630-.03	.132-.01	.477-.01	.436-.02	.933-.02
52	.248-.01	.119-.02	.140-.01	.358-.03	.507-.02	.457-.03	.626-.03	.179-.03
53	.140-.01	.266-.03	.590-.02	.209-.03	.845-.03	.212-.03	.943-.04	.160-.04
54	.637-.02	.261-.04	.127-.02	.131-.03	.713-.04	.795-.05	.588-.05	.369-.06
55	.166-.02	.794-.04	.129-.03	.352-.04	.306-.04	.728-.05	.147-.05	.419-.06
56	-.104-.06	-.157-.04	.069-.00	.000	.000	.000	.000	.000

57 58 59 60 61 62 63 64

	49	50	51	52	53	54	55
K	.000	.000	.000	.000	.000	.000	.000
1	.000	.000	.000	.000	.000	.000	.000
2	.000	.000	.000	.000	.000	.000	.000
3	.000	.000	.000	.000	.000	.000	.000
4	.000	.000	.000	.000	.000	.000	.000
5	.000	.000	.000	.000	.000	.000	.000
6	.000	.000	.000	.000	.000	.000	.000
7	.000	.000	.000	.000	.000	.000	.000
8	.000	.000	.000	.000	.000	.000	.000
9	.000	.000	.000	.000	.000	.000	.000
10	.000	.000	.000	.000	.000	.000	.000
11	.000	.000	.000	.000	.000	.000	.000
12	.000	.000	.000	.000	.000	.000	.000
13	.000	.000	.000	.000	.000	.000	.000
14	.000	.000	.000	.000	.000	.000	.000
15	-.148-.05	.379-.CS	.000	.000	.000	.000	.000
16	-.139-.04	.255-.04	.105-.05	.280-.05	.000	.000	.000
17	.160-.04	.220-.04	.147-.04	.117-.04	.123-.05	.175-.04	.000
18	.140-.04	.316-.03	.257-.04	.413-.04	.197-.04	.162-.04	.252-.05
19	-.135-.02	.192-.03	.460-.02	.270-.03	.150-.03	.123-.03	.197-.04
20	.220-.02	.061-.02	.110-.02	.256-.03	.764-.03	.709-.03	.215-.04
21	.130-.01	.116-.01	.295-.02	.376-.02	.612-.03	.188-.03	.643-.03
22	.283-.01	.199-.01	.115-.01	.108-.01	.277-.02	.406-.02	.136-.03
23	.464-.01	.280-.01	.293-.01	.191-.01	.906-.02	.905-.01	.216-.02
24	.654-.01	.352-.01	.383-.01	.274-.01	.811-.01	.180-.01	.637-.02
25	.843-.01	.418-.01	.542-.01	.350-.01	.295-.01	.255-.01	.127-.01
26	.102-.00	.488-.01	.690-.01	.418-.01	.422-.01	.323-.01	.210-.01
27	.119-.00	.558-.01	.814-.01	.480-.01	.537-.01	.378-.01	.298-.01
28	.135-.00	.628-.01	.976-.01	.539-.01	.647-.01	.424-.01	.382-.01
29	.151-.00	.659-.01	.112-.01	.599-.01	.762-.01	.473-.01	.321-.01
30	.165-.00	.765-.01	.125-.00	.656-.01	.873-.01	.521-.01	.550-.01
31	.177-.00	.826-.01	.134-.00	.699-.01	.953-.01	.552-.01	.615-.01
32	.182-.00	.849-.01	.140-.00	.721-.01	.987-.01	.542-.01	.630-.01
33	.182+.00	.835-.01	.138+.00	.694-.01	.934-.01	.536-.01	.616-.01
34	.155-.00	.669-.01	.111-.00	.512-.01	.707-.01	.343-.01	.375-.01
35	.139-.00	.577-.01	.978-.01	.433-.01	.618-.01	.259-.01	.319-.01
36	.123-.00	.495-.01	.857-.01	.532-.01	.652-.01	.473-.01	.523-.01
37	.108-.00	.418-.01	.743-.01	.296-.01	.652-.01	.181-.01	.222-.01
38	.944-.01	.342-.01	.635-.01	.227-.01	.378-.01	.129-.01	.129-.01
39	.810-.01	.261-.01	.532-.01	.160-.01	.369-.01	.924-.02	.140-.01
40	.681-.01	.182-.01	.436-.01	.977-.02	.259-.01	.411-.02	.102-.02
41	.545-.01	.107-.01	.336-.01	.439-.02	.113-.01	.109-.02	.104-.03
42	.413-.01	.458-.02	.240-.01	.558-.03	.113-.01	.765-.03	.560-.02
43	.271-.01	.640-.04	.142-.01	.156-.02	.556-.02	.122-.02	.381-.03
44	.140-.01	.192-.02	.616-.02	.165-.02	.193-.02	.822-.03	.159-.03
45	.405-.12	.125-.02	.131-.02	.608-.03	.185-.03	.102-.03	.659-.04
46	-.192-.03	.461-.04	.202-.03	.164-.03	.516-.04	.263-.06	.176-.05
47	-.635-.04	.109-.03	.302-.04	.465-.05	.121-.05	.558-.05	.128-.05
48	-.899-.15	.313-.06	.113-.05	.877-.05	.249-.05	.556-.06	.535-.05
49	-.367-.06	.470-.05	.660-.05	.107-.05	.573-.05	.107-.05	.000
50	.770-.05	.175-.05	.555-.05	.821-.07	.000	.000	.000
51	-.377-.05	.339-.06	.000	.000	.000	.000	.000
52	.000	.000	.000	.000	.000	.000	.000
53	.200	.000	.000	.000	.000	.000	.000
54	.000	.000	.000	.000	.000	.000	.000
55	.000	.000	.000	.000	.000	.000	.000
56	.000	.000	.000	.000	.000	.000	.000



1	.600
2	.000
3	.000
4	.000
5	.000
6	.000
7	.000
8	.000
9	.000
10	.000
11	.000
12	.000
13	.000
14	.000
15	.000
16	.000
17	.000
18	.000
19	.000
20	.000
21	.000
22	.000
23	.000
24	.000
25	.000
26	.000
27	.000
28	-.159-05-.116-05
29	-.243-03-.181-03
30	-.739-03-.462-03
31	-.132-02-.680-03
32	-.152-02-.768-03
33	-.156-02-.765-03
34	-.712-03-.309-03
35	-.567-03-.171-03
36	-.366-03-.646-04
37	-.165-03-.710-05
38	.000
39	.000
40	.000
41	.000
42	.000
43	.000
44	.000
45	.000
46	.000
47	.000
48	.000
49	.000
50	.000
51	.000
52	.000
53	.000
54	.000
55	.000
56	.000
57	.000
58	.000
59	.000
60	.000
61	.000
62	.000
63	.000
64	.000

57	58	59	60	61	62	63	64
55	56	57	58	59	60	61	62
53	54	55	56	57	58	59	60
51	52	53	54	55	56	57	58
49	50	51	52	53	54	55	56
47	48	49	50	51	52	53	54
45	46	47	48	49	50	51	52
43	44	45	46	47	48	49	50
41	42	43	44	45	46	47	48
39	40	41	42	43	44	45	46
37	38	39	40	41	42	43	44
35	36	37	38	39	40	41	42
33	34	35	36	37	38	39	40
31	32	33	34	35	36	37	38
29	30	31	32	33	34	35	36
27	28	29	30	31	32	33	34
25	26	27	28	29	30	31	32
23	24	25	26	27	28	29	30
21	22	23	24	25	26	27	28
19	20	21	22	23	24	25	26
17	18	19	20	21	22	23	24
15	16	17	18	19	20	21	22
13	14	15	16	17	18	19	20
11	12	13	14	15	16	17	18
9	10	11	12	13	14	15	16
7	8	9	10	11	12	13	14
5	6	7	8	9	10	11	12
3	4	5	6	7	8	9	10
1	2	3	4	5	6	7	8
0	1	2	3	4	5	6	7

THE MTF AND RTF VALUES ARE PRINTED AS A PAIR IN 8 BLOCKS OF 65(MEWS) BY 8(COLUMNS)

7  
6  
5  
4  
3  
2  
1  
X  
1 2 3 4 5 6 7 8 9 10 11 12 13 14 15 16 17 18 19 20 21 22 23 24 25 26 27 28 29 30 31 32 33 34 35 36 37 38 39 40 41 42 43 44 45 46 47 48







	17	18	19	20	21	22	23	24
K	.000	.000	.000	.000	.000	.000	.000	.000
1	.000	.000	.000	.000	.000	.000	.000	.000
2	.000	.000	.000	.000	.000	.000	.000	.000
3	.000	.000	.000	.000	.000	.000	.000	.000
4	.000	.000	.000	.000	.000	.000	.000	.000
5	.000	.000	.000	.000	.000	.000	.000	.000
6	.000	.000	.000	.000	.000	.000	.000	.000
7	.000	.000	.000	.000	.000	.000	.000	.000
8	.000	.000	.000	.000	.000	.000	.000	.000
9	.000	.000	.000	.000	.000	.000	.000	.000
10	.000	.000	.000	.000	.000	.000	.000	.000
11	.000	.000	.000	.000	.000	.000	.000	.000
12	.000	.000	.000	.000	.000	.000	.000	.000
13	.000	.000	.000	.000	.000	.000	.000	.000
14	.000	.000	.000	.000	.000	.000	.000	.000
15	.378-.05	.000	.135-.04	.652-.02	.924-.05	.000	.219-.04	.000
16	.79-.05	.000	.182-.04	.600+.00	.264-.03	.305-.01	.204-.02	.973-.01
17	.872-.05	.000	.679-.04	.261+.01	.211-.03	.236+.01	.557-.02	.258-.01
18	.908-.05	.000	.445-.04	.195+.01	.412-.03	.299+.01	.166-.02	.119+.00
19	.126-.03	.210+.01	.473-.03	.226+.01	.783-.03	.226+.01	.103-.01	.726-.01
20	.197-.03	.291+.01	.165-.02	.394+.00	.101+.01	.175+.00	.294-.01	.499-.01
21	.422-.02	.299+.00	.125-.01	.138+.00	.289-.01	.151-.01	.54-.01	.164+.00
22	.161-.01	.136+.00	.285-.01	.274-.02	.506-.01	.131+.00	.244+.00	.113+.00
23	.27-.01	.236-.02	.466-.01	.114+.00	.735-.01	.217+.00	.107+.00	.302+.00
24	.416-.01	.111+.00	.645-.01	.190+.00	.954-.01	.269+.00	.134+.00	.311+.00
25	.555-.01	.193+.00	.831-.01	.250+.00	.117+.00	.305+.00	.175+.00	.345+.00
26	.705-.01	.261+.00	.102+.00	.294+.00	.136+.00	.325+.00	.177+.00	.356+.00
27	.851-.01	.312+.00	.120+.00	.326+.00	.158+.00	.338+.00	.199+.00	.356+.00
28	.100+.00	.347+.00	.138+.00	.346+.00	.178+.00	.364+.00	.222+.00	.342+.00
29	.118+.00	.389+.00	.160+.00	.385+.00	.215+.00	.385+.00	.242+.00	.385+.00
30	.138+.00	.382+.00	.175+.00	.363+.00	.220+.00	.346+.00	.134+.00	.310+.00
31	.154+.00	.354+.00	.196+.00	.371+.00	.243+.00	.349+.00	.206+.00	.330+.00
32	.169+.00	.408+.00	.208+.00	.386+.00	.265+.00	.386+.00	.231+.00	.350+.00
33	.201+.00	.429+.00	.245+.00	.395+.00	.269+.00	.358+.00	.331+.00	.375+.00
34	.201+.00	.436+.00	.246+.00	.394+.00	.290+.00	.362+.00	.322+.00	.328+.00
35	.195+.00	.437+.00	.239+.00	.364+.00	.261+.00	.353+.00	.322+.00	.315+.00
36	.182+.00	.434+.00	.224+.00	.266+.00	.267+.00	.341+.00	.310+.00	.300+.00
37	.166+.00	.434+.00	.207+.00	.377+.00	.249+.00	.327+.00	.290+.00	.282+.00
38	.149+.00	.434+.00	.189+.00	.370+.00	.230+.00	.314+.00	.271+.00	.239+.00
39	.131+.00	.438+.00	.170+.00	.364+.00	.210+.00	.301+.00	.254+.00	.244+.00
40	.111+.00	.447+.00	.149+.00	.364+.00	.167+.00	.291+.00	.222+.00	.227+.00
41	.941-.01	.460+.00	.127+.00	.368+.00	.163+.00	.286+.00	.202+.00	.216+.00
42	.763-.01	.494+.00	.106+.00	.379+.00	.140+.00	.341+.00	.176+.00	.210+.00
43	.543-.01	.543+.00	.840-.01	.411+.00	.116+.00	.308+.00	.150+.00	.220+.00
44	.346-.01	.613+.00	.611-.01	.465+.00	.918-.01	.339+.00	.123+.00	.238+.00
45	.17-.01	.727+.00	.395-.01	.554+.00	.672-.01	.406+.00	.941-.01	.284+.00
46	.461-.02	.107+.01	.203-.01	.724+.00	.443-.01	.521+.00	.705-.01	.364+.00
47	.137-.02	.300+.01	.612-.02	.1	.243-.01	.735+.00	.470-.01	.507+.00
48	.217-.03	.150+.01	.100-.02	.25	.963-.02	.113+.01	.276+.00	.173+.01
49	.275-.04	.929+.00	.641-.01	.441+.00	.229+.01	.150-.01	.918+.00	.314-.01
50	.279-.04	.207+.01	.959-.04	.125+.01	.269-.03	.239+.01	.672-.02	.103+.01
51	.440-.05	.000	.620-.05	.000	.378-.03	.166+.01	.114-.02	.139+.01
52	.000	.344-.05	.000	.393-.05	.000	.39-.03	.196+.00	.339-.02
53	.000	.000	.127-.01	.724+.00	.119-.04	.000	.278-.04	.137+.01
54	.000	.000	.000	.000	.000	.000	.000	.000
55	.000	.000	.000	.000	.000	.000	.000	.000
56	.000	.000	.000	.000	.000	.000	.000	.000

57 100 100 100 100 100 100  
58 100 100 100 100 100 100  
59 100 100 100 100 100 100  
60 100 100 100 100 100 100  
61 100 100 100 100 100 100  
62 100 100 100 100 100 100  
63 100 100 100 100 100 100  
64 100 100 100 100 100 100  
65 100 100 100 100 100 100

	25	26	27	28	29	30	31	32
K	.000	.000	.000	.000	.000	.000	.000	.000
1	.000	.000	.000	.000	.000	.000	.000	.000
2	.000	.000	.000	.000	.000	.000	.000	.000
3	.000	.000	.000	.000	.000	.000	.000	.000
4	.000	.000	.000	.000	.000	.000	.000	.000
5	.000	.000	.000	.000	.000	.000	.000	.000
6	.000	.000	.000	.000	.000	.000	.000	.000
7	.000	.000	.000	.000	.000	.000	.000	.000
8	.000	.000	.000	.000	.000	.000	.000	.000
9	.000	.000	.000	.000	.000	.000	.000	.000
10	.181-04	.216+01	.146-02	.100+01	.346-02	.110+00	.695-02	.320+00
11	.156-02	.480-01	.569-02	.251+01	.106-01	.148+00	.165-01	.229+00
12	.63-02	.410-02	.129-01	.574-01	.207-01	.142+00	.279-01	.315+00
13	.180-01	.190-01	.235-01	.879-01	.326-01	.251+00	.417-01	.313+00
14	.249-01	.478-01	.360-01	.135+00	.473-01	.218+00	.582-01	.313+00
15	.286-01	.551-01	.516-01	.164+00	.647-01	.238+00	.777-01	.319+00
16	.587-01	.135+00	.702-01	.168+00	.854-01	.264+00	.101+00	.321+00
17	.748-01	.162+00	.926-01	.234+00	.110+00	.286+00	.127+00	.324+00
18	.592-01	.238+00	.120+00	.274+00	.139+00	.303+00	.158+00	.324+00
19	.139+03	.289+00	.151+00	.305+00	.172+00	.314+00	.193+00	.317+00
20	.164+00	.326+00	.187+00	.329+00	.210+00	.332+00	.231+00	.340+00
21	.202+03	.350+00	.227+00	.339+00	.250+00	.324+00	.272+00	.339+00
22	.241+00	.383+00	.268+00	.343+00	.293+00	.318+00	.316+00	.328+00
23	.260+00	.386+00	.310+00	.341+00	.336+00	.310+00	.362+00	.327+00
24	.318+00	.364+00	.351+00	.334+00	.380+00	.299+00	.409+00	.260+00
25	.354+03	.352+00	.322+00	.322+00	.386+00	.288+00	.455+00	.226+00
26	.387+00	.338+00	.426+00	.305+00	.464+00	.275+00	.499+00	.237+00
27	.418+00	.320+00	.461+00	.255+00	.503+00	.263+00	.542+00	.227+00
28	.447+00	.304+00	.493+00	.285+00	.539+00	.303+00	.582+00	.219+00
29	.475+00	.289+03	.524+00	.279+00	.573+00	.245+00	.622+00	.213+00
30	.502+00	.274+00	.552+00	.254+00	.604+00	.235+00	.655+00	.226+00
31	.527+00	.259+00	.577+00	.249+00	.629+00	.221+00	.682+00	.207+00
32	.564+00	.240+00	.594+00	.219+00	.646+00	.207+00	.699+00	.195+00
33	.583+00	.218+00	.601+00	.197+00	.653+00	.171+00	.701+00	.164+00
34	.551+00	.187+00	.630+00	.164+00	.652+00	.140+00	.704+00	.115+00
35	.533+00	.163+00	.576+00	.111+00	.622+00	.091+00	.694+00	.079+00
36	.522+00	.137+00	.576+00	.111+00	.622+00	.080+00	.669+00	.069+00
37	.507+00	.111+00	.550+00	.099+00	.593+00	.070+00	.593+00	.050+00
38	.486+00	.889+01	.520+00	.711+01	.516+00	.471+01	.549+00	.374+01
39	.448+00	.703+01	.483+00	.500+01	.516+00	.471+01	.502+00	.392+01
40	.414+00	.548+01	.444+00	.447+01	.473+00	.358+01	.502+00	.302+01
41	.378+00	.393+01	.404+00	.426+01	.429+00	.313+01	.453+00	.267+01
42	.336+00	.247+01	.362+00	.162+01	.365+00	.091+00	.406+00	.022+01
43	.299+00	.981+02	.321+00	.125+02	.342+00	.061+02	.362+00	.021+01
44	.262+00	.638+02	.282+00	.215+01	.302+00	.281+01	.320+00	.341+01
45	.226+00	.226+01	.245+00	.442+01	.263+00	.543+01	.286+00	.614+01
46	.191+00	.386+01	.210+00	.700+01	.227+00	.861+01	.738+00	.336+00
47	.158+00	.544+01	.176+00	.592+01	.193+00	.124+00	.208+00	.136+00
48	.129+00	.679+01	.146+00	.129+00	.161+00	.167+00	.176+00	.181+00
49	.102+00	.774+01	.119+00	.157+00	.134+00	.209+00	.147+00	.231+00
50	.801+01	.789+01	.948+01	.184+00	.109+00	.246+00	.121+00	.279+00
51	.608+01	.732+01	.738+01	.965+01	.705+00	.975+01	.355+00	.873+00
52	.441+01	.590+01	.555+01	.217+00	.663+01	.321+00	.762+01	.371+00
53	.293+01	.452+01	.394+01	.176+00	.222+00	.487+01	.535+00	.639+01
54	.167+01	.367+01	.251+01	.241+00	.331+01	.386+00	.400+01	.496+00
55	.653+02	.414+01	.130+01	.254+00	.194+01	.420+00	.251+01	.526+00
56	.203+03	.311+01	.300+02	.286+00	.777+02	.438+00	.123+01	.685+01



	33	34	35	36	37	38	39	40
1	.000	.000	.000	.000	.000	.000	.000	.000
2	.000	.000	.000	.000	.000	.000	.000	.000
3	.000	.000	.000	.000	.000	.000	.000	.000
4	.000	.000	.000	.000	.000	.000	.000	.000
5	.000	.000	.000	.000	.000	.000	.000	.000
6	.000	.000	.000	.000	.000	.000	.000	.000
7	.000	.000	.000	.000	.000	.000	.000	.000
8	.000	.000	.000	.000	.000	.000	.000	.000
9	.723-.02-.514+.00	.723-.02-.101+.01	.729-.02-.922+.00	.404-.02-.759+.03	.292-.02-.759+.03	.079-.02-.345+.00	.308-.02-.345+.00	.308-.02-.240+.00
10	.185-.01-.823+.00	.183-.01-.764+.00	.185-.01-.681+.00	.178-.01-.676+.00	.159-.01-.643+.00	.123-.01-.562+.00	.777-.02-.345+.00	.130-.01-.259+.00
11	.338-.01-.713+.00	.328-.01-.654+.00	.326-.01-.605+.00	.324-.01-.566+.00	.299-.01-.541+.00	.251-.01-.522+.00	.154-.01-.420+.00	.130-.01-.241+.00
12	.517-.01-.621+.00	.497-.01-.527+.00	.49-.01-.495+.00	.490-.01-.495+.00	.456-.01-.496+.00	.400-.01-.473+.00	.721-.01-.371+.00	.251-.01-.241+.00
13	.736-.31-.534+.00	.709-.01-.452+.00	.696-.01-.415+.00	.681-.01-.432+.00	.638-.01-.439+.00	.569-.01-.423+.00	.481-.01-.353+.00	.394-.01-.227+.00
14	.100.00-.459+.00	.961-.01-.382+.00	.931-.01-.356+.00	.898-.01-.373+.00	.842-.01-.387+.00	.762-.01-.371+.00	.661-.01-.321+.00	.555-.01-.217+.00
15	.131.00-.387+.00	.125.00-.332+.00	.120.00-.301+.00	.114.00-.316+.00	.107.00-.316+.00	.975-.01-.325+.00	.845-.01-.285+.00	.738-.01-.205+.00
16	.165.00-.339+.00	.158.00-.279+.00	.150.00-.258+.00	.142.00-.255+.00	.125.00-.255+.00	.112.00-.256+.00	.102.00-.224+.00	.948-.01-.184+.00
17	.202.00-.275+.00	.194.00-.238+.00	.183.00-.216+.00	.172.00-.218+.00	.160.00-.218+.00	.121.00-.210+.00	.109.00-.209+.00	.115.00-.157+.00
18	.242.00-.233+.00	.233.00-.197+.00	.219.00-.180+.00	.204.00-.178+.00	.190.00-.178+.00	.181.00-.176+.00	.161.00-.167+.00	.146.00-.129+.00
19	.284.00-.156+.00	.274.00-.146+.00	.256.00-.149+.00	.240.00-.149+.00	.224.00-.149+.00	.208.00-.138+.00	.192.00-.124+.00	.178.00-.992+.01
20	.326.00-.164+.00	.315.00-.138+.00	.299.00-.118+.00	.277.00-.107+.00	.259.00-.102+.00	.243.00-.095+.01	.222.00-.086+.01	.210.00-.073+.01
21	.368.00-.160+.00	.358.00-.114+.00	.338.00-.096+.00	.316.00-.082+.01	.298.00-.068+.01	.260.00-.061+.01	.245.00-.042+.01	.215.00-.021+.01
22	.412.00-.119+.00	.402.00-.094+.01	.361.00-.074+.01	.349.00-.055+.01	.339.00-.045+.01	.302.00-.025+.01	.281.00-.019+.01	.248.00-.009+.01
23	.458.00-.099+.01	.447.00-.077+.01	.427.00-.055+.01	.404.00-.036+.01	.382.00-.022+.01	.362.00-.012+.01	.342.00-.009+.01	.321.00-.009+.01
24	.505.00-.037+.01	.495.00-.015+.01	.475.00-.006+.01	.452.00-.006+.01	.429.00-.009+.02	.406.00-.006+.02	.385.00-.005+.02	.362.00-.004+.02
25	.553.00-.079+.01	.544.00-.049+.01	.526.00-.028+.01	.502.00-.009+.02	.477.00-.007+.02	.453.00-.004+.02	.429.00-.003+.02	.403.00-.003+.02
26	.603.00-.059.01	.592.00-.021+.01	.557.00-.004+.01	.516.00-.004+.01	.452.00-.004+.01	.427.00-.004+.01	.392.00-.003+.01	.368.00-.003+.01
27	.656.00-.047.01	.651.00-.004+.01	.631.00-.007+.01	.611.00-.010+.01	.580.00-.010+.01	.545.00-.010+.01	.514.00-.009+.01	.481.00-.008+.01
28	.701.00-.035.01	.706.00-.013.01	.687.00-.009.01	.659.00-.009.01	.629.00-.009.01	.595.00-.009.01	.564.00-.009.01	.531.00-.009.01
29	.756.00-.023.01	.763.00-.000.01	.733.00-.000.02	.711.00-.000.01	.682.00-.000.01	.654.00-.000.01	.622.00-.000.01	.591.00-.000.01
30	.825.00-.113.01	.818.00-.078.02	.793.00-.050.02	.758.00-.034.01	.715.00-.019.01	.670.00-.005.00	.649.00-.000.00	.618.00-.000.00
31	.884.00-.222.02	.871.00-.150.01	.839.00-.089.00	.805.00-.055.01	.751.00-.025.01	.712.00-.000.00	.679.00-.000.00	.641.00-.000.00
32	.943.00-.233.02	.921.00-.092.01	.892.00-.061.01	.853.00-.040.01	.792.00-.016.01	.747.00-.000.00	.706.00-.000.00	.664.00-.000.00
33	.100.00-.000.00	.943.00-.025.01	.886.00-.059.01	.821.00-.053.01	.763.00-.025.01	.707.00-.000.00	.654.00-.000.00	.611.00-.000.00
34	.543.00-.222.02	.518.00-.070.01	.495.00-.070.01	.461.00-.060.00	.419.00-.040.00	.370.00-.010.00	.327.00-.000.00	.285.00-.000.00
35	.684.00-.220.02	.671.00-.032.01	.636.00-.032.01	.604.00-.027.01	.575.00-.017.01	.534.00-.006.00	.494.00-.000.00	.451.00-.000.00
36	.825.00-.113.01	.816.00-.076.00	.781.00-.050.00	.742.00-.027.00	.705.00-.012.00	.661.00-.000.00	.624.00-.000.00	.582.00-.000.00
37	.766.00-.224.01	.741.00-.099.00	.701.00-.069.00	.651.00-.049.00	.612.00-.021.00	.573.00-.000.00	.535.00-.000.00	.494.00-.000.00
38	.710.00-.035.01	.705.00-.011.01	.669.00-.004.00	.649.00-.004.00	.611.00-.000.00	.574.00-.000.00	.535.00-.000.00	.495.00-.000.00
39	.656.00-.070.01	.637.00-.040.00	.605.00-.029.01	.561.00-.017.00	.515.00-.005.00	.479.00-.000.00	.441.00-.000.00	.401.00-.000.00
40	.603.00-.059.01	.592.00-.016.00	.563.00-.009.00	.523.00-.006.00	.484.00-.000.00	.455.00-.000.00	.424.00-.000.00	.384.00-.000.00
41	.553.00-.070.01	.548.00-.010.00	.533.00-.004.00	.503.00-.001.00	.469.00-.000.00	.434.00-.000.00	.406.00-.000.00	.375.00-.000.00
42	.505.00-.037.01	.499.00-.016.00	.468.00-.014.00	.438.00-.010.00	.408.00-.000.00	.373.00-.000.00	.342.00-.000.00	.312.00-.000.00
43	.468.00-.099.01	.453.00-.051.00	.428.00-.034.00	.393.00-.016.00	.363.00-.000.00	.333.00-.000.00	.303.00-.000.00	.273.00-.000.00
44	.412.00-.011.00	.407.00-.004.00	.384.00-.000.00	.350.00-.000.00	.316.00-.000.00	.287.00-.000.00	.253.00-.000.00	.223.00-.000.00
45	.368.00-.163.00	.343.00-.030.00	.313.00-.000.00	.283.00-.000.00	.253.00-.000.00	.227.00-.000.00	.197.00-.000.00	.167.00-.000.00
46	.326.00-.164.00	.304.00-.031.00	.273.00-.000.00	.243.00-.000.00	.213.00-.000.00	.183.00-.000.00	.153.00-.000.00	.122.00-.000.00
47	.284.00-.164.00	.257.00-.031.00	.228.00-.000.00	.198.00-.000.00	.168.00-.000.00	.138.00-.000.00	.108.00-.000.00	.078.00-.000.00
48	.242.00-.233.00	.237.00-.027.00	.219.00-.000.00	.186.00-.000.00	.153.00-.000.00	.124.00-.000.00	.094.00-.000.00	.064.00-.000.00
49	.203.00-.275.00	.199.00-.040.00	.167.00-.000.00	.145.00-.000.00	.116.00-.000.00	.086.00-.000.00	.056.00-.000.00	.026.00-.000.00
50	.165.00-.330.00	.163.00-.016.00	.133.00-.000.00	.109.00-.000.00	.070.00-.000.00	.040.00-.000.00	.010.00-.000.00	.-0.00-.000.00
51	.121.00-.361.00	.120.00-.036.00	.100.00-.000.00	.049.00-.000.00	.019.00-.000.00	.-0.00-.000.00	.-0.00-.000.00	.-0.00-.000.00
52	.100.00-.459.00	.101.00-.050.00	.522.00-.000.00	.532.00-.000.00	.506.00-.000.00	.473.00-.000.00	.443.00-.000.00	.413.00-.000.00
53	.736.01-.534.00	.745.01-.021.00	.531.01-.000.00	.531.01-.000.00	.505.01-.000.00	.477.01-.000.00	.447.01-.000.00	.417.01-.000.00
54	.517.01-.621.00	.521.01-.021.00	.419.01-.000.00	.409.01-.000.00	.383.01-.000.00	.356.01-.000.00	.327.01-.000.00	.297.01-.000.00
55	.338.01-.713.00	.341.01-.036.00	.321.01-.000.00	.309.00-.000.00	.287.00-.000.00	.257.00-.000.00	.227.00-.000.00	.198.00-.000.00
56	.185.01-.823.00	.171.01-.017.01	.144.01-.000.00	.139.00-.000.00	.114.01-.000.00	.101.00-.000.00	.066.00-.000.00	.010.00-.000.00



	41	42	43	44	45	46	47	48
1	.000	.000	.000	.000	.000	.000	.000	.000
2	.000	.000	.000	.000	.000	.000	.000	.000
3	.000	.000	.000	.000	.000	.000	.000	.000
4	.000	.000	.000	.000	.000	.000	.000	.000
5	.000	.000	.000	.000	.000	.000	.000	.000
6	.000	.000	.000	.000	.000	.000	.000	.000
7	.000	.000	.000	.000	.000	.000	.000	.000
8	.000	.000	.000	.000	.000	.000	.000	.000
9	.000	.000	.000	.000	.000	.000	.000	.000
10	.203-.02	.311+.01	.000	.000	.000	.000	.000	.000
11	.653-.02	-.14-.01	.224-.02	.262+.00	.910-.04	-.288+.01	.000	.000
12	1.67-.01	-.147-.01	.934-.02	.227+.00	.344-.02	.552+.00	.128-.03	.266+.01
13	.293-.01	-.152-.01	.193-.01	.194-.01	.106-.01	.475+.00	.373-.02	.797+.00
14	.441-.01	-.190-.01	.322-.01	.152+.00	.210-.01	.414+.03	.111-.01	.706+.00
15	.608-.31	-.732-.01	.476-.01	.111+.00	.337-.01	.340+.00	.629-.01	.905+.00
16	.801-.01	-.729-.01	.652-.01	.725-.01	.495-.01	.262+.00	.336-.01	.493+.00
17	.102+.00	-.774-.01	.856-.01	.395-.01	.683-.01	.194+.00	.499-.01	.387+.00
18	.129+.00	-.679-.01	.111+.00	.185-.01	.910-.01	.136+.00	.607-.01	.680+.00
19	.158+.00	-.544-.01	.140+.00	.867-.02	.118+.00	.950-.01	.197+.00	.610-.01
20	.191+.00	-.356-.01	.171+.00	.591-.02	.148+.00	.633-.01	.123+.00	.139+.00
21	.226+.00	-.226-.01	.205+.00	.874-.02	.180+.00	.500-.01	.154+.00	.107+.00
22	.262+.00	-.228-.02	.248+.00	.162-.01	.473-.01	.248+.00	.925-.01	.186+.00
23	.259+.00	.981-.02	.276+.00	.263-.01	.249+.00	.509-.01	.217+.00	.929-.01
24	.339+.00	-.247-.01	.313+.00	.381-.01	.283+.00	.603-.01	.248+.00	.981-.01
25	.378+.00	.393-.01	.347+.00	.530-.01	.314+.00	.755-.01	.278+.00	.112+.00
26	.414+.00	.584-.01	.380+.00	.705-.01	.344+.00	.936-.01	.306+.00	.129+.00
27	.488+.00	.703-.01	.412+.00	.887-.01	.372+.00	.117+.00	.332+.00	.152+.00
28	.480+.00	.689-.01	.439+.00	.113+.00	.397+.00	.143+.00	.355+.00	.177+.00
29	.507+.00	.111+.00	.462+.00	.463+.00	.420+.00	.168+.00	.202+.00	.286+.00
30	.529+.00	.137+.00	.48+.00	.164+.00	.439+.00	.194+.00	.394+.00	.225+.00
31	.543+.00	.163+.00	.495+.00	.188+.00	.452+.00	.218+.00	.410+.00	.250+.00
32	.551+.00	.187+.00	.505+.00	.213+.00	.464+.00	.240+.00	.477+.00	.265+.00
33	.553+.00	.218+.00	.520+.00	.520+.00	.482+.00	.258+.00	.484+.00	.278+.00
34	.544+.00	.240+.00	.496+.00	.260+.00	.450+.00	.277+.00	.453+.00	.287+.00
35	.527+.00	.259+.00	.477+.00	.273+.00	.429+.00	.288+.00	.381+.00	.331+.00
36	.502+.00	.274+.00	.426+.00	.288+.00	.404+.00	.299+.00	.357+.00	.323+.00
37	.475+.00	.289+.00	.426+.00	.304+.00	.379+.00	.316+.00	.332+.00	.287+.00
38	.447+.00	.304+.00	.401+.00	.321+.00	.355+.00	.334+.00	.309+.00	.341+.00
39	.416+.00	.320+.00	.374+.00	.339+.00	.350+.00	.352+.00	.362+.00	.358+.00
40	.387+.00	.338+.00	.347+.00	.358+.00	.305+.00	.371+.00	.262+.00	.376+.00
41	.354+.00	.332+.00	.316+.00	.372+.00	.276+.00	.384+.00	.236+.00	.385+.00
42	.318+.00	.364+.00	.283+.00	.383+.00	.277+.00	.391+.00	.208+.00	.389+.00
43	.286+.00	.386+.00	.304+.00	.387+.00	.214+.00	.392+.00	.178+.00	.385+.00
44	.241+.00	.363+.00	.212+.00	.377+.00	.180+.00	.376+.00	.146+.00	.360+.00
45	.202+.00	.350+.00	.175+.00	.355+.00	.186+.00	.345+.00	.115+.00	.321+.00
46	.164+.00	.324+.00	.139+.00	.317+.00	.113+.00	.294+.00	.639-.01	.252+.00
47	.130+.00	.269+.00	.106+.00	.263+.00	.811-.01	.222+.00	.555-.01	.163+.00
48	.592-.01	.218+.00	.776-.01	.200+.00	.557-.01	.146+.00	.335-.01	.872-.01
49	.748-.01	.182+.00	.563-.01	.123+.00	.387-.01	.214+.00	.392+.00	.556-.01
50	.547-.01	.135+.00	.391-.01	.761-.31	.232-.01	.491-.01	.102-.01	.640-.01
51	.380-.01	.981-.01	.252-.01	.329-.01	.132-.01	.362-.01	.592-.03	.190+.00
52	.249-.01	.477-.01	.140-.01	.256-.01	.509-.02	.898-.01	.651-.03	.278+.00
53	.143-.01	.190-.01	.59-.02	.261-.01	.246-.01	.951-.04	.361-.01	.193-.04
54	.437-.02	-.010-.02	.128-.02	.103-.00	.717-.04	-.303+.01	.954-.05	.000
55	.166-.02	-.040-.01	.130-.03	-.287+.01	.729-.05	.000	.000	.000
56	.168-.04	-.216+.01	.000	.000	.000	.000	.000	.000

57 58 59 60 61 62 63 64 65

	49	50	51	52	53	54	55	56
1	.000	.000	.000	.000	.000	.000	.000	.000
2	.000	.000	.000	.000	.000	.000	.000	.000
3	.000	.000	.000	.000	.000	.000	.000	.000
4	.000	.000	.000	.000	.000	.000	.000	.000
5	.000	.000	.000	.000	.000	.000	.000	.000
6	.000	.000	.000	.000	.000	.000	.000	.000
7	.000	.000	.000	.000	.000	.000	.000	.000
8	.000	.000	.000	.000	.000	.000	.000	.000
9	.000	.000	.000	.000	.000	.000	.000	.000
10	.000	.000	.000	.000	.000	.000	.000	.000
11	.000	.000	.000	.000	.000	.000	.000	.000
12	.000	.000	.000	.000	.000	.000	.000	.000
13	.000	.000	.000	.000	.000	.000	.000	.000
14	.000	.000	.000	.000	.000	.000	.000	.000
15	.407-.05	.000	.000	.000	.000	.000	.000	.000
16	.277-.04	-.207+.01	.759-.05	-.000	.000	.000	.000	.000
17	.275-.04	-.325+.00	.187-.04	-.247+.01	.176-.04	.000	.000	.000
18	-.217-.03	-.150+.01	.491-.04	-.697+.00	.747-.03	.028-.05	.000	.000
19	.137-.02	-.300+.01	.523-.03	-.261+.01	.19-.03	.689+.00	.268-.04	.745-.00
20	.461-.02	.107+.01	.113-.02	-.291+.01	.104-.02	-.239+.01	.141+.01	.116-.04
21	.174-.01	.727+.00	.473-.02	.905+.00	.618-.03	.286+.01	.114-.02	.217+.01
22	.346-.01	.613+.00	.157-.01	.756+.00	.491-.02	.974+.00	.161-.03	.255+.01
23	.542-.01	.533+.00	.333-.01	.682+.00	.139-.01	.860+.00	.428-.02	.372-.03
24	.743-.01	.494+.00	.471-.01	.621+.00	.255-.01	.782+.00	.110-.01	.552+.00
25	.941-.01	.460+.00	.645-.01	.573+.00	.300-.01	.713+.00	.196-.01	.864+.00
26	.113+.00	.467+.00	.107-.01	.544+.00	.531-.01	.653+.00	.296-.01	.782+.00
27	.131+.00	.438+.00	.612-.01	.562-.01	.657-.02	.286+.01	.114-.02	.286+.01
28	.165+.00	.434+.00	.111+.00	.505+.00	.774-.01	.581+.00	.484-.01	.663+.00
29	.182+.00	.434+.00	.127+.00	.452+.00	.899-.01	.556+.00	.570-.01	.620+.00
30	.195+.00	.437+.00	.141+.00	.485+.00	.102+.00	.538+.00	.661-.01	.588+.00
31	.201+.00	.437+.00	.151+.00	.480+.00	.110-.01	.524+.00	.729-.01	.565+.00
32	.205+.00	.436+.00	.157+.00	.477+.00	.113+.00	.512+.00	.739-.01	.546+.00
33	.231+.00	.426+.00	.155+.00	.463+.00	.112+.00	.498+.00	.713-.01	.528+.00
34	.169+.00	.404+.00	.122+.00	.432+.00	.786-.01	.452+.00	.436+.00	.352-.01
35	.150+.00	.394+.00	.107+.00	.417+.00	.692-.01	.436+.00	.112-.01	.460+.00
36	.133+.00	.382+.00	.931-.01	.401+.00	.581-.01	.413+.00	.295-.01	.412+.00
37	.116+.00	.367+.00	.800-.31	.378+.00	.487-.01	.381+.00	.240-.01	.364+.00
38	.105+.00	.347+.00	.674-.01	.344+.00	.399-.01	.330+.00	.189-.01	.266+.00
39	.851-.01	.312+.00	.555-.01	.292+.00	.350-.01	.261+.00	.143-.01	.210+.00
40	.705-.01	.261+.00	.446-.01	.221+.00	.213-.01	.210+.00	.102-.01	.998-.01
41	.559-.01	.193+.00	.139-.01	.130+.00	.174-.01	.630-.01	.681-.02	.205-.01
42	.416-.01	.111+.00	.240-.01	.233-.01	.114-.01	.675-.01	.348-.02	.162+.00
43	.271-.01	.236-.02	.143-.01	.110-.00	.570-.02	.224+.00	.106-.03	.302+.00
44	.141-.01	.136+.00	.674-.01	.263+.00	.210-.02	.402+.00	.175-.03	.424+.00
45	.424-.02	.299+.00	.144-.02	.435+.00	.211-.03	.304+.00	.716-.04	.273+.01
46	.197-.03	.291+.01	.260-.03	.246+.01	.581-.04	.266+.01	.176-.05	.979-.05
47	.126-.03	.210+.01	.305-.04	.249+.01	.571-.05	.000	.000	.113-.05
48	.900-.65	.000	.143-.04	-.248+.01	.256-.05	.000	.000	.538-.05
49	.472-.05	.000	.669-.95	.000	.570-.05	.000	.000	.000
50	.790-.65	.000	.555-.95	.000	.000	.000	.000	.000
51	.378-.65	.000	.000	.000	.000	.000	.000	.000
52	.000	.000	.000	.000	.000	.000	.000	.000
53	.000	.000	.000	.000	.000	.000	.000	.000
54	.000	.000	.000	.000	.000	.000	.000	.000
55	.000	.000	.000	.000	.000	.000	.000	.000
56	.000	.000	.000	.000	.000	.000	.000	.000

57 58 59 60 61 62 63 64



.000  
.000 .000 .000 .000  
.000 .000 .000 .000  
.000 .000 .000 .000  
.000 .000 .000 .000  
.000 .000 .000 .000  
.000 .000 .000 .000  
.000 .000 .000 .000  
.000 .000 .000 .000  
.000 .000 .000 .000  
.000 .000 .000 .000  
.000 .000 .000 .000  
.000 .000 .000 .000  
.000 .000 .000 .000  
.000 .000 .000 .000  
.000 .000 .000 .000  
57 .000  
58 .000  
59 .000  
60 .000  
61 .000  
62 .000  
63 .000  
64 .000

THE FOLLOWING PARAMETERS, IN ADDITION TO THE DE AND GTF VALUES, ARE WRITTEN ON TAPE WHICH BECOMES INPUT TO THE PLOTTING PROGRAM  
THIS LISTING SHOULD BE CHECKED BEFORE RUNNING PLOTTING PROGRAM

```
DELTAY = 4.680      DELTXY = 7.399
RADIUS = 57.777    WAVELENGTH = .6328-03
DEVMIN = -1.66     DEVMAX = -126
NS1 = 26           NS2 = 26
FNUMBER = 8.650
RUSHMAX = LAMDDA/ 20.625
EXCEPT PRINTS
```

## APPENDIX B

### COMPUTER PROGRAM TO PLOT WSI TEST DATA

The computer program used to generate machine plotting of WSI test data is presented. An outline of program operation is given together with an input description, auxiliary definitions of program variables, listing of subroutines, computational program listing, and a sample printout.

#### Outline of Program Operation

The program uses a set of subroutines, termed the Graphical Display System, to produce graphic elements which are independent of any given display device. These graphic elements, or plotter directives, are placed in intermediate drum storage, and for the present program, these directives are transferred to actual plotter commands by two other independent programs called the PRINTER post-processor and the CALCOMP (California Computer Products, Inc., Anaheim, Ca.) post-processor. The PRINTER post-processor provides plots on a standard computer line printer, and the CALCOMP post-processor provides plots on an incremental pen-and-ink device. The printer plots provide an inexpensive and speedy set of plots for general inspection. The CALCOMP plots are high quality and suitable for final presentation in reports or slides. Examples of both types of plots are given later in the sample printout.

- A. Input data - magnetic tape containing parameters, pupil function, and OTF as generated by WSI data-reduction program
- B. Calculations
  - 1. Compute coordinates of circular lens aperture
  - 2. Compute coordinates of grid values at which pupil function is known
  - 3. Compute contour levels for plotting pupil function
  - 4. Determine normalized MTF
  - 5. Compute spatial-frequency coordinates at which MTF is known
  - 6. Compute contour levels for plotting MTF

7. Determine PTF relative to value at maximum MTF
8. Compute contour levels for plotting PTF
9. Determine tangential and sagittal MTF and spatial-frequency coordinates at which the MTF is known
10. Determine tangential and sagittal PTF

C. Output data

1. Paper printout (See sample printout.)
  - a. Parameters and pupil function written on input tape
  - b. Contour levels for pupil function
  - c. Contour levels for MTF
  - d. Contour levels for PTF
  - e. Spatial-frequency cut-off for diffraction-limited lens of same f/number as test lens
  - f. Printout plot (See sample printout.)
    - (i) Contour map of pupil function
    - (ii) Contour map of MTF
    - (iii) Contour map of PTF
    - (iv) MTF vs spatial frequency for test lens (0 to diffraction-limited spatial-frequency cut-off)
    - (v) MTF vs spatial frequency for test lens\* (0 to lowest spatial frequency at which MTF is less than 0.05)
    - (vi) MTF vs spatial frequency for diffraction-limited lens of same f/number as test lens
    - (vii) PTF vs spatial frequency for test lens

\*This plot is optional; for highly aberrated lenses for which the RMS of the wavefront is greater than 2.00, this plot will be generated with an expanded scale for low values of spatial frequency.

2. Magnetic tape containing plotting directives for CALCOMP plotters; the resulting plots will be versions of the printer plots f.(i) through f.(vii) listed above.

#### Input Description

The input quantities for the plotting program exist on magnetic tape generated by the data-reduction program. The FORTRAN program statement for reading these unformatted data on tape unit 7 or A is given below to indicate presence and order of the variables.

```
READ TAPE 7, DEVMIN, DEVMAX, RADIUS, WAVEI, DELTA, DELTXY,  
DE, OTF, NS1, NS2, FNO, RMSMAX
```

### Auxiliary Definitions

Variables which are common to the data-reduction and plotting programs and have been defined previously are not listed below unless a different symbol is used in the plotting program.

<u>FORTRAN Variable</u>	<u>Description</u>
BUFX(500)	Array of 500 consecutive words provided as work region for routine to process data
BUFXY(LENGTH)	Variable-sized array of words provided as work region for routine to process data
BUFY(500)	Array of 500 consecutive words provided as work region for routine to process data
DL(I)	Values of MTF for diffraction-limited lens with f-number equal to that of test lens
DY	Coordinate increment along y-axis
GIVEN(I)	Parameters specify maximum and minimum values of given x and y ordinate ranges and upper limit to number of scale subdivisions; used by subroutines to plot linear x and y-axes
LENGTH	Size of array BUFXY; LENGTH = 10,000 is recommended for present program
MTF(J,K)	Modulation transfer function
PHIMAX	Maximum value of PTF
PHIMIN	Minimum value of PTF
PTF(J,K)	Phase transfer function
SPECS(I)	Array of values that specify construction parameters necessary to produce various plot components
SF(I)	Spatial frequency
SFCTOF	Spatial-frequency cut-off for diffraction-limited lens with f-number equal to that of test lens
X	x-coordinate of plotted values
XCONTR	Length (inches) of x-scale in plot of pupil-function phase

<u>FORTRAN Variables</u>	<u>Description</u>
XINCRE	Incremental difference between plotted contour levels
X1	x-coordinate of circular lens aperture
Y	y-coordinate of plotted values
YCONTR	Length (inches) of y-scale in plot of pupil-function phase
Y1	y-coordinate of circular lens aperture
Y2(I)	Tangential MTF or tangential PTF
Y3(I)	Sagittal MTF or sagittal PTF
ZLEVEL(I)	Values of plotted contour levels

### Subroutines

A list of the subroutines used in this program is presented below.

<u>FORTRAN Name</u>	<u>Called by</u>	<u>Function</u>
PLOTPU	MAIN	Provide directives for plot of isocontour values of pupil-function phase
GDLILI	PLOTPU, PLTMOD	Construct rectangular grid having linear subdivisions of both axes
TITLET	PLOTPU, PLTMOD	Construct lines of text above plot
FABLIX	PLOTPU, PLTMOD	Determine linear scale for x-ordinate range
FABLIY	PLOTPU, PLTMOD	Determine linear scale for y-ordinate range
NODLIL	PLOTPU, PLYMOD	Construct linear numeric scale to left of plot
NODLIB	PLOTPU, PLTMOD	Construct linear numeric scale below plot
AXLILI	PLOTPU, PLTMOD	Construct pair of axes having linear subdivisions
TITLEB	PLOTPU, PLTMOD	Construct lines of text below plot
TITLEL	PLOTPU, PLTMOD	Construct lines of text to left of plot
PFLILI	PLOTPU, PLTMOD	Construct a trend curve through set of points in linear rectangular system
CONLI	PLOTPU, PLTMOD	Construct contour lines from rectangular grid of values
PLTMOD	MAIN	Provide directives for plots of MTF, PTF, and isocontour values
NXTFRM	PLTMOD	Initiate a new frame
GDSEND	PLTMOD	Terminate plotting

Computation Program Listing

```
C THIS PROGRAM PLOTS PUPIL FUNCTION, MTF, AND PHASE USING PRINTER UNIT
C AND GENERATES TAPE FOR CALCOMP PLOTTING OF THESE LENS PROPERTIES
DIMENSION DE(32,32)
COMPLEX GTF(65,65)
READ TAPE 7, DEVMIN, DEVMAX, RADIUS, WAVELENGTH, DELTXY, DE, GTF, NS1,
1NS2, FNG, RMSMAX
WRITE(6,5)DELTXY, RADIUS, WAVELENGTH, DEVMIN, DEVMAX, NS1, NS2, FNG,
1RMSMAX
5 FORMAT(1B11'THE FOLLOWING PARAMETERS, IN ADDITION TO THE DE AND GTF
1VALUES, WERE READ IN FROM TAPE OR DRUM GENERATED BY // PROGRAM FOR
2 DATA REDUCTION OF WSI INTERFEROGRAMS - //'
3      ' DELTA = 'F8.3,10X'DELTXY = 'F8.3//' RADIUS = 'F8.3,9
4X'WAVELENGTH = 'E9.4//' DEVMIN = 'F8.3,9X'DEVMAX = 'F8.3//' NS1 =
5'I2,18X'NS2 = 'I2//' F/NUMBER = 'F8.3//' RMSMAX = LAMBDA/'F8.3)

CALL PLGTPU( DE, NS1, DELTXY, DEVMIN, DEVMAX, RADIUS, NS2 )

NSMAX=MAX0( NS1, NS2 )
CALL PLTMOD( GTF, DELTXY, NSMAX, WAVELENGTH, FNG, RMSMAX )
STOP
END
```

```

C THIS SUBROUTINE PROVIDES 1 PRINTER PLOT (FRAME) PLUS GENERATES
C CODE FOR CAL-COMP PLOTTER
C PUPIL FUNCTION IS PLOTTED IN ACTUAL LENS COORDINATES
C SUBROUTINE PLGTPU(DE,NS1,DELTA,DEVMAX,DEVMIN,RADIUS,NS2)
C DIMENSION BUPX(500),BUFY(500),BUFXYZ(10000),DE(32,32),GIVEN(3),
C 1 SPECS(35),X(32),X1(122),Y(32),Y1(122),ZLEVEL(10)

      WRITE(6,211)
211  FORMAT(1H1' VALUES OF DE(I,K) FOR THE BEST FITTING WAVEFRONT ARE
     1 PRINTED BELOW -'//1' TERMS INVOLVING R(1),B(2),B(3),B(4) HAVE BEEN
     2 SUBTRACTED FROM DE VALUES'//1' ALSO, THE VALUE OF DE AT THE CENTE
     3R OF THE APERTURE HAS BEEN SUBTRACTED FROM THE DE VALUES'//1' THESE
     4 DE VALUES SHOULD COMPARE EXACTLY WITH THE DE VALUES GENERATED BY
     5 THE MAIN PROGRAM FOR REDUCING INTERFEROGRAMS AND'//1' TRANSFERRED TO
     6 THIS PROGRAM BY A TAPE UNIT'////)
      WRITE(6,66)
66  FORMAT(1H 2X'I'4X'2'7X'3'7X'4'7X'5'7X'6'7X'7'7X'8'7X'9'6X'10'6X'11
     1'6X'12'6X'13'6X'14'6X'15'6X'16'6X'17'/' K')
      DO 761 K=1,32
761  WRITE(6,68)K,(DE(I,K),I=2,17)
68  FORMAT(1H I2,1X16F8.3/)
      WRITE(6,69)
69  FORMAT(1H 2X'J'3X'18'6X'19'6X'20'6X'21'6X'22'6X'23'6X'24'6X'25'6
     1X'26'6X'27'6X'28'6X'29'6X'30'6X'31'6X'32'6X'33'/' K')
      DO 762 K=1,32
762  WRITE(6,68)K,(DE(I,K),I=18,33)

C SET UP COORDINATES, X1 AND Y1, FOR CIRCULAR LENS APERTURE IN SAME
C SYSTEM AS COORDINATES FOR PUPIL FUNCTION TO BE PLOTTED, I.E.
C THE ACTUAL LENS COORDINATES
C DY=(2.*RADIUS/60.0) - 0.001
C K=122
C D=0
C DO 10 I=1,61
C Y1(I)=D
C Y1(K)=Y1(I)
C X1(I)=(RADIUS - SQRT(2.*RADIUS*D - D**2))
C X1(K)=(RADIUS + SQRT(2.*RADIUS*D - D**2))
C D=D+DY
10  K=K-1

C DRAW A BOX AROUND THE PLOTTING AREA
C SET UP XDIST AND YDIST (IN INCHES)
C SPECS(1)=2.0
C SPECS(2)=2.0
C SET UP XLENGTH AND YLENGTH (IN INCHES)
C SPECS(7)=5.50
C SPECS(8)=5.50
C SET UP GRIDLESS CONTOURING AREA, XDIV AND YDIV =1
C SPECS(9)=1.
C SPECS(10)=1.
C SET UP PRINTING TOOL (ONLY ONE AVAILABLE AT NBS)
C SPECS(11)=1.
C SET UP TAPE NUMBER
C SPECS(12)=8.
C CALL GDLILI(SPECS)

```

```

C      SET SPECS TO PRINT TITLE
SPECS( 17 )=0.2
SPECS( 18 )=0.2
SPECS( 19 )=0.0
SPECS( 21 )=1.0
SPECS( 25 )=0.75
CALL TITLET( 27PHASE OF THE PUPIL FUNCTION, SPECS)

C      SET UP X AND Y ARRAYS (LENS COORDINATES OF PUPIL-FUNCTION VALUES)
DO 30 I=1,32
X(I)=DELTA*(I-1)
30 Y(I)=X(I)

C      SET SPECS TO DETERMINE X,Y COORDINATES FOR A LINEAR SCALE.
GIVEN(1)=2.*RADIUS
GIVEN(2)=0.0
GIVEN(3)=6
C      FALBLIX SETS SPECS(3), SPECS(4), AND SPECS(9).
CALL FABLIB(GIVEN,SPECS)
GIVEN(1)=2.*RADIUS
C      FABLIY SETS SPECS(5), SPECS(6), AND SPECS(10).
CALL FABLY(GIVEN,SPECS)

C      SET SPECS TO CONSTRUCT NUMERICAL SCALES ALONG X AND Y AXES.
SPECS( 17 )=0.15
SPECS( 18 )=0.15
SPECS( 20 )=0.0
SPECS( 26 )=0.1
SPECS( 28 )=0.0
CALL NODLIL(SPECS)
SPECS( 24 )=0.1
CALL NODLIB(SPECS)

C      RESET THE NUMBER OF DIVISIONS FOR TICK MARKS
SPECS( 9 )=2.*SPECS( 9 )
SPECS( 10 )=2.*SPECS( 10 )
CALL AXLILI(SPECS)
C      LABEL X AND Y AXES
CALL TITLEB(6HX (MM),SPECS)
CALL TITLEL(6HY (MM),SPECS)

C      SET UP SPECS TO PLOT CIRCULAR LENS APERTURE
SPECS( 13 )=122
SPECS( 14 )=1.
SPECS( 15 )=1.
CALL PFLILI(X1,Y1,BUFX,BUFY,SPECS)

C      COMPUTE LEVELS AT WHICH CONTOURS ARE TO BE MADE
XINCRE=(DEVMAX-DEVMIN)*.1
ZLEVEL(1)=DEVMIN*XINCRE
DO 40 I=2,9
40 ZLEVEL(I)=ZLEVEL(I-1)+XINCRE
WRITE(6,8)
8 FORMAT(//!!! CONTOUR LEVELS COMPUTED FOR THE PUPIL-FUNCTION PHASE(
1DE) ARE -!/)
WRITE(6,6) (ZLEVEL(I),I=1,9)
6 FORMAT(9F11.3)

```

C SET REMAINING SPECS NECESSARY FOR CONTOURING SUBROUTINE -  
C (1) CONTOUR PLOTTING AREA AS MEASURED IN INCHES ON PLOT PAPER IS  
C DETERMINED BY SPECS(7) AND SPECS(8)  
C (2) ARRAY VALUES OF PUPIL-FUNCTION PHASE USED IN CONTOUR  
C SUBROUTINE ARE LIMITED BY SPECS(4), SPECS(6), AND NEWLY  
C COMPUTED VALUES OF SPECS(3) AND SPECS(5)  
XCONTR=(2.\*RADIUS/SPECS(3))\*SPECS(7)  
SPECS(7)=XCONTR  
YCONTR=(2.\*RADIUS/SPECS(5))\*SPECS(8)  
SPECS(8)=YCONTR  
C RESET SPECS(3), SPECS(4), SPECS(5), AND SPECS(6)  
SPECS(3)=X(NS1)  
SPECS(4)=X(2)  
SPECS(5)=Y(NS2)  
SPECS(6)=Y(2)  
C SET UP SCRATCH TAPE OR DRUM  
SPECS(30)=12.  
C SET UP XCOLMS  
SPECS(31)=32.  
C SET UP YROWS  
SPECS(32)=32.  
C SET UP NUMBER OF CONTOURS  
SPECS(33)=9.  
LENGTH=10000  
C CALL THE CONTOURING SUBROUTINE  
CALL CONLI(X,Y,DE,ZLEVEL,BUFXYZ,LENGTH,SPECS)

100 RETURN  
END

```

C THIS SUBROUTINE PROVIDES 5 PRINTER PLOTS (FRAMES) PLUS GENERATES
C CODE FOR CAL-COMP PLOTTER
C SUBROUTINE PLTMOD (OTF,DELTXY,NSMAX,WAVEL,FNG,RMSMAX)
C DIMENSION BUFX(500),BUFY(500),BUFXYZ(10000),DL(24),GIVEN(3),
1 PTF(65,65),SF(24),SPECs( 35 ),X( 65 ),Y( 65 ),Y2( 32 ),Y3( 32 ),ZLEVEL(10)
C COMPLEX OTF(65,65)
REAL MTF(65,65)

C COMPUTE CUTOFF SPATIAL FREQUENCY FOR DIFFRACTION-LIMITED CASE
SPECtcf=1.0/(WAVEL*FNG)

C THE FOLLOWING SPECIFICATIONS ARE COMMON TO THE REMAINING 4 PLOTS
C SET UP XDIST AND YDIST ( INCHES )
SPECs( 1 )=2.0
SPECs( 2 )=2.0
C SET UP XLENGTH AND YLENGTH ( INCHES )
SPECs( 7 )=5.50
SPECs( 8 )=5.50
C SET UP PRINTING TOOL
SPECs( 11 )=1.0
C SET UP TAPE NUMBER
SPECs( 12 )=8.0
C SET SPACER
SPECs( 19 )=0.0
SPECs( 20 )=0.0
C SET FONTS
SPECs( 21 )=1.0
C SET UP SCRATCH TAPE OR DRUM
SPECs( 30 )=12.0
C ALTHOUGH SPECs( 24 ), SPECs( 25 ), AND SPECs( 26 ) HAVE THE SAME VALUE
C FOR EACH FRAME, THESE SPECs MUST BE REPEATED PRIOR TO EACH FRAME-
C OTHERWISE THEIR VALUES ARE INCREMENTED SUCCESSIVELY FROM THE
C INITIAL VALUE

C BEGIN COMPUTATIONS FOR FRAME 2 (ISOCOUNTS OF MTF)
C FIND MAXIMUM VALUE OF THE REAL PART OF THE OTF AND RECORD THE
C SUBSCRIPTS
XM1=0
XM2=0
DO 10 K=1,65
DO 10 J=1,65
MTF( J, K )=0
XM1=AMAX1(XM1,REAL(OTF( J, K )))
IF( XM1 .LE. XM2 ) GO TO 10
XM2=XM1
JORD=J
KORD=K
10 CONTINUE

C CALCULATE NORMALIZED MTF
DO 20 K=1,65
DO 20 J=1,65
20 MTF( J, K )=REAL(OTF( J, K ))/REAL(OTF( JORD, KORD ))

C SET UP X AND Y ARRAYS
DO 25 I=1,65

```

```

X(I)=(I-KORD)*DELTXY
25 Y(I)=X(I)

C COMPUTE LEVELS AT WHICH CONTOURS ARE TO BE MADE
Z=0
DO 35 I=1,5
ZLEVEL(I)=Z*.1
35 Z=Z*.2
WRITE(6,36)
36 FORMAT(//,' CONTOUR LEVELS COMPUTED FOR THE MTF ARE -')
WRITE(6,37) (ZLEVEL(I),I=1,5)
37 FORMAT(1X,6F10.3)

CALL NXTRFM(SPECS)
C SET UP GRIDLESS CONTOURING AREA, XDIV=YDIV=1
SPECS(9)=1.
SPECS(10)=1.
C DRAW A BOX AROUND CONTOURING AREA
CALL GDLILI(SPECS)
C SET UP XRIGHT AND XLEFT
GIVEN(1)=SFCTOF
GIVEN(2)=-1.*SFCTOF
GIVEN(3)=10
CALL FABLIX(GIVEN,SPECS)
C SET YTOP AND YBOTTOM
CALL FABLIY(GIVEN,SPECS)
C CONSTRUCT SCALE VALUES AT REGULAR INTERVALS ALONG THE AXES
SPECS(17)=.15
SPECS(18)=.15
SPECS(28)=0.0
SPECS(26)=0.10
CALL NDLIL(SPECS)
SPECS(24)=0.10
CALL NDLIB(SPECS)
C RESET THE NUMBER OF DIVISIONS FOR TICK MARKS
SPECS(9)=2.*SPECS(9)
SPECS(10)=2.*SPECS(10)
CALL AXLILI(SPECS)
SPECS(17)=.2
SPECS(18)=.2
SPECS(25)=0.75
CALL TITLET(28HOF OPTICAL TRANSFER FUNCTION,7HMODULUS,SPECS)
SPECS(17)=.15
SPECS(18)=.15
CALL TITLEB(29HSpatial FREQUENCY (CYCLES/MM),SPECS)
CALL TITLEL(29HSpatial FREQUENCY (CYCLES/MM),SPECS)
C SET UP XCOLMS
SPECS(31)=65.
C SET UP YROWS
SPECS(32)=65.
C SET UP NUMBER OF CONTOURS
SPECS(33)=5.
LENGTH =10000
C CALL THE CONTOURING SUBROUTINE
CALL CONLI(X,Y,MTF,ZLEVEL,BUFXYZ,LENGTH,SPECS)

C BEGIN COMPUTATIONS FOR FRAME 3 ( ISOCOUNTOURS OF PTF )
C CALCULATE PTF RELATIVE TO VALUE AT MAXIMUM MTF

```

```

PHIMIN=0
PHIMAX=0
DO 55 K=1,65
DO 55 J=1,65
PTF(J,K)=0
PTF(J,K)=AIMAG(OTP(J,K))-AIMAG(OTP(JORD,KORD))
PHIMIN=AMIN1(PHIMIN,PTF(J,K))
PHIMAX=AMAX1(PHIMAX,PTF(J,K))
55 CONTINUE

C COMPUTE CONTOUR LEVELS FOR THE PHASE PLOT
XINCRE=(PHIMAX-PHIMIN)*.15
ZLEVEL(1)=PHIMIN+XINCRE
DO 30 I=2,6
ZL=ZLEVEL(I-1)+XINCRE-AIMAG(OTP(JORD,KORD))
IF(ABS(ZL).LE.1.0E-6) GO TO 28
ZLEVEL(I)=ZLEVEL(I-1)+XINCRE
GO TO 30
28 ZLEVEL(I)=ZLEVEL(I-1)*2*XINCRE
30 CONTINUE
WRITE(6,38)
38 FORMAT(//!!! CONTOUR LEVELS COMPUTED FOR THE PTF ARE -/)
WRITE(6,37) (ZLEVEL(I),I=1,6)

CALL NXTFRM(SPECS)
C SET UP GRIDLESS CONTOURING AREA
SPECS(9)=1.
SPECS(10)=1.
CALL GDLILI(SPECS)
CALL FABLIX(GIVEN,SPECS)
CALL FABLIY(GIVEN,SPECS)
C SET UP NUMBER OF CONTOUR LEVELS TO BE PLOTTED
SPECS(33)=6.0
SPECS(17)=.15
SPECS(18)=.15
SPECS(24)=0.1
CALL NDLIB(SPECS)
SPECS(26)=0.1
CALL NDLIL(SPECS)
C RESET THE NUMBER OF DIVISIONS FOR TICK MARKS
SPECS(9)=2.*SPFCS(9)
SPECS(10)=2.*SPECS(10)
CALL AXLILI(SPECS)
SPECS(17)=.2
SPECS(18)=.2
SPECS(25)=0.75
CALL TITLET(28HOF OPTICAL TRANSFER FUNCTION,5HPHASE,SPECS)
SPECS(17)=.15
SPECS(18)=.15
CALL TITLEB(29HSpatial Frequency (CYCLES/MM),SPECS)
CALL TITLEL(29HSpatial Frequency (CYCLES/MM),SPECS)
CALL CONLI(X,Y,PTF,ZLEVEL,BUFXYZ,LENGTH,SPECS)

C BEGIN COMPUTATIONS FOR FRAME 4 (MTF VS. SPATIAL FREQUENCY)
75 JR0W=JORD
KC0L=KORD
NSMAX=NSMAX*2
DO 80 I=1,NSMAX

```

```

Y2(1)=REAL( GTF( JRGW, KORD ))/REAL( GTF( JORD, KORD ))
Y3(1)=REAL( GTF( JORD, KCOL ))/REAL( GTF( JORD, KORD ))
X(1)=DELTXY*(I-1)
JRGW=JRGW+1
80 KCOL=KCOL+1

      CALL NXTRFM( SPECS )
C      DETERMINE LINEAR SCALE FOR X AXIS
      GIVEN(1)=SFCTGF
      GIVEN(2)=0.0
      GIVEN(3)=10
      CALL FABLIX(GIVEN,SPECS)
C      DETERMINE LINEAR SCALE FOR Y AXIS
      GIVEN(1)=Y2(1)
      GIVEN(2)=Y2(NSMAX)
      GIVEN(3)=6
      CALL FABLIY(GIVEN,SPECS)
C      SET UP SPECS ARRAY TO PLOT TWO DIMENSIONAL MTF
      SPECS(13)=NSMAX
      SPECS(14)=1.
      SPECS(15)=1.
      CALL GDLILI(SPECS)
C      SET FONTB AND FONTH
      SPECS(17)=.15
      SPECS(18)=.15
      SPECS(24)=0.1
      CALL NODLIB(SPECS)
      SPECS(26)=0.1
      SPECS(28)=1.
      CALL NODLIL(SPECS)
      CALL TITLEB(29HSPATIAL FREQUENCY (CYCLES/MM),SPECS)
      CALL TITLEL(28HMODULATION TRANSFER FUNCTION,SPECS)
C      PLOT TANGENTIAL MTF
      CALL PFLILI(X,Y2,BUFX,BUFY,SPECS)
      SPECS(17)=0.2
      SPECS(18)=0.2
      SPECS(25)=0.75
      CALL TITLET(32HOF THE OPTICAL TRANSFER FUNCTION,31HTANGENTIAL AND
      1SAGITTAL MODULUS,SPECS)
      SPECS(6)=Y3(NSMAX)
C      PLOT SAGITTAL MTF
      CALL PFLILI(X,Y3,BUFX,BUFY,SPECS)

      IF( RMSMAX.GT. 2.00) GO TO 84
C      BEGIN COMPUTATION FOR OPTIONAL FRAME (EXPANDED PLOT OF MTF VS.
C      SPATIAL FREQUENCY) - THIS FRAME IS PLOTTED FOR HIGHLY ABERRATED
C      TEST LENS
      LIMIT=NSMAX
      DO 800 I=NSMAX,1,-1
      IF(Y2(I).GT. 0.05) GO TO 800
      LIMIT=I
800  CONTINUE
      CALL NXTRFM( SPECS )
C      DETERMINE LINEAR SCALE FOR X AXIS
      GIVEN(1)=X(LIMIT)
      GIVEN(2)=0.0
      GIVEN(3)=10.
      CALL FABLIX(GIVEN,SPECS)

```

```

C DETERMINE LINEAR SCALE FOR Y AXIS
GIVEN(1)=Y2(1)
GIVEN(2)=Y2(NSMAX)
GIVEN(3)=6.
CALL FABLIY(GIVEN,SPECS)
SPECS(13)=LIMIT
C SET UP SPECS ARRAY TO PLOT TWO DIMENSIONAL MTF
SPECS(14)=1.
SPECS(15)=1.
CALL GDLILI(SPECS)
C SET PONTB AND PONTH
SPECS(17)=.15
SPECS(18)=.15
SPECS(24)=0.1
SPECS(28)=0.0
CALL NDLIB(SPECS)
SPECS(26)=0.1
SPECS(28)=1.
CALL NDNLIL(SPECS)
CALL TITLEB(29HSPATIAL FREQUENCY (CYCLES/MM),SPECS)
CALL TITLER(28HMODULATION TRANSFER FUNCTION,SPECS)
C PLOT TANGENTIAL MTF
CALL PFLILI(X,Y2,BUFX,BUFY,SPECS)
SPECS(17)=0.2
SPECS(18)=0.2
SPECS(25)=0.75
CALL TITLET(32HOF THE OPTICAL TRANSFER FUNCTION,31HTANGENTIAL AND
1SAGITTAL MODULUS,SPECS)
SPECS(6)=Y3(NSMAX)
C PLOT SAGITTAL MTF
CALL PFLILI(X,Y3,BUFX,BUFY,SPECS).
84 CONTINUE

C BEGIN COMPUTATIONS FOR FRAME 5 (DIFFRACTION-LIMITED MTF VS.
C SPATIAL FREQUENCY)
C ENTER DIFFRACTION-LIMITED MTF VALUES FOR FRAME 5
C SOURCE - L. LEVI AND R. AUSTING, APP. OPT. 7, 967(1968)
DATA DL(1),DL(2),DL(3),DL(4),DL(5),DL(6),DL(7),DL(8),DL(9),DL(10),
1DL(11),DL(12),DL(13),DL(14),DL(15),DL(16),DL(17),DL(18),DL(19),DL(
220),DL(21),DL(22),DL(23),DL(24)/1.000,.936,.873,.810,.747,.685,.62
34,.564,.505,.447,.391,.337,.285,.235,.188,.144,.104,.068,.037,.027
4,.017,.010,.003,.000/,SF(1),SF(2),SF(3),SF(4),SF(5),SF(6),SF(7),SF
5(8),SF(9),SF(10),SF(11),SF(12),SF(13),SF(14),SF(15),SF(16),SF(17),
6SF(18),SF(19),SF(20),SF(21),SF(22),SF(23),SF(24)/.00,.05,.10,.15,.
720,.25,.30,.35,.40,.45,.50,.55,.60,.65,.70,.75,.80,.85,.90,.92,.94
8,.96,.98,1.00/
C CONVERT NORMALIZED SPATIAL FREQUENCY TO VALUES WITH UNITS OF
C CYCLES/MM
DO 85 I=1,24
85 SF(I)=SF(I)*SFCTOF
WRITE(6,86)SFCTOF
86 FORMAT(//1' CUTOFF FREQUENCY FOR DIFFRACTION-LIMITED PERFORMANCE I
1S 'P8.2,1X'CYCLES/MM')
CALL NXTRNM(SPECS)
C USE SAME VALUES OF GIVEN AND SPECS AS THOSE USED FOR FRAME 4
C EXCEPT WHERE NOTED OTHERWISE

```

```

GIVEN( 1 )=SF( 24 )
GIVEN( 2 )=SF( 1 )
GIVEN( 3 )=10
CALL FABLIX(GIVEN,SPECS)
GIVEN( 1 )=DL( 1 )
GIVEN( 2 )=DL( 24 )
GIVEN( 3 )=6
CALL FABLIY(GIVEN,SPECS)
SPECS( 13 )=24
CALL GDLILI(SPECS)
SPECS( 17 )=.15
SPECS( 18 )=.15
SPECS( 24 )=.1
SPECS( 28 )=0.0
CALL NDLIB(SPECS)
SPECS( 26 )=.1
SPECS( 28 )=1.0
CALL NDLIL(SPECS)
CALL TITLEB( 29HSPATIAL FREQUENCY (CYCLES/MM),SPECS)
CALL TITEL( 28HMODULATION TRANSFER FUNCTION,SPECS)
CALL PFLILI(SF,DL,BUFX,BUFY,SPECS)
SPECS( 17 )=0.2
SPECS( 18 )=0.2
SPECS( 25 )=0.75
CALL TITLET( 31HDIFFRACTION-LIMITED PERFORMANCE,30H OPTICAL TRANSFER FUNCTION FOR,19H MODULUS OF THE,SPECS)

C BEGIN COMPUTATIONS FOR FRAME 6 (PTF VS. SPATIAL FREQUENCY)
C RESET PARAMETERS TO PLOT TWO DIMENSIONAL PHASE
JROW=JORD
KCOL=KORD
PHIMIN=0
PHIMAX=0
DO 90 I=1,NSMAX
Y2( I )=AIMAG( GTF( JROW,KORD ) )-AIMAG( GTF( JORD,KORD ) )
Y3( I )=AIMAG( GTF( JORD,KCOL ) )-AIMAG( GTF( JORD,KORD ) )
JROW=JROW+1
KCOL=KCOL+1
PHIMIN=AMIN1( PHIMIN,Y2( I ),Y3( I ) )
90 PHIMAX=AMAX1( PHIMAX,Y2( I ),Y3( I ) )

CALL NXTRFM( SPECS )
C DETERMINE LINEAR SCALE FOR X AXIS
GIVEN( 1 )=SFCTDF
GIVEN( 2 )=0.0
GIVEN( 3 )=10
CALL FABLIX(GIVEN,SPECS)
C DETERMINE LINEAR SCALE FOR Y AXIS
GIVEN( 1 )=PHIMAX
GIVEN( 2 )=PHIMIN
GIVEN( 3 )=6
CALL FABLIY(GIVEN,SPECS)
SPECS( 13 )=NSMAX
CALL GDLILI(SPECS)
SPECS( 25 )=0.75
CALL TITLET( 32HOF THE OPTICAL TRANSFER FUNCTION,29HTANGENTIAL AND
1SAGITTAL PHASE,SPECS )
SPECS( 17 )=0.15

```

```
SPECS(18)=0.15
SPECS(26)=0.1
CALL NODLIL(SPECS)
SPECS(24)=0.1
SPECS(28)=0.0
CALL NGDLIB(SPECS)
CALL TITLEB(29)SPATIAL FREQUENCY (CYCLES/MM),SPECS)
CALL TITLEL(29)PHASE TRANSFER FUNCTION (RAD),SPECS)
CALL PFLILI(X,Y2,BUFX,BUFY,SPECS)
CALL PFLILI(X,Y3,BUFX,BUFY,SPECS)
```

```
C THIS IS LAST CALL IN GDS PLOTTING
CALL GDSEND(SPECS)
RETURN
END
```

## Sample Printout

THE FOLLOWING PARAMETERS, IN ADDITION TO THE DE AND OFF VALUES, WERE READ IN FROM TAPE OR DRUM GENERATED BY  
PROGRAM FOR DATA REDUCTION OF WSI INTERFERograms -

DELTA =	4.680	DELTXY =	7.399
RADIUS =	57.777	WAVELNGTH =	-6326-03
DEVMIN =	-166	DEVMAX =	126
NS1 =	26	NS2 =	26
F/NURBEN =	8.050		
RMSM1 = LAMBDA/	20.625		

VALUES OF DE(I,K) FOR THE BEST FITTING WAVEFRONT ARE PRINTED BELOW -

TERMS INVOLVING B(1),B(2),B(3),B(4) HAVE BEEN SUBTRACTED FROM DE VALUES

ALSO, THE VALUE OF DE AT THE CENTER OF THE APERTURE HAS BEEN SUBTRACTED FROM THE DE VALUES  
 THESE DE VALUES SHOULD COMPARE EXACTLY WITH THE DE VALUES GENERATED BY THE MAIN PROGRAM FOR REDUCING INTERFERograms AND  
 TRANSFERRED TO THIS PROGRAM BY A TAPE UNIT

	1	2	3	4	5	6	7	8	9	10	11	12	13	14	15	16	17
1	-000	-000	-000	-000	-000	-000	-000	-000	-000	-000	-000	-000	-000	-000	-000	-000	-000
2	-000	-000	-000	-000	-000	-000	-000	-000	-000	-001	-005	-0127	-0147	-0154	-0148	-0125	-0125
3	-000	-000	-000	-000	-000	-000	-000	-000	-000	-006	-0093	-0122	-0144	-0158	-0166	-0164	-0151
4	-000	-000	-000	-000	-000	-000	-000	-000	-000	-001	-0051	-0104	-0123	-0138	-0149	-0155	-0147
5	-000	-000	-000	-000	-000	-000	-000	-000	-000	-008	-0088	-0102	-0114	-0124	-0132	-0136	-0137
6	-000	-000	-000	-000	-000	-000	-000	-000	-000	-007	-0095	-0101	-0108	-0113	-0117	-0118	-0115
7	-000	-000	-000	-000	-000	-000	-000	-000	-000	-0062	-0083	-0085	-0088	-0091	-0095	-0097	-0097
8	-000	-000	-000	-000	-000	-000	-000	-000	-000	-0072	-0083	-0088	-0090	-0094	-0096	-0098	-0098
9	-000	-000	-000	-000	-000	-000	-000	-000	-000	-0075	-0083	-0088	-0092	-0095	-0097	-0098	-0098
10	-000	-000	-000	-000	-000	-000	-000	-000	-000	-0073	-0081	-0086	-0090	-0093	-0096	-0097	-0097
11	-039	-064	-100	-105	-100	-100	-100	-100	-100	-093	-093	-093	-093	-093	-093	-093	-093
12	-062	-105	-111	-111	-100	-100	-100	-100	-100	-096	-096	-096	-096	-096	-096	-096	-096
13	-074	-109	-115	-115	-108	-108	-108	-108	-108	-097	-097	-097	-097	-097	-097	-097	-097
14	-077	-108	-112	-112	-104	-104	-104	-104	-104	-093	-093	-093	-093	-093	-093	-093	-093
15	-074	-105	-105	-105	-100	-100	-100	-100	-100	-089	-089	-089	-089	-089	-089	-089	-089
16	-069	-101	-105	-109	-098	-098	-098	-098	-098	-097	-097	-097	-097	-097	-097	-097	-097
17	-069	-098	-104	-104	-097	-097	-097	-097	-097	-086	-086	-086	-086	-086	-086	-086	-086
18	-060	-106	-106	-106	-100	-100	-100	-100	-100	-089	-089	-089	-089	-089	-089	-089	-089
19	-060	-104	-107	-107	-096	-096	-096	-096	-096	-078	-078	-078	-078	-078	-078	-078	-078
20	-060	-099	-117	-117	-107	-107	-107	-107	-107	-095	-095	-095	-095	-095	-095	-095	-095
21	-000	-000	-121	-131	-123	-110	-110	-110	-110	-084	-084	-084	-084	-084	-084	-084	-084
22	-000	-000	-101	-100	-100	-100	-100	-100	-100	-097	-097	-097	-097	-097	-097	-097	-097



18	-0.028	-0.025	-0.021	-0.018	-0.020	-0.027	-0.040	-0.051	-0.060	0.000	0.000	0.000	0.000	0.000
19	-0.027	-0.022	-0.017	-0.015	-0.018	-0.026	-0.039	-0.045	-0.050	0.000	0.000	0.000	0.000	0.000
20	-0.022	-0.016	-0.011	-0.010	-0.013	-0.022	-0.030	-0.036	-0.040	0.000	0.000	0.000	0.000	0.000
21	-0.015	-0.007	-0.003	-0.002	-0.005	-0.010	-0.016	-0.020	-0.024	0.000	0.000	0.000	0.000	0.000
22	-0.003	.004	-0.009	.012	.012	.017	.017	.020	.020	0.000	0.000	0.000	0.000	0.000
23	.012	.021	.029	.037	.046	.060	.060	.060	.060	0.000	0.000	0.000	0.000	0.000
24	.036	.050	.066	.080	.090	.090	.090	.090	.090	0.000	0.000	0.000	0.000	0.000
25	.079	.106	.106	.090	.080	.060	.050	.040	.030	0.000	0.000	0.000	0.000	0.000
26	.000	.000	.000	.000	.000	.000	.000	.000	.000	0.000	0.000	0.000	0.000	0.000
27	.000	.000	.000	.000	.000	.000	.000	.000	.000	0.000	0.000	0.000	0.000	.000
28	.000	.000	.000	.000	.000	.000	.000	.000	.000	0.000	0.000	0.000	0.000	.000
29	.000	.000	.000	.000	.000	.000	.000	.000	.000	0.000	0.000	0.000	0.000	.000
30	.000	.000	.000	.000	.000	.000	.000	.000	.000	0.000	0.000	0.000	0.000	.000
31	.000	.000	.000	.000	.000	.000	.000	.000	.000	0.000	0.000	0.000	0.000	.000
32	.000	.000	.000	.000	.000	.000	.000	.000	.000	0.000	0.000	0.000	0.000	.000

CONTOUR LEVELS COMPUTED FOR THE PUPIL-FUNCTION PHASE(0E) ARE -  
 CONTOUR LEVELS COMPUTED FOR THE PTF ARE -  
 CONTOUR LEVELS COMPUTED FOR THE MTF ARE -

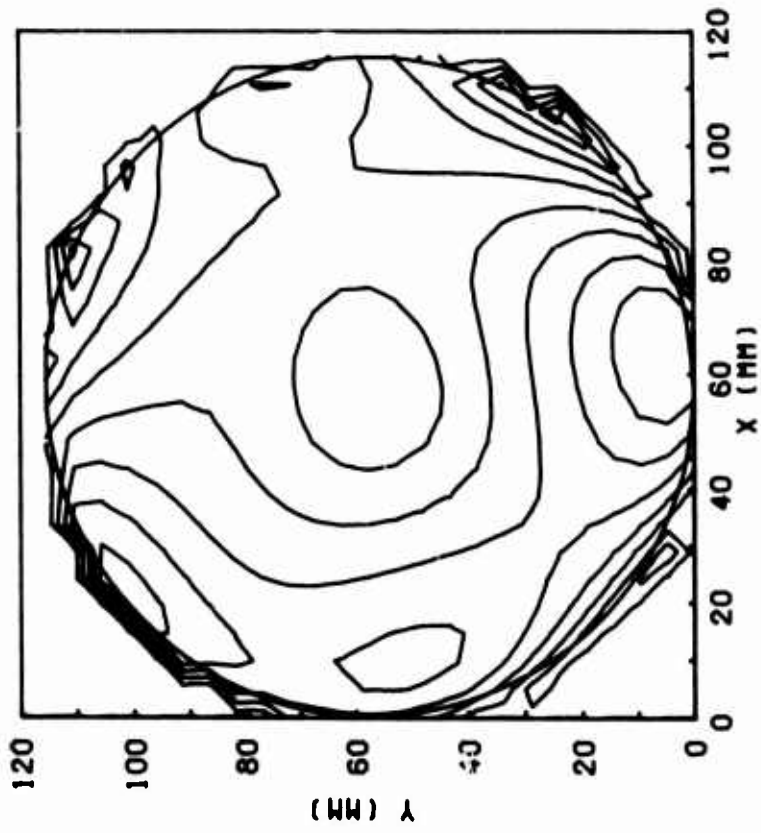
~1.36 ~-1.07 ~-0.98 ~-0.99 ~-0.90 ~-0.92 ~0.018 ~0.039 ~0.097

CONTOUR LEVELS COMPUTED FOR THE MTF ARE -  
 CONTOUR LEVELS COMPUTED FOR THE PTF ARE -

.100 .300 .500 .700 .900

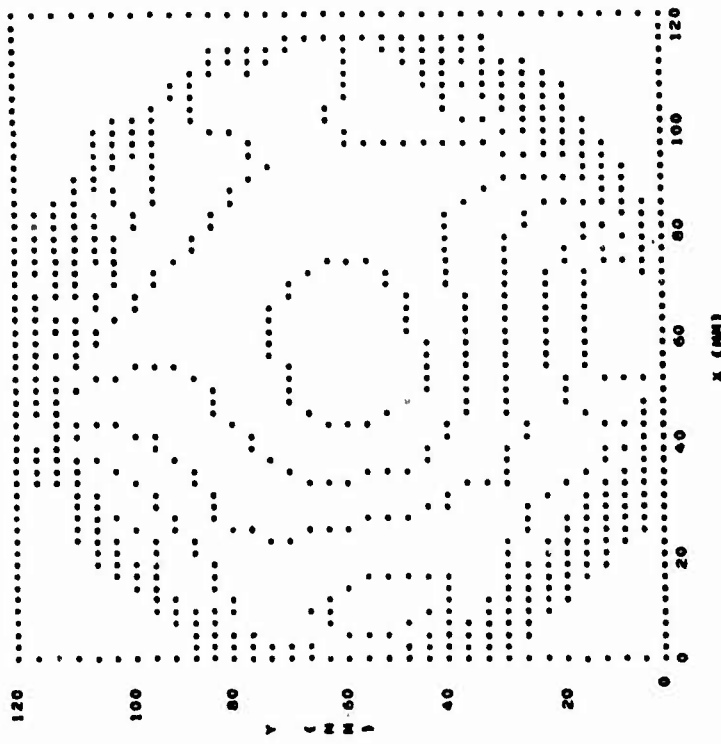
CUTOFF FREQUENCY FOR DIFFRACTION-LIMITED PERFORMANCE IS 102.69 CYCLES/MM

PHASE OF THE PUPIL FUNCTION



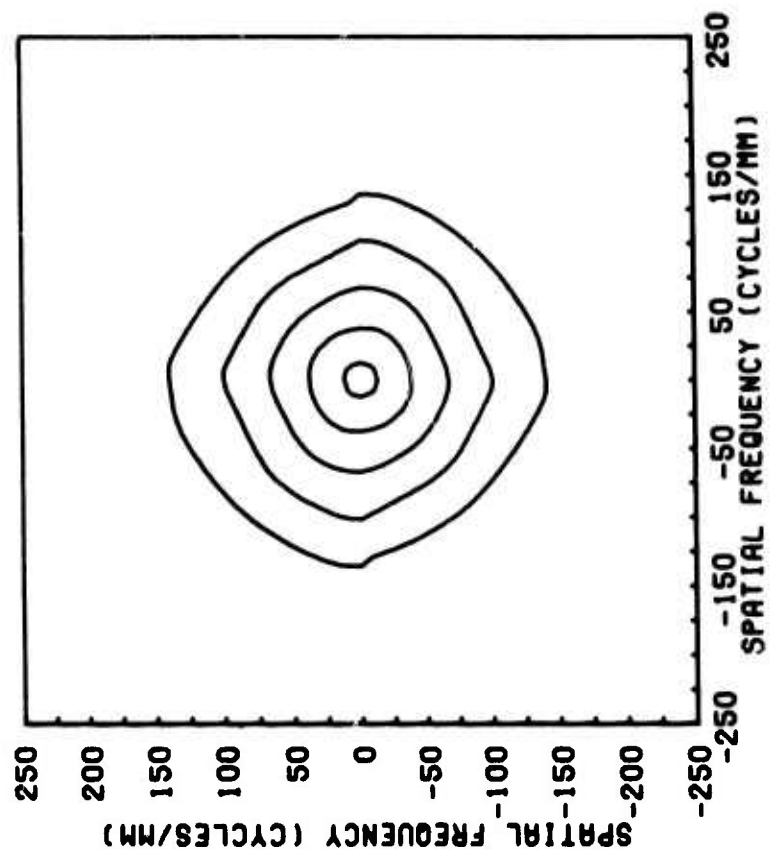
CALCOMP Plot

PHASE OF THE PUPIL FUNCTION



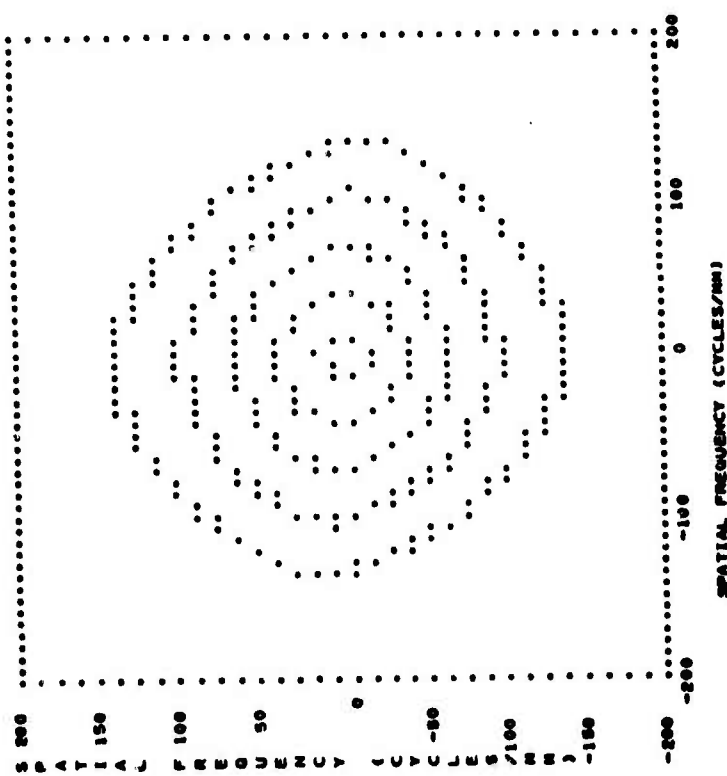
Printer Plot

OF OPTICAL TRANSFER FUNCTION  
MODULUS



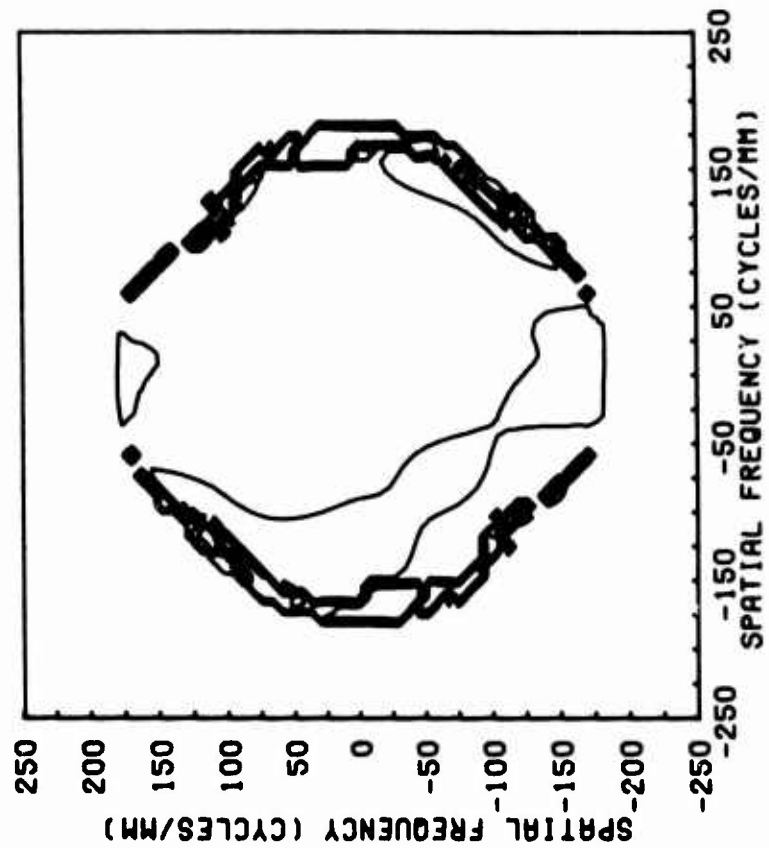
CALCOMP Plot

MODULUS  
OF OPTICAL TRANSFER FUNCTION



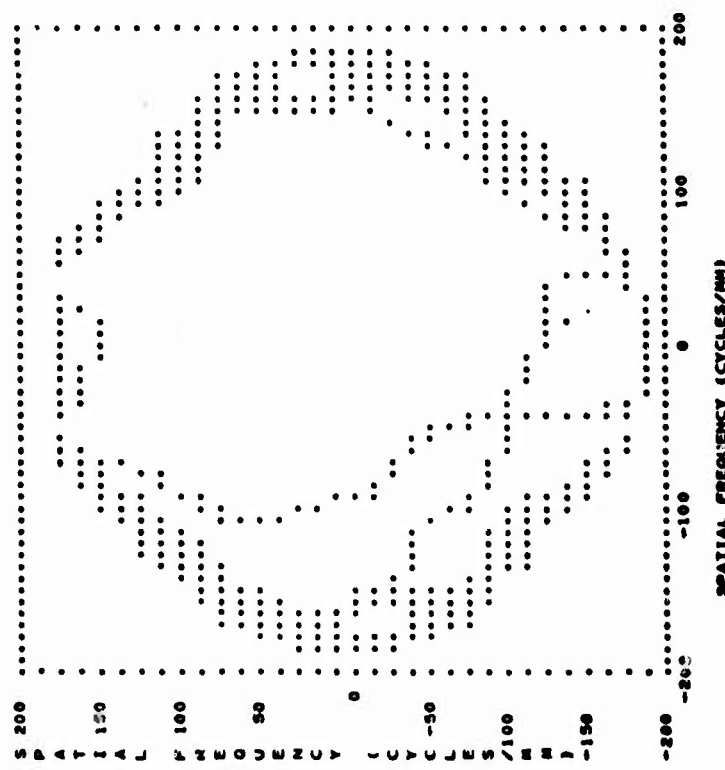
Printer Plot

PHASE  
OF OPTICAL TRANSFER FUNCTION



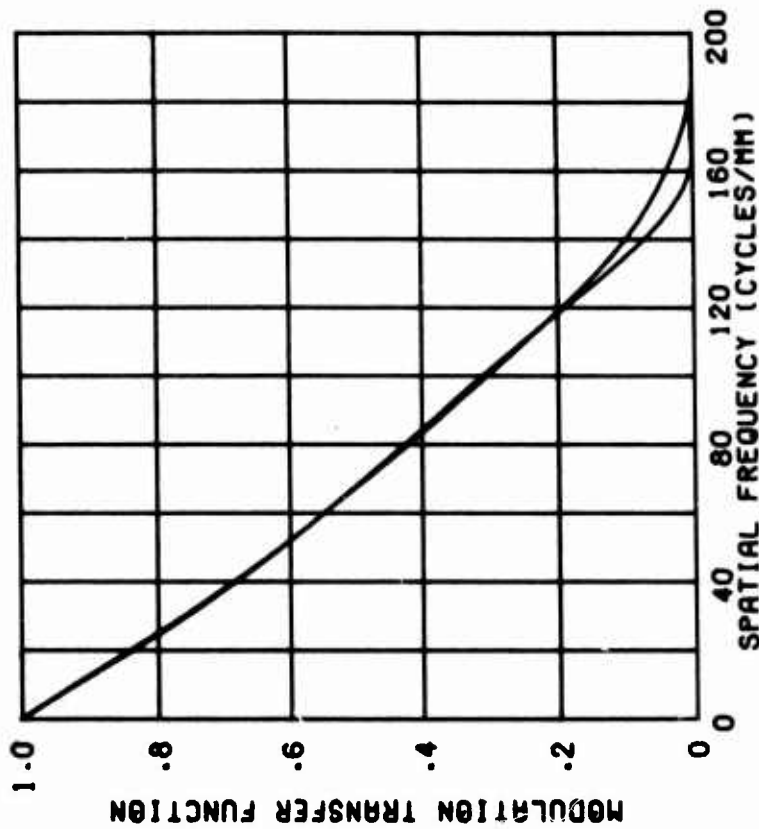
CALCOMP Plot

PHASE  
OF OPTICAL TRANSFER FUNCTION

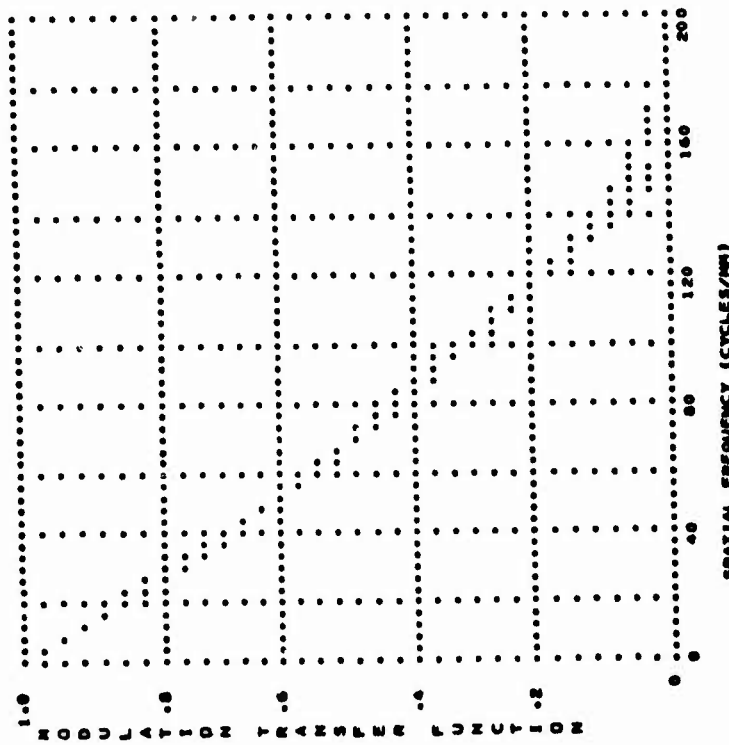


Printer Plot

TANGENTIAL AND SAGITTAL MODULUS  
OF THE OPTICAL TRANSFER FUNCTION

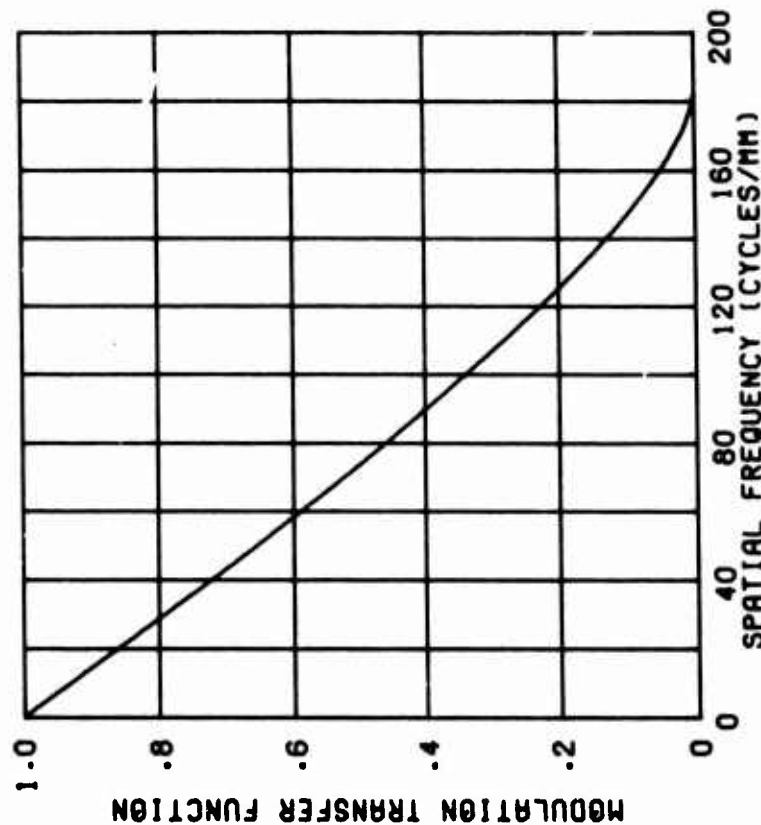


Printer Plot



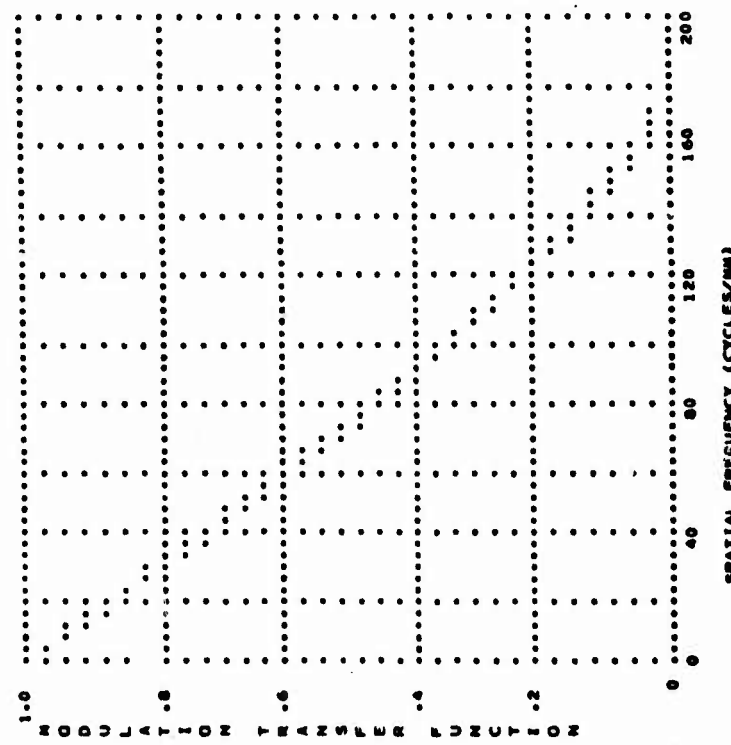
CALCOMP Plot

MODULUS OF THE  
OPTICAL TRANSFER FUNCTION FOR  
DIFFRACTION-LIMITED PERFORMANCE



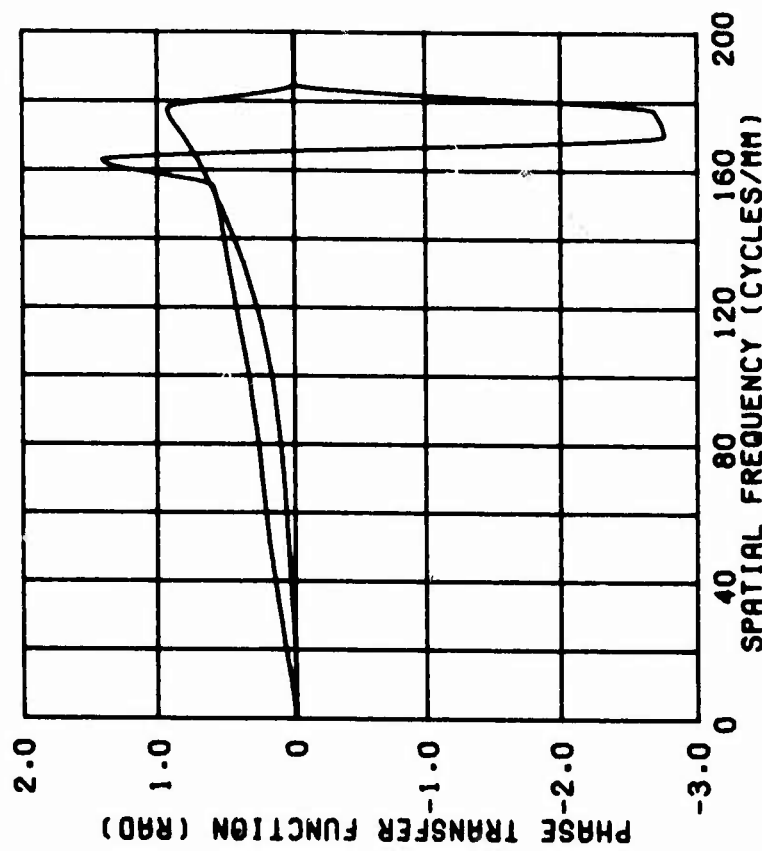
CALCOMP Plot

MODULUS OF THE  
OPTICAL TRANSFER FUNCTION FOR  
DIFFRACTION-LIMITED PERFORMANCE



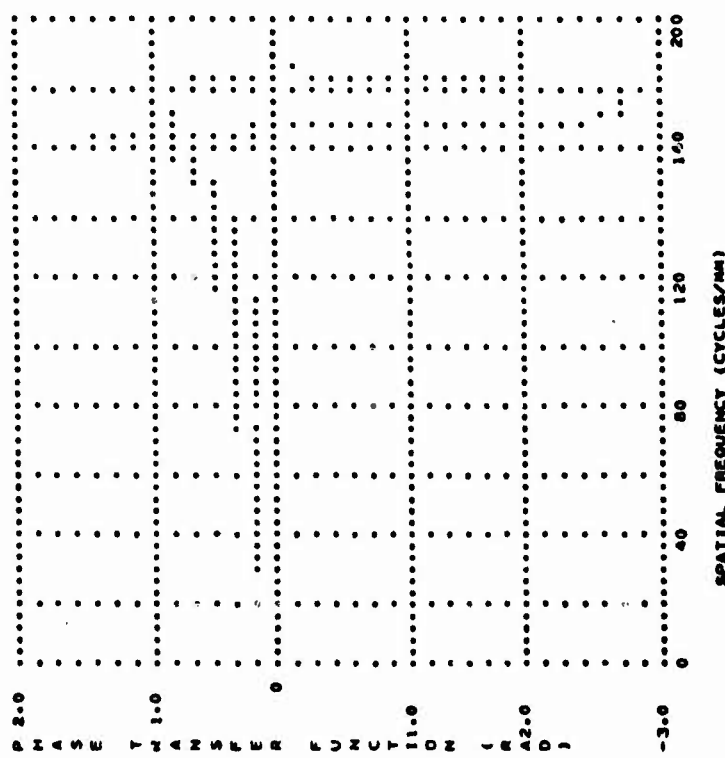
Printer Plot

TANGENTIAL AND SAGITTAL PHASE  
OF THE OPTICAL TRANSFER FUNCTION



CALCOMP Plot

TANGENTIAL AND SAGITTAL PHASE  
OF THE OPTICAL TRANSFER FUNCTION



Printer Plot

## APPENDIX C

### COMPUTER PROGRAM TO OBTAIN WSI FRINGE DATA FROM AUTOMATIC-SCANNER DENSITY DATA

The computer program used to obtain fringe data from photographic-density data generated by automatic scanning of WSI interferograms is presented in part. The present version is neither a complete program nor a final version. This version consists of three subroutines that require the development of a main program by the user to read the density data and to call these subroutines; in addition, the user must already have available certain external subroutines for "unpacking" and reading density data stored on magnetic tape. The additional programming required depends on the particular scanning procedures and data format of the user's automatic scanner. Furthermore, the present version has been used very infrequently and may contain deficiencies which could be uncovered during extended usage.

The three subroutines are used to obtain fringe-peak coordinates, fringe-order numbers, and the coordinates of the test-lens aperture boundary. The basic input data are gray levels corresponding to density values generated on magnetic tape by automatic raster scanning of prepared interferogram transparencies with a digital microdensitometer. Since these subroutines involve the reading of magnetic tapes, alterations in some statements may be required in order to render the programming compatible with the user's computer facilities. Furthermore, these subroutines could be eliminated entirely in a computer-controlled scanning system with internal programming to determine the fringe and lens-aperture parameters required for the WSI data-reduction program.

The following description of each of the three subroutines includes a brief discussion of calculations, definitions of input-output arguments, and a listing of additional external subroutines required. A computational program listing for each subroutine is given. A sample printout resulting from a main computer program that uses the three subroutines to generate WSI fringe data is also presented. The subroutines assume the following: (1) one magnetic-tape file contains all the scans from one interferogram; (2) lens aperture is circular and unobscured; (3) a hole with a diameter roughly equal to a fringe width has been punched at both terminals of every fringe on the interferogram; and (4) one scan does not contain density data from more than one profile on the same fringe, i.e., closed or looped fringes cannot be treated.

### A. Subroutine SEARCH

This subroutine locates the x and y coordinates of the center of the circular holes punched at the fringe terminals on the interferogram. These holes serve to identify the fringe boundaries and the lens aperture. The subroutine first skips a selected number (NBORD) of density values at the beginning of each scan and then tests every other density value in order to locate zero values which may correspond to the punched holes. If the number of adjacent zero density values is less than a selected number (NCT), the location is considered to be noise, such as a film pinhole, and the search for the punched holes continues. Upon locating a punched hole from one scan, the density values from the next scan are tested to determine if part of the hole is also located along that next scan. This procedure continues until the extent of the hole is completely known. The search also continues on the other side of the hole since another hole may lie along these same scans. Eventually, all of the x and y coordinates (BOUNDX and BOUNDY) of the punched holes are determined.

Caution: The holes should be punched to follow closely the circular arcs of the lens aperture. Otherwise, the subroutine may miss one or more of these holes and thus, lead to an error in the ordering of fringes in the subroutine SORT.

If a device error (hardware, parity, or specification of illegal unit) occurs while reading the magnetic tapes in subroutines SEARCH and PEAKS, an error message (ERROR1) is printed and program execution stops. Furthermore, if an end-of-file mark is encountered before the physical end of the file, an error message (ERROR9) is printed and program execution stops. Therefore, the user should ideally use new magnetic tape for recording density values, and the tape transport unit used to transfer data from the scanner to the tape should be in good working condition.

FORTRAN <u>Variable</u>	<u>Source</u>	<u>Definitions</u>
NS	input	Total number of scans; in present version, every other scan is used (this may be altered to fit needs of user)
ND	input	Number of density values in each scan
NBORD	input	Number of density values skipped at beginning of each scan
NBUF	input	Density value; accessed through subroutine SUNPAC
BOUNDX	output	Average x-coordinate of center of punched hole denoting fringe terminus
BOUNDY	output	Average y-coordinate of center of punched hole denoting fringe terminus

<u>FORTRAN Variable</u>	<u>Source</u>	<u>Definition</u>
LL	output	Total number of punched holes

The following list of external subroutines called by SEARCH must be provided by the user; a computational listing of those subroutines as used at the NBS is not available for the present report.

<u>External subroutine and arguments</u>	<u>Function</u>
NTRAN (8, 7, N)	Position tape by skipping N records (scans)
NTRAN (8, 2, N, IWORD, L)	Reads N words from tape into array IWORD
NTRAN (8, 22)	Assures that all previous operations on tape unit are completed before returning control to user; this feature allows programs to be swapped in multiprogrammed computer system
NTRAN (8, 24)	Allows a record (scan) which has incomplete words to be read without stopping on an error; the automatic scanner used in the present report generates an incomplete word at the end of each record
SUNPAC (IWORD, NBUF, NW)	Unpacks density values from every other word on tape; one density value is put into one storage location of array NBUF

## B. Subroutine SORT

This subroutine associates the punched-hole coordinates (BOUNDX and BOUNDY) with the proper fringes and assigns fringe-order numbers. As noted earlier, the punched-hole coordinates obtained from subroutine SEARCH locate the fringe terminals as well as the test-lens aperture boundary. It is assumed in SORT that all punched holes located above the center of the frame (interferogram) denote the top of a fringe and those located below the frame center denote the bottom of a fringe. The fringes are assigned increasing order numbers in the direction of increasing x-coordinate (BOUNDX) of the punched holes.

<u>FORTRAN Variable</u>	<u>Source</u>	<u>Definition</u>
NS	input	Total number of scans from interferogram
BOUNDX	input	See SEARCH
BOUNDY	input	See SEARCH
LL	input	See SEARCH
J2	output	Total number of fringes

No external subroutines are used by SORT.

### C. Subroutine PEAKS

This subroutine determines the fringe-peak locations which are the basic input data for the WSI data-reduction computer program. The subroutine starts by curvefitting two circular arcs to the x and y-coordinates (BOUNDX and BOUNDY) of the punched holes; one arc is fit to the coordinates on the left side of the frame (interferogram), and the other arc is fit to the coordinates on the right side of the frame. The x and y-coordinates of the center and the radius of each of these arcs is determined, and their average values are used as the center coordinates and radius for a circular aperture of the test lens. From this circular aperture, the boundaries (LIMLOW and LIMUP) for fringe scanning are set. Three scans are then read consecutively, and their density values are averaged. An approximate fringe peak (AVG) is located, and this resulting fringe profile is autoconvolved to give a far more accurate location (PKS) of the fringe peak. Next, the fringe order associated with each peak is determined by finding the coordinates of the nearest punched hole. In addition, the fringes are checked by comparing adjacent fringe peaks with the first set of fringe peaks. Finally, cards are punched that contain the fringe-peak coordinates required for the WSI data-reduction program. (See appendix A.) Values of the radius (RAD) of the test-lens aperture and the parameters NF1 or NF2, NSX or NSY, CX or CY, and POSY or POSY are determined in this subroutine; these values are also required for the WSI data-reduction program.

This subroutine also uses a set of subroutines, termed the Graphical Display System, to produce one plot on both a computer line printer and an incremental pen-and-ink device. (See appendix B.) The plots show two circular apertures and the location of their centers; each circle is an extension of the circular arcs discussed above. The location of the fringe peaks (PKS) and the punched holes (BOUNDX and BOUNDY) are also plotted. Examples of both types of plots are included in the sample printout.

Caution: If holes are punched too far outside of the lens aperture, the aperture boundary may be interpreted as fringe peaks by this subroutine, particularly if diffraction fringes are significant. In an effort to reduce this possibility, the subroutine discards apparent fringe peaks which lie outside of the circular aperture determined from curvefitting of the punched-hole coordinates.

## FORTRAN

<u>Variable</u>	<u>Source</u>	<u>Definition</u>
ND	input	See SEARCH
J2	input	See SORT
IDELTA	input	Number of scans contained within shear distance as measured on interferogram, i.e., shear distance/scan raster
PKS	output (printout and punched cards)	x-coordinates (x-sheared interferogram) or y-coordinates (y-sheared interferogram) of fringe peaks
NS	input	See SORT
BOUNDX	input	See SEARCH
BOUNDY	input	See SEARCH
TEST1	input	Identifies test lens and test number or date
TEST2	input	Identifies frame, i.e., x-sheared or y-sheared
IFRAME	input	Identifies frame IFRAME = 1 for x-sheared interferogram IFRAME = 2 for y-sheared interferogram

The following list of external subroutines called by PEAKS must be provided by the user. Some of these subroutines are similiar to those listed previously for SEARCH.

<u>External subroutine and arguments</u>	<u>Function</u>
NTRAN (8, 7, NSKIP)	See SEARCH
UNPACK (IWORD, NBUF1, ND)	Same as SUNPAC in SEARCH except that density values are unpacked from every other word on tape
NTRAN (8, 2, 750, IWORD, L)	See SEARCH

<u>External subroutine and arguments</u>	<u>Function</u>
NTRAN (8, 22)	See SEARCH
NTRAN (8, 24)	See SEARCH
GJR*	Solve simultaneous equations by method of Gauss-Jordan Elimination (See reference 39.)
FABLIX (GIVEN, SPECS)	Determine linear scale for x-ordinate range
FABLIY (GIVEN, SPECS)	Determine linear scale for y-ordinate range
GDLILI (SPECS)	Construct rectangular grid having linear subdivisions of both axes
NODLIB (SPECS)	Construct linear numeric scale below plot
TITLEB*	Construct lines of text below plot
NODLIL (SPECS)	Construct linear numeric scale to left of plot
TITEL*	Construct lines of text to left of plot
TITLET*	Construct lines of text above plot
PSLILI*	Plot data with symbols in linear rectangular system
PFLILI*	Construct a trend curve through set of points in linear rectangular system
GDSEND (SPECS)	Terminate plotting

---

\*The arguments for these subroutines are either lengthy or vary throughout program. Note computation program listing for details.

### Computation Program Listing

```

C THIS SUBROUTINE LOCATES COORDINATES OF BOUNDARY MARKS
C BOUNDARY MARKS ARE HOLES IN THE FILM WHICH REGISTER GRAY LEVELS
C OF ZERO. A COUNT IS MADE OF THE NUMBER OF ADJACENT ZEROS. A
C COUNT OF LESS THAN FIVE IS CONSIDERED NOISE. THE AVERAGE VALUE OF
C THE X AND Y COORDINATES ARE STORED IN BOUNDX AND BOUNDY AS THE
C CENTER OF THE HOLE. THE REMAINING LOOPS IN THE PROGRAM INSURE THAT
C THE ENTIRE FRAME IS SEARCHED.
SUBROUTINE SEARCH(NS,ND,NBORD,NBUF,BOUNDX,BOUNDY,LL)
CALL NTRAN(8,24,22)
DIMENSION BOUNDX(100),BOUNDY(100),IWORD(750),NBUF(3000)
WRITE(6,800)
800 FORMAT(1H1 'THE FOLLOWING VALUES INCLUDE X AND Y COORDINATES OF PUN
1CHED HOLES IN SAME ORDER AS FOUND BY THIS SUBROUTINE -'////)
NW=ND
M=1
NAREA=1
NRET=0
LL=0
LF=0
MLIM=NS
JMIN=1
ND=ND/2
JMAX=ND-NBORD
J=1
10 CALL NTRAN(8,7,1)
CALL NTRAN(8,2,750,IWORD,L,22)
CALL NTRAN(8,22)
IF(L+1)12,14,14
12 IF(L.EQ.-2)GO TO 998
STOP ERROR1
14 M=M+1
CALL SUNPAC(IWORD,NBUF,NW)
15 IF(NBUF(J).LT.1) GO TO 20
16 J=J+1
IF(J.LT.JMAX)GO TO 15
J=JMIN
17 IF(M.LT.MLIM) GO TO 10
IF(M.GE.NS) GO TO 900
WRITE(6,906)NAREA
18 GO TO (900,140,150,150),NAREA
20 IF(J.LT.NBORD) GO TO 16
NCT=1
NSCAN=M
SUMX=J
SUMY=M
JMIN=J
22 J=J+1
IF(NBUF(J).GE.1) GO TO 25
NCT=NCT+1
SUMX=SUMX+J
SUMY=SUMY+M
GO TO 22
25 JMAX=J
26 KSW=0
30 CALL NTRAN(8,7,1)
CALL NTRAN(8,2,750,IWORD,L,22)
CALL NTRAN(8,22)

```

```

      IF(L+1)32,33,33
32  IF(L.EQ.-2)GO TO 998
      STOP ERROR1
33  M=M+1
      J=JMIN
      CALL SUNPAC(IWORD,NBUF,NW)
34  IF(NBUF(J).GE.1) GO TO 35
      IF(J.LE.1) GO TO 35
      J=J-1
      GO TO 34
35  IF(JMIN.LE.J)GO TO 36
      JMIN=J
36  J=J+1
      IF(NBUF(J).GE.1) GO TO 38
      NCT=NCT+1
      SUMX=SUMX+J
      SUMY=SUMY+M
      KSW=1
      GO TO 36
38  IF(J.LT.JMAX)GO TO 36
      JMAX=J
40  IF(KSW.NE.1)GO TO 42
      GO TO 26
42  GO TO (45,50,60,70),NAREA
45  NB = NSCAN - M -1
      JMXR = JMIN-1
      JMRD = NBORD
      MRET=NSCAN
      MXR=M
      MLIM = M
      JMIN = JMAX+1
      JMAX = ND - NBORD
      M = NSCAN -1
      NAREA = 2
      NB=2*NB
      CALL NTRAN(8,7,NB)
      GO TO 100
50  IF (MXR - M) 56,54,54
54  NB=NSCAN-M-1
      NB=2*NB
      CALL NTRAN(8,7,NB)
      JMIN=JMAX+1
      JMAX=ND-NBORD
      M=NSCAN -1
      MLIM=MXR
      NAREA=2
      GO TO 100
56  NB=NSCAN-M-1
      NB=2*NB
      CALL NTRAN(8,7,NB)
      MXR=M
      IF(JMIN .LT. JMXR) JMXR=JMIN-1
      JMIN=JMAX+1
      JMAX=ND-NBORD
      MLIM=M
      M=NSCAN -1
      NAREA=2
      GO TO 100

```

```

60 IF(MLIN - M) 66,64,62
62 NB=NSCAN-M -1
    NB=2*NB
    CALL NTRAN(8,7,NB)
    JMAX=JMIN-1
    JMIN=NBOARD
    M=NSCAN -1
    NAREA=3
    GO TO 100
64 NB=NSCAN-M-1
    NB=2*NB
    CALL NTRAN(8,7,NB)
    JMAX=JMIN-1
    JMIN=NBOARD
    MLIM=M
    M=NSCAN -1
    NAREA=3
    GO TO 100
66 JMXR=JMIN-1
    JMIN=JMAX+1
    JMAX=MD-NBOARD
    NB=MLIM-M
    NB=2*NB
    CALL NTRAN(8,7,NB)
    JMNR=NBOARD
    MRET=NSCAN
    NAREA=2
    MXR=M
    MXZ=MLIM
    MLIM=M
    M=MXZ
    GO TO 100
70 IF (MLIM - M)76,74,72
72 NB=NSCAN-M-1
    NB=2*NB
    CALL NTRAN(8,7,NB)
    JMIN=JMAX+1
    JMAX=ND-NBOARD
    M=NSCAN -1
    NAREA=4
    GO TO 100
74 NB=NSCAN-M -1
    NB=2*NB
    CALL NTRAN(8,7,NB)
    JMIN=JMAX+1
    JMAX=ND-NBOARD
    MLIM=M
    M=NSCAN -1
    NAREA=4
    GO TO 100
76 NB=NSCAN-M -1
    NB=2*NB
    CALL NTRAN(8,7,NB)
    JMNR=NBOARD
    JMZR=JMIN-1
    MRET=MLIM
    MXR=M
    JMIN=JMAX+1

```

```

JMAX=ND-NBORD
MLIM=M
M=NSCAN -1
NAREA=2
100 IF(NCT.LT.10) GO TO 120
110 LL=LL+1
BOUNDX(LL)=SUMX/NCT
BOUNDY(LL)=SUMY/NCT
BOUNDX(LL)=2*BOUNDX(LL)
BOUNDY(LL)=2*BOUNDY(LL)
WRITE(6,907)LL
WRITE(6,903)BOUNDX(LL),BOUNDY(LL)
WRITE(6,906)NAREA
WRITE(6,908)NSCAN
120 J=JMIN
GO TO 17
140 NAREA = 3
JMIN = JMNR
JMAX = JMNR
M = MRET -1
NB = MLIM - MRET +1
NB=2*N
CALL NTRAN (8,7,-NB)
GO TO 10
150 NAREA = 1
J=NBORD
WRITE(6,906) NAREA
JMIN = NBORD
JMAX = ND - NBORD
MLIM = NS
GO TO 10
900 WRITE(6,901)NS,ND
901 FORMAT(//1H 'THIS FRAME USED = '14,' SCANS EACH CONTAINING '14,'  

'DENSITY VALUES'//)
904 FORMAT(1H1 'THE COORDINATES OF THE BOUNDARY MARKS BEFORE ORDERING A  

'RE GIVEN BELOW -'//)
SUMX=0.0
SUMY=0.0
DO 202 J=1,LL
SUMX=SUMX+BOUNDX(J)
SUMY=SUMY+BOUNDY(J)
202 SUMX=SUMX/LL
SUMY=SUMY/LL
SUMR=0.0
DO 204 J=1,LL
SUMR=SUMR+(BOUNDX(J)-SUMX)**2+(BOUNDY(J)-SUMY)**2
204 SUMR=SQR(SUMR/LL)=0.85
DO 216 J=1,LL
RR= SQR((BOUNDX(J)-SUMX)**2+(BOUNDY(J)-SUMY)**2)
IF(RR.LT.SUMR.OR.RR.GT.(1.4*SUMR))GO TO 210
GO TO 216
210 JG=J+1
DO 212 K=JG,LL
BOUNDX(K-1)=BOUNDX(K)
212 BOUNDY(K-1)=BOUNDY(K)
LL=LL-1
WRITE(6,214)

```

```
214 FORMAT(1H0,'POINT DROPPED')
      GO TO 205
216 CONTINUE
      WRITE(6,903)(BOUNDX(J),BOUNDY(J),J=1,LL)
903 FORMAT(1H 'X = 'F8.2,10X'Y = 'F8.2/)
      ND=NW
906 FORMAT(1H 'NAREA = 'I4/) -
907 FORMAT(1H 'LL = 'I4/)
908 FORMAT(1H 'NSCAN = 'I4//++)
      GO TO 999
998 WRITE(6,950)
950 FORMAT(1X,' THIS IS ERROR NINE')
      ND=M
      GO TO 900
999 RETURN
      END
```

C THIS SUBROUTINE ORDERS THE BOUNDARY MARKS THEREBY ASSIGNING ORDER  
 C NUMBERS TO THE FRINGES. IT IS ASSUMED THAT ALL BOUNDARY MARKS ABOVE THE  
 C CENTER OF THE FRAME ARE AT THE BEGINNING OF A FRINGE AND THOSE IN THE  
 C BOTTOM HALF ARE AT THE END OF A FRINGE. BOUNDARY MARKS IN THE TOP  
 C AND BOTTOM RESPECTIVELY ARE ORDERED IN INCREASING VALUES OF X.  
 SUBROUTINE SORT(NS, BOUNDX, BOUNDY, LL, J2)  
 DIMENSION BOUNDX(100), BOUNDY(100)  
 J=0  
 YHALF=0  
 DO 2 K=1,LL  
 2 YHALF=YHALF+BOUNDY(K)  
 YHALF=YHALF/LL  
 3 J=J+1  
 IF( BOUNDX(J+1).LT. BOUNDX(J) ) GO TO 12  
 6 IF( BOUNDY(J+2).LT. YHALF ) GO TO 3  
 GO TO 20  
 12 STORE=BOUNDX(J+1)  
 BOUNDX(J+1)=BOUNDX(J)  
 BOUNDX(J)=STORE  
 STORE=BOUNDY(J+1)  
 BOUNDY(J+1)=BOUNDY(J)  
 BOUNDY(J)=STORE  
 IP(J.LE.1)GO TO 3  
 K=J+1  
 14 IF( BOUNDX(K+1).LT. BOUNDX(K) ) GO TO 15  
 GO TO 6  
 15 STORE=BOUNDX(K+1)  
 BOUNDX(K+1)=BOUNDX(K)  
 BOUNDX(K)=STORE  
 STORE=BOUNDY(K+1)  
 BOUNDY(K+1)=BOUNDY(K)  
 BOUNDY(K)=STORE  
 IF(K.LE.1) GO TO 6  
 K=K+1  
 GO TO 14  
 20 J2=J+2  
 J=J+1  
 23 J=J+1  
 IF( BOUNDX(J+1).LT. BOUNDX(J) ) GO TO 32  
 26 IF( J+1.LT. LL ) GO TO 23  
 GO TO 40  
 32 STORE=BOUNDX(J+1)  
 BOUNDX(J+1)=BOUNDX(J)  
 BOUNDX(J)=STORE  
 STORE=BOUNDY(J+1)  
 BOUNDY(J+1)=BOUNDY(J)  
 BOUNDY(J)=STORE  
 IF( J.LE.J2 ) GO TO 23  
 K=J+1  
 34 IF( BOUNDX(K+1).LT. BOUNDX(K) ) GO TO 35  
 GO TO 26  
 35 STORE=BOUNDX(K+1)  
 BOUNDX(K+1)=BOUNDX(K)  
 BOUNDX(K)=STORE  
 STORE=BOUNDY(K+1)  
 BOUNDY(K+1)=BOUNDY(K)  
 BOUNDY(K)=STORE

```
IF(K.LE.J2)GO TO 26
K=K-1
GO TO 34
40 J2=J2-1
WRITE(6,50)J2
50 FORMAT(1H1 'BOUNDARIES, OR COORDINATES OF PUNCHED HOLES, FOR 'I3,1
1 FRINGES ARE GIVLN BELOW -'//1X'BOUNDX(J)'8X'BOUNDY(J)'41X'BOUNDX(
2J+J2)'4X'BOUNDY(J+J2)')
      WRITE(6,52)(BOUNDX(J),BOUNDY(J),BOUNDX(J+J2),BOUNDY(J+J2),J=1,J2)
52 FORMAT(1H0,F7.2,10X,F7.2,45X,F7.2,10X,F7.2)
RETURN
END
```

```

C THIS SUBROUTINE FINDS AND CHECKS FRINGE PEAKS
C USES AVERAGING OF 9 POINTS TO SMOOTH DATA
C SUBROUTINE PEAKS(ND,J2, IDELT,A,PKS,NS,BOUNDX,BOUNDY,TEST1,TEST2,
21FRAME)
CALL NTRAN(8,24,22)
DIMENSION NBUF1(3000),NBUF2(3000),NBUF3(3000),AVG(3000),PKS(60,60)
DIMENSION BOUNDX(50),BOUNDY(50),AUTG(200),NPK(50),WORD(750)
DIMENSION NCNT(50)
DIMENSION FNC(50),YLY(50)
DIMENSION SPECS(30),GIVEN(3)
DIMENSION XIX1(50),XIX2(50)
DIMENSION XC(2),YC(2),BUFX(500),BUFY(500),X1(122),Y1(122)
DIMENSION AZ(3,4),V(4),JC(4)
DIMENSION TEST1(6),TEST2(2)

C THE FOLLOWING INSTRUCTIONS DIVIDE THE INTERFEROGRAM INTO TWO ARCS
C AND COMPUTE THE CENTERS AND RADII OF EACH
    V(1)=5
    XC1=0.0
    YC1=0.0
    R1=0.0
    XC2=0.0
    YC2=0.0
    R2=0.0
    NZ=0
    NH=0
    IHALF=J2/2
    DO 500 K=1,4
    DO 500 J=1,3
500 AZ(J,K)=0.0
    DO 8 I=1,J2
    J=I
    IF( I.GT.IHALF ) J=I+IHALF
7   IF( BOUNDX(J) .LT. 0.0001) NZ=NZ+1
    IF( BOUNDX(J) .LT. 0.0001) GO TO 8
    AZ(1,1)=AZ(1,1)+BOUNDX(J)
    AZ(1,2)=AZ(1,2)+BOUNDY(J)
    AZ(1,3)=AZ(1,3)+1
    AZ(2,1)=AZ(2,1)+BOUNDX(J)**2
    AZ(2,2)=AZ(2,2)+BOUNDX(J)*BOUNDY(J)
    AZ(2,4)=AZ(2,4)+BOUNDX(J)**3+BOUNDX(J)*BOUNDY(J)**2
    AZ(3,2)=AZ(3,2)+BOUNDY(J)**2
    AZ(3,4)=AZ(3,4)+BOUNDX(J)**2*BOUNDY(J)+BOUNDY(J)**3
8   CONTINUE
    AZ(1,4)=AZ(2,1)+AZ(3,2)
    AZ(2,3)=AZ(1,1)
    AZ(3,1)=AZ(2,2)
    AZ(3,3)=AZ(1,2)
    CALL GJR(AZ,4,3,3,4,$998,JC,V)
    XC1=AZ(1,4)/2.0
    YC1=AZ(2,4)/2.0
    P1=SQRT( AZ(3,4)*XC1**2+YC1**2 )
    XC1MM=XC1*.05
    YC1MM=YC1*.05
    R1MM=R1*.05
    WRITE(6,36) XC1,YC1,R1,XC1MM,YC1MM,R1MM
36 FORMAT(1HI 'COORDINATES FOR LEFT ARC ARE -1//1X' XCENTER = 'F10.4,

```

```

110X'YCENTER = 'F10.4,10X'RADIUS = 'F10.4//1X' XCENTER = 'F10.4,
2MM'7X'YCENTER = 'F10.4,' MM'7X'RADIUS = 'F10.4,' MM'//)
NH=J2 = IHALF
NZ=0
DO 510 K=1,4
DO 510 J=1,3
510 AZ(J,K)=0.0
V(1)=5
DO 13 I=1,J2
J=I+IHALF
IF(I.GT.IHALF) J=I+J2
11 IF(BOUNDX(J).LT.0.0001) NZ=NZ + 1
IF(BOUNDX(J).LT.0.0001) GO TO 13
AZ(1,1)=AZ(1,1)+BOUNDX(J)
AZ(1,2)=AZ(1,2)+BOUNDY(J)
AZ(1,3)=AZ(1,3)+1
AZ(2,1)=AZ(2,1)+BOUNDX(J)**2
AZ(2,2)=AZ(2,2)+BOUNDX(J)*BOUNDY(J)
AZ(2,4)=AZ(2,4)+BOUNDX(J)**3+BOUNDX(J)*BOUNDY(J)**2
AZ(3,2)=AZ(3,2)+BOUNDY(J)**2
AZ(3,4)=AZ(3,4)+BOUNDX(J)**2+BOUNDY(J)+BOUNDY(J)**3
13 CONTINUE
AZ(1,4)=AZ(2,1)+AZ(3,2)
AZ(2,3)=AZ(1,1)
AZ(3,1)=AZ(2,2)
AZ(3,3)=AZ(1,2)
CALL GJR(AZ,4,3,3,4,SS98,JC,V)
XC2=AZ(1,4)/2.0
YC2=AZ(2,4)/2.0
R2=SQRT(AZ(3,4)*XC2**2+YC2**2)
XC2NM=XC2.
YC2NM=YC2*.05
R2MM=R2*.05
WRITE(6,37) XC2, YC2, R2, XC2NM, YC2NM, R2MM
37 FORMAT(1H0 'COORDINATES FOR RIGHT ARC ARE -'//1X' XCENTER = 'F10.4
1,10X'YCENTER = 'F10.4,10X'RADIUS = 'F10.4//1X' XCENTER = 'F10.4,
2 MM'7X'YCENTER = 'F10.4,' MM'7X'RADIUS = 'F10.4,' MM'//)
SHEAR=ABS(XC1MM-XC2MM)
DISPLT=ABS(YC1MM-YC2MM)
WRITE(6,38) SHEAR, DISPLT
38 FORMAT(//1H 'SHEAR = 'F10.4,5X'THIS VALUE SHOULD BE EQUAL OR CLOSE
1SE TO SHEAR VALUE AS MEASURED ON INTERFEROGRAM'//1H 'DISPLT = 'F10
2.4,5X'THIS VALUE SHOULD EQUAL OR BE CLOSE TO ZERO'//)
SUMX1=XC1MM + R1MM
SUMX2=XC2MM + R2MM
SUMY1=YC1MM + R1MM
SUMY2=YC2MM + R2MM
AMAXX=AMAX1(SUMX1,SUMX2)
AMAXY=AMAX1(SUMY1,SUMY2)

DM 300 J=1,J2
BOUNDX(J)=0.05*BOUNDX(J)
BOUNDY(J)=0.05*BOUNDY(J)
BOUNDX(J+J2)=0.05*BOUNDX(J+J2)
BOUNDY(J+J2)=0.05*BOUNDY(J+J2)
300 CONTINUE
WRITE(6,320) J2
320 FORMAT(1H1 'BOUNDARIES, OR COORDINATES OF PUNCHED HOLES, IN MM FOR

```

```

1'i3.' FRINGES ARE GIVEN BELOW -'//1X'BOUNDX(J)'8X'BOUNDY(J)'41X'B0
2UNDX(J+J2)'4X'BOUNDY(J+J2)'''
      WRITE(6,321)(BOUNDX(J),BOUNDY(J),BOUNDX(J+J2),BOUNDY(J+J2),J=1,J2)
321 FORMAT(1H0,F7.2,10X,F7.2,45X,F7.2,10X,F7.2)

      GIVEN(1)=AMAXX
      GIVEN(2)=0.0
      GIVEN(3)=20.0
      CALL FABLIX(GIVEN,SPECS)
      GIVEN(1)=AMAXY
      GIVEN(2)=0.0
      GIVEN(3)=20.0
      CALL FABLIX(GIVEN,SPECS)
      SPECS(1)=0.75
      SPECS(2)=0.5
      SPECS(8)=9.00
      SPECS(7)=SPECS(3)/(SPECS(5)/SPECS(8))
      SPECS(11)=1.0
      SPECS(12)=10.0
      CALL GDLILI(SPECS)
      SPECS(17)=0.10
      SPECS(18)=0.10
      SPECS(19)=0.0
      SPECS(21)=1.0
      SPECS(24)=0.1
      SPECS(28)=0.0
      CALL NDLIB(SPECS)
      SPECS(24)=0.25
      CALL TITLEB(6HX(MM),SPECS)
      SPECS(26)=0.1
      CALL NDLIL(SPECS)
      SPECS(26)=0.25
      CALL TITLET(6HY(MM),SPECS)
      SPECS(25)=0.2
      IF(IFRAME.EQ.2) GO TO 325
      CALL TITLET(7HY SHEAR,SPECS)
      GO TO 328
325 CALL TITLET(7HY SHEAR,SPECS)
328 CONTINUE
      SPECS(25)=0.6
      SPECS(17)=0.20
      SPECS(18)=0.20
      CALL TITLET(53HMAP OF WSI INTERFEROGRAM SCANNED BY AUTOMATIC SCANN
1ER,SPECS)
      SPECS(13)=2.*J2
      SPECS(14)=1.0
      SPECS(15)=1.0
      SPECS(16)=1.0
      SPECS(17)=0.10
      SPECS(18)=0.10
      CALL PSLILI(BOUNDX,BOUNDY,SPECS)

      DO 330 J=1,J2
      BOUNDX(J)=BOUNDX(J)/0.05
      BOUNDY(J)=BOUNDY(J)/0.05
      BOUNDX(J+J2)=BOUNDX(J+J2)/0.05
330 BOUNDY(J+J2)=BOUNDY(J+J2)/0.05

```

C PLOT CENTERS OF LEFT AND RIGHT ARCS WHICH HAVE BEEN FIT TO PUNCHED  
 C HOLES AND PLOT CIRCLES ABOUT EACH CENTER  
 XC( 1 )=XC1MM  
 YC( 1 )=YC1MM  
 XC( 2 )=XC2MM  
 YC( 2 )=YC2MM  
 SPECSS( 13 )=2.0  
 SPECSS( 16 )=14.  
 CALL PSLILI(XC,YC,SPECSS)  
 DY=(2.\*R1MM/60.0)-0.001  
 K=122  
 D=YC1MM-R1MM  
 DO 400 I=1,61  
 Y1(I)=D  
 Y1(K)=Y1(I)  
 ARG= R1MM\*\*2 + 2.\*D\*YC1MM - YC1MM\*\*2 - D\*\*2  
 ARG1=ABS(ARG)  
 X1(I)=XC1MM + SORT(ARG1)  
 X1(K)=XC1MM - SORT(ARG1)  
 D=D\*DY  
 400 K=K-1  
 SPECSS( 13 )=122  
 CALL PFLILI(X1,Y1,BUFX,BUFY,SPECSS)  
 DY=(2.\*R2MM/60.0)-0.001  
 K=122  
 D=YC2MM-R2MM  
 DO 401 I=1,61  
 Y1(I)=D  
 Y1(K)=Y1(I)  
 ARG= R2MM\*\*2 + 2.\*D\*YC2MM - YC2MM\*\*2 - D\*\*2  
 ARG1=ABS(ARG)  
 X1(I)=XC2MM + SORT(ARG1)  
 X1(K)=XC2MM - SORT(ARG1)  
 D=D\*DY  
 401 K=K-1  
 SPECSS( 13 )=122  
 CALL PFLILI(X1,Y1,BUFX,BUFY,SPECSS)  
 C COMPUTE STANDARD DEVIATION OF FIT RADIALLY  
 NZ=0  
 IHALF=J2/2  
 SS=0.0  
 DO 77 I=1,IHALF  
 J=I  
 6 IF( BOUNDX(J) .LT. 0.0001) NZ=NZ + 1  
 IF( BOUNDX(J) .LT. 0.0001) GO TO 77  
 CR=( BOUNDX(J) - XC1)\*\*2 + ( BOUNDY(J) - YC1)\*\*2  
 CR=SQRT(CR)  
 H3=(CR - R1)\*\*2  
 SS=SS + H3  
 IF(J .GT. 1) GO TO 77  
 J=I + J2  
 GO TO 6  
 77 CONTINUE  
 IHALF=IHALF + 1  
 DO 9 I=IHALF,J2  
 J=I  
 4 IF( BOUNDX(J) .LT. 0.0001) NZ=NZ + 1

```

1F( BOUNDX(J) .LT. 0.0001 ) GO TO 9
CR=( BOUNDX(J) - XC2)**2 + (BOUNDY(J) - YC1)**2
CR=SORT( CR )
R3=(CR - R2)**2
SS=SS+ R3
1F( J .GT. I ) GO TO 9
J=I + J2
GO TO 4
9 CONTINUE
SS=SS/(2*J2 - NZ)
SSMM = SS*0.05
WRITE(6,2) SS,SSMM
2 FORMAT(////////1X'THE STANDARD DEVIATION OF FITTING ALL THE PUNCHED
1HOLE COORDINATES TO TWO ARCS IS 'F8.3,' OR 'F8.3,' MM'//)

IRAD=(R1 + R2)/2.0
IDIFF=R1 + R2
IK=(YC1 + YC2)/2.0
IHALF=J2/2
K=IDIFF/IDELTA
NSKIP=(IDIFF-K*IDELTA)/2
IDELT4=IDELTA/4
IF(NSKIP .LT. IDELT4) NSKIP=NSKIP + IDELT4
LINUP=IK+IRAD-NSKIP
LIMLOW=IK-IRAD-NSKIP
DO 5 J=1,60
DO 5 K=1,60
5 PKS(J,K)=0
WRITE(6,71)
71 FORMAT(1H1)
C NEXT SMOOTH DATA BY AVERAGING
NSKIP=LIMLOW-1
CALL NTRAN(8,7,NSKIP)
NSKIP=IDELTA-3
NSS=0
DO 200 LY=LIMLOW,LINUP, IDELT4
NSS=NSS+1
IX1=XC1-SQRT((0.985*R1)**2-(LY-IK)**2)
IX2=XC2-SQRT((0.985*R2)**2-(LY-IK)**2)
WRITE(6,811) NSS
811 FORMAT(////////1X'SCAN NO. 'I2)
WRITE(6,81) LY,IX1,IX2
81 FORMAT(//1X'Y = 'I5.8X'X1 = 'I5.8X'X2 = 'I5)
XIX1(NSS)=0.05*IX1
XIX2(NSS)=0.05*IX2
YLY(NSS)=0.05*LY
WRITE(6,82)YLY(NSS),XIX1(NSS),XIX2(NSS)
82 FORMAT(/1X'Y = 'F7.2,' MM'3X'X1 = 'F7.2,' MM'3X'X2 = 'F7.2,' MM')
WRITE(6,73)
73 FORMAT(///1X'PEAK', ' KO', ' CENTER', ' CENTER(MM)')
10 CALL NTRAN(8,2,750,IWORD,L)
CALL NTRAN(8,22)
IF(L+1)12,14,14
12 IF(L.EQ.-2)GO TO 968
STOP ERR0R1
14 M=M+1
CALL UNPACK(IWORD,NBUFI,ND)
20 CALL NTRAN(8,2,750,IWORD,L,22)

```

```

CALL NTRAN(8,22)
IF(L=1)22,24,24
22 IF(L.EQ.-2) GO TO 998
STOP ERROR1
24 M=M+1
CALL UNPACK(IWORD,NBUF2,ND)
30 CALL NTRAN(8,2,750,IWORD,L,22)-
CALL NTRAN(8,22)
IF(L=1)32,34,34
32 IF(L.EQ.-2)GO TO 998
STOP ERROR1
34 M=M+1
CALL UNPACK(IWORD,NBUF3,ND)
JFRWD=0
KP=0
NCOUNT=0
JMAX=0
DO 50 J=IX1,IX2
AVG(J)=(NBUF1(J-1)*NBUF1(J)*NBUF1(J+1)*NBUF2(J-1)*NBUF2(J)*NBUF2(J
2+1)*NBUF3(J-1)*NBUF3(J)*NBUF3(J+1))/9
IF(J .LT. JFRWD) GO TO 50
IF(JMAX .NE. 0) GO TO 42
IF(AVG(J) .LT. AVG(J-1)) JMAX=J-1
GO TO 50
42 IF(AVG(J) .LT. AVG(J-1)) NCOUNT=NCOUNT+1
IF(NCOUNT .EQ. 5) GO TO 43
IF(AVG(J) .GT. AVG(J-1)) GO TO 44
GO TO 50
43 KP=KP+1
NPK(KP)=JMAX
JFRWD=JMAX+IDELTA/2
44 NCOUNT=0
JMAX=0
50 CONTINUE
C DETERMINE POSITION OF PEAKS
DO 80 I=1,KP
JMIN=NPK(I)-(IDELTA/2)
JMAX=NPK(I)+(IDELTA/2)
IF(I .EQ. KP .AND. IX2 .LT. JMAX) JMAX=IX2
IF(I .EQ. 1 .AND. IX1 .GT. JMIN) JMIN =IX1
LIM=2*(JMAX-JMIN)+1
AMXX=0
KO=0
DO 75 I1=1,LIM
K=I1-(JMAX-JMIN+1)
IF(K .GT. 0) GO TO 60
JL=JMIN
JU=JMAX+K
GO TO 65
60 JL=JMIN+K
JU=JMAX
65 A=0
DO 72 I2=JL,JU
72 A=A+AVG(I2)*AVG(JU-I2+JL)
AUTG(I1)=A
IF(AUTG(I1) .GE. AMXX) KO=I1
75 AMXX=AMAX(AUTG(I1),AMXX)
K=KO-(JMAX-JMIN+1)

```

```

NCNT( I )=( JMAX+JMIN)/2 *K
FNC( I )=0.05*NCNT( I )
WRITE( 6,85 ) NPK( I ),K,NCNT( I ),FNC( I )
85 FORMAT( 1X,3( I5,2X ),2(F10.2) )
YLY( I )=YLY( NSS )
80 CONTINUE

SPECs( 13 )=1.0*K
SPECs( 16 )=3.0
SPECs( 17 )=0.1
SPECs( 18 )=0.1
CALL PSLILI( FNC,YLY,SPECs )

CALL NTRAN( 8,7,NSkip )
C THE FOLLOWING INSTRUCTION DETERMINE THE FRINGE ORDER ASSOCIATED
C WITH EACH PEAK
NB=J2+1
DO 150 IJ=1,KP
DO 100 JY=2,NB
DIFF1=ABS( BOUNDx( JY-1 )-NCNT( J ) )
IF( NSS .EQ. 1 ) GO TO 87
IF( PKS( JY,NSS-1 ) .NE. 0 ) DIFF1=ABS( PKS( JY,NSS-1 )-NCNT( IJ ) )
87 CONTINUE
IF( DIFF1 .NE. ABS( PKS( JY,NSS-1 )-NCNT( IJ ) ) .AND. DIFF1 .GT. IDELTa/
12 ) GO TO 100
IF( DIFF1 .GT. ( IDELTa/2 ) ) GO TO 100
IF( PKS( JY,NSS ) .EO. 0 ) GO TO 90
IF( NSS .EQ. 1 ) DIFF2=ABS( BOUNDx( JY-1 )-PKS( JY,NSS ) )
IF( NSS .GT. 1 ) DIFF2=ABS( PKS( JY,NSS-1 )-PKS( JY,NSS ) )
DIFF3=ABS( DIFF2-DIFF1 )
IF( DIFF1 .LT. DIFF3 ) GO TO 90
IF( DIFF2 .LT. DIFF3 ) GO TO 100
PKS( JY,NSS )=( PKS( JY,NSS ) + NCNT( IJ ) )/2.0
GO TO 100
90 PKS( JY,NSS )=NCNT( IJ )
IF( PKS( JY-1,NSS ) .NE. PKS( JY,NSS ) ) GO TO 100
IF( NSS .EO. 1 .OR. PKS( JY-1,NSS-1 ) .EQ. 0 ) GO TO 98
DIFF2=ABS( PKS( JY-1,NSS-1 ) -NCNT( IJ ) )
GO TO 99
98 DIFF2=ABS( BOUNDx( JY-2 ) -NCNT( IJ ) )
99 CONTINUE
IF( DIFF1 .LT. DIFF2 ) PKS( JY-1,NSS )=0
IF( DIFF1 .GT. DIFF2 ) PKS( JY,NSS )=0
100 CONTINUE
150 CONTINUE
200 CONTINUE
DO 170 I=1,NSS
DO 168 J=2,NB
168 PKS( J,I )=PKS( J,I )*.05
170 CONTINUE
WRITE( 6,71 )
CX=( XC1 - IRAD )*.05
POSX=( LIMLOW-( IK-IRAD ))*.05
RAD=IRAD*.05
IF( IPFRAME .EQ. 2 ) GO TO 225
WRITE( 6,212 ) J2,NSS,CX,POSX,RAD
212 FORMAT( 1H1 J2 ( NF1 ) = 'I3//I' NSS ( NSX ) = 'I3//I' CX = 'F8.3//I' POSX
1 = 'F8.3//I' RADIUS = 'F8.3//////////')

```

```

00 TO 226
225 WRITE(6,224)J2,NSS,CX,P0SX,RAD
224 FORMAT(1H1J2 (NP2) - 'I3// NSS (NSY) = 'I3// CY = 'F8.3// P0SY
1 = 'F8.3// RADIUS = 'F8.3//////////)
226 WRITE(6,213)
213 FORMAT(1H 'FRINGE-PEAK POSITIONS PKS(J,K) RESULTING FROM AUTOMATIC
1 SCANNING ARE PRINTED BELOW -'// J = FRINGE NUMBER 5X1K = SCAN NU
2MBER'//)
    WRITE(6,214)
214 FORMAT(1H 3X1J13X117X1217X1317X1417X1517X1617X1717X1817X1916X101
16X1116X1216X1316X1416X1516X161// K1)
    DD 215 K=1,29
215 WRITE(6,216)K,(PKS(J,K),J=1,16)
216 FORMAT(1H I2,1X16F8.3)
    WRITE(6,217)
217 FORMAT(//1H 3X1J12X1716X1816X1916X12016X12116X12216X12316X12416
1X12516X12616X12716X12816X1291// K1)
    DD 218 K=1,29
218 WRITE(6,216)K,(PKS(J,K),J=17,29)
    WRITE(1,209)((PKS(J,K),J=1,8),K=1,NSS)
    WRITE(1,209)((PKS(J,K),J=9,16),K=1,NSS)
    WRITE(1,209)((PKS(J,K),J=17,24),K=1,NSS)
    WRITE(1,209)((PKS(J,K),J=25,30),K=1,NSS)
220 FORMAT(7X,7F7.2)
209 FORMAT(8F7.2)
205 FORMAT(16F7.2)
203 FORMAT(2I10,F10.2)
210 FORMAT(2F10.2)
    CALL GDSEND(SPECS)
    RETURN
998 STOP ERROR9
END

```

Sample Printout

THE FOLLOWING DATA WERE GENERATED FROM AUTOMATIC SCANNING OF  
V-SHEARED INTERFACES OF  
P/8.7 COLLIMATOR A

THE FOLLOWING QUANTITIES ARE INPUT VALUES -

NS = 2100      TOTAL NUMBER OF SCANS - THIS VALUE MAY BE SMALLER THAN NUMBER OF SCANS ON TAPE,  
                BUT SHOULD BE LARGE ENOUGH TO INCLUDE ALL PUNCHED HOLES AND PRIMES

IDELTA = 74      NUMBER OF SCANS CONTAINED WITHIN SHEAR DISTANCE AS MEASURED ON INTERFACORAN

NBORD = 20      NUMBER OF DENSITY VALUES SKIPPED AT BEGINNING OF EACH SCAN

THE FOLLOWING VALUES INCLUDE X AND Y COORDINATES OF PUNCHED HOLES IN SAME ORDER AS FOUND BY THIS SUBROUTINE -

LL = 1  
X = 1034.48 Y = 23.50  
NAREA = 2  
NSCAN = 6

LL = 2  
X = 1108.66 Y = 27.71  
NAREA = 2  
NSCAN = 6

LL = 3  
X = 1164.68 Y = 44.19  
NAREA = 2  
NSCAN = 16

LL = 4  
X = 1262.06 Y = 59.95  
NAREA = 2  
NSCAN = 24

NAREA = 2  
LL = 5  
X = 955.63 Y = 30.90  
NAREA = 3  
NSCAN = 9

LL = 6  
X = 877.83 Y = 44.67  
NAREA = 3  
NSCAN = 16

LL = 7  
X = 802.32 Y = 66.32  
NAREA = 2  
NSCAN = 27

LL = 8  
X = 1345.67 Y = 89.00  
NAREA = 2  
NSCAN = 38

NAREA = 2  
LL = 9  
X = 720.43 Y = 99.83  
NAREA = 2  
NSCAN = 44

LL = 10  
X = 1425.24 Y = 124.76  
NAREA = 2  
NSCAN = 56

LL = 11  
X = 642.61 Y = 137.32  
NAREA = 2  
NSCAN = 63

LL = 12  
X = 1499.06 Y = 163.01  
NAREA = 2  
NSCAN = 75

NAREA = 2  
LL = 13  
X = 565.67 Y = 188.34  
NAREA = 2  
NSCAN = 86

NAREA = 2  
LL = 14  
X = 1573.37 Y = 222.14  
NAREA = 2  
NSCAN = 105

NAREA = 2  
LL = 15  
X = 490.79 Y = 247.68

NAREA -	2
NSCAN -	118
NAREA -	2
NAREA -	3
NAREA -	1
LL -	16
X -	1653.04
Y -	296.69
NAREA -	2
NSCAN -	142

NAREA -	2
LL -	17
X -	411.14
Y -	315.91
NAREA -	2
NSCAN -	152

NAREA -	2
NAREA -	3
NAREA -	1
LL -	16
X -	1726.31
Y -	306.13
NAREA -	2
NSCAN -	167
NAREA -	2
LL -	19

X = 339.42 Y = 390.56  
NAREA = 2  
NSCAN = 189

NAREA = 2  
NAREA = 3  
NAREA = 1  
LL = 20  
X = 1610.92 Y = 510.98  
NAREA = 2  
NSCAN = 249

NAREA = 2  
LL = 21  
X = 260.43 Y = 510.91  
NAREA = 2  
NSCAN = 254

NAREA = 2  
NAREA = 3  
NAREA = 1  
LL = 22  
X = 1605.62 Y = 696.70  
NAREA = 2  
NSCAN = 342

NAREA = 2

NAREA =	3	
NAREA =	1	
LL =	23	
X =	1851.00	Y = 1314.63
NAREA =	2	
NSCAN =	651	
NAREA =	2	
NAREA =	3	
NAREA =	1	
LL =	24	
X =	266.34	Y = 1399.74
NAREA =	2	
NSCAN =	674	
NAREA =	2	
NAREA =	3	
NAREA =	1	
LL =	25	
X =	1779.80	Y = 1435.19
NAREA =	2	
NSCAN =	712	
NAREA =	2	
NAREA =	3	
NAREA =	1	
LL =	26	
X =	343.12	Y = 1496.34

NAREA = 2  
NSCAN = 742

NAREA = 2  
NAREA = 3  
NAREA = 1  
LL = 27  
X = 1708.41 Y = 1530.12  
NAREA = 2  
NSCAN = 759

NAREA = 2  
NAREA = 3  
NAREA = 1  
LL = 26  
X = 417.67 Y = 1588.29  
NAREA = 2  
NSCAN = 766

LL = 29  
X = 1630.42 Y = 1610.12  
NAREA = 2  
NSCAN = 796

NAREA = 2  
NAREA = 3  
NAREA = 1

LL = 30  
X = 697.47 Y = 1665.62  
NAREA = 2  
NSCAN = 627

LL = 31  
X = 1545.69 Y = 1685.83  
NAREA = 2  
NSCAN = 637

NAREA = 2  
NAREA = 3  
NAREA = 1  
LL = 32  
X = 575.91 Y = 1719.14  
NAREA = 2  
NSCAN = 654

LL = 33  
X = 1473.68 Y = 1733.58  
NAREA = 2  
NSCAN = 860

NAREA = 2  
NAREA = 3  
NAREA = 1  
LL = 34

X = 651.52 Y = 1763.74  
NAREA = 2  
NSCAN = 876

LL = 35 X = 1400.96 Y = 1772.35  
NAREA = 2  
NSCAN = 880

NAREA = 2  
NAREA = 3  
NAREA = 1  
LL = 36 X = 725.00 Y = 1797.96  
NAREA = 2  
NSCAN = 895

LL = 37 X = 1324.33 Y = 1805.50  
NAREA = 2  
NSCAN = 896

NAREA = 2  
NAREA = 3  
NAREA = 1  
LL = 38 X = 601.74 Y = 1828.89  
NSCAN = 897

NAREA = 2  
NSCAN = 911

LL = 39  
X = 1236.77 Y = 1636.81  
NAREA = 2  
NSCAN = 912

NAREA = 2  
NAREA = 3  
NAREA = 1  
LL = 40  
X = 948.97 Y = 1660.35  
NAREA = 2  
NSCAN = 926

LL = 41  
X = 1027.40 Y = 1662.73  
NAREA = 2  
NSCAN = 926

LL = 43

X = 1164.50 Y = 1659.00

NAREA = 2

NSCAN = 926

NAREA = 2

NAREA = 3

NAREA = 1

THIS FRAME USED • 1050 SCANS EACH CONTAINING 1050 DENSITY VALUES

THE COORDINATES OF THE BOUNDARY MARKS BEING ORDERED AND GIVEN BELOW.

X =	1034.48	Y =	23.50
X =	1108.66	Y =	27.71
X =	1184.68	Y =	44.19
X =	1262.06	Y =	59.95
X =	955.63	Y =	30.90
X =	877.83	Y =	44.67
X =	802.32	Y =	64.32
X =	1345.87	Y =	89.00
X =	720.43	Y =	99.83
X =	1425.24	Y =	124.76
X =	642.61	Y =	137.32
X =	1499.48	Y =	163.01
X =	565.67	Y =	188.34
X =	1573.37	Y =	222.14
X =	490.79	Y =	247.66
X =	1653.04	Y =	296.09
X =	411.14	Y =	315.91
X =	1726.31	Y =	366.13
X =	339.42	Y =	390.58
X =	1810.92	Y =	510.98
X =	260.43	Y =	519.91
X =	1685.62	Y =	696.70
X =	1851.08	Y =	1314.53
X =	266.34	Y =	1359.74
X =	1775.80	Y =	1435.19
X =	343.12	Y =	1496.34
X =	1708.41	Y =	1530.12

X =	417.67	Y =	1588.29
X =	1630.42	Y =	1610.12
X =	497.47	Y =	1665.82
X =	1545.69	Y =	1685.83
X =	575.91	Y =	1719.14
X =	1673.68	Y =	1733.58
X =	651.52	Y =	1763.74
X =	1400.06	Y =	1772.35
X =	725.00	Y =	1797.96
X =	1324.33	Y =	1805.50
X =	601.74	Y =	1828.89
X =	1236.77	Y =	1836.51
X =	948.97	Y =	1860.35
X =	1027.40	Y =	1862.73
X =	1091.54	Y =	1865.41
X =	1164.58	Y =	1859.60

BOUNDARIES, OR COORDINATES OF PURCHASED LANDS.	PRICES ARE GIVEN BELOW -	BOUNDARY(J+J2)
BOUNDARY(J)	BOUNDARY(J)	BOUNDARY(J+J2)
260.43	519.91	1359.74
339.42	360.58	1496.34
411.14	315.91	1588.29
490.79	247.68	417.47
565.67	188.34	497.47
642.61	137.32	575.91
720.43	99.83	1719.14
802.32	66.32	651.52
877.83	44.67	1763.74
955.63	30.90	726.00
1034.48	23.50	1767.96
1108.66	27.71	801.74
1184.68	44.19	1028.89
1262.06	59.95	948.97
1345.87	89.00	1027.40
1425.24	124.78	1062.73
1499.48	163.01	1091.54
1573.37	222.14	1164.58
1653.04	296.09	1236.77
1726.31	366.13	1314.93
1810.92	510.98	.00
1885.62	696.70	.00

COORDINATES FOR 'LEFT' ARC ARE -

XCENTER =	1062.6129	YCENTER =	946.3886	RADIUS =	922.4545
XCENTER =	54.1306 MM	YCENTER =	47.3294 MM	RADIUS =	46.1227 MM
XCENTER =					

COORDINATES FOR 'RIGHT' ARC ARE -

XCENTER =	996.0717	YCENTER =	944.5528	RADIUS =	923.8361
XCENTER =	49.8036 MM	YCENTER =	47.2276 MM	RADIUS =	46.1919 MM
XCENTER =					

THIS VALUE SHOULD BE EQUAL OR CLOSE TO SHEAR VALUE AS MEASURED ON INTUMESCON

SHEAR =	.3271	THIS VALUE SHOULD BE EQUAL OR CLOSE TO SHEAR VALUE AS MEASURED ON INTUMESCON
DISPLT =	.1016	THIS VALUE SHOULD EQUAL OR BE CLOSE TO ZERO

BOUNDARIES, OR COORDINATES OF PUNCHED HOLES, IN MM FOR 22 PRIMES ARE GIVEN BELOW.

BOUNDARY(J)	BOUNDARY(J)	BOUNDARY(J+J2)	BOUNDARY(J+J2)
13.02	26.00	13.32	67.99
16.97	19.53	17.16	74.82
20.56	19.80	20.87	79.41
24.54	12.36	24.87	83.29
26.26	9.42	26.80	85.96
32.13	6.87	32.58	88.19
36.02	4.99	36.25	89.90
40.12	3.32	40.09	91.44
43.89	2.23	47.45	93.02
47.78	1.54	51.37	93.14
51.72	1.18	54.58	93.27
55.43	1.39	58.23	92.98
59.23	2.21	61.94	91.83
63.10	3.00	66.22	90.26
67.29	4.45	70.00	88.62
71.26	6.24	73.68	86.68
74.97	8.15	77.28	84.29
78.67	11.11	81.52	80.51
82.65	14.80	85.42	76.51
86.32	19.31	88.99	71.76
90.55	25.55	92.55	65.73
94.28	34.84	.00	.00

THE STANDARD DEVIATION OF FITTING ALL THE PUNCHED HOLE COORDINATES TO TWO ARCS IS 12.582 MM .034 MM

## SCAN NO. 1

Y =	57	X1 =	690	X2 =	1194
Y =	2.85 MM	X1 =	44.50 MM	X2 =	59.70 MM

PEAK	X0	CENTER	CENTER (MM)
690	0	698	45.40
659	0	659	47.95
1038	0	1038	51.90
1112	0	1112	55.60
1186	10	1181	59.05

## SCAN NO. 2

Y =	131	X1 =	676	X2 =	1492
Y =	6.55 MM	X1 =	33.90 MM	X2 =	76.10 MM

PEAK	X0	CENTER	CENTER (MM)
676	20	716	35.80
721	0	721	36.05
797	-1	796	39.80
875	0	875	43.75
957	-1	956	47.80
1040	-1	1039	51.95
1112	0	1112	55.60
1152	-1	1188	59.40
1265	0	1269	63.45
1349	0	1349	67.45

## SCAN NO. 3

Y =	205	X1 =	555	X2 =	1625
Y =	10.25 MM	X1 =	27.75 MM	X2 =	76.25 MM

PEAK	X0	CENTER	CENTER (MM)
566	-16	562	26.10
638	-1	637	31.05
710	-1	709	35.45

789	-5	784	39.20
869	1	870	43.50
952	0	952	47.60
1034	0	1034	51.70
1113	0	1113	55.65
1158	-6	1192	59.60
1274	0	1274	63.70
1310	0	1310	65.50
1356	0	1356	67.80
1434	0	1434	71.70
1507	1	1498	74.90

## SCAN NO. 4

Y = 279      X1 = 464      X2 = 1616  
 Y = 13.05 MM    X1 = 23.20 MM    X2 = 80.00 MM

PEAK	X0	CENTER	CENTER(MM)
468	-14	480	24.00
554	-1	553	27.65
623	0	623	31.15
700	0	700	35.00
782	-5	777	38.85
866	-4	862	43.10
944	4	942	47.40
980	0	980	49.00
1028	2	1030	51.50
1112	0	1112	55.60
1146	0	1148	57.40
1200	0	1200	60.00
1282	0	1282	64.10
1364	-3	1361	68.05
1435	4	1435	71.95
1515	-6	1509	75.45
1585	1	1583	79.15

## SCAN NO. 5

Y = 353      X1 = 393      X2 = 1687  
 Y = 17.65 MM    X1 = 19.65 MM    X2 = 84.35 MM

PEAK    X0    CENTER    CENTER(MM)

				19.00
412	-23	396		23.55
473	-2	471		26.05
544	-5	539		30.70
613	1	614		34.55
685	-1	651		38.70
775	-1	774		42.05
861	-4	857		47.25
940	3	945		51.35
1025	2	1027		55.65
1118	-5	1113		59.95
1203	-4	1199		64.25
1285	0	1285		68.25
1368	-2	1365		72.25
1445	0	1445		75.90
1518	0	1518		79.70
1597	-3	1564		83.00
1659	0	1660		

SCAN NO. 6

T = 427      X1 = 324      X2 = 1764  
 Y = 21.35 MM    X1 = 16.74 MM    X2 = 87.20 MM

PEAK	X0	CENTER	CENTER(MM)
336	-24	330	16.50
396	-2	394	19.70
462	-3	459	22.95
523	-4	525	26.45
608	-3	605	30.25
690	-6	684	34.20
768	0	768	38.40
853	0	853	42.65
939	1	940	47.00
1026	-1	1025	51.25
1119	-5	1114	55.70
1205	-6	1199	59.95
1288	1	1289	64.45
1372	0	1372	68.60
1452	0	1452	72.60
1528	1	1525	76.45
1602	1	1603	80.15
1671	-1	1670	83.50
1732	23	1742	87.10

SCAN NO. 7

	X1	X1	X2	X2	
Y - 501	-	-	269	-	1790
Y - 25.05 MM	X1 -	X1 -	14.45 MM	X2 -	89.50 MM

PEAK	KO	CENTER	CENTER(MM)
269	20	327	16.35
326	-3	323	16.15
385	-5	380	19.00
451	0	451	22.55
523	-2	521	26.05
601	-2	559	29.95
684	-2	682	34.10
764	-1	763	38.15
848	-2	846	42.30
932	3	935	46.75
1027	-3	1024	51.20
1118	-6	1112	55.60
1207	1	1208	60.40
1291	0	1291	64.55
1376	0	1376	68.80
1454	3	1457	72.85
1537	-3	1534	76.70
1612	0	1612	80.60
1678	0	1678	83.90
1745	-3	1742	87.10

	X1	X1	X2	X2	
Y - 575	-	-	252	-	1827
Y - 26.75 MM	X1 -	X1 -	12.60 MM	X2 -	91.35 MM

PEAK	KO	CENTER	CENTER(MM)
232	-23	247	12.35
312	0	312	15.60
380	-5	375	18.75
447	4	447	22.35
517	0	517	25.85
598	-2	596	29.80
676	-3	673	33.65
757	-4	753	37.65
843	-4	839	41.95
931	1	932	46.60
1026	-4	1022	51.10
1116	-1	1115	55.75
1212	-2	1210	60.50
1257	-1	1256	64.80
1381	-2	1379	68.95
1461	0	1461	73.05

1541	1	1542		77.10
1619	-4	1615		60.75
1686	1	1687		64.35
1755	-3	1752		67.60
1815	16	1820		91.00

SCAN NO. 9

Y - 649      X1 -      223      X2 - 1656  
 Y - 32.45 MM    X1 -      11.15 MM    X2 - 92.80 MM

PEAK	KO	CENTER	CENTER (MM)
223	11	252	12.60
259	-21	236	11.90
303	0	303	15.15
367	1	366	16.40
440	1	441	22.05
516	-3	513	25.65
595	-4	591	29.55
669	-3	666	33.30
751	-8	743	37.15
836	-4	834	41.70
931	-2	929	46.45
1026	-3	1023	51.15
1118	0	1116	55.90
1213	-2	1211	60.55
1248	3	1301	65.05
1385	0	1385	69.25
1466	0	1466	73.30
1544	1	1545	77.25
1620	0	1620	81.00
1694	-2	1652	84.60
1756	0	1756	87.90
1821	2	1822	91.10

SCAN NO. 10

Y - 723      X1 -      201      X2 - 1676  
 Y - 36.15 MM    X1 -      10.05 MM    X2 - 63.90 MM

PEAK	KO	CENTER	CENTER (MM)
201	0	219	10.95

				12.00
242	-2	302	15.10	
299	-3	367	16.35	
366	-1	435	21.75	
436	-1	509	25.45	
509	0		29.35	
568	-1	587	32.95	
665	-6	659		
665	-6		37.05	
742	-1	741		
836	-4	832	41.60	
931	-7	924	46.20	
1027	-10	1017	50.85	
1120	-4	1116	55.80	
1214	-3	1211	60.55	
1304	-4	1300	65.00	
1391	-2	1389	69.45	
1470	2	1472	73.60	
1549	-1	1548	77.40	
1622	-4	1626	81.30	
1656	0	1696	84.80	
1764	0	1764	88.20	
1827	-1	1826	91.30	

SCAN NO. 11  
Y = 797      X1 =      186      X2 = 1893  
Y = 39.85 MM    X1 =      9.30 MM    X2 = 94.65 MM

PEAK	X0	CENTER	CHIRIKIN MM)
186	-28	176	8.80
238	-1	237	11.65
266	-1	298	14.90
362	-1	361	18.05
436	-4	432	21.60
505	-1	505	25.25
578	-1	579	28.95
657	0	657	32.65
745	-2	743	37.15
825	11	840	42.00
927	-8	919	45.95
1024	-9	1015	50.75
1125	1	1126	56.30
1215	1	1216	60.80
1304	1	1305	65.25
1386	11	1359	69.95
1448	50	1498	74.90
1486	-19	1467	73.35
1553	-2	1551	77.55
1627	-2	1625	81.25
1701	-2	1699	84.95
1770	-2	1768	88.40

1631	0	1631	91.56
1685	20	1654	54.70

## SCAN NO. 12

Y =	871	X1 =	177	X2 =	1903
Y =	43.55 MM	X1 =	8.65 MM	X2 =	95.15 MM

PEAK	X0	CENTER	CENTER(MM)
177	-23	172	8.60
237	-2	235	11.75
296	-1	295	14.75
361	-2	359	17.95
430	-2	428	21.40
503	-2	501	25.05
578	-5	573	28.65
655	-2	653	32.65
745	-3	742	37.10
832	-2	830	41.50
913	4	917	45.85
1021	0	1021	51.05
1122	3	1125	56.25
1158	-50	1108	55.40
1222	0	1222	61.10
1305	0	1305	65.25
1392	0	1392	69.60
1481	-6	1475	73.75
1554	-2	1552	77.60
1626	0	1628	81.40
1702	-2	1700	85.00
1770	0	1770	89.50
1832	0	1832	91.60
1885	20	1855	54.75

## SCAN NO. 13

Y =	945	X1 =	173	X2 =	1906
Y =	47.25 MM	X1 =	8.65 MM	X2 =	95.30 MM

PEAK	X0	CENTER	CENTER(MM)
173	-17	174	8.70
237	-2	235	11.75

				14.70
297	-3	294		
360	-1	361		18.05
431	-2	429		21.45
502	0	502		25.10
571	4	575		28.75
654	-1	655		32.75
744	-1	743		37.15
831	-3	828		41.40
917	-1	916		45.60
1017	-1	1018		50.90
1124	0	1124		56.20
1160	-49	1111		55.55
1224	0	1224		61.20
1305	0	1305		65.25
1394	-1	1393		69.65
1460	-3	1477		73.65
1553	0	1553		77.65
1627	2	1629		81.45
1700	0	1700		85.00
1771	-3	1768		88.40
1835	0	1835		91.75
1885	0	1877		93.65

SCAN NO. 14		X1 = 177		X2 = 1963	
Y =	1019	X1 =		X2 =	
Y =	50.95 MM	X1 =	0.05 MM	X2 =	95.15 MM

PEAK	NO	CENTER	CENTER(MM)
177	-25	170	6.50
236	0	236	11.80
295	0	295	14.75
363	0	363	16.15
436	-6	430	21.50
504	1	505	25.25
576	0	576	28.80
656	-2	654	32.70
745	-4	741	37.05
831	-2	829	41.45
913	0	919	45.95
1014	7	1021	51.05
1053	-52	1001	50.05
1126	0	1126	56.30
1163	-52	1111	55.55
1217	0	1217	60.85
1303	3	1306	65.30
1353	0	1393	66.65
1476	0	1476	73.60
1551	-1	1550	77.50
1627	-2	1625	81.25

	-5	1666	84.80
1701	-1	1767	68.38
1768	0	1632	91.60
1632	11	1685	94.25
1682			

## SCAN NO. 15

Y =	1093	X1 =	186	X2 =	1893
Y =	54.65 MM	X1 =	9.30 MM	X2 =	64.65 MM

PEAK	X0	CENTER	CENTER (MM)
186	-28	176	8.80
239	0	239	11.95
296	0	269	14.95
367	-6	361	16.05
435	1	436	21.80
509	-2	507	25.35
580	-1	579	28.95
660	-7	653	32.65
743	0	743	37.15
835	-6	829	41.45
923	-1	922	46.10
1021	-4	1017	50.85
1118	2	1120	56.00
1209	4	1213	60.65
1296	-4	1302	65.10
1393	-3	1390	69.50
1473	-4	1469	73.45
1545	1	1546	77.30
1629	-10	1619	80.95
1656	1	1697	84.85
1762	0	1762	88.10
1821	1	1822	91.10
1881	17	1885	94.25

## SCAN NO. 16

Y =	1167	X1 =	201	X2 =	1878
Y =	58.35 MM	X1 =	10.05 MM	X2 =	63.90 MM

PEAK	X0	CENTER	CENTER (MM)
201	0	216	10.95

	244	12.20
205	304	15.20
370	367	18.35
439	1	440
510	0	510
587	1	583
663	15	658
748	13	745
831	4	835
929	16	923
1021	13	1016
1117	13	1114
1210	1	1209
1300	1	1301
1388	1	1384
1465	1	1466
1543	0	1543
1617	11	1616
1691	12	1689
1756	1	1757
1818	13	1815
1864	26	1881

SCAN NO. 17

	$y = 1241$	$x_1 =$	$x_2 = 1056$
	$y = 62.05 \text{ MM}$	$x_1 =$	$x_2 = 92.80 \text{ MM}$

PEAK	$x_0$	CENTER (MM)
223	21	13.10
259	18	251
312	13	309
375	13	372
447	15	442
519	16	513
588	1	589
665	13	666
751	11	750
836	11	835
933	16	924
1024	14	1020
1115	11	1114
1213	10	1203
1259	12	1297
1384	13	1381
1462	11	1461
1538	0	1538
1609	1	1610
1685	1	1684
1748	2	1750

1811 0 1811 90.95

SCAN NO. 18

Y = 1315 X1 = 252 X2 = 1827  
Y = 65.75 MM X1 = 12.60 MM X2 = 91.35 MM

PEAK	X0	CENTER	CENTER MM)
257	-25	248	12.60
319	-4	315	15.75
391	-2	379	18.95
449	-1	448	22.40
526	-2	524	26.20
596	0	566	29.80
677	-5	672	33.60
754	1	755	37.75
838	2	840	42.00
931	0	931	46.55
1020	-1	1019	50.95
1114	-3	1111	55.55
1204	0	1204	60.20
1296	-6	1290	64.50
1371	5	1376	68.80
1454	-12	1452	72.60
1533	-1	1532	76.60
1607	-1	1606	80.30
1676	-3	1673	83.65
1742	-4	1738	86.90
1803	6	1801	90.65

SCAN NO. 19

Y = 1369 X1 = 289 X2 = 1790  
Y = 69.45 MM X1 = 14.05 MM X2 = 69.50 MM

PEAK	X0	CENTER	CENTER MM)
289	0	307	15.35
327	0	327	16.35
391	-1	360	19.50
458	-5	453	22.65
527	0	527	26.35
603	-4	559	29.95

680	-2	678	33.90
765	-3	762	38.10
844	0	844	42.20
639	-14	925	46.25
1018	2	1020	51.00
1111	-2	1109	55.45
1200	-2	1158	59.90
1253	0	1283	64.15
1366	0	1266	68.30
1446	-2	1445	72.25
1526	-3	1523	76.15
1567	0	1597	79.85
1666	-1	1665	83.25
1727	0	1727	86.35
1779	24	1790	89.50

SCAN #4. 23  
 Y = 1463      X1 = 336      X2 = 1744  
 Y = 73.15 MM    X1 = 16.00 MM    X2 = 97.20 MM

PEAK	E0	CENTER	CENTER (MM)
338	-26	329	16.45
402	-1	401	20.05
465	0	465	23.25
535	-11	534	26.70
608	-11	607	30.35
689	-3	686	34.30
771	-2	769	38.45
847	-3	850	42.50
934	0	934	46.70
1018	2	1020	51.00
1107	-1	1106	55.30
1193	-2	1191	59.55
1280	-5	1275	63.75
1360	-1	1359	67.95
1441	-3	1438	71.90
1520	0	1520	76.00
1592	0	1592	75.60
1653	0	1653	82.65
1713	0	1710	85.50

SCAN #4. 21  
 Y = 1537      X1 = 373      X2 = 1687

$\gamma$  - 78.85 MM     $x_1$  - 10.65 MM     $x_2$  - 64.35 MM

PEAK	KO	CENTER	CENTER(MM)
393	0	411	20.55
429	-28	401	20.05
477	0	477	23.85
544	-1	543	27.15
617	0	617	30.85
693	-2	661	34.55
774	-2	772	36.60
852	3	855	42.75
935	0	935	46.75
1023	-2	1021	51.05
1108	-3	1105	55.25
1189	0	1169	59.45
1273	-2	1271	63.55
1354	0	1354	67.70
1435	-2	1433	71.65
1505	2	1507	75.35
1579	-7	1572	78.60
1640	-1	1639	81.95

SCAN NO. 22

$\gamma$  - 1611     $x_1$  - 464     $x_2$  - 1616  
 $\gamma$  - 60.55 MM     $x_1$  - 23.20 MM     $x_2$  - 60.80 MM

PEAK	KO	CENTER	CENTER(MM)
464	0	462	24.10
500	-11	469	24.45
555	0	555	27.75
627	0	627	31.35
700	1	701	35.05
778	-2	776	39.60
856	0	856	42.80
940	-3	937	46.85
1020	2	1022	51.10
1103	0	1103	55.15
1186	-4	1182	59.10
1265	-1	1264	63.20
1349	-3	1346	67.30
1422	0	1422	71.10
1491	0	1491	74.55
1560	-1	1559	77.95

## SCAN NO. 23

$\gamma = 1685$        $x_1 = 555$        $x_2 = 1625$   
 $\gamma = 84.25 \text{ MH}$        $x_1 = 27.75 \text{ MH}$        $x_2 = 76.25 \text{ MH}$

PEAK	KO	CENTER	CENTER(MH)
565	-24	554	27.70
639	0	639	31.95
709	-1	706	35.40
784	0	784	39.20
863	-1	862	43.10
939	-1	938	46.90
1020	1	1021	51.05
1101	-2	1099	54.95
1180	0	1180	59.00
1260	-2	1258	62.90
1335	1	1336	66.80
1413	0	1413	70.65
1479	0	1479	73.95

## SCAN NO. 24

$\gamma = 1759$        $x_1 = 678$        $x_2 = 1482$   
 $\gamma = 87.95 \text{ MH}$        $x_1 = 33.90 \text{ MH}$        $x_2 = 76.10 \text{ MH}$

PEAK	KO	CENTER	CENTER(MH)
678	0	695	34.80
725	-1	724	36.20
793	0	793	39.65
865	-2	863	43.15
942	0	942	47.10
1024	-3	1021	51.05
1095	1	1096	54.80
1174	0	1174	58.70
1251	-3	1246	62.40
1326	0	1326	66.40
1366	21	1397	69.85

## SCAN NO. 25

$\gamma = 1833$        $x_1 = 890$        $x_2 = 1194$

Y	91.65 MM	X1	44.50 MM	X2	59.70 MM
PEAK	X0	CENTER	CENTER MM)		
890	0	908	45.40		
946	0	648	47.40		
1022	0	1022	51.10		
1052	0	1092	54.60		
1165	13	1174	58.70		

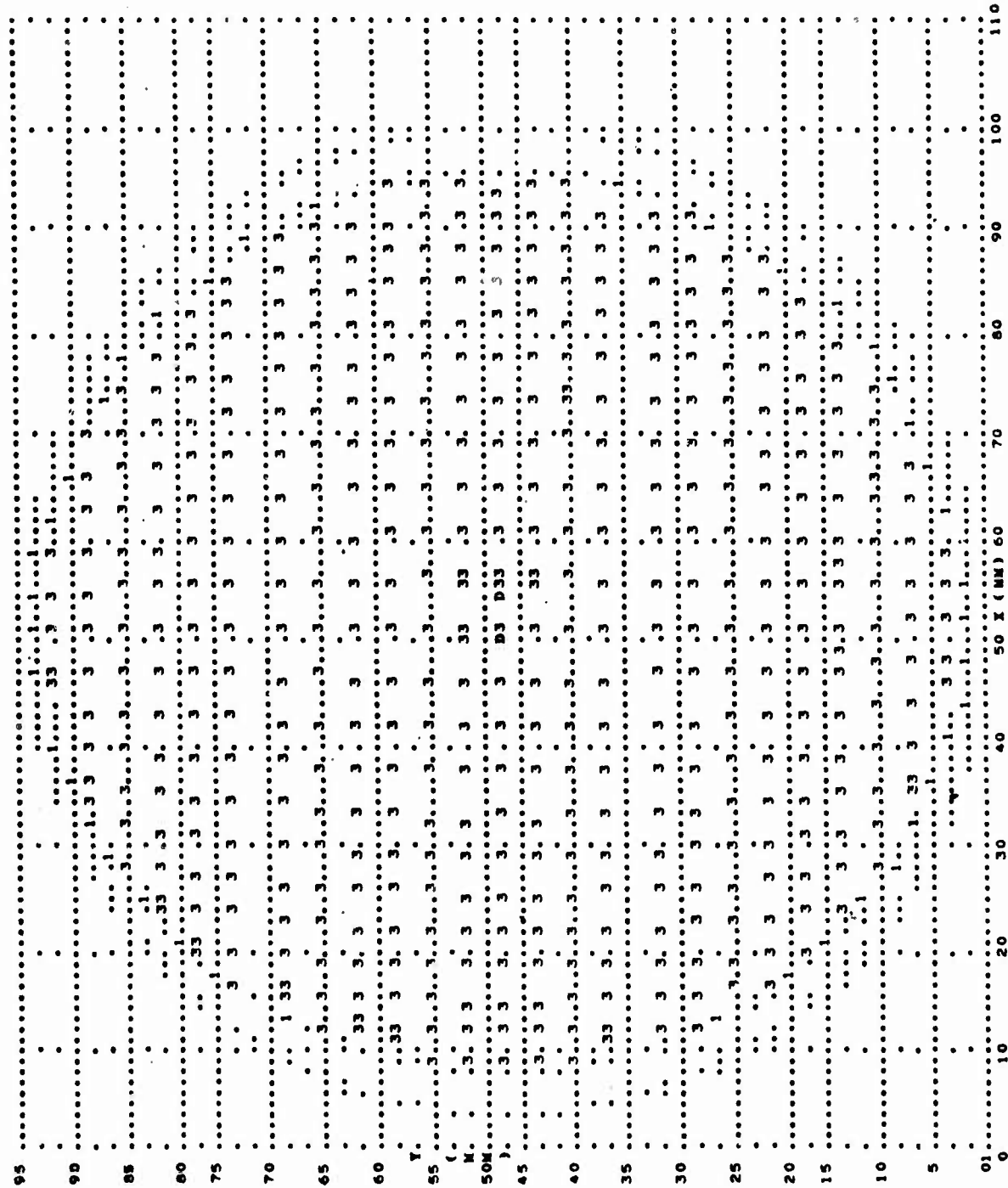
CLJ2 (HF2) -	22
NSS (NST) -	25
CTI -	7.981
PCSY -	1.750
RADIUS -	46.150

PRINCE-PEAK POSITIONS PEG(J,K) RESULTING FROM AUTOMATIC LEARNING ARE PRINTED BELOW:  
J = PRINCE NUMBER      K = SCAN NUMBER



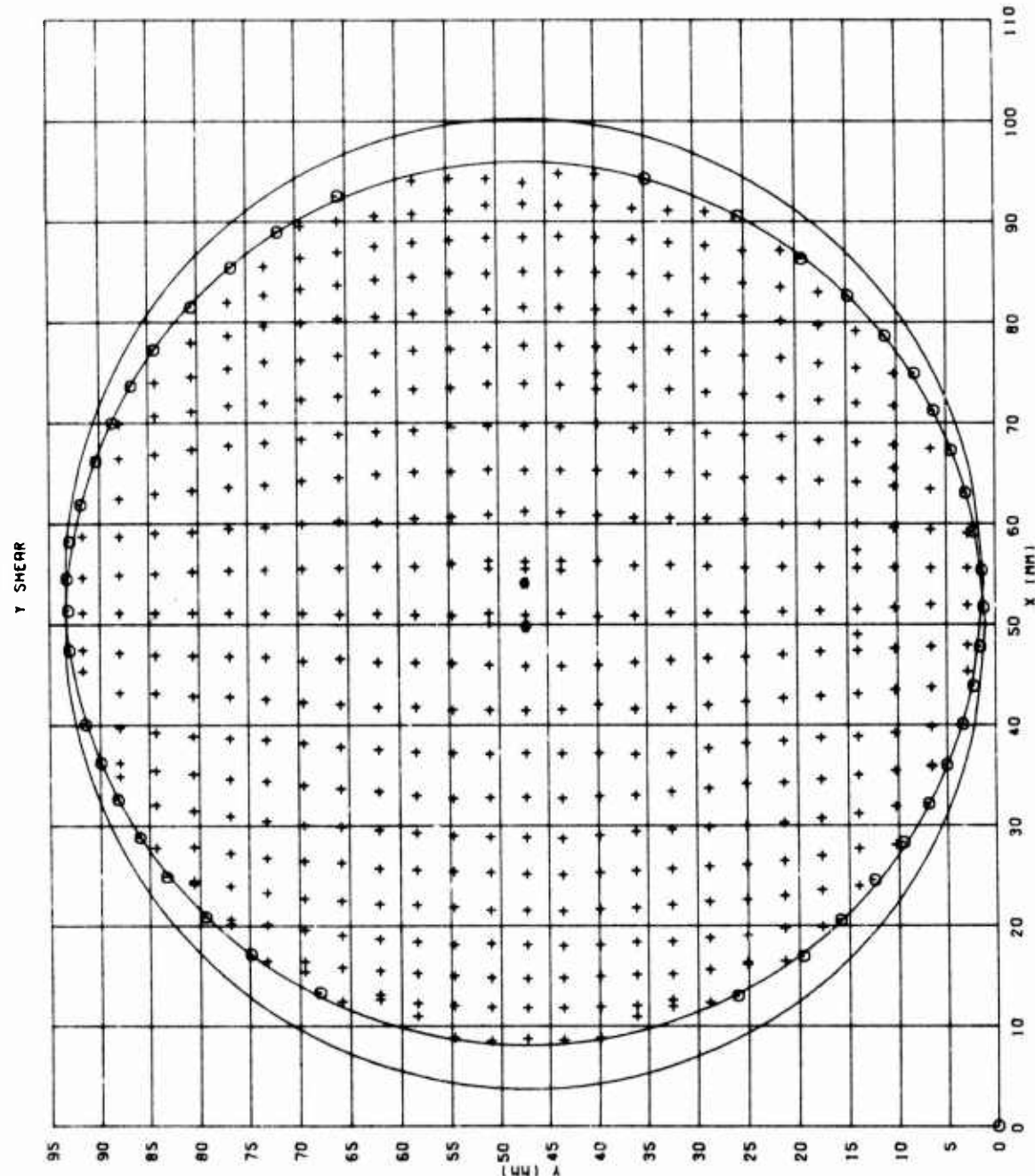
Printer Plot

MAP OF VSI INTERFACED SCANNED BY AUTOMATIC SCANNER  
Y SEPAR



MAP OF WSI INTERFERGRAM SCANNED BY AUTOMATIC SCANNER

CALCOMP Plot



## APPENDIX D

### REGISTRATION OF INTERFEROGRAMS

The registration of the fringe-peak data obtained from scanning a pair of x and y-sheared interferograms is equivalent to the coordinate transformation of these two sets of fringe data to a common coordinate system. Fiducial marks placed in an interferometric test system are generally used to identify coordinates of the test lens, thereby permitting subsequent registration of fringe data from two or more scanned interferograms. However, such an approach usually results in the partial obscuration of fringes and, in addition, requires that the scanning system, or operator, distinguish between fiducial marks and fringes. The present approach for registering interferograms from the WSI uses such fiducial marks, but owing to the inherent stability of the WSI, a second set of interferograms identical to an earlier set except for the absence of fiducial marks within the aperture is taken and used for scanning.

The main data-reduction computer program performs the registration of the x and y-sheared interferograms provided that the fringe-peak data from the scanner are in a required format. The data-reduction program assumes the following: (1) shear directions were along the positive x and negative y axes for the x and y-sheared interferograms, respectively; and (2) the y-sheared interferogram was obtained by rotating either the test lens 90° clockwise or the cube interferometer 90° counterclockwise as viewed from the back of the cube. A left-hand cartesian coordinate system chosen to ensure that the fringe data will satisfy both conditions for registration is illustrated in Figure 36.

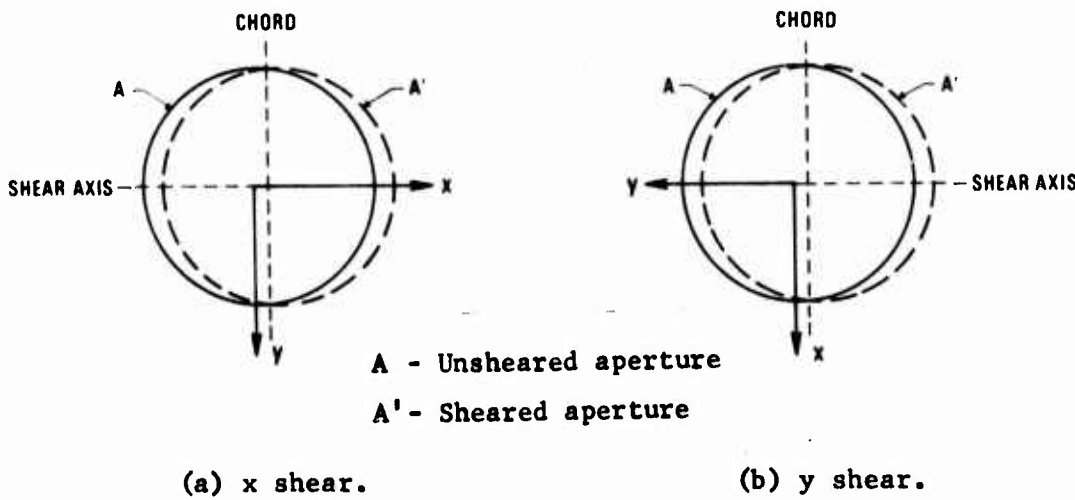


Figure 36.- Coordinate system for WSI interferograms.

As shown in figure 36, the shear direction, or shear axis, is perpendicular to an imaginary chord connecting the two points of intersection of the original and sheared aperture boundaries. Since the interferogram is scanned parallel to the shear axis, it is necessary to locate this axis on both the x and y-sheared interferograms. The simple construction of the shear axis by drawing a line perpendicular to the chord connecting the two points of intersection of the original and sheared aperture boundaries is generally not an accurate method; these points of intersection are not very distinct in the resulting interferograms since the shear distance is typically only a few percent of the test-lens diameter. The approach used for locating the shear axis is based on the following property of a lateral-shearing interferometer with a fixed shear angle such as the WSI: the number of fringes in the fringe pattern of a test lens can be increased until all the fringes eventually appear straight and parallel to the shear axis even for a lens with large aberrations. As the cube interferometer is moved along the test-system optical axis and away from the test-lens focus, the tilt between the unsheared and sheared wavefronts is increased, thereby increasing the number of fringes.

The test and scanning procedures used to ensure the proper registration of the fringe data from the x and y-sheared interferograms are outlined in the following steps and illustrations. It is assumed that the test lens and cube interferometer have been aligned using cross hairs as discussed in section 11.3 and that a fringe pattern is visible in the film plane.

- (1) Place right-angle cross hairs near test lens so that a sharp image of these cross hairs is formed in film plane; place a small and different pattern on each cross hair at bottom and right side near aperture edge; mark test-lens edge or mounting collar at bottom and right side so that these fiducial marks coincide with shadows of cross hairs as shown in figure 37.

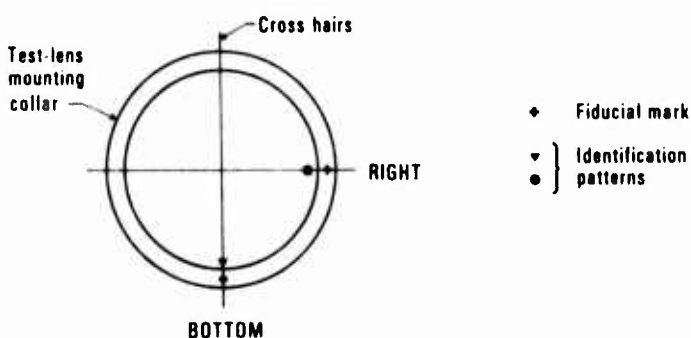


Figure 37.- Schematic of test lens with cross hairs, fiducial marks, and identification patterns as viewed from cube interferometer.

- (2) Move cube interferometer along test-system optical axis and away from test-lens focus until fringes are so numerous (typically 75 to 100 fringes) that they all appear straight; rotate the cube interferometer about test-system optical axis until these fringes are parallel to one of the cross hairs as shown in figure 38.

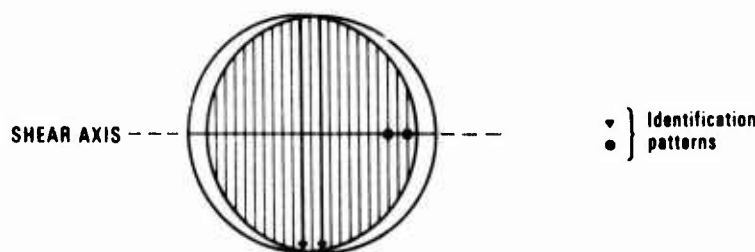
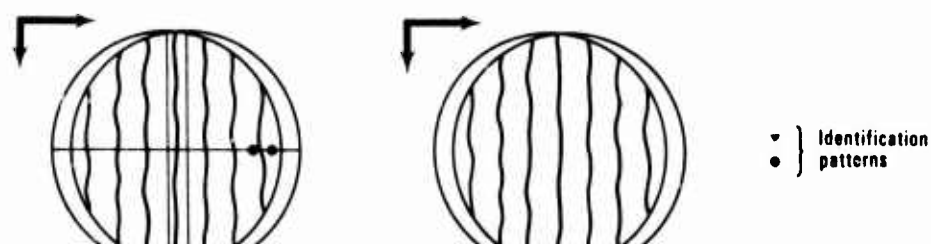


Figure 38.- Schematic of WSI fringe pattern with cross hairs and identification patterns.

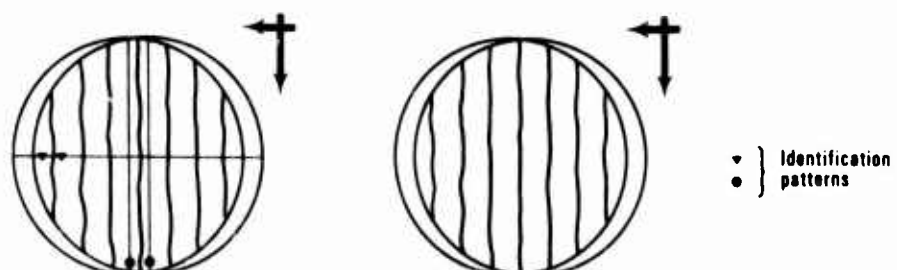
- (3) Move cube interferometer back along test-system optical axis and towards test-lens focus to selected test position ( $\lambda$  setting); photograph resulting fringe pattern (x-sheared interferogram) with and without cross hairs.
- (4) Replace cross hairs and rotate either cube interferometer  $90^\circ$  counterclockwise or test lens  $90^\circ$  clockwise as viewed from back of cube interferometer; photograph resulting fringe pattern (y-sheared interferogram) with and without cross hairs. Note - if test lens is rotated, the small patterns on the cross hairs will have to be removed and also rotated  $90^\circ$  clockwise.
- (5) Mark each of the resulting four interferograms with left-handed Cartesian-coordinate axes outside of fringe pattern; for automatic scanning, these axes should also be outside region of scanning; positive direction of these axes is in direction of small patterns on cross hairs.

hairs, i.e., towards bottom and right side of lens; x-axis is roughly parallel to shear axis in x-sheared interferogram, and y-axis is roughly parallel to shear axis in y-sheared interferogram; x-axis is longer than y-axis, and these axes terminate at origin in x-sheared interferogram and extend through origin in y-sheared interferogram as shown in figure 39. Note - if strip film is not used for photographing fringe patterns, the original orientation among the interferograms will have to be preserved until coordinate axes can be applied.



(i) With cross hairs.      (ii) Without cross hairs.

(a) x shear.



(i) With cross hairs.      (ii) Without cross hairs.

(b) y shear.

**Figure 39.- Schematic of WSI interferograms marked with coordinate axes to preserve relative orientation.**

- (6) Make photographic transparencies of both interferogram pairs using same magnification; these transparencies must have a size and fringe contrast ratio suitable for scanning and must be free of distortion; superimpose the two transparencies in each pair until aperture and fringes coincide; punch small holes (approximately 0.5 mm diameter) through each matched pair of interferograms at both ends of cross hairs as shown in figure 40.

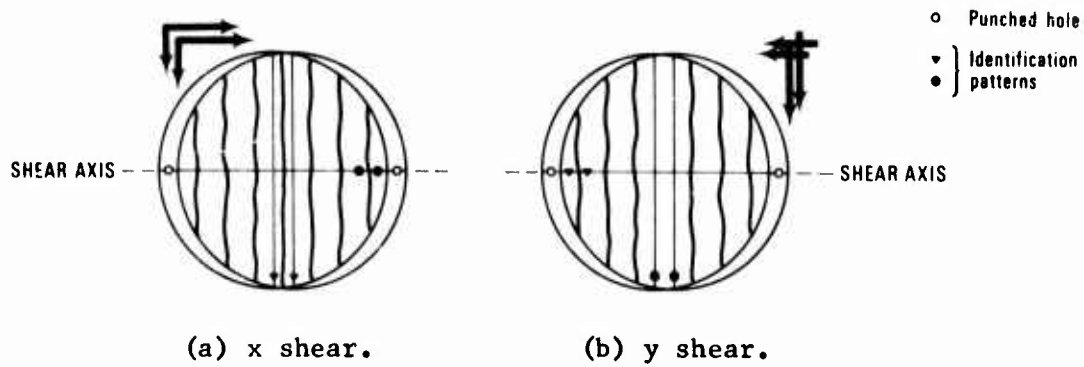
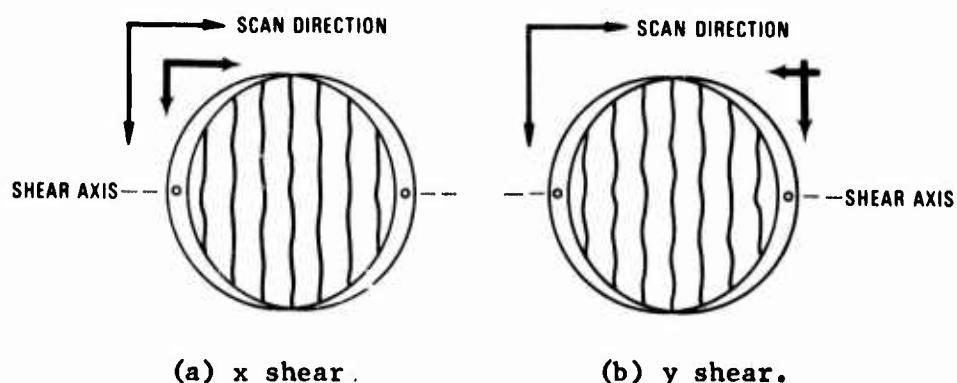


Figure 40.- Schematic of superimposed WSI interferograms with punched holes for manual-scanning alignment.

- (7) Place interferogram without cross hairs on scanner with emulsion side facing pick-up optics (efflux side); scanning direction should be parallel to shear axis or imaginary line through centers of punched holes; orient x-sheared interferogram so that scan coordinates are increasing in directions of positive x and y-axes and orient y-sheared interferogram so that scan coordinates are increasing in directions of positive x-axis and negative y-axis as shown in figure 41. Note - the computer software should be modified to translate and interpolate fringe data if interferograms cannot be oriented so that automatic scanner scans parallel to shear axis.



**Figure 41.- Schematic of placement of WSI interferograms for scanning.**

APPENDIX E  
SPECIFICATIONS AND ASSEMBLY OF WSI CUBES

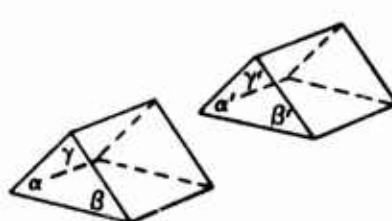
The parameters of the eight cubes assembled for the sponsor are given in table 2(b). The shear angles  $\phi$  are selected on the bases of the f-numbers of the optical systems expected to be tested and approximately twenty-five fringes in the interference pattern for a well-corrected optical system. The cube parameters  $l$  and the minimum working distance are defined in figure 7.

The prisms used to make the cube interferometers are high-purity synthetic fused silica (Suprasil 1-T19) with a high degree of optical homogeneity and uniform transmittance over the visible spectrum. The pair of prisms used for each cube is cut from the same original prism to assure that the two pairs of adjacent angles,  $\alpha/\alpha'$  and  $\beta/\beta'$  shown in figure 42, are equal. Therefore, the cube interferometer can be adjusted during assembly to provide equal optical paths for the two light beams. The tolerance on the  $90^\circ$  prism angle is  $\pm 1$  minute, whereas the tolerance of  $\pm 30$  minutes on the  $45^\circ$  angles is less stringent because the two prisms for each cube are cut from the same original prism. If the prism angles are not within the specified tolerances, additional tilt may be introduced into the cube interferometer. However, this is not a serious problem for angular deviation less than about  $1/2^\circ$ .

$$\alpha = \alpha' = 45^\circ$$

$$\beta = \beta' = 45^\circ$$

$$\gamma = \gamma' = 90^\circ$$



(a) General view.



(b) End view.

Figure 42.- Schematic of pair of  $45^\circ$ -  $90^\circ$ -  $45^\circ$  prisms for WSI cube.

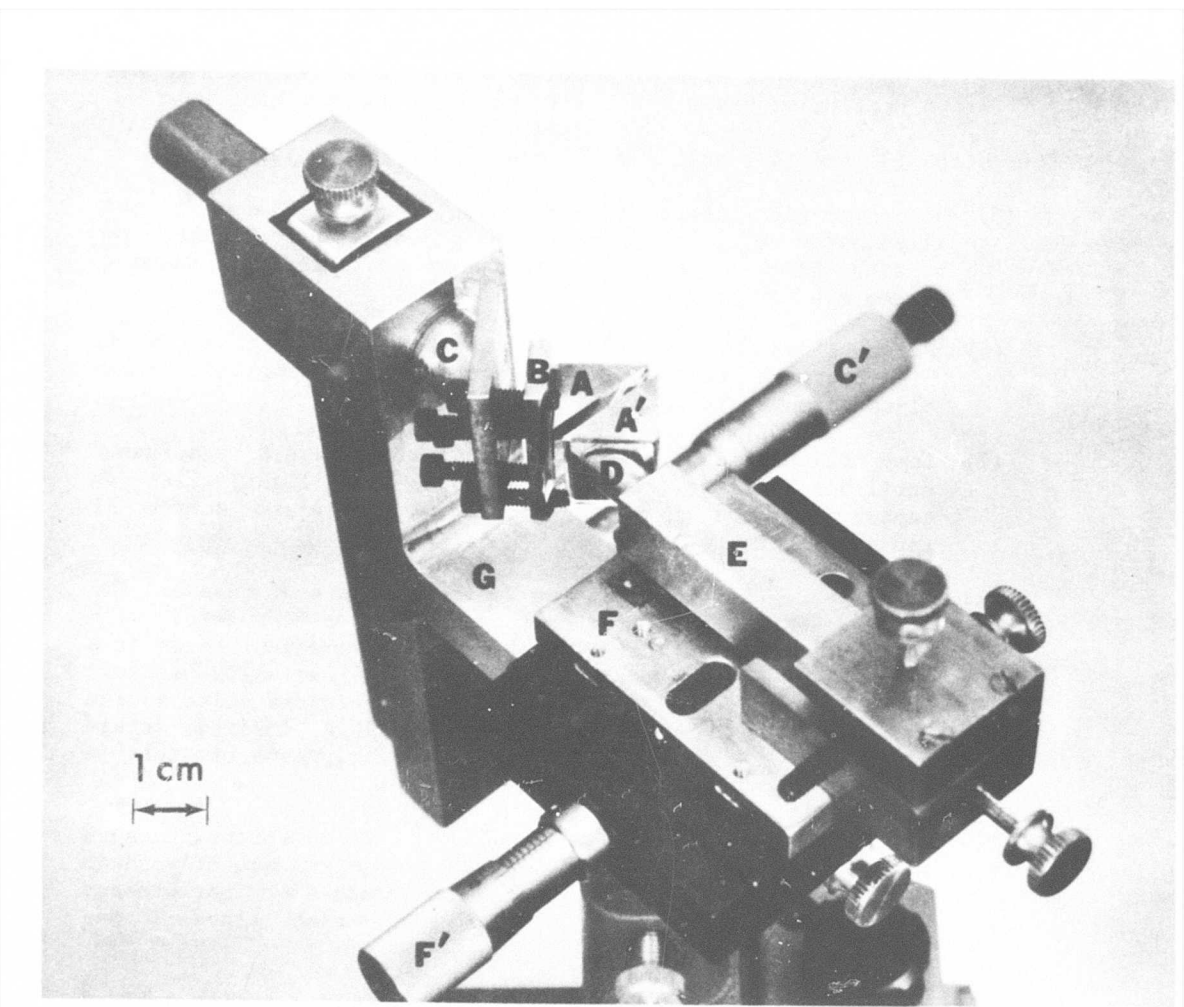
The sides of the prism, except the hypotenuse or base, are 13 mm in length. Thus, the assembled cube interferometer also measures 13 mm on a side. This choice for the cube dimension exceeds the minimum thickness required for testing relatively low f-number optical systems, as discussed in section VI.1, and provides cube surfaces which are not difficult to polish optically flat. All prism surfaces used to transmit or to reflect light are polished flat to  $\lambda/10$  for  $\lambda = 546.1$  nm. One surface on each prism has a vapor-deposited aluminum coating which is totally reflective for visible radiation and overcoated with silicon monoxide for protection. The hypotenuse face on one prism from each pair also has a bare vapor-deposited aluminum coating to provide the beam-dividing surface. It is unnecessary that this coating exhibit equal transmittance and reflectance; the two beams emerging from the cube interferometer will have traveled equal optical paths, and the resultant intensity of each beam will be the product of the transmittance and reflectance of the beam-dividing coating (neglecting minor absorption and scattering losses).

A 1.0-mm-thick glass plate is attached to the totally-reflective prism surface. This thin plate allows the prism to be mounted rigidly during assembly without directly damaging the reflective coating or the prism surface. After assembly of the cube, these plates could be removed or left in place provided their adhesion does not introduce stresses in the cube. In the present instance, no stresses are evident, and it has been decided that the removal of the glass plates is unnecessary.

The primary requirements for assembly of the cube interferometer are the following: (1) a mount for each prism; (2) controls for the independent movement of each prism in order to produce the fringe pattern and to adjust it for chromatic compensation; and (3) a control to rotate one prism about an axis perpendicular to its hypotenuse face in order to set the desired shear angle. For assembly of the present cube set, a special device was built and is shown in figure 43 with a pair of prisms mounted. This assembly rig consists basically of two separable parts or sub-assemblies - a prism mounting plate (B) attached to a shaft (C) and a prism mounting rod (D) housed in a block (E) attached to a translation stage (F); the two sub-assemblies are mounted in a frame (G). The differential micrometers (C' and F') provide very fine adjustments of the prisms. The steps required for assembling the cube interferometer from a pair of prisms with attached glass plates are as follows:

- (1) Prism A with partially aluminized base is attached to mounting plate B by fastening prism side (with glass plate) with hot wax.
- (2) Shaft C with attached plate B and prism A is secured in frame G; with a laser beam incident on the reflective prism base, the prism mounting plate B is adjusted until laser beam reflected from base does not shift while rotating shaft C.

After steps (1) and (2), the prism has effectively been adjusted so that its axis of rotation is now perpendicular to its reflective base.



A - Prism	C - Rotating shaft	F - Translation stage
A' - Prism	C' - Micrometer	F' - Micrometer
B - Mounting plate	D - Mounting shaft	G - Frame
	E - Housing block	

Figure 43.- Photograph of device for assembling WSI cube.

- (3) Frame G is tilted so that base of prism A is horizontal; other prism A' is placed on prism A with their bases congruent; other sub-assembly is placed in frame and prism A' is fastened to mounting shaft D with adhesive.
- (4) Prisms are then separated by withdrawing mounting shaft D and Translating stage F; cement for attaching two prisms together is poured onto base of prism A, and prism A' is repositioned so that prism bases are nearly parallel and touching.

After steps (3) and (4), the cube is ready for fringe adjustments.

- (5) Monochromatic light (Hg-arc lamp with 546.1-nm filter) illuminates cube, and prism A' is adjusted by controls on housing block E until cube images projected onto viewing screen are congruent.
- (6) Prism A' is moved very slowly with translation stage F until high-contrast fringes appear; controls on housing block E are adjusted until fringes are horizontal.
- (7) Lamp filter is removed and translation stage F is adjusted until black fringe (zero order for white light) lies in center of cube image on screen; mercury-arc source is replaced by He-Ne laser.
- (8) Laser beam is incident on entrance face of cube and two sheared beams emerge from exit face; prism A is rotated with shaft C until measured separation of emergent beams at a known distance yields the desired shear angle; alternatively for small shear angles (about 6 mrad or less), a point source is used and prism A is adjusted until a desired fringe spacing at a known distance is obtained; prisms are left in this position until cement sets.
- (9) Mounting plate B is separated from cube by slight pressure required to break wax bond; cube is freed from mounting shaft D by a means which depends on choice of adhesive (for present cubes, a firm mechanical blow to housing block E was satisfactory).

After steps (5) through (9), the cube interferometer with a fixed value of shear is complete.

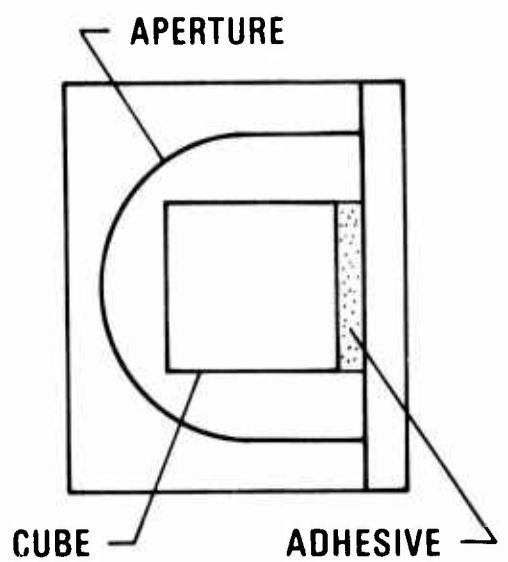
Complete assembly of each cube interferometer required two to three days; the cube was allowed to set for two days before being separated from the assembly rig.

The cement used to seal the two prisms together is a silicone resin (Sylgard 184) which is a low-viscosity liquid during application. After setting, this material is clear with a index of refraction (1.430) in the visible region close to that of the prisms (1.460), thereby permitting nearly perfect chromatic compensation for a very thin layer between the prisms. In addition, Sylgard 184 is

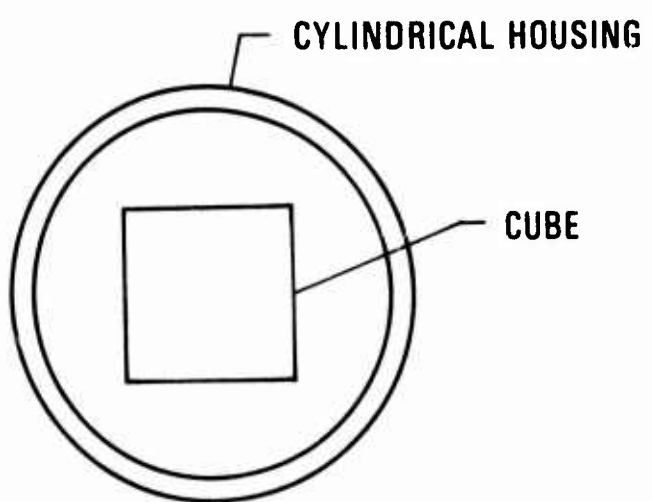
noncorrosive to both glass and aluminum and has a potting life of over two hours at 25°C so that sufficient time is available to adjust the prisms. Also, Sylgard is readily soluble in trichloroethylene, thereby allowing the prisms to be cleaned easily without damage whenever the assembly must be redone or excess Sylgard oozes out onto the cube faces. However, it is necessary to put the Sylgard in a vacuum (70 mm Hg) to outgas air bubbles trapped during mixing of the base and curing agent. Sylgard is also used to attach the glass plates to the prisms. Since this resin has low shrinkage during cure and 100 percent elongation, there should be very little, if any, stresses induced in the prisms by the resin. On a cautionary note, it should be added that the linear coefficient of thermal expansion of Sylgard is about 500 times higher than the prism fused silica at room temperature (22°C); therefore, the cube interferometers should not be subjected to large thermal gradients during use.

The adhesive used to attach prism A' to the mounting shaft D is an extremely fast drying (a few seconds) liquid (Eastman Kodak 910). The drying speed of this adhesive allowed assembly of the prisms to proceed without delay, and the high strength provided a very secure bond for one prism. Eastman 910 could be been used for mounting both prisms, but separation of the finished cube from the assembly rig would have been very difficult. However, the rapid drying introduces stresses into the attached prism, and these are evidenced by distorted fringes which appear during assembly; they vanish when the cube is removed from the assembly rig.

The cube should be mounted in a holder to facilitate laboratory use; a suggested holder is shown in figure 44. A commercial two-part epoxy adhesive was used to fasten the present cubes in the holders. A final inspection of the cube mounted in the holder should be made to determine if the cube is free of aberrations. For this test, a point source is placed close to the cube entrance face, and the resulting interference pattern is examined. Deviations of these fringes from straight parallel lines indicate surface imperfections. If the fringes are rotated with respect to the intended shear direction, additional tilt is present. This method of inspecting the cube may reveal a relatively large cumulative error across the cube. Since only a small part of the cube is usually used for lens testing, particularly for high f-number lenses, another approach is suggested for determining local aberrations. In this method, a near diffraction-limited lens is stopped down to essentially diffraction-limited conditions, and after aligning the front surface of the cube normal to the optical axis of the lens, the cube is placed near the focal plane of the lens as shown in figure 2 or 3. With only a few fringes in the field, this method can be very sensitive to small aberrations (less than  $\lambda/20$ ) in the cube. The cube can be moved laterally and, therefore, inspected over most of its surface. The fringe patterns can also be photographed and scanned to provide a quantitative analysis of any aberrations present.



(a) Side view.



(b) End view.

Figure 44.- Schematic of cylindrical holder for WSI cube.

## REFERENCES

1. Brock, A. C., *Image Evaluation for Aerial Photography*, pp. 53-55 (Focal Press, London, 1970).
2. Rosenthaler, K., Measurement of Aberrations and Optical Transfer Functions of Optical Systems, Chap. 18, *Advanced Optical Techniques*, A. C. S. Van Heel, ed., pp. 647-654 (North Holland Publishing Co., Amsterdam, 1967).
3. Barnes, K. R., *The Optical Transfer Function, Monographs on Applied Optics*, No. 3, Chap. 3 (American Elsevier Publishing Co., Inc., New York, 1971).
4. Swing, R. E., Conditions for Microdensitometer Linearity, *J. Opt. Soc. Am.* 62, No. 2, 199-207 (Feb. 1972).
5. O'Neill, E. L., *Introduction to Statistical Optics*, pp. 75-79 (Addison-Wesley Publishing Co., Inc., Reading, Mass., 1963).
6. Swing, R. E., The Case for the Pupil Function, *Image Assessment and Specification*, Vol. 46 (Society of Photo-Optical Instrumentation Engineers, Palos Verdes Estates, Ca., 1974).
7. DeVelis, J. B., and Parrent, Jr., G. B., Transfer Function for Cascaded Optical Systems, *J. Opt. Soc. Am.* 57, No. 12, 1486-1490 (Dec. 1967).
8. Swing, R. E., and Clay, J. R., Ambiguity of the Transfer Function with Partially Coherent Illumination, *J. Opt. Soc. Am.* 57, No. 10, pp. 1180-1189 (Oct. 1967).
9. Steel, W. H., *Interferometry*, p. 169 (Cambridge University Press, Cambridge, 1967).
10. Saunders, J. B., A Simple, Inexpensive Wavefront Shearing Interferometer, *Appl. Opt.* 6, No. 9, 1581-1583 (Sept. 1967).
11. Born, M., and Wolf, E., *Principles of Optics*, Third ed., p. 481 (Pergamon Press Inc., New York, 1965).
12. Beran, M. J., and Parrent, Jr., G. B., *Theory of Partial Coherence*, p. 3 (Prentice-Hill, Inc., Englewood Cliffs, N. J., 1964).
13. Grimes, D. N., Measurement of the Second-Order Degree of Coherence by Means of a Wavefront Shearing Interferometer, *Appl. Opt.* 10, No. 7, pp. 1567-1570 (July 1971).

REFERENCES (CONTINUED)

14. Grimes, D., and Jerke, J. M., *Interferometric Lens Testing*, Nat. Bur. Stand. (U.S.), Report 10-827, 124 pages (March 1972).
15. Certain commercial instruments and equipment are identified in this report in order to specify the experimental procedures adequately. In no case does such identification imply recommendation or endorsement by NBS, nor does it imply that the equipment identified is necessarily the best available for the purpose.
16. Pennington, R. H., *Introductory Computer Methods and Numerical Analysis*, Second ed., pp. 445-452 (The Macmillan Co., New York, 1970).
17. Ref. 5, p 91.
18. Saunders, J. B., and Bruening, R. J., A New Interferometric Test and Its Application to the 84-in. Reflecting Telescope at Kitt Peak National Observatory, *Astron. J.* 73, No. 6, 415-430 (Aug. 1968).
19. Ref. 11, pp. 464-468.
20. Smith, W. J., *Modern Optical Engineering*, pp. 300-302 (McGraw-Hill Book Co., Inc., New York, 1966).
21. Hopkins, H. H., The Numerical Evaluation of the Frequency Response of Optical Systems, *Proc. Phys. Soc. (London)*, Sec. B, 70, No. 454B, 1002-1005 (Oct. 1, 1975).
22. Barakat, R., Computation of the Transfer Function of an Optical System from the Design Data for Rotationally Symmetric Aberrations. Part I. Theory, *J. Opt. Soc. Am.* 52, No. 9, 985-991 (Sept. 1962).
23. Lerman, S. H., Application of the Fast Fourier Transform to the Calculation of the Optical Transfer Function, *Modulation Transfer Function*, Vol. 13 (Society of Photo-Optical Instrumentation Engineers, Palos Verdes Estates, Ca., 1969).
24. Ref. 11, p. 441.
25. Ref. 20, pp. 82-84.
26. Wilf, H. S., *Mathematics for the Physical Sciences*, pp. 133-136 (John Wiley and Sons, Inc., New York, 1962).
27. Birch, K. C., The Construction and Proving of Three 50 mm Focal Length Standard Reference Lenses, *Optica Acta* 18, No. 2, p. 144 (Feb. 1971).

REFERENCES (CONTINUED)

28. Anon., *Military Standard Photographic Lenses MIL-STD-150A* (U.S. Government Printing Office, Washington, D. C., 1959).
29. Anon., *Catalog of NBS Standard Reference Materials*, Nat. Bur. Stand. (U.S.), Spec. Publ. 260, 1975-76 ed., 92 pages (June 1975).
30. Murty, M. V. R. K., The Use of a Single Plane Parallel Plate as a Lateral Shearing Interferometer with a Visible Gas Laser Source, *Appl. Opt.* 3, No. 4, 531-534 (April 1964).
31. Briers, J. D., Interferometric Testing of Optical Systems and Components: A Review, *Optics and Laser Technol.* 4, No. 1, 28-41 (Feb. 1972).
32. Black, G., and Linfoot, E. H., Spherical Aberration and the Information Content of Optical Images, *Proc. Roy. Soc. (London)* A239, No. 1219, 522-540 (April 1957).
33. Taylor, C. A., and Thompson, B. J., Some Improvements in the Operation of the Optical Diffractometer, *J. Sci. Instr.* 34, No. 11, 439-446 (Nov. 1957).
34. Cox, A., *Photographic Optics*, pp. 147-150 (Focal Press, London, 1971).
35. Ref. 20, pp. 135-139.
36. Williams, T. L., and Ashton, A., The Use of Standard Test Lenses for Verifying the Accuracy of OTF Equipment, *Appl. Opt.* 8, No. 10, 2007-2012 (Oct. 1969).
37. Becherer, R. J., and Parrent, Jr., G. B., Nonlinearity in Optical Imaging Systems, *J. Opt. Soc. Am.* 57, No. 12, pp. 1479-1486 (Dec. 1967).
38. Ref. 16, pp. 341-348.
39. Anon., *Univac Large Scale Systems MATH PACK Abstracts*, UP-4051 Rev. 2, Section 7, pp. 7-8 (Sperry Rand Corp., 1967, 1970).